A Paleomagnetic Study of Central Harrat Rahat, Western Saudi Arabia

by

Ismail Ebrahim San Linn Kaka

A Thesis Presented to the

FACULTY OF THE COLLEGE OF GRADUATE STUDIES

KING FAHD UNIVERSITY OF PETROLEUM & MINERALS

DHAHRAN, SAUDI ARABIA

In Partial Fulfillment of the
Requirements for the Degree of

MASTER OF SCIENCE

In

GEOLOGY

June, 1993

INFORMATION TO USERS

This manuscript has been reproduced from the microfilm master. UMI films the text directly from the original or copy submitted. Thus, some thesis and dissertation copies are in typewriter face, while others may be from any type of computer printer.

The quality of this reproduction is dependent upon the quality of the copy submitted. Broken or indistinct print, colored or poor quality illustrations and photographs, print bleedthrough, substandard margins, and improper alignment can adversely affect reproduction.

In the unlikely event that the author did not send UMI a complete manuscript and there are missing pages, these will be noted. Also, if unauthorized copyright material had to be removed, a note will indicate the deletion.

Oversize materials (e.g., maps, drawings, charts) are reproduced by sectioning the original, beginning at the upper left-hand corner and continuing from left to right in equal sections with small overlaps. Each original is also photographed in one exposure and is included in reduced form at the back of the book.

Photographs included in the original manuscript have been reproduced xerographically in this copy. Higher quality 6" x 9" black and white photographic prints are available for any photographs or illustrations appearing in this copy for an additional charge. Contact UMI directly to order.

University Microfilms International
A Bell & Howell Information Company
300 North Zeeb Road, Ann Arbor, MI 48106-1346 USA
313/761-4700 800/521-0600

Order Number 1354096

A paleomagnetic study of central Harrat Rahat, western Saudi Arabia

Kaka, Ismail Ebrahim San Linn, M.S.

King Fahd University of Petroleum and Minerals (Saudi Arabia), 1993

U·M·I
300 N. Zeeb Rd.
Ann Arbor, MI 48106

A PALEOMAGNETIC STUDY OF CENTRAL HARRAT RAHAT, WESTERN SAUDI ARABIA

BY

ISMAIL EBRAHIM SAN LINN KAKA

A Thesis Presented to the

FACULTY OF THE COLLEGE OF GRADUATE STUDIES

KING FAHD UNIVERSITY OF PETROLEUM & MINERALS

DHAHRAN, SAUDI ARABIA

In Partial Fulfillment of the
Requirements for the Degree of

MASTER OF SCIENCE

In

GEOLOGY

JUNE 1993

530

KING FAHD UNIVERSITY OF PETROLEUM AND MINERALS

DHAHRAN, SAUDI ARABIA

COLLEGE OF GRADUATE STUDIES

This thesis, written by **ISMAIL EBRAHIM SAN LINN KAKA** under the direction of his Thesis Advisor and approved by his Thesis Committee, has been presented to and accepted by the Dean of the College of Graduate Studies, in partial fulfillment of the requirements for the degree of **MASTER OF SCIENCE** in **GEOLOGY.**

Thesis Committee

Dr. ABDUL-WAHAB A. ABOKHODAIR
Thesis Advisor

Dr. KHALIL A. ZIQ
Member

Dr. MEHMET N. CAGATAY
Member

Dr. ZAGHLOUL R. EL-NAGGAR
Member

Dr. ZAKI Y. AL-HARARI
Chairman, Earth Sciences Department

Dr. ALA H. AL-RABEH
Dean, College of Graduate Studies

Date: 5-7-93

To Whom I Cherish Infinitely and More

ACKNOWLEDGEMENT

Praise be to ALLAH, the Almighty, for giving me the help that enable me to accomplish this work successfully and may peace be upon His prophet Mohammad.

I wish to express my deepest gratitude to my thesis committee chairman, Dr. A.A Abokhodair, for his invaluable support and guidance throughout the period of the research.

I am also grateful to other members of my thesis committee, Dr. M.N Cagatay, Dr. Z.R El-Naggar and Dr. K.A Ziq for their constructive suggestions and ideas which have contributed greatly to the success of the thesis.

Acknowledgement is also due to the King Fahd University of Petroleum and Minerals, Earth Sciences Department for providing the opportunity to carry out this research work.

I am also thankful to all the people, faculty and students alike, who helped ease my somewhat difficult life at the University.

Finally, my sincerest gratitude to my parents, my uncle and all the relatives for their moral support and encouragement.

TABLE OF CONTENTS

ACKNOWLEDGEMENT ..... *iv*

LIST OF ABBREVIATIONS ..... *viii*

LIST OF TABLES ..... *ix*

LIST OF FIGURES ..... *x*

LIST OF PLATES ..... *xi*

ABSTRACT(Arabic) ..... *xii*

ABSTRACT(English) ..... *xiii*

Chapter One

1.1 Introduction 1

1.2 Geology of the Harrat Rahat 4

1.3 Previous Paleomagnetic Work in Saudi Arabia 16

Chapter Two

2.1 A Review of Paleomagnetic Principles 21

2.1.1 Natural Remanent Magnetization (NRM) 21

2.1.2 Thermal Remanent Magnetization (TRM) 21

2.1.3 Demagnetization Techniques 22

2.1.3.1 Alternating Field Demagnetization 23

2.1.3.2 Thermal Demagnetization 24

2.1.4 Representation of demagnetization data 24

2.1.5 Statistical Analyses of Paleomagnetic Data 25

Chapter Three

3. Field and Laboratory Procedures 29

3.1.1 Sampling Scheme 29

3.1.2 Laboratory Procedures 32

Chapter Four

4.1 Paleodirection Measurement 35

4.1.1 Analysis of NRM components 35

4.1.2 Results and Discussion 37

4.1.3 Apparent Polar Wander Path (APWP) 51

4.2 Paleo-intensity Measurement 56

4.2.1 Introduction 56

4.2.2 The Thellier-Thellier Method 58

4.2.3 Data and Results 61

4.3 Opaque Mineralogy 63

4.3.1 Crystal Chemistry and Magnetism 63

4.3.2 Ore Microscopic Study 66

Chapter Five

Conclusions and Recommendations 75

REFERENCES 78

APPENDIX-A : Sample Chart for Central Harrat Rahat 86

APPENDIX-B : NRM-TRM Curves 109

APPENDIX-C : Vector Diagrams
(during thermal demagnetization) 202

APPENDIX-D : Vector Diagrams
(during a.f demagnetization) 226

LIST OF ABBREVIATIONS

AF	Alternating field.
AOB	Alkali olivine basalt.
APWP	Apparent polar wander Path.
ChRM	Characteristic remanent magnetization.
Oe	Oersted
OTB	Olivine transitional basalt.
NRM	Natural remanent magnetization.
PNRM	Partial natural remanent magnetization.
PTRM	Partial thermoremanent magnetization.
TRM	Thermoremanent magnetization.
VGP	Virtual paleomagnetic pole.

LIST OF TABLES

Table		*Page*
1.1	Calculation of total area and volume of Harrat Rahat	8
1.2	Comparison of average rate of lava	8
1.3	Numbers and types of mapped vents on Harrat Rahat grouped by exposed stratigraphic units	15
1.4	Volume calculations for stratigraphic units of Harrat Rahat	15
4.1	Compilation of Paleomagnetic Data	48
4.2	Africa and Arabia Paleomagnetic Poles	52

LIST OF FIGURES

Figures *Page*

1.1 Location map of the study area 3

1.2 Cenozoic lava fields and major tectonic elements of Arabia and northeast Africa 6

1.3 Distribution of Harrat Rahat volcanic fields on the western coast of Saudi Arabia 7

1.4 Isopach map of Harrat Rahat 9

1.5 Stratigraphic units of Harrat Rahat 11

1.6 Distribution of Stratigraphic units of Harrat Rahat 13

3.1 Sampling site locations 30

4.1 First type vector diagram representing the behavior of remanent magnetization during alternating field demagnetization 38

4.2 Second type vector diagram representing the behavior of remanent magnetization during alternating field demagnetization 40

4.3 Type three vector diagram representing the behavior of remanent magnetization during alternating field demagnetization 41

4.4 Type three vector diagram representing the behavior of remanent magnetization during alternating field demagnetization 42

4.5 Equal-area stereographic projection of the site mean directions 44

4.6 Equal-area stereographic projection showing the first and second group are not significantly different at 95% confidence level 47

4.7 Equal-area stereographic projection of the site mean direction 50

4.8 Cenozoic Apparent polar wonder (APWP) for Arabia 55

LIST OF PLATES

Plate		*Page*
1.A	A titanomagnetite grain containing few pale laths of ilmenite.	69
1.B	Ilmenite associated with titanomagnetite subdivided by exsolution lamellae of second phase ilmenite set along planes of the titanomagnetite host.	69
2.A	Whitened heterogeneous lamellae of metailmenite in a titanomagnetite host.	70
2.B	Rhombohedral and triangular areas of titanomagnetite (M) which is in the process of being altered to titanohematite (H). The original ilmenite lamellae has been transformed first to metailmenite and then to titanohematite.	70
3 A	A grain of titanomagnetite with trellis texture of ilmenite lamellae.	71
3.B	Mermaketic texture of Hematite at the boundary of titanomagnetite grain.	71

خلاصة الرسالة

ألاسم : أسماعيل أبراهيم سان لين كلكا

عنوان الرسالة : دراسة المغناطيسية القديمة لحرات رهاط الوسطى, غرب المملكة العربية السعودية.

ألتخصص : جيولوجيا

تاريخ الدرجة : يونيو ١٩٩٣.

تم الحصول على قيم المغناطيسية القديمة من ٢٣ موقع فى حرات رهاط الوسطى , غرب المملكة العربية السعودية. بعد أخذ متوسط ألاتجاهات القطبية المتوسطة لثمان مواقع ذات قطبية عادية و ألاتجاهات الضد القطبية لخمسة عشر موقعا ذو قطبية منعكسة لوحظ أن ألاتجاه المتوسط للمغناطيسية يميل بمقدار ٣٨,٥ درجة و ينحرف بأتجاه ٣٥٣,٢ و له معامل a_{95} بقيمة ٥,٤. لقد كان موقع القطب المغناطيسى فى زمن البليوسين المتأخر- البليستوسين عند خط عرض ٨٦,٧٤ درجة شمالا و خط طول ٣٤٥,٤٩ درجة شرقا. و يبدى المسار الظاهرى لطواف ألاقطاب فى منطقة شبه الجزيرة انحرافا بدءا من ألاوليجوسين المتأخر الى البليستوسين و هذا يتفق جيدا مع انفتاح البحر ألاحمر. تم تحديد اثنين و تسعون منحنى NRM -TRM بطريقة ثيلير في هذه الثلاثه والعشرون موقعا. معظم هذه المنحنيات تحيد عن الخط المستقيم المطلوب بدرجة جعلت تحديد الشدة القديمة غير ممكنة. أسفرت دراسة تركيب المعادن المعتمة للناقلات المغناطيسية فى الصخرعن أنه كلما زادت نسبة التيتانوماجنيتيت المؤكسد قلت قابليتها الى التغيرأثناء التسخين.

درجة الماجستير فى العلوم
جامعة الملك فهد للبترول و المعادن
الظهران, المملكة العربية السعودية
يونيو ١٩٩٣

THESIS ABSTRACT

Name : Ismail Ebrahim San Linn Kaka

Title : A Paleomagnetic Study of Central Harrat Rahat, Western Saudi Arabia

Major Field : Geology

Date of Degree : June 1993

Paleomagnetic results have been obtained from 23 sites in central Harrat Rahat, western Saudi Arabia. After averaging the site mean directions for the 8 normal polarity sites along with the antipoles of the 15 reversed polarity sites, the mean direction of magnetization has an inclination of 38.5 and declination of 353.2 with a_{95} of 5.4. The Late Pliocene-Pleistocene pole position is at Lat. 86.74° N, long. 345.49° E. Apparent polar wander path for Arabia shows divergence for Late Oligocene to Pleistocene time that is in good agreement with the opening of the Red Sea. A total of 92 NRM-TRM curves were determined by Thellier's method from all 23 sites. Most of them deviated from straight line of interest so much that reliable paleo-intensities determination could not be made. Observations of opaque mineralogy of magnetic carriers of the rocks indicate that samples with more oxidized titanomagnetite minerals are less susceptible to further alteration during heating.

MASTER OF SCIENCE

KING FAHD UNIVERSITY OF PETROLEUM AND MINERALS
DHAHRAN, SAUDI ARABIA
June 1993

CHAPTER 1

1.1 INTRODUCTION

Paleomagnetism is an effective tool in Earth Sciences because of its potential to provide reliable information about the earth's magnetic field in the geologic past. Paleomagnetic research has greatly extended our knowledge about the history of the geomagnetic field including its polarity reversals. It also provided the needed direct evidence for continental drift, sea-floor spreading, and plate tectonics. Moreover, in recent years paleomagnetism has been increasingly used as a structural and correlation tool in the study of local, regional and global geologic problem (McElhinny,1973).

The basis of paleomagnetism is the ability of rocks to acquire a permanent magnetization at the time of their formation. This magnetization, which is found in most rocks, usually points in the direction of the magnetizing field and its strength is proportional to the strength of the field. If this magnetization remains unchanged throughout the history of the rocks, it provides a good compass pointing to the ancient magnetic north with an intensity proportional to that of the ancient magnetic field (Strangway,1970).

Very limited paleomagnetic investigations have so far been carried out in Saudi Arabia, despite the need for it to solve various geological and geophysical problems. Therefore the objective of this research work

is to conduct a paleomagnetic study of the Cenozoic basaltic flows in central Harrat Rahat area, western Saudi Arabia (Fig. 1.1).

The study area in the central Harrat Rahat volcanic field was chosen because of the availability of good exposures for the basaltic lava flows in streams, road-cuts and moderately deep trenches. Geological mapping of the area has also been updated recently and the basalt stratigraphy reworked with considerably more reliable radiometric dating than ever before.

The research aims at providing basic data on the direction and the intensity of the Cenozoic geomagnetic field in the study area and attempts to develop reliability criteria for paleo-intensity determination.

In paleo-intensity experiments, rock samples are subjected to several heating and cooling cycle up to their Curie point (approx. 600° C). Frequently, these rocks undergo irreversible alterations that affect the chemical composition, texture, size and shape of their magnetic minerals. Such changes make the experiments more difficult to perform and render their results unreliable. Because these experiments are extremely time consuming, it is of great practical importance to develop a set of petrological, mineralogical and magnetic criteria to aid in the selection of samples suitable for these experiments. Moreover, one approach to this goal is to investigate relationship between the ideal behavior of rock samples in these experiments and their opaque

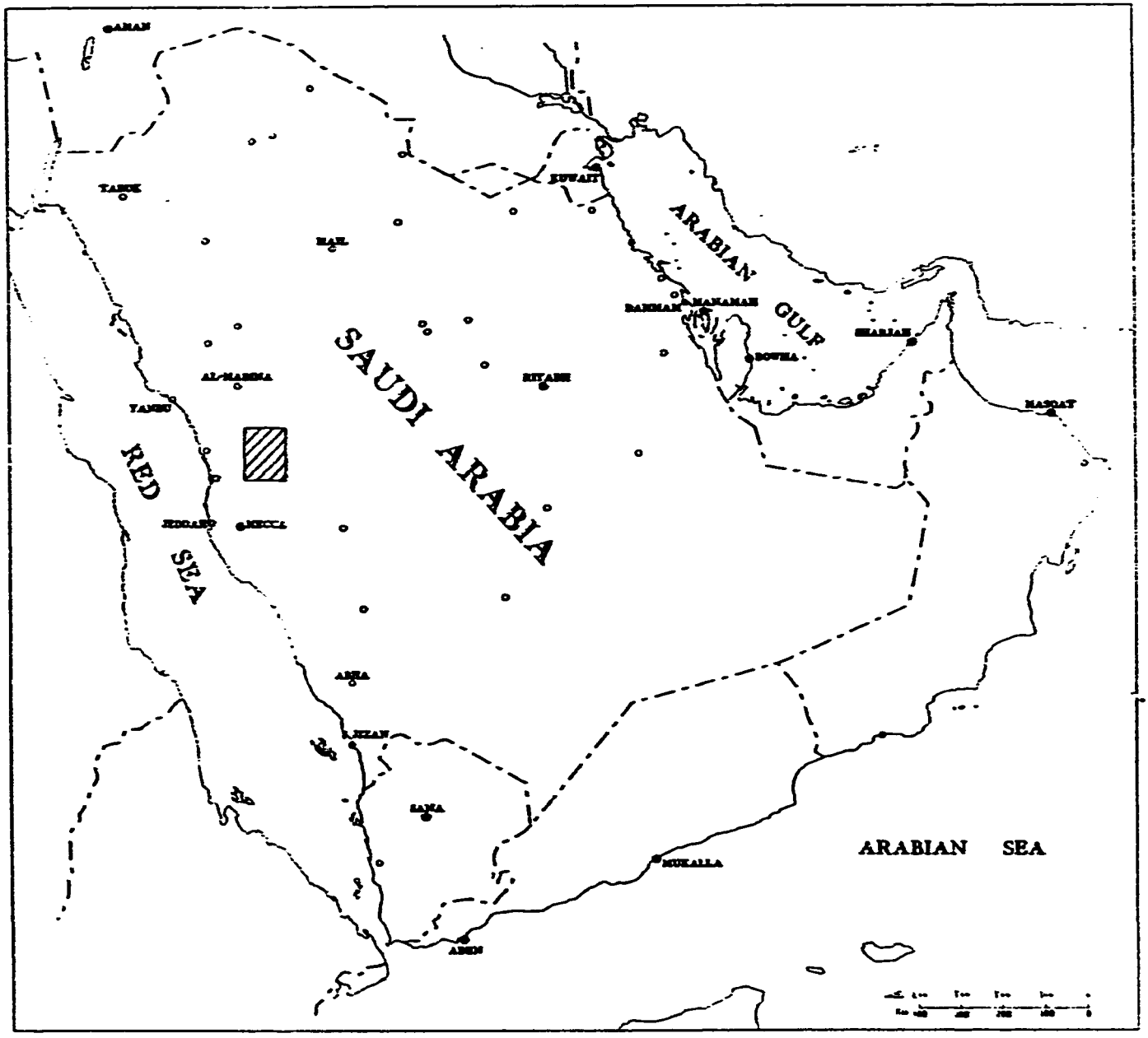

Figure 1.1 Location Map of the Study Area

mineralogy.

The data generated by the present study can be used in a wide range of studies such as determination of the Cenozoic poles for Arabia, correlation of lava flow sequences within and between al-harrat lava fields. Moreover, the raw data will be an addition to the paleomagnetic database for Saudi Arabia which is essential for an investigation relating to the determination of time and amount of Red Sea rifting.

Consequently, the research work is undertaken with a view to carrying out a study of the Cenozoic rocks in central Harrat Rahat volcanic field. Specifically my objectives are as follows:

(1) To determine paleomagnetic directions from suitable samples of these basaltic flows, using standard paleomagnetic sampling techniques.
(2) To investigate paleo-intensities of the geomagnetic field by the Thellier's method from suitable samples.
(3) To study the opaque mineralogy of magnetic carriers of the rocks by reflected light microscope.
(4) To investigate the relationship between ideal behavior in the Thellier's experiments and the magnetic mineralogy of the samples.

1.2. GEOLOGY OF THE HARRAT RAHAT

Several prominent Cenozoic volcanic lava fields known as Harrats, occur in the western part of the Arabian Peninsula from Yemen in the

south, through Saudi Arabia and Jordan, to Syria in the north (Fig. 1.2). The lava fields of the Arabian Peninsula constitute one of the world's largest volcanic provinces with an approximate area of 180,000 square km (Coleman & others, 1983). In Saudi Arabia these rocks cover about 90,000 sq kilometers in thirteen different lava fields (harrats) namely Harrat As Sirat, Al Birk, Al Buqum-Nawasif, Hadan, Al Kishb, Rahat, Lunayyir, Khybar-Ithnayn-Kura-Kurama, Ishara-Khirsat-Harairah, Al Uwayrid-Ar Raha, Hutaymah, Ash Shamah and Al Hamad (Fig. 1.3). Most of these volcanic fields lie along the eastern coast of the Red Sea, approximately 150-200 km in land from the shore line.

The Harrat Rahat , a major feature of western Saudi Arabia, extends from Al-Madinah al Munawwarah (Lat 24.30') to Wadi Fatimah near Makkah (Lat 21.40'), a distance of 310 km. Its average width is 60 km and area is 19,830 sq km (Table 1.1). It is a composite harrat made up of four connected smaller harrats which are, from south to north, Harrat ar Rukhq, Harrat Turrah, Harrat Bani Abdullah and Harrat Rashid (Fig. 1.4). Their north-south lengths are 80, 100, 70, and 60 km respectively, in the form of an elongated shield-like body marked by radially oriented flows extruded from a group of north-west trending linear vent systems. In the central vent axis, the vent systems are offset by gaps that mark the boundaries between the major component harrats (Camp & Roobol, 1991). The average thickness of the Harrat Rahat lava field was determined geophysically by Blank and Sadik (1983) who

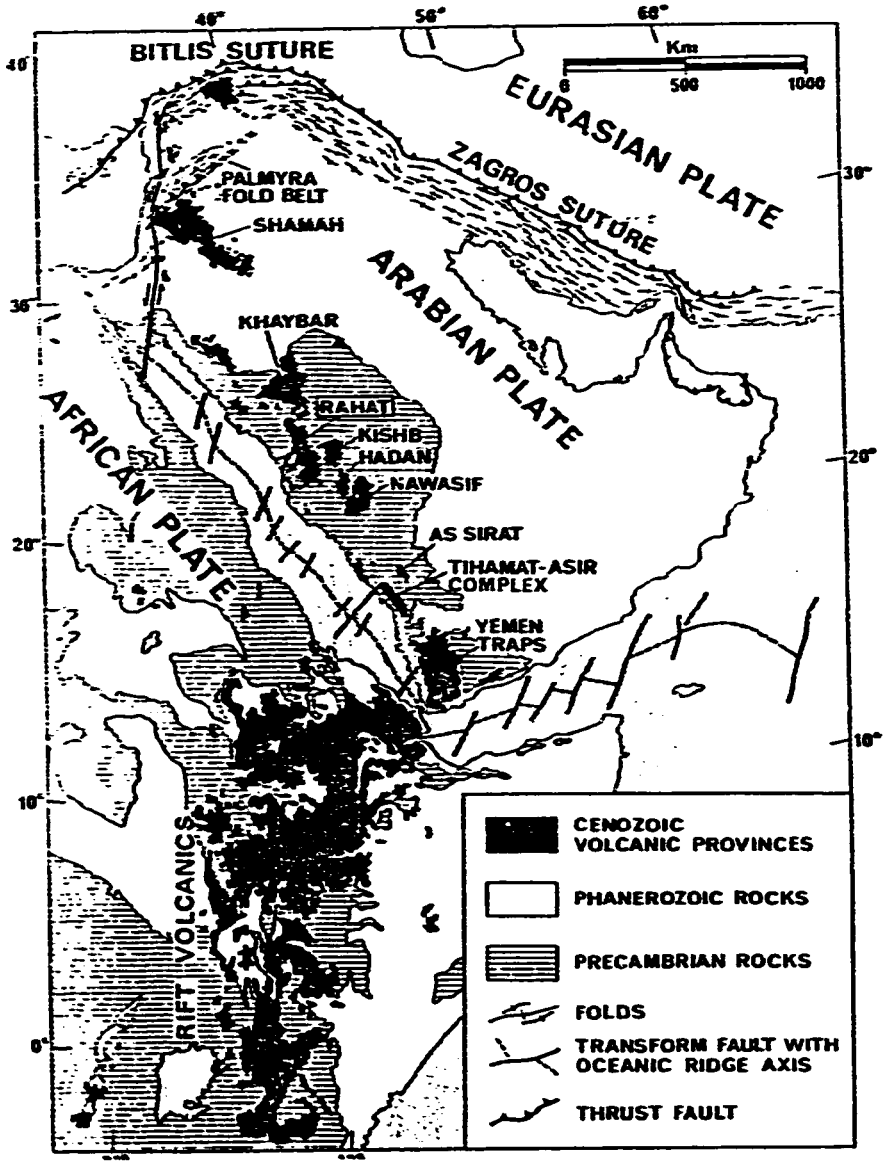

Figure 1.2 Cenozoic lava fields and major tectonic elements of Arabia and Northeast Africa. After Coleman & others(1983).

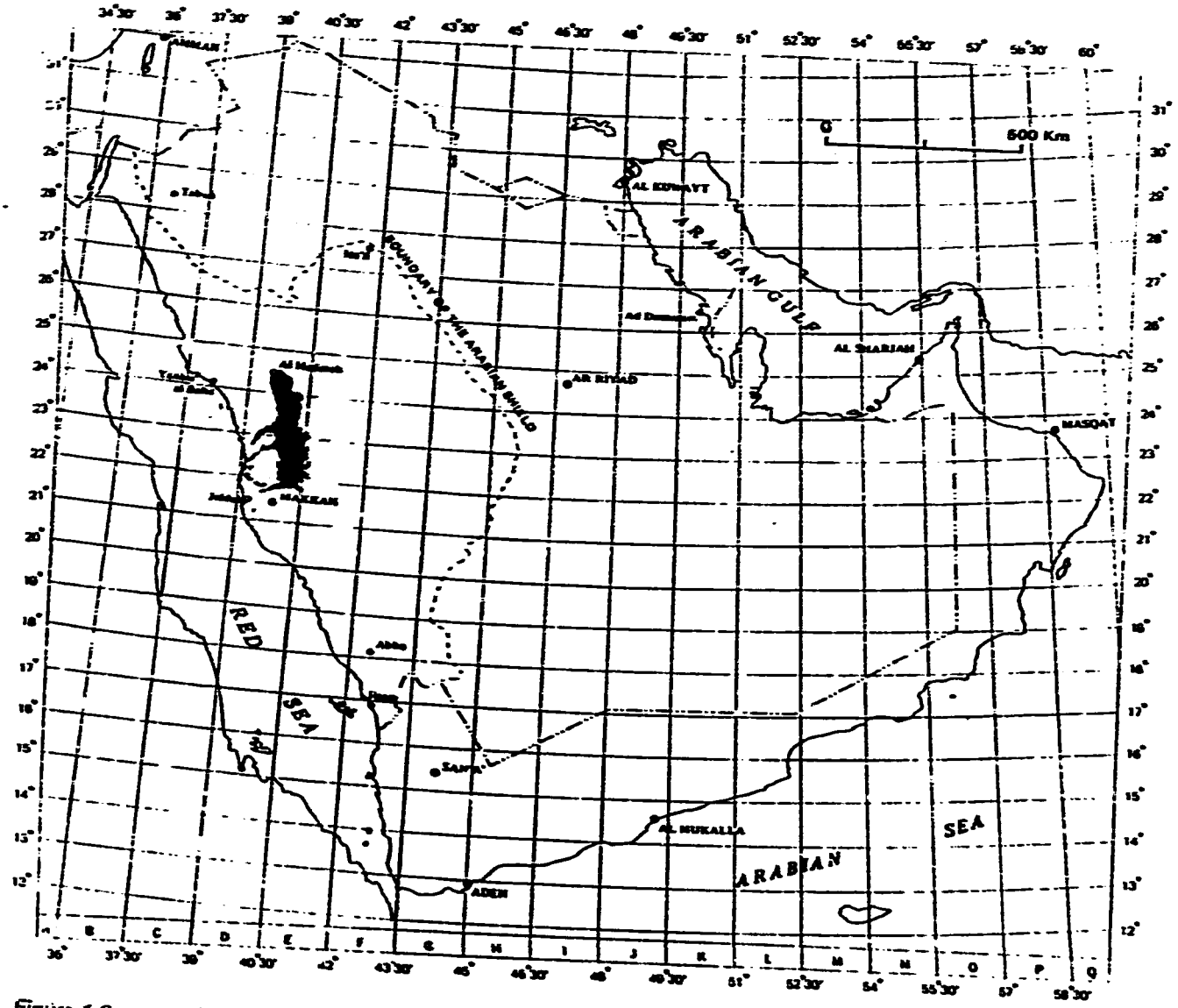

Figure 1.3 Distribution of Harrat Rahat volcanic fields on the western coast of Saudi Arabia. After Camp & Roobol (1991).

Table 1.1 Calculation of total area and total volume of Harrat Rahat. After Camp & Roobol (1991)

Area underlain by	>300 m =	110	km^2	volume =	110 x 0.35	=	38.50	km^3
" "	" 200-300 m =	1,399	km^2	" =	1,399 x 0.25	=	349.75	km^3
" "	" 100-200 m =	6,947	km^2	" =	6,947 x 0.15	=	1042.05	km^3
" "	" <100 m =	11,374	km^2	" =	11,374 x 0.05	=	568.70	km^3
	Total area =	19,830	km^2		Total volume =		1,999	km^3

Table 1.2 Comparison of average rate of lava production of Harrat Rahat with other basaltic areas. After Camp & Roobol (1991).

Location	Time period	Rate of lava production km^3/year	Reference
Harrat Rahat	10 m.y.	0.02×10^{-2}	Camp & Roobol (1991)
Hawaii today	-	10×10^{-2}	Swanson (1972)
Hawaii	6 m.y.	3.3×10^{-2}	Shaw (1973)
Iceland	10,000 years	4×10^{-2}	Thorarinsson (1967)
Ireland	10,000 years	4.8×10^{-2}	Jakobsson (1972)
Yakima Basalt of Columbia River Plateau	3 m.y.	7×10^{-2}	Swanson and others (1975)

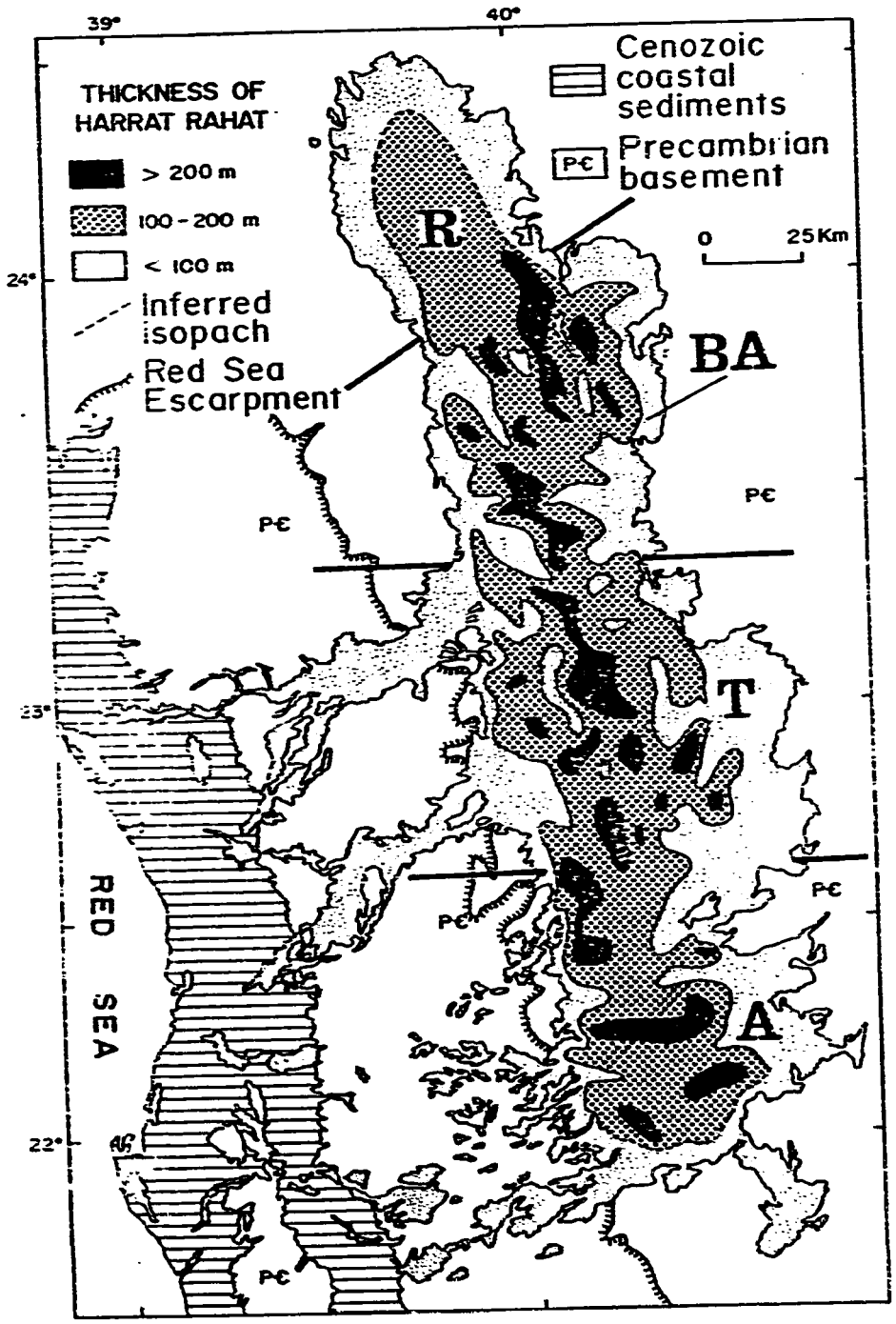

Figure 1.4 Isopach map of Harrat Rahat (After Camp and Roobol,1991). Straight solid lines represent approximate boundaries between Harrat subdivisions: R, Harrat Rashid; BA, Harrat Bani Abdullah; T, Harrat Turrah; A, Harrat ar Rukhq.

produced an isopach map for the harrat south of Lat 24° North. (Fig 1.4). and calculated the average thickness to be approximately 100 meters. The lava field is believed to have been intermittently active for the past 10 Ma with an average lava production rate of about 0.02×10^{-2} km^3 per year. Table 1.2 shows a comparison of the average rate of lava production by Harrat Rahat with other well known basaltic provinces.

The lava flow sequences in the Harrat Rahat are divided into three main successive lava flow sequences that have been treated as three litho-stratigraphic units as follows (from base to top): the Shawahit (10-2.5 Ma), the Hammah (2.5-1.7 Ma) and the Madina (1.7 Ma-Recent) Basalts (Camp et al., 1991).

All exposures of volcanic rocks in the study area are considered part of the Harrat Rahat in that they were extruded in successive eruptions during the past 10 Ma from vents associated with the Harrat Rahat proper.

The Shawahit lithostratigraphic unit was named by Smith (1980) as the 'Shawahit Formation', after Jabal Shawahit, but the name was later modified to the 'Shawahit Basalt' by Camp & Roobol (1987). The unit is best exposed on both Harrat Ar Rukhq and Harrat Turah.

The Shawahit Litho-stratigraphic unit has two disconformity surfaces within its own body (Fig. 1.5) and is followed by a third one (Smith,1980), and hence, it is suggested here to raise this rock unit to a

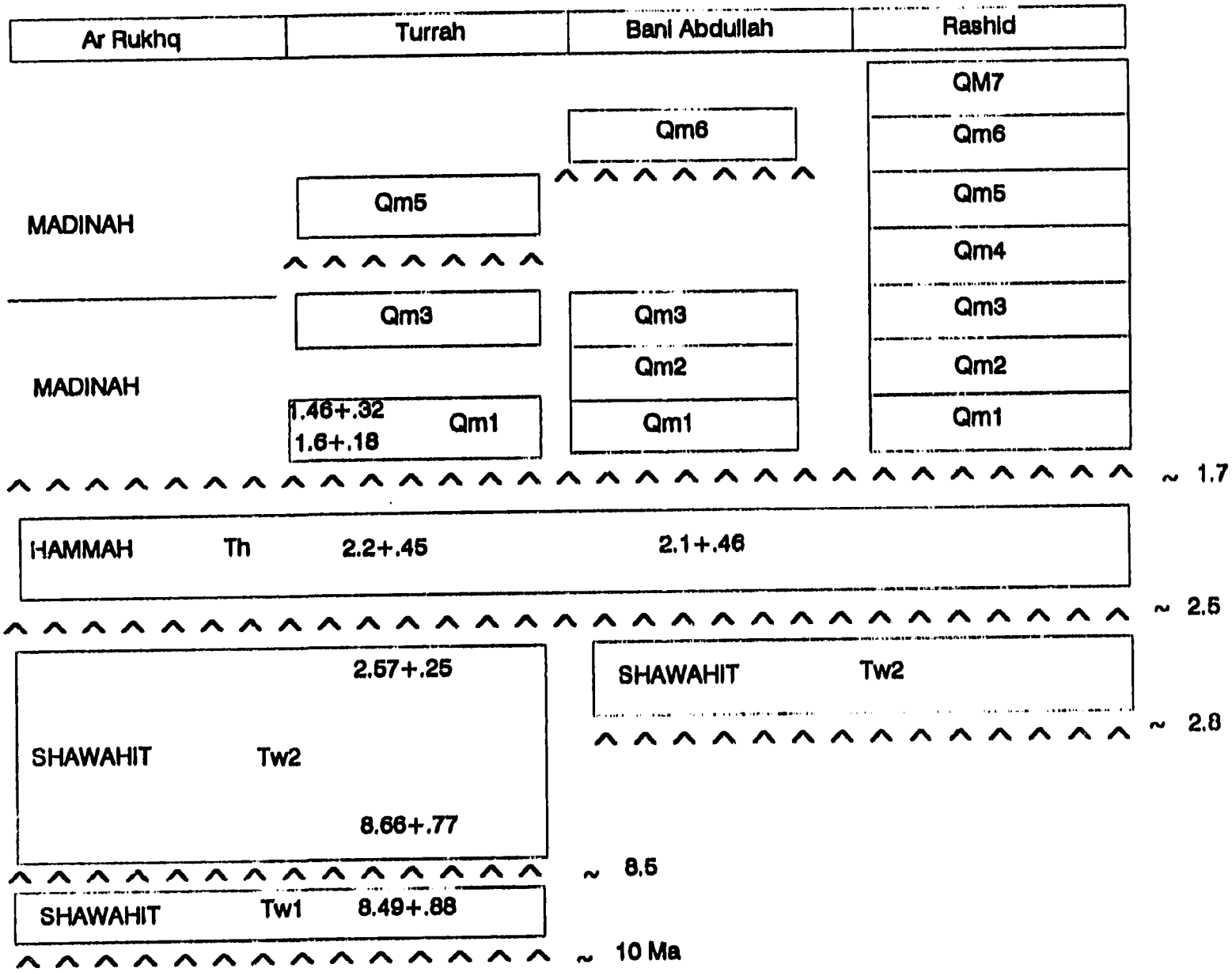

Figure 1.5 Stratigraphic Units of Harrat Rahat (Modified from Camp & Roobol 1987).

group status. All three disconformities in the Shawahit Group represent mature erosional surfaces characterized by incised dendritic drainage patterns. Where these surfaces are exposed, the individual lava flow cannot be recognized. The oldest disconformity occurs on both Harrat ar Rukhq and Harrat Turrah (Figs. 1.3, 1.6). K-Ar isotopic ages indicate that the surface of this oldest disconformity has an age of about 8.5 Ma (Camp & Roobol 1991). This surface is used to separate the lower Shawahit Basalt (Tw1) from the Upper Shawahit basalt (Tw2). The second surface of disconformity is dated at about 2.8 Ma, and occurs on Harrat Bani Abdullah, while the third surface of disconformity truncates the upper part of the Shawahit Group throughout the Harrat Rahat, and represents a hiatus in the volcanic activity at about 2.5 Ma.

The Shawahit Group, comprising about 70 percent of the total volume of Harrat Rahat, is made up of alkali dictytaxitic olivine transitional basalt (OTB) and minor alkali olivine basalt (AOB) which covers large areas over an east west distance of 100 km on Harrat ar Rukhq (Camp & Roobol, 1987).

In the olivine transitional basalt (OTB) megacrysts are usually absent or poorly represented by corroded olivine and very rare corroded plagioclase and microcryst of skeletal olivine are common. In the alkali olivine basalt (AOB) megacrysts are common and microphenocrysts of skeletal olivine are found in most samples. (Camp & Roobol, 1987).

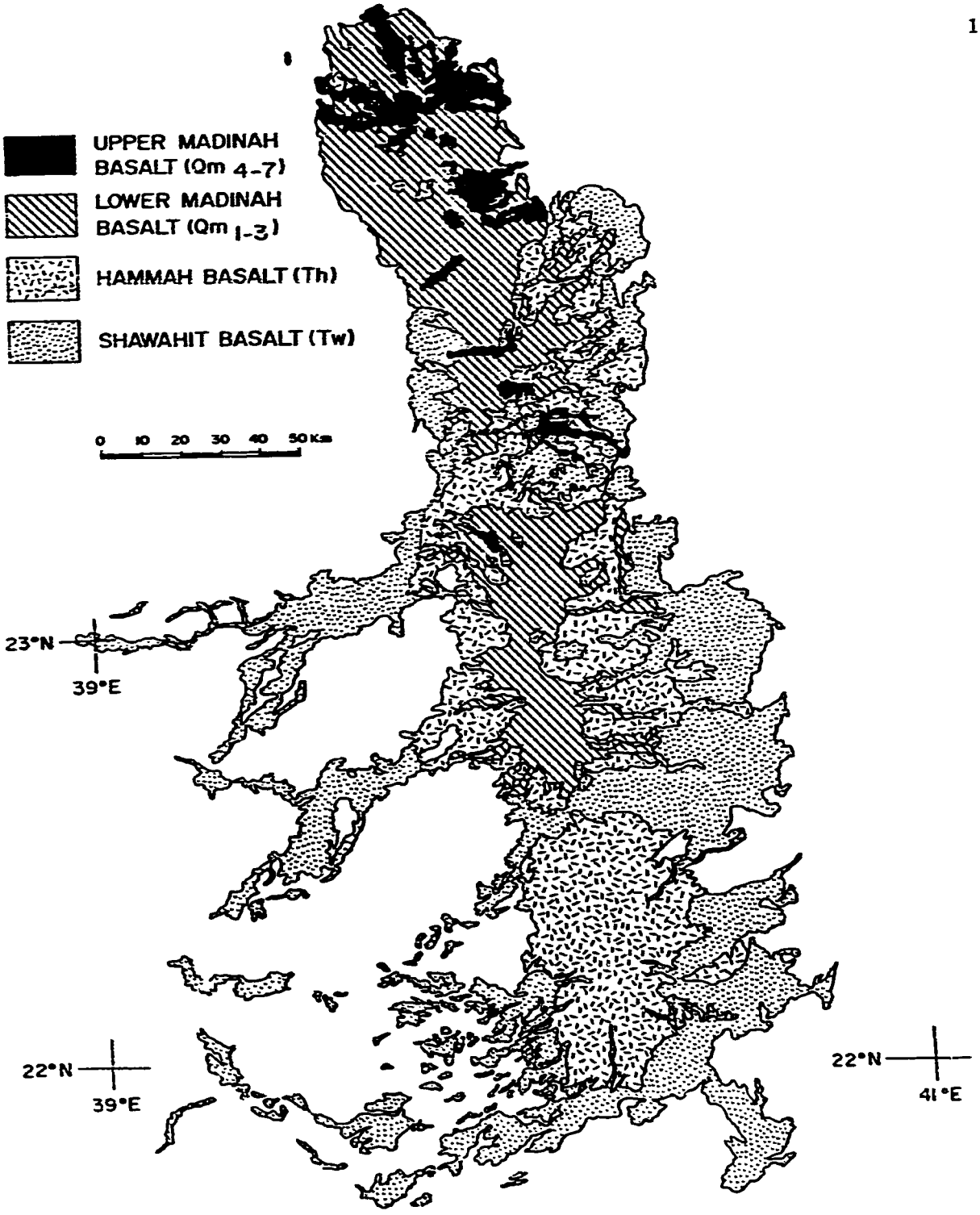

Figure 1.6 Distribution of the stratigraphic units of Harrat Rahat. (from Camp and Roobol, 1991)

Similarly, the name 'Hammah Formation' was also named by Smith (1980) after Wadi Hammah for the alkali olivine basalts which appear to overlie the Shawahit Group on the southern part of Harrat Turrah. The name is modified to 'Hammah Basalt (Th)' by Camp & Roobol in 1987.

The Hammah Basalt consists of fine-grained alkali olivine basalt (AOB) and the hawaiite and is overlain by the Madinah Basalt on a disconformable surface that is considerably less mature than those of the underlying Shawahit Group.

The term Madinah Basalt was suggested by Camp & Roobol (1987) as a new lithostratigraphic unit to include all volcanic eruptions younger than the Hammah basalt. The unit is best developed on Harrat Rashid and diminishes in extent southward to be completely absent in Harrt ar Rukhq (Fig. 1.6).

Based on specifically defined increasing degree of erosion, the Madinah Basalt is stratigraphically subdivided into seven subunits Qm1 to Qm7. The younger lavas (Qm7 to Qm4) lack erosion and their surfaces are progressively covered by dust ponds, while the older lavas (Qm1 to Qm3) are increasingly dissected. The oldest Madinah subunit Qm1 has been dated by the K-Ar method at 1.6 and 1.46 Ma which suggest that the age of the boundary between the Madinah Basalt and the underlying Hammah Basalt is approximately 1.7 Ma (Fig 1.6). The Madina Basalt is composed of alkali olivine basalt (AOB), olivine transitional basalt (OTB), hawaiite and a significant amount of

Table 1.3 Numbers and type of mapped vents on Harrat Rahat grouped by exposed stratigraphic units. After Camp & Roobol (1991). 15

Stratigraphic unit	Exposed area of unit (km^2)	Scoria cones	Shield volcanoes	Domes	Vent ratios Cone:Shield:Dome
Upper Madinah basalt (Qm_4-Qm_7)	760 *	44	0	11	100:0:25
Lower Madinah basalt (Qm_1-Qm_3)	c.5,000 *	401	5	12	100:1:3
Hammah basalt	c.6,000 *	122	22	1	100:18:1
Shawahit basalt	c.8,000 *	17	9	0	100:53:0
Total	c.19,760 *	644	36	24	100:6:4

* These figures are for areas exposed and do not include areas of, for example, Hammah basalt buried beneath Madinah basalt. For the lower Madinah, Hammah, and Shawahit basalts the figures are rounded so that the total area is approximate and less accurate than those of table 1. Similarly, the vent ratios only take into account vents that are now exposed.

Table 1.4 Volume calculation for stratigraphic units of Harrat Rahat. After Camp & Roobol (1991).

Stratigraphic unit	Total area (km^2)	Average thickness (m)	Volume (km^3)	Volume %	Rounded %
Upper Madinah basalt (Qm_4-Qm_7)	760 *	20	15	0.7	1
Lower Madinah basalt (Qm_1-Qm_3)	5,700 *	45	257	12.4	10
Hammah basalt	8, 500 *	45	323	18.5	20
Upper Shawahit basalt (T_{sh2})	17,000 *	50	850	41.2	40
Lower Shawahit basalt (T_{sh1})	8,000 *	70	560	27.1	30
		TOTAL	2065	99.9	

* These figures are for the total area occupied by each stratigraphic unit. They include for example the area of Hammah basalt exposed plus the area of Hammah basalt hidden beneath the Madinah basalt.

differentiated rock types, and its lavas are finer grained and less extensive than those of the older basalts.

The stratigraphic analysis of vent types reveals a systematic temporal change in volcanic style (Table 1.3). Shield volcanos are common in the Shawahit Group but are few in the Hammah Basalt and are absent in the upper Madinah Basalt. On the contrary, volcanic domes are absent from the Shawahit, first appear in the Hammah, and are most abundant in the upper Madinah Basalt (Camp & Roobol,1989). Detailed stratigraphy of the basaltic flows and problems of correlation are discussed in detail by Mufti (1985).

1.3. PREVIOUS PALEOMAGNETIC WORK IN SAUDI ARABIA

The number of paleomagnetic studies that have so far been carried out in Saudi Arabia is very limited. These include Kellogg and Reynolds (1980) on As Sarat volcanic field, Yousif and Beckmann (1981) on some Cretaceous and Paleogene (Tertiary) rocks in western Saudi Arabia, Kellogg and Blank (1982) on the Coastal Plain of Tihamat Asir, Kellog and Beckmann (1981) on Late (upper) Proterozoic rocks in the eastern Arabian Shield, and Hussain and Bakor (1988) on the Basaltic flows of southwest Harrat Rahat, Saudi Arabia.

Kellogg and Reynolds (1980) carried out a paleomagnetic investigation of the As Sarat Volcanic Field of Oligocene-Miocene age,

southwestern Saudi Arabia. The purpose was to drive a paleomagnetic pole, to improve the resolution of the rotational history of Arabia relative to Africa during the past 30 m.y. Their results also provided information relating to the periodicity of volcanic eruption and to the dispersion of the Late Oligocene- Early Miocene field due to secular variation. They compared their results with both Arabian and African results and suggested that the Red Sea has opened at least 2° in the past 5 Ma, and at least 4° in the past 25 Ma. They also suggest that the Arabian Peninsula was equatorial in late Oligocene to early Miocene time than it is now, by an amount compatible with the opening of the Gulf of Aden.

Kellogg & Beckmann (1981) investigated a suite of rocks from the Late Proterozoic rocks in the vicinity of Bir Juqjuq, lat.21.4°N,long.43.7°E), which lies in the eastern part of the Arabian Shield. Their samples include andesitic volcanic rocks and hematized metasediments from Arfan and Juqjuq formation (610 Ma), a younger andesite porphyry stock, a granitic batholith (596 Ma), and two felsic dikes that intruded the granitic batholith. They concluded that most rocks appeared to have been magnetically reset and are not suitable for paleomagnetic analysis. Result from many sites showed unstable or scattered paleomagnetic directions. In most cases, resetting is approximately in the same direction of the present fields. No reversals of magnetization were noted in the volcanic rocks and there is no recent

viscous remanent magnetization was detected. A Late Proterozoic dike was shown to possessed both reversed and normal components of magnetization. The country rock at its margin is magnetized in an identical manner, substantiating the TRM nature of remanence. Major thermal activity associated with granitic to quartz monzonitic plutonism is known to have occurred approximately 600 Ma B.P in the region. They suggested the need for more paleomagnetic work on some of the younger dated rocks to help resolve the apparent polar-wandering path for the region.

Yusif and Beckmann (1981) determined the preliminary paleomagnetic poles for three sequences of Paleogene (Tertiary) basaltic lava and for the Usfan Formation near Jeddah. They reported that poles from the rocks older than 19 m.y deviated from African polar wander path, and suggested that this departure is consistent with the opening of the Red Sea. They also pointed out that for the period from about 67 to 19 m.y ago, the Arabian Plate had a northward movement with an average speed of 5 cm per year, and it reached its present latitude about 19 m.y ago.

Kellogg and Blank (1982) conducted a paleomagnetic study on the Paleogene (Tertiary) of the Tihamat Asir coastal plain, southwestern Saudi Arabia. The objective of their work was to test several hypotheses related to the tectonics rifting along the eastern margin of the red sea. They concluded: (1) All data are consistent with a tilt of

approximately 20° of the coastal-plain region toward the Red Sea subsequent to the emplacement of the Tihamat Asir gabbros and granophyres. (2) The paleomagnetic evidence does not support significant rotation during the period of emplacement of that most dikes. (3) The ratio of normally to reversely magnetized dikes changes significantly along a traverse normal to the Red Sea. (4) The paleomagnetic data support the hypothesis that the Jabal at Tirf gabbro cooled with an internal geometry similar to its present configuration, allowing only a small amount of relative warping after emplacement.

Hussain and Bakor (1989) investigated the paleomagnetism and opaque mineralogy of basalts (3.3 to 3.73 Ma) exposed along Jeddah-Madina road. They constructed a preliminary apparent polar wonder path (APWP) for Arabia and Africa during the Paleogene-Neogene period and concluded that the paleomagnetic data at hand is still far too meager to allow to trace the tectonic history of the Red Sea.

From the above literature review, it is apparent that the amount of the paleomagnetic research so far been conducted in Saudi Arabia is inadequate to resolve the many and complex questions of tectonic history of the Red Sea and Arabian Shield regions. Especially if one realizes the geological importance (in terms of plate tectonics) as well as mineral resource potential of the Red Sea and Arabian Shield. There are a number of important questions that can not be answered until adequate paleomagnetic data become available such as the timing and

amount of relative motion between the Arabian and African plate. As such data accumulates, it could also bring evidence to the origin of the Arabian Shield.

Evidently, none of the researchers attempted to determine the paleo-intensity. Such measurement provides an important information about the time variation of the intensity of the geomagnetic field which can lead to the understanding of paleosecular variation. Such understanding is important for both age determination and correlation purposes in the studied area.

This is why we decided to carry out a paleomagnetic study of basaltic flows in the Central Harrat Rahat area. The results of this research is a contribution to the Geology of the Kingdom of Saudi Arabia and provide a better understanding for the volcanic activities in the Central Harrat Rahat area.

CHAPTER 2

2.1. A REVIEW OF PALEOMAGNETIC PRINCIPLES

In this chapter, some background material is reviewed which will be helpful in understanding the experimental results obtained in this investigation.

2.1.1 Natural Remanent Magnetization (NRM)

The natural remanent magnetization (NRM) is the "permanent" magnetization acquired by a rock at the time of its initial formation in the earth's magnetic field. Typically, it is composed of more than one component. The NRM component acquired during the time of the formation of the rock is referred to as primary NRM (characteristic remanence) and is the component (or signal) sought in paleomagnetic investigations. Whereas components acquired subsequent to the formation of the rock is termed as secondary NRM and is the undesirable component (or noise).

2.1.2 Thermoremanent Magnetization (TRM)

Mafic igneous rocks are formed by the cooling of magma from temperatures well above 1000° C accompanied by the crystallization of various mineral phases including iron oxides. As the iron oxides continue to cool after crystallization, an exchange interaction

between atoms begins to dominate thermal disordering. The temperature at which this happens is known as the Curie point. This results in strong spontaneous magnetization setting in within the crystals, and this magnetization become closely aligned with the ambient geomagnetic field at that location. Just below the Curie point the response time (relaxation time) of the magnetic moments of the grains to changes in the applied field is very short. in the order of seconds. However relaxation time increases exponentially with increasing grain volume and with decreasing temperature. On cooling to a particular temperature called the blocking temperature the relaxation time rapidly increase and the magnetization of the grain then becomes effectively fixed in the direction of the ambient field. As the grain continues to cool the relaxation time may reach 10^9 years or more, so that a record of the geomagnetic field at the time of cooling is effectively frozen into the rock, this type of magnetization is called a TRM.

2.1.3 Demagnetization Techniques

As discussed earlier, most rock samples carry more than one component of magnetization which have been acquired at different times in the rock's history. These components will reside in different populations of magnetic mineral grain within the rock sample which commonly will have different magnetic stabilities. The stability of the magnetization in a grain could be specified in

terms of its blocking temperature or its coercivity. Coercivity is the reversed field required to destroy the remanent magnetization of the grain.

The separation of the different components of magnetism in the rock is normally achieved by progressive demagnetization procedures, the lower stability components being removed during the early stage and the higher stability components during the later stage of the demagnetization process. Progressive demagnetization techniques used in this experiment were Alternating-field (AF) and Thermal demagnetization techniques.

2.1.3.1 Alternating-field (AF) demagnetization

During the demagnetization process, the rock specimen is tumbled in the center of a demagnetizing coil which generates alternating field. The coil is inside the magnetic shield to remove the effect of any other magnetic fields present in laboratory. A specimen holder provides for rotating the rock specimen about two of its axes by means of the mechanical tumbler. Removal of the unstable components of remanence is accomplished by demagnetizing in an applied alternating field which decays linearly to zero from a pre-set peak value (H1). During each half-cycle of the applied field, the magnetization of all grains in the rock specimen with coercivities up to H1 will follow the applied field and alternate in direction along the demagnetizing coil axis. As a

result of progressive reduction of the alternating field to zero, equal number of grains will be left with their magnetic moments pointing in the opposite direction along this axis, so that no net magnetization results form these grains. Thus, the magnetization of all grains with coercivities up to H1 is effectively randomized. This treatment is repeated at progressively higher applied fields, H1, H2, etc., and the magnetization of the rock specimen is measured after each step.

2.1.3.2 Thermal demagnetization

The rock specimen is heated to determined temperatures and cooled back to room temperature in field-free space. The thermal fluctuations due to heating will randomize the magnetization of all grains with blocking temperatures up to this applied temperature. Then magnetization of the rock specimen is measured at room temperature. This process is continued until the magnetism of the rock specimen is destroyed.

2.1.4 Representation of demagnetization data

The results of progressive demagnetization investigations can be plotted in either of two ways: as stereographic projections of the direction of remanent magnetism, with accompanying graphs showing the changes in intensity of magnetization diagrams, or as vector diagrams also known as Zijderveld diagrams (Zijderveld,

1967). In the last diagram, the tip of the NRM vector after each magnetization step is projected onto the horizontal and the vertical planes. The vector diagram was used in this study because it has the advantage that it combines both the directional and intensity changes on to a single plot, rather than treating these parameters separately. It also shows both single and multi-component in a way that might not be evident from spherical projections, where only one direction of magnetization can be illustrated. As the rock specimen is demagnetized, the projection will trace out a path defined by the collective changes in declination, inclination and intensity. If the NRM comprises only a single component, its magnitude will be progressively reduced by demagnetization but its direction will remain unchanged and the projection will migrate along two straight lines (the vertical and horizontal components) towards the origin of the coordinates. If the magnetization is multi-component, the vector path will trace out a straight line provided that only one component is being subtracted at a time, but these straight lines will not pass through the origin.

2.1.5 Statistical analyses of Paleomagnetic data

The initial stage in the interpretation of paleomagnetic data is the determination of a mean direction of NRM from a set of observed (measured) directions together with an estimate of uncertainty in the mean direction and a measure of the reliability

of the paleomagnetic data. For this purpose, the most widely used statistical technique in paleomagnetic research is that of Fisher.

In this section, the statistical parameters used in this study are described.

To compute the mean direction from a set of N unit vectors, first individual vectors are computed:

$l_i = \cos I_i \cos D_i$

$m_i = \cos I_i \sin D_i$

$n_i = \sin I_i$

where (I_i, D_i) are the inclination and declination of the ith vector respectively and l_i, m_i, n_i are its direction cosines with respect to north, east and down direction.

The direction cosines, l, m ,n of the mean directions are given by

$$l = \sum_{i=1}^{N} l_i / R$$

$$m = \sum_{i=1}^{N} m_i / R$$

$$n = \sum_{i=1}^{N} n_i / R$$

where R is the resultant vector with length R given by

$$R^2 = (\sum_{i=1}^{N} l_i)^2 + (\sum_{i=1}^{N} m_i)^2 + (\sum_{i=1}^{N} n_i)^2$$

R is always ≤N and approaches N only when the vectors are tightly

clustered. Declination and inclination are computed by

$$D_m = \tan^{-1}\left(\frac{m}{l}\right)$$

$$I_m = \sin^{-1}(n)$$

To compute the precision parameter (k). a measure of the scatter data points. can be calculated by

$$k = \frac{N - l}{N - R}$$

The advantage of using the precision parameter is that it is a normalized quantity and is not dependent upon the number of rock samples used in the study. provided that a sufficient number of samples is used and scattering in directions is not too great. When 'N' is large, the expression reduces approximately to N/(N-R), and it then becomes a true measure of the scatter of points. If the point are closely grouped, 'R' approaches 'N' so that the value of 'k' is large, while if the data are highly scattered. 'R' is small and the value of 'k' is small. The precision parameter k varies from infinity when all the direction are identical down to one when the directions are uniformly distributed over the surface of the sphere.

For a directional data set with N directions, the angle α_{1-p} within which the unknown true mean lies at confidence level (1-p)

is given by

$$\cos\alpha_{1-p} = 1 - \frac{N-R}{R}\left\{\frac{1}{p}\right\}^{\frac{1}{N-1}} - 1$$

Probability level 95% was chosen and the confidence limit is usually denoted as $\alpha 95$.

Small value of $\alpha 95$ implies that the mean has been precisely estimated while large value implies that it has been poorly estimated.

CHAPTER 3

FIELD AND LABORATORY PROCEDURES

3.1 SAMPLING SCHEME

For paleomagnetic studies rock units have to be sampled in sufficient detail to obtain reliable information about the ancient geomagnetic field in the area of investigation. Consequently, the first stage in any paleomagnetic study is the collection of oriented samples. Sample orientation consists of defining a set of sample-fixed coordinates removed from their original field (x,y,z) and recording the orientation of this coordinate system with respect to local geographic coordinates (N,E,V). This is necessary for subsequent conversion of the sample magnetization directions to a common geographic reference system.

The basaltic flows were sampled at sites distributed along a circular traverse that covers the entire area of Central Harrat Rahat (Fig. 3.1). The sampling scheme was designed to satisfy the following considerations:

-Variation in lithologic composition,

-Changes in texture

-Evidence of relative movement between different parts of the exposure,

-Presence or absence of weathering, and

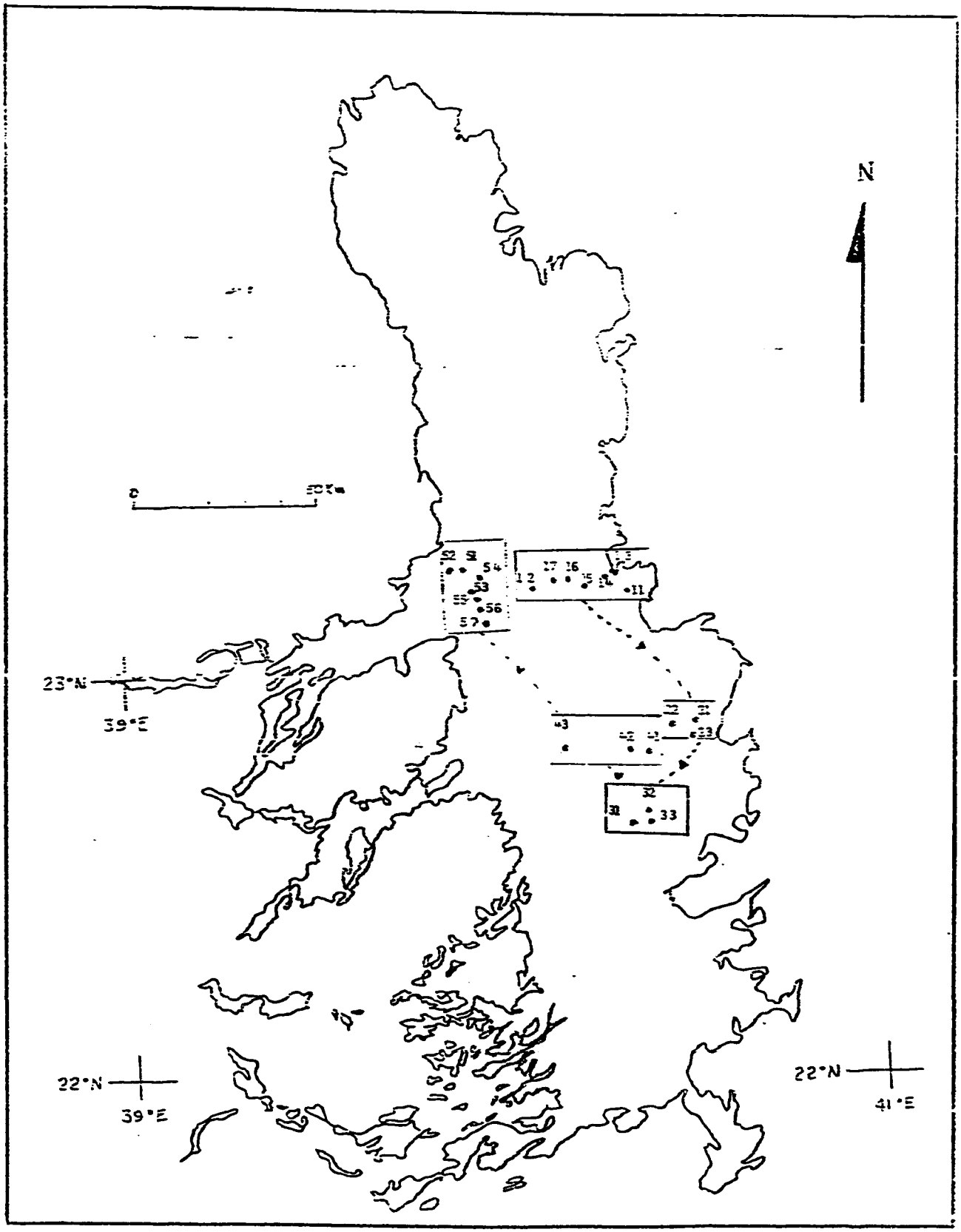

Figure 3.1 Sampling site locations.

-Suitable mechanical properties for drilling of samples.

The area was divided into five localities, at each of which, oriented samples were collected from three to seven separate exposures referred to as sampling sites. Samples for this study were collected according to the standards for any careful paleomagnetic study. Special care was taken to avoid outcrops that had been rotated or displaced by faulting. Fresh outcrops were preferred for sampling, but effort was made to sample as many physically distinguishable parts of the flow unit as possible. A minimum of five and a maximum of eighteen cores were drilled at each site in order to average out small orientation errors and other sources of local variability and to improve the precision of the mean site remanence direction. Little advantage is to be gained by sampling more than five cores at each site unless more than one component of magnetization is present. At some sites, additional hand specimens were also taken. A total of 202 oriented and 39 un-oriented core samples, representing 7 different litho-stratigraphic units were obtained from 5 localities (23 sites) shown in (Fig. 3.1). The samples from the different sites in each locality are listed in the Appendix A, along with their orientation angles and site location.

All samples were taken in the form of cores 2.49 cm in diameter and from 8 to 18 cm in length, drilled in situ with a portable water cooled diamond core drill. A nonmagnetic device was used to mark the core before they were detached from the outcrop in such a way as to preserve

the geographic orientation. Although orientation is not necessary for studies concerned with the past intensity of the geomagnetic field, it is desirable that some control over the remanence direction of the samples is obtained whenever possible as this allows more reliable evaluation of the nature of components of their remanence.

3.2 LABORATORY PROCEDURES

All the samples for this study were treated in the Paleomagnetism Laboratory of the Earth Sciences Department, King Fahd University of Petroleum & Minerals.

The aims of paleomagnetic laboratory procedures are to examine the stability of the remanent magnetization of the rock, attempt to remove the secondary components of magnetization present, and isolate the characteristic magnetization.

In the laboratory, two or three cylinder 2.49 cm long were cut from the lower end of each (core) sample giving a suitable specimen for magnetometer measurements. First two specimens were used for direction and intensity measurements, but occasionally, only one specimen was obtained from a sample. The remaining material from the core was used to make both thin and polished sections.

Measurement of remanence directions and intensities were made on a Digital Spinner Magnetometer (DSM-1). Step-wise partial demagnetization (magnetic cleaning) was carried out using both

Schonstedt AC Tumbling Demagnetizer (GSD-5) and Thermal Specimen Demagnetizer (TDS-1). General discussion of the use of these instruments are given in detail by both McElhinny (1973) and Tharling (1983).

Two core samples per site were step-wise thermally demagnetized up to 600° C and the remaining core samples were stepwise AF (alternating field) cleaned. After initial measurement of remnant magnetization (NRM), the specimens were treated by alternating field demagnetization at field strengths of 50, 100, 150, 200, 300, 400, 600, 800 and 1000 oersted ; and by thermal demagnetization at increasing temperature intervals of 50 in the range of 50 to 600° C. Special care was taken to randomize the positions of the specimens in the thermal demagnetizing chamber in order to minimize the possible effects imposed by any small residual fields during cooling.

Paleo-intensity determination by Thelliers' technique was carried out on specimens from all 23 sampling sites. From each sampling site four specimens were selected, a total of 92 specimens from all seven litho-stratigraphic units. The measurement and determination of paleo-intensity is described in detail in section 2 of next chapter.

Polished sections of the samples collected (from all seven stratigraphic unit) were examined under reflected light microscope to determine if there were any unifying mineralogical characteristics

governing stability of magnetization. Chapter 4.3 gives detailed discussion.

CHAPTER 4

4.1 PALEO-DIRECTION MEASUREMENTS

4.1.1 Analysis of NRM components

On the basis of lithostratigraphic sequence, the sites were divided into two groups. First group contains sites from all Madinah basalt which consists of 13 sampling sites and second group consists of 10 sampling sites from Hammah and Shawahit basalts.

Vector diagrams (for all the specimens used in this study) showing the changes in NRM direction that occur during demagnetization are displayed in Appendix(D). The aim is to remove all secondary magnetization and identify the ChRM. A BASIC program which uses principal component analysis described by Sherwood (1989) was used to determine the characteristic remanent magnetization direction for each specimen. The procedure is essentially that of fitting by least squares criterion the best straight line along the demagnetization path. The data are displayed as vector diagram and a series of points which make up a single component can be selected. If a specimen has multi-component, new points may be selected and analyzed. In this way,

ChRM direction was isolated by removing the secondary NRM.

These ChRM directions of specimens from each core (sample) are combined first to give a sample-mean ChRM directions. A site-mean ChRM direction is then calculated form the sample-mean ChRM directions. The site-mean ChRM are in turn combined to yield the average ChRM directions form the stratigraphic rock unit. Then set of VGPs is used to determine the mean pole position (Paleomagnetic pole) by Fisher statistics. It is important here to know the difference between VGP and paleomagnetic pole.

By definition, a pole position that is calculated from a single observation of the direction of the geomagnetic field is called a Virtual Geomagnetic Pole (VGP). It represents magnetic field direction at one location and at one point in time (secular variation is not meaned out). In paleomagnetism a site-mean ChRM direction is a record of past geomagnetic field direction at the sampling site location during the interval of time over which the ChRM was acquired. Therefore, a pole position calculated form a single site-mean ChRM direction is a virtual geomagnetic pole (VGP).

It is known that the dipolar geomagnetic field undergoes secular variation, causing the geomagnetic pole to randomly walk about the rotation axis with periodicities dominantly from 10^3 to 10^4 year.

The geocentric axial dipole hypothesis states that, if geomagnetic secular variation has been adequately sampled, the average position of the geomagnetic pole coincides with the rotation axis. Thus a set of paleomagnetic sites magnetized over about 10^4 to 10^5 year should yield an average pole position (average of site-mean VGPs) coinciding with the rotation axis. Pole positions calculated with these criteria satisfied are called paleomagnetic poles. The term paleomagnetic pole implies that the pole position has been determined from a paleomagnetic data set that has averaged geomagnetic secular variation and thus gives the position of the rotation axis with respect to the sampling area at the time of ChRM was acquired.

4.1.2 Results and Discussion

Observations of initial NRM behavior (all vector diagram plots) during both alternating field demagnetization and thermal demagnetization treatments allow classification of remanence into three major types.

First type remanence is interpreted as uncomplicated, original TRM. For instance, sample No. 14R129 from Qm1 shows mostly the decay of only a single component of magnetization (Fig. 4.1). It can be interpreted that the ChRM of the specimen to be a TRM imparted to the specimen at the time of its initial cooling. Little

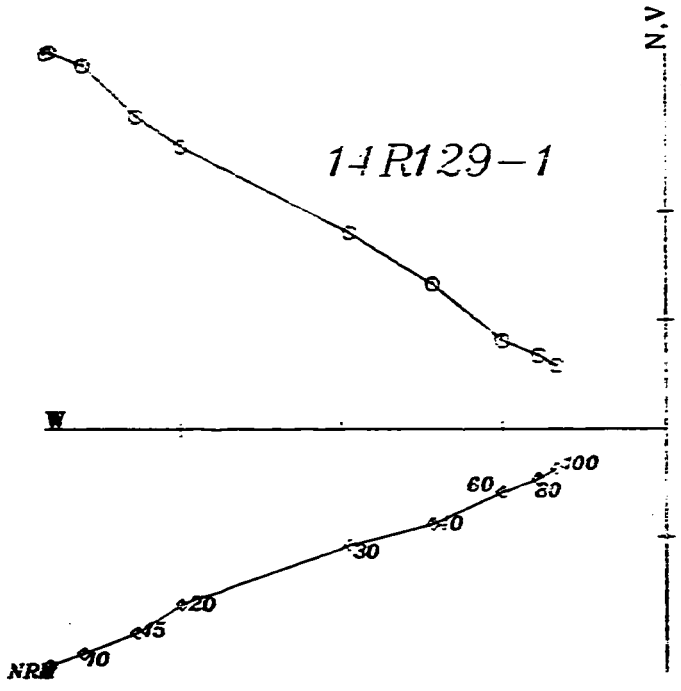

Horizontal Vertical

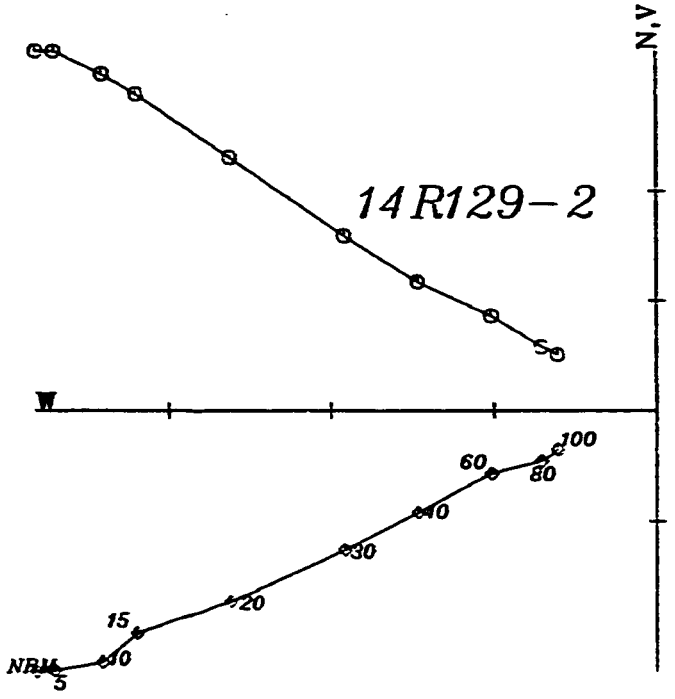

Figure 4.1 First Type : vector diagram representing the behavior of remanent magnetization during alternating field (a.f) demagnetization.

or no secondary component of magnetization is present.

Second type is a TRM overprinted by a weak to moderate isothermal remanent magnetization (IRM) (Fig. 4.2). Initial NRM of this type of specimens (e.g 21R020, 13R113 from Tw1, Qm1) show low to moderate dispersion, and progressive AF demagnetization reveals a low to moderate coercivity component (removed using peak fields 5 to 15 mT).

Third type remanence is a TRM overprinted by a strong secondary remanence (Fig. 4.3, 4.4). AF (alternating field) demagnetization of this type of specimens (e.g 56R195, 16R138 from Qm3, Th) show evidence for more than one component. It is very likely that these secondary components are due to multiple lightning strike or to secondary partial thermal or chemical remagnetization following the acquisition of initial TRM.

From each site, 4 specimens (2 core samples) were step-wise thermally demagnetized and the remaining core samples were step-wise AF cleaned. It is very interesting to note that the thermal demagnetization behavior of more than 42 specimens are consistent with (similar to) that of AF (alternating field) demagnetization. The fact that alternating field demagnetization behaviors reveal the same ChRM directions as did thermal demagnetization (their ChRM directions do not differ significantly form specimens to specimens after they have been subjected to AF and thermal

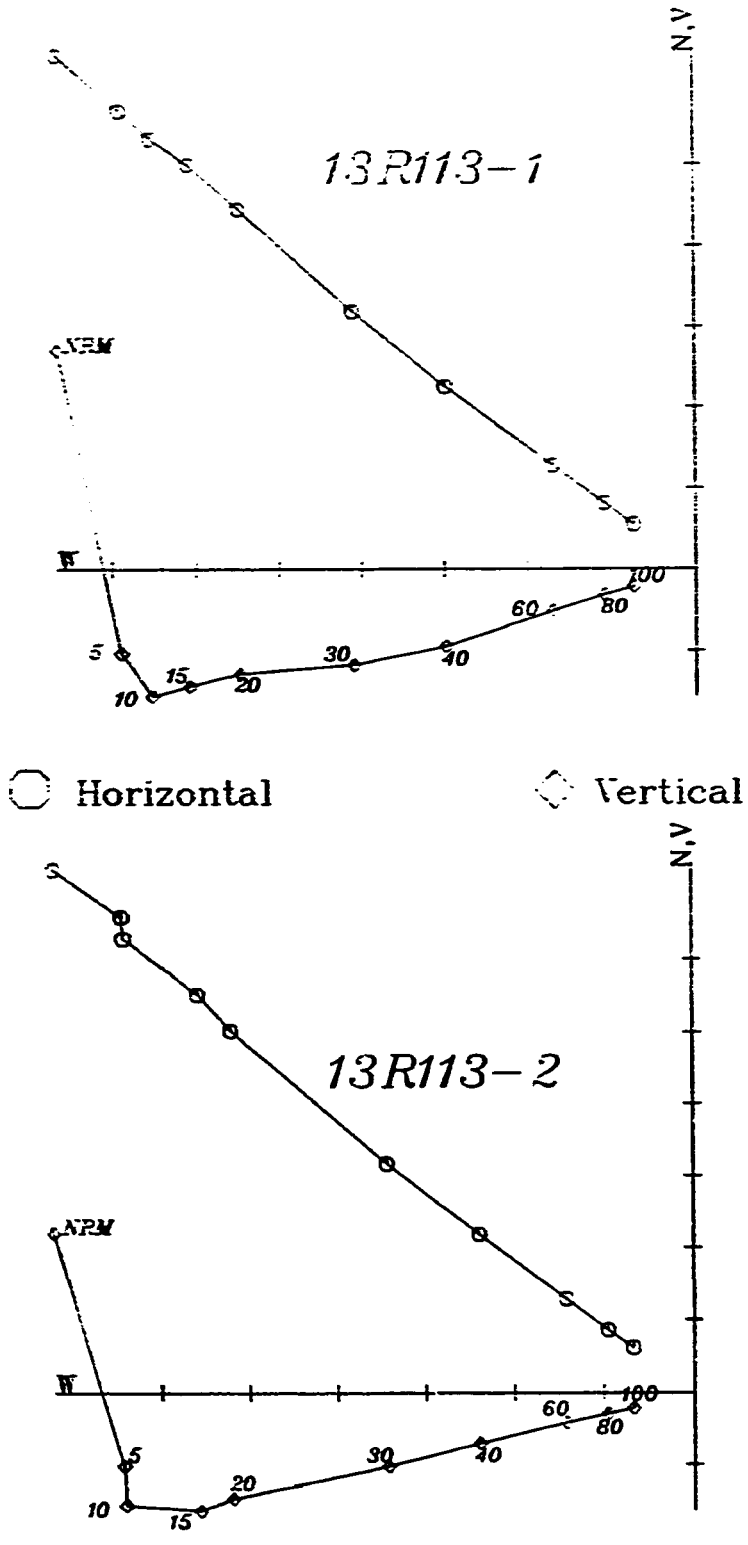

Figure 4.2 Second type : vector diagram representing the behavior of remanent magnetization during alternating field (a.f) demagnetization.

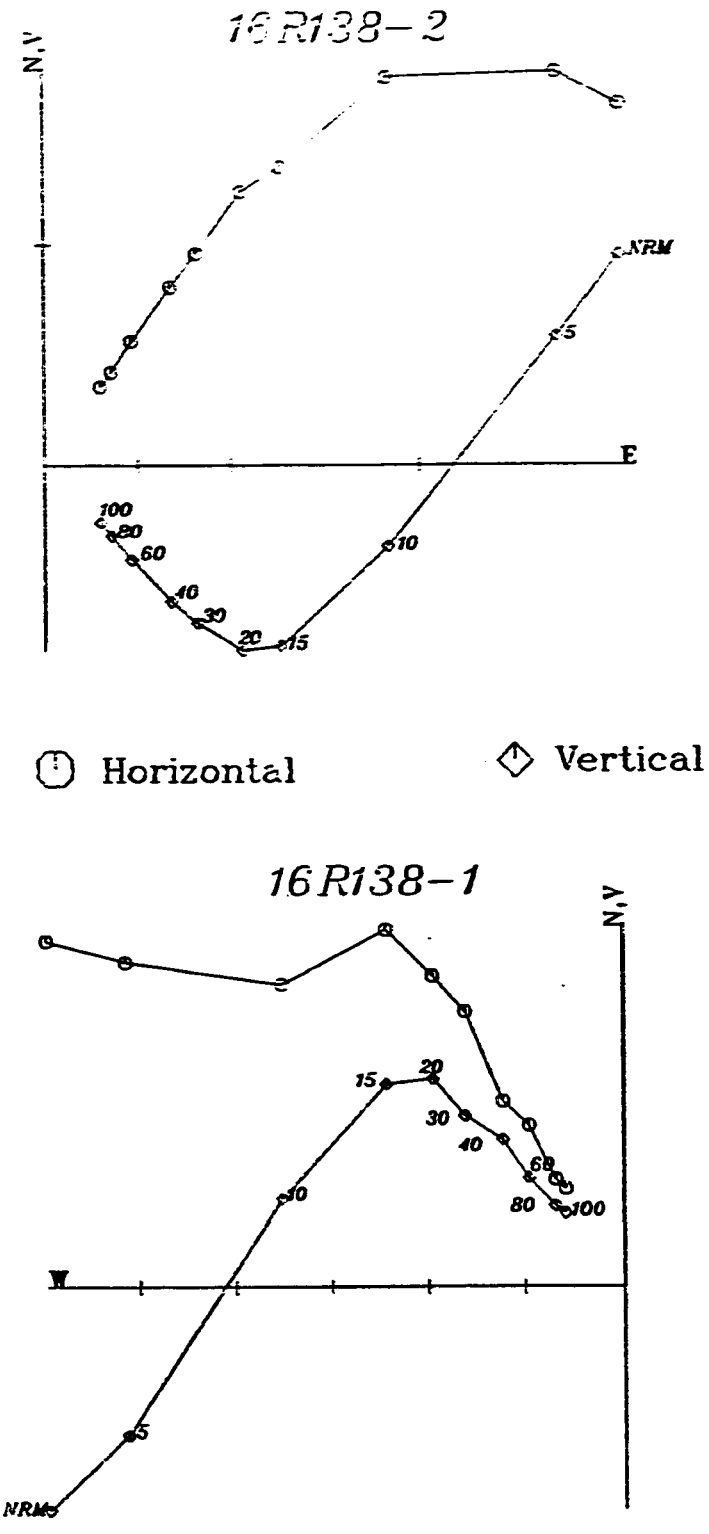

Figure 4.3 Type three: vector diagram representing the behavior of remanent magnetization during alternating field (a.f) demagnetization.

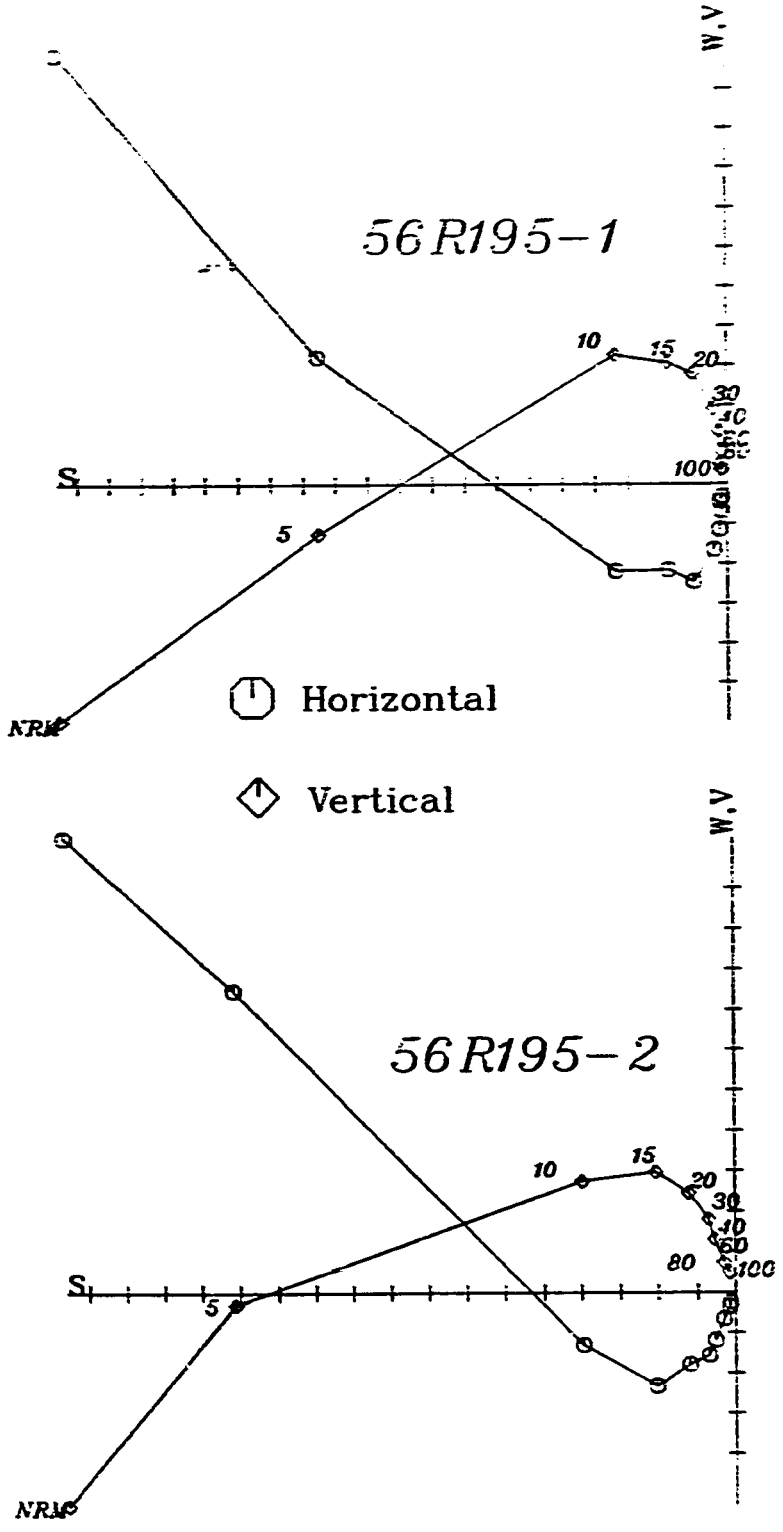

Figure 4.4 Type three:. vector diagrams representing the behavior of remanent magnetization during alternating fields (a.f) demagnetization.

demagnetization) suggests that the secondary components were successfully removed and the ChRM from each specimen was successfully isolated.

As in most paleomagnetic studies, we encountered specimens (from site Nos. 15 & 21, Th & Tw1) that grouped poorly despite magnetic cleaning. To deal with such situation objectively, we discarded the specimen direction that fell well outside the cluster defined by the remainder of the specimens of the same site.

Equal-area stereographic projection of mean directions for each of the sites used in this analysis are shown in Fig. 4.5. Eight sites are of normal polarity and fifteen have reversed polarity. A mean direction for normal sites was calculated by giving unit weight to each normal site mean and a mean direction for reversed sites was also calculated using the same method. These mean directions are also shown in the same Figure 4.5 along with the circles of 95% confidence interval.

It is well established that the earth's field has reversed its polarity many times in the geological past. Accordingly, a group of data in which the reversal is about 180 degree (antipodal) generally taken that the rocks involved have not acquired a magnetization since the time of the formation of the rocks. Therefore, a comparison of normal and reverse subsets is very useful as evidence of adequate magnetic cleaning, if the subsets are

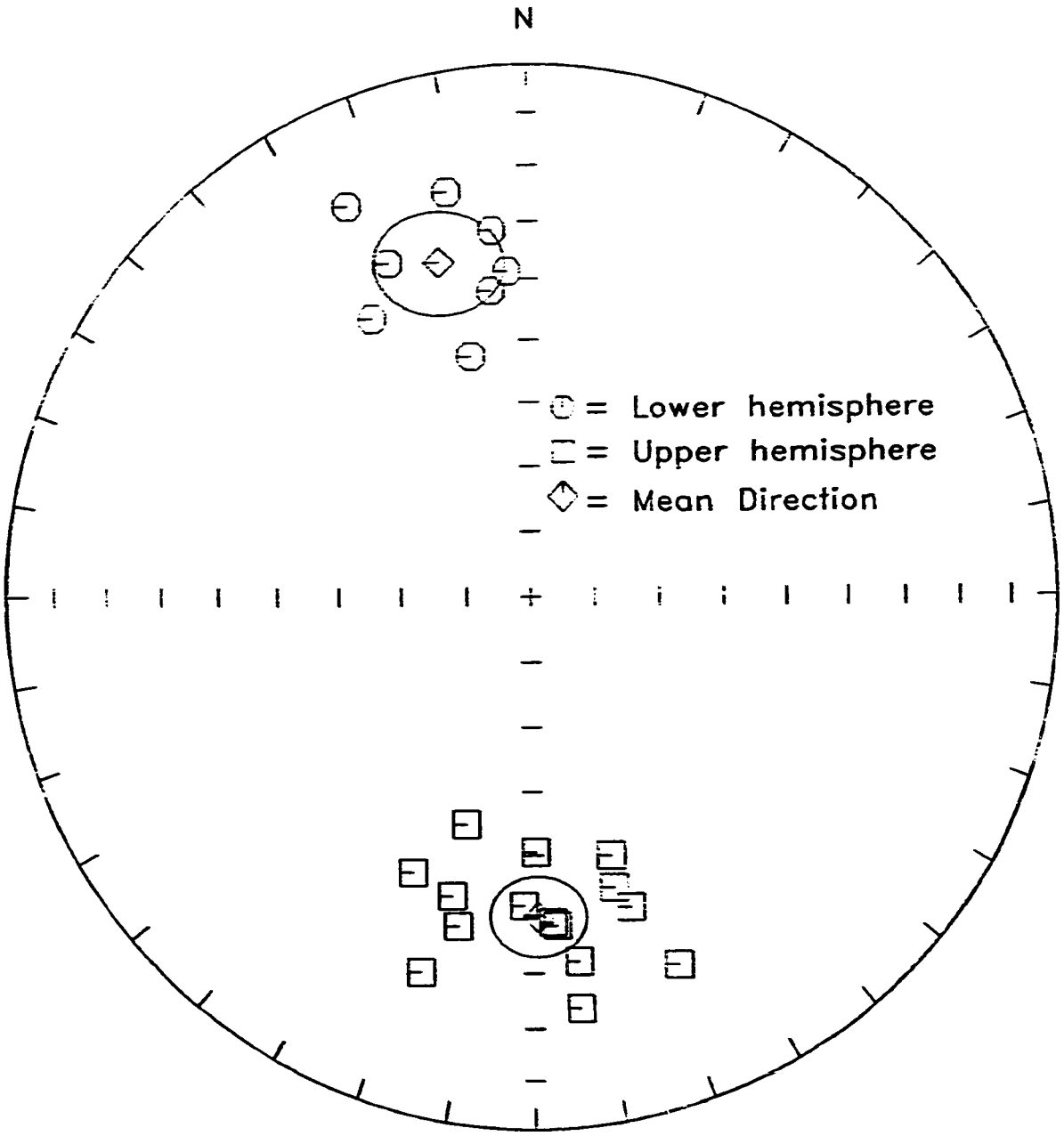

Figure 4.5 Equal–area stereographic projection of the site mean directions.
08 normal polarity sites
15 reversed polarity sites.

not antipodal, an un-remove secondary magnetization may be present. If secondary component exists in the rock sample, the effect would be to give an apparent reversal that was not exact antipodal. In our case, it is observed that the mean direction of normal and reversed are almost antipodal. Thus, it could be argued that all secondary component were removed by magnetic cleaning and the ChRM are that of primary. Mc Elhinny (1973) pointed out that the parallelism between tightly grouped mean directions of magnetization in two groups of sample which are reversely magnetized with respect to each other is a much stronger test than simple consistency of directions without reversal.

Having successfully removed the secondary components, we next compare two groups of directions on the basis of stratigraphic sequence, the first and the second group. The first group contains sites from all Madinah Basalt which consists of thirteen sampling sites and the second group consists of ten sampling sites form Hammah and Shawahit Basalts. This comparison (known as significance test) is necessary in order to establish if there are significant differences, which may be interpreted in terms of age differences. And also to see whether the data can statistically be combined to obtain an overall mean. If the confidence limits of two mean directions do not overlap, the directions are judged to be significantly different at that probability level. The test reveals that mean ChRM directions for the first

(Madinah) and second (Hammah & Shawahit) group are not significantly different form each other at the 95% probability (Fig. 4.6). Thus, it could be concluded from the test that the overall mean direction closely approximate the average direction of Late Pliocene to Pleistocene age. It seems, therefore, that the Shawahit basalts sampled in this study are from the upper parts of the flow sequence and are less than 3 Ma old.

The paleomagnetic results are summarized in Table 4.1. All the reverse directions were inverted 180 degrees, the results from 23 sites yields a mean paleomagnetic direction of
I = 38.52, D = 353.21 with $\alpha 95 = 5.42$ (Fig. 4.7).

Inversion of 180 degrees was made for all the reversed directions according to the geocentric axial dipole hypothesis which states that, if geomagnetic secular variation has been adequately sampled, the average position of the geomagnetic pole coincides with the rotation axis.

A paleomagnetic pole for:
-Al-Madinah is Lat = 86.36, Long. = 22.8, K = 25, A95 = 8.6, N = 10
-the Hammah & Shawahit is Lat = 85.3, Long. = 308, K = 24, A95 = 10.1, N = 13.

The calculated pole position for central Harrat Rahat lies at latitude 86.74 N and longitude 345.49 E.

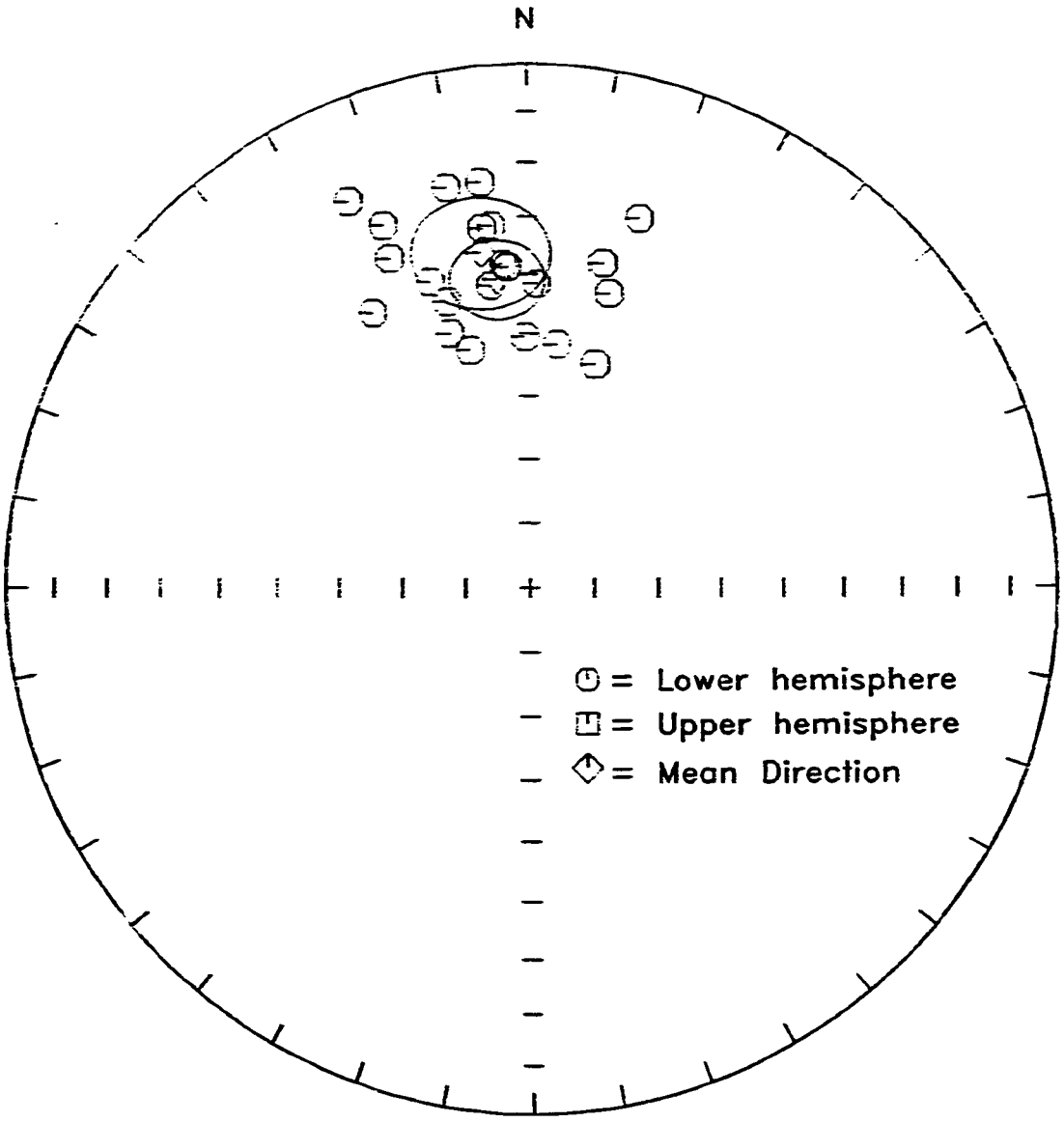

Figure 4.6 Equal-area stereographic porjection showing mean directions for the first and second group are not significantly different at 95% condidence level.

Table 4.1 Compilation of Paleomagnetic data.

Madinah Basalt.

Site	N	Im	Dm	R	k	a95	VGPs	
							Lat.	Long.
Site 1.2	5	43.10	23.90	3.90	3.60	33.20	68.15	120.46
Site 1.3	6	36.70	13.20	5.80	21.40	12.40	77.43	140.89
Site 1.4	5	41.60	1.70	4.90	53.20	8.60	88.31	107.39
Site 1.7	3	23.30	353.30	2.90	16.70	19.80	77.16	151.16
Site 4.2	7	41.50	15.50	6.70	19.60	12.00	75.74	123.16
Site 4.3	4	50.50	359.30	3.70	10.90	21.20	81.58	36.32
Site 5.1	3	38.80	342.20	2.80	10.60	22.70	73.52	308.44
Site 5.2	5	39.60	330.30	4.60	10.90	19.00	62.67	45.94
Site 5.3	4	41.60	352.80	3.70	8.70	23.80	83.36	42.81
Site 5.4	5	38.60	356.20	4.60	8.90	20.90	86.17	287.24
Site 5.5	5	32.40	337.10	5.00	152.00	5.10	67.84	299.45
Site 5.6	3	51.50	346.10	3.00	42.20	12.40	64.57	11.68
Site 5.7	6	31.30	354.20	5.60	12.40	16.20	81.72	262.12
All Sites	13	40.63	354.25	12.69	38.62	6.67	86.36	22.80

Hammah & Shawahit Basalts.

Site	N	Im	Dm	R	k	a95	VGPs	
							Lat.	Long.
Site 1.1	6	27.40	17.00	5.40	8.30	19.90	71.72	155.86
Site 1.5	3	26.51	338.10	2.40	3.40	43.80	67.27	289.77
Site 1.6	5	31.60	352.70	4.90	45.90	9.20	80.76	269.43
Site 2.1	2	53.40	16.70	1.90	10.88	29.19	71.65	89.70
Site 2.2	5	48.00	342.80	4.90	42.10	9.60	73.37	24.13
Site 2.3	5	42.80	344.10	5.00	159.80	5.00	75.33	38.61
Site 3.1	5	23.30	348.50	4.90	49.40	8.90	74.87	268.62
Site 3.2	3	38.70	356.40	2.90	18.50	18.80	86.57	297.07
Site 3.3	5	19.90	334.90	4.80	24.10	12.80	62.99	287.17
Site 4.1	3	38.10	355.70	2.90	25.30	16.10	85.77	291.57
All Sites	10	35.73	361.93	9.65	25.61	9.73	85.29	307.96
Mean, (Madinah,Hammah & Shawahit)	23	38.52	353.21	22.32	32.12	5.42	86.74	345.49

N..... : Number of samples or sites averaged.
Im.... : Inclination (mean) in degree.
Dm.... : Declination (mean) in degree.
R .... : Resultant vector.
k .... : Precision parameter estimate.
a95....: Radius of 95% confidence in degrees.
Lat....: Latitude degree North.
Long...: Longitude degree East.
VGP....: Virtual geomagnetic pole.
Mean directions are Fisherian averages of site mean directions.
Pole positions are obtined from Fisherian averages of VGPs.

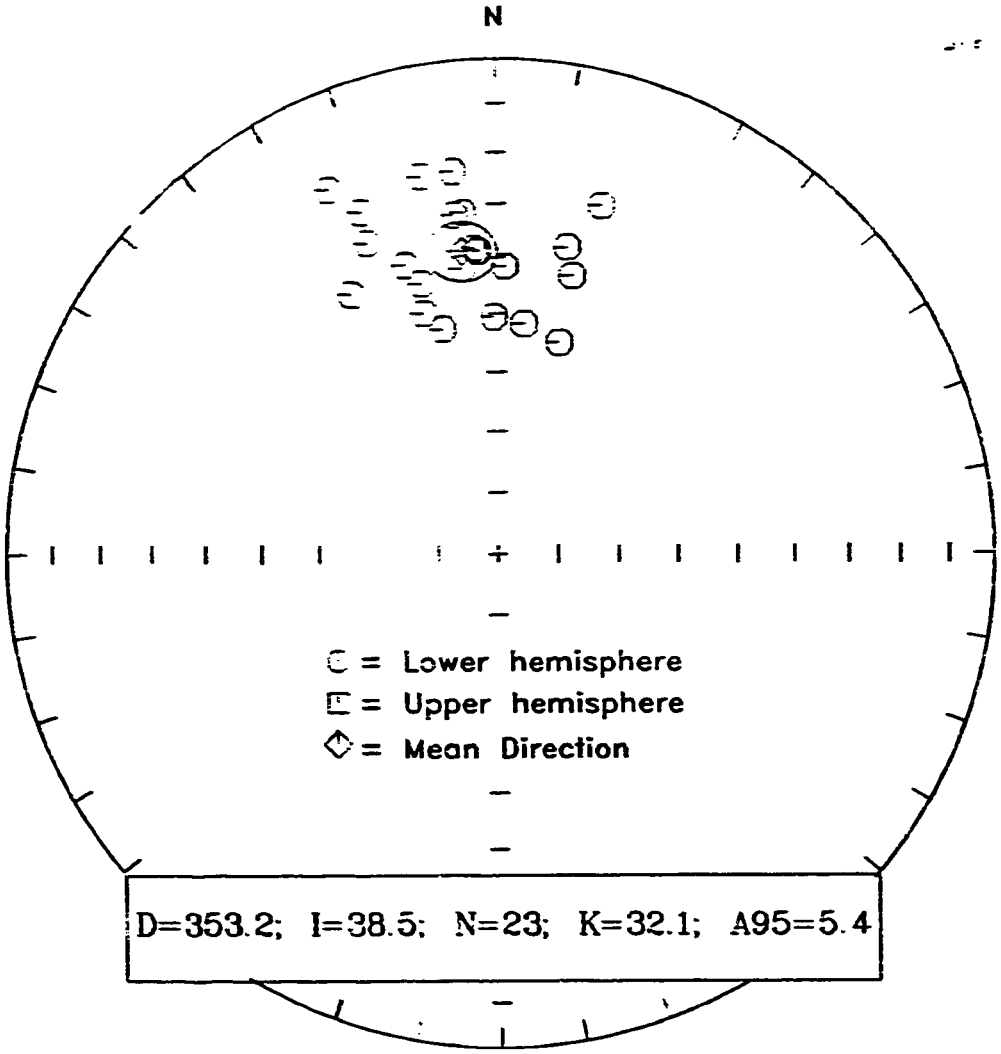

Figure 4.7 Equal-area stereographic projection of the site mean directions. (Reversed directions were inverted 180 degree).

4.1.3 Apparent Polar Wonder Path (APWP)

The paleomagnetic poles for the Arabian and African plates are compiled in Table 4.2. For comparison, the result from this study is also given in Table 4.2.

The pole generated by this study, together with other available pole for the Arabian plate were used to construct a preliminary apparent polar wonder path (APWP- plot of the sequential positions of paleomagnetic pole) for Arabia during the Tertiary (Eocene-Pliocene) and Quaternary (Pleistocene-Holocene) (Fig. 4.8). Both poles 4 and 5 on Fig. 4.8 are almost identical (not significantly different). This similarity of two poles suggests that little or no apparent polar wander path is observable during approximately 40 to 29 Ma ago. However, poles 4, 3, 2 and 1 on Fig. 4.8 are significantly diverged. The divergence of the apparent polar wonder path defines the essential evidence that the Arabia has changed its position during Neogene and Quaternary time. It seems very likely that this divergence could be the result of the opening of the Red Sea. This is reasonably agree with the existing work in the literature. It is reported that the Arabian plate separated form the African plate during two phases of sea floor spreading occurred that formed the Red Sea (Hall et al., 1977; Camp & Roobol 1991). The early phase was in the Late Oligocene, at about 30 Ma, and lasted until Early Miocene at

Table 4.2 Africa and Arabian Tertiary Paleomagnetic Poles

Rocks studied and regions	Pole position (Lat.N	Long. E)	a95	Reference
A. African Data				
1. Rift Valley Lavas Kenya & Tanzania				Reilly & others (1976)
0-1.8 Ma (Quaternary)	88.7	104.0	3	
1.8-7.0 Ma (Pliocene)	86.5	147.6	2	
11-13 Ma (Miocene)	86.5	186.6	6	
2. Haruj Assad Volcanics, Libya, (0.2 - 2.2 Ma)	84	169	7	Ade-Hall & others (1974)
3. Guinea Volcanics,				
Cameroon Gulf(Quaternary)	85	122	6	Piper &Richardson (1972)
Fernando Poo Gulf(Quat.)	85	189	4	
Sao Tome Gulf(Pliocene)	86	199	5	
4. Narosura & Magadi Volcanics, Kenya.				Patel & Raja (1979)
0.64 - 0.72 Ma	85	116	6	
1.60 - 6.90 Ma	84	297	4	
12.00 - 15 Ma	80	34	9	
5. Canary Islands & Madeira				Watkins (1973)
0 - 1.6 Ma	83	120	3	
1.6 - 5.1 Ma	82	125	4	
5.2 - 25 Ma	87	82	6	
6. Danakil Deprission, Ethiopia (Pliocene)	80	258	3	Schult (1974)
7. Jabal Soda, Libya				McElhinny (1977)
10.5 - 12.3 Ma	73.0	195.0	5.6	

Rocks studied and regions	Pole position (Lat.N	Long. E)	a95	Reference
8. Afars and Issas Volcanics Quaternary	81	260		Pouchan & Roche (1971)
9. Kapiti Phonolite, Kenya 12.9 -13.4 Ma	81	118	17	Patel & Gracci (1972)
10. Algerian Volcanics (Miocene)	88	154	2	Bobier & Robin (1969)
11. Ethiopian Plateau (Oligocene)	75	170	22	Schult (1975)
12. Ethiopian Traps (45+15 Ma)	87	253	11	McElhinny (1973)
13. Ethiopian Traps (45+15 Ma)	81	168	5	Brock & others (1970)
14. Garian Basalts and Phonolite, Libya (Miocene - Eocene)	86	152	4	Schult & Soffel (1973)
15. Oligocene Basalts, Egypt				Hussain & others (1976)
Abu Rawash	78.6	81		
Abu Zaa'bal	75.8	70.2		
16. Wadi Abu Teregwiya Basalts, Egypt				Hussain & others (1979)
(< Mid-Eocene)	69.4	189.4	5.8	
(< Upper-Eocene)	58.2	186.7	9.9	
17. Baharia Basalt Egypt, 16 Ma	62.2	206.0	16.3	"

Rocks studied and regions	Pole position (Lat.N	Long. E)	a95	Reference
B. Arabian Plate Pole				
1. Aden volcanics (5 Ma)	83.0	310.0	5	Tarling (1970)
2. Basalt, Jordan (<2 Ma)	73.8	241.3	4.9	Sallomy & Krs (1980)
3. Basalt, SW Harrat Rahat Saudi Arabia	80.0	310.4	3.9	Hussain & Bakor (1989)
4. Jabal Khariz Aden (10 Ma)	80	297	7	Tarling (1979)
5. As Sarat Volcanics Saudi Arabia.(24-29 Ma) Oligocene-Miocene	78.8	247.8	4	Kellogg & Reynolds (1980)
6. Tertiary & Cretaceous Western Saudi Arabia. Usfan Formation				Yousif & Beckmann (1981)
19 Ma	86.3	199.5	5.0	"
24 - 29 Ma	80.9	247.9	10.8	"
about 40 Ma	68.0	242.8	2.6	"
65 - 70 Ma	62.9	231.2	11.5	"
7. Al-Shumaysi Formation Oligocene?- Eocene	88.9	246.9	4.0	"
8. Centeral Harrat Rahat Pliocene - Pleistocene	86.74	345.49	6.19	This study

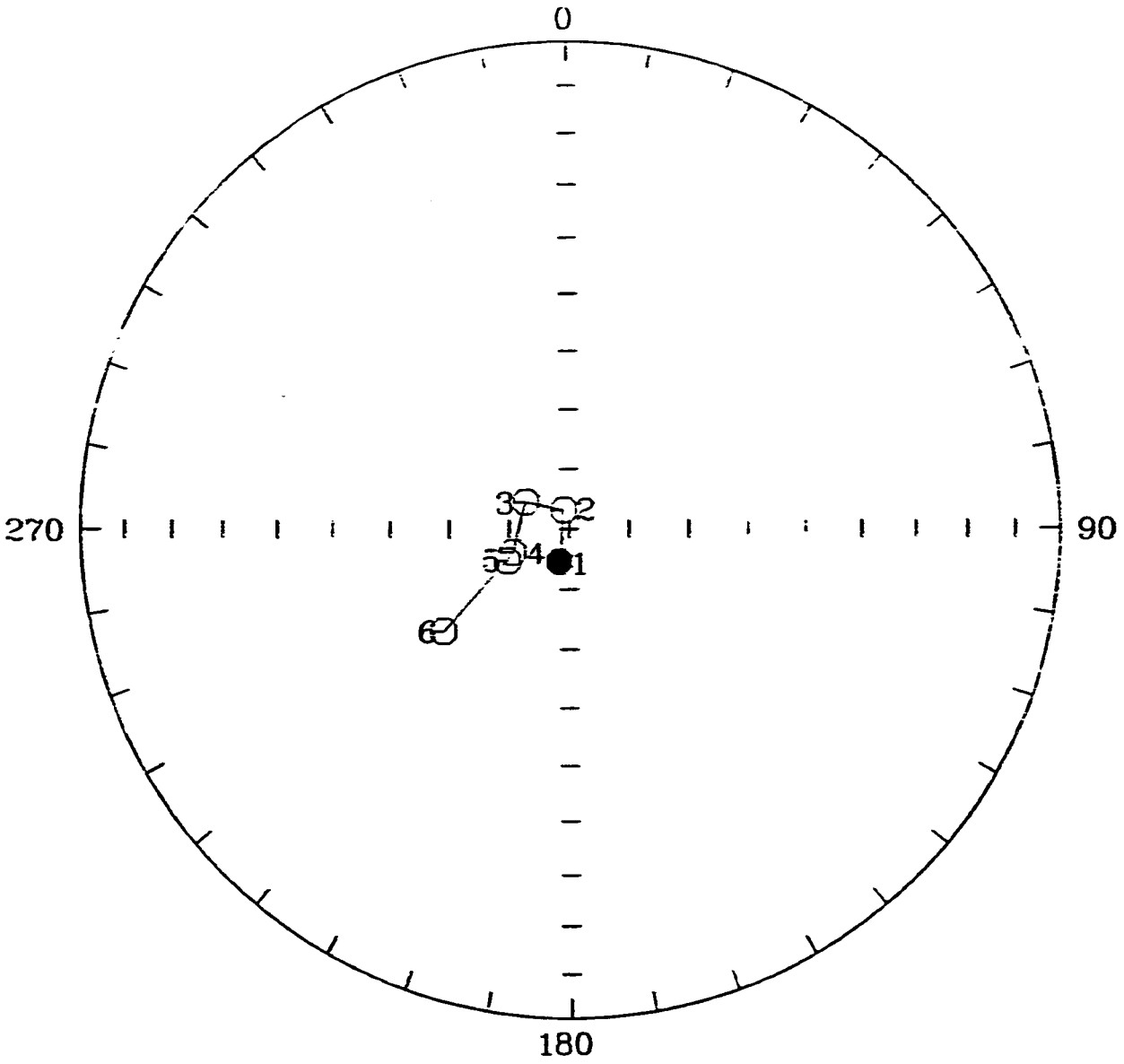

Figure 4.8 Cenozoic (APWP) Apparent polar wander path for Arabia.
1=Present Pole (April, 1993)
2=Pole generated by this study (~<3 Ma)
3=Late Miocene Pole (~5-10Ma)
4=Late Oligocene Pole (~24-29)
5=Early Late Miocene Pole (~40 Ma)
6=Early Paleocene (~65 Ma)

about 15 Ma: and the final phase was in the Pliocene at about 4.5 Ma to the present. However, the available paleomagnetic data are not adequate to explain the details of opening of the Red Sea (determining the timing and amount of Red Sea rifting) by paleomagnetic means. This problem will only be resolved when more and more paleomagnetic results from carefully dated rocks become available.

4.2 PALEO-INTENSITY MEASUREMENTS

4.2.1 Introduction

Paleo-intensity study provides important information about the time variation of the intensity of the geomagnetic field. This information contributes to the knowledge of geomagnetic variation and constitutes a valuable input for those researchers constructing models of the generation of the geomagnetic field. The number of paleo-intensities determined are still very few, and almost no intensity determination has yet been done in Saudi Arabia. The reason is that in paleo-intensity experiments, rock samples are subjected to several heating and cooling cycle up to their Curie point (approx. 600° C). Frequently, these rocks undergo irreversible alterations that affect the chemical composition, texture, size and shape of their magnetic minerals. Such changes make the

experiments more difficult to perform and render their results unreliable. Moreover, these experiments are extremely time consuming, one also needs to investigate the relationship between the ideal behavior of rock samples in these experiments and their opaque mineralogy.

Several methods for paleo-intensity determinations have been proposed (Thellier, 1938; Thellier and Thellier,1959; Wilson,1961; Van Zijl et al.,1962; Carmichael, 1967; Shaw,1974). All these methods are similar in principle. Some of which have the advantage of being considerably less time consuming and others were designed to avoid repeated heating. Yet, these methods do not seem to provide a generally better alternative for the Thelliers' method which is now considered to be the standard method for the determination of the ancient geomagnetic field intensities from rocks.

Coe and Gromme (1973) compared three of the more common paleo-intensity methods in their study of historic lava that erupted in known fields. They concluded that the Thellier method yields the most reliable results. Salis et al. (1989) also suggested that Thelliers' method appears to be the most reliable for paleo-intensity determination of volcanic rocks. Moreover, Abokhodair and Shebl (1989) suggest a new approach for the determination of paleo-intensity by the Thelliers' method which could provide a more

direct means to detect the effect of alterations and judge the reliability of paleo-intensity.

In principle paleo-intensity measurement is simple. Samples of basaltic lavas, having cooled from temperature above their Curie point in the geomagnetic field acquire a TRM proportional to the intensity of the ambient magnetic field in which they cooled. In order to measure the field one need to heat the sample to a temperature above its Curie point, cool it in a known field, and compare its new TRM to its NRM.

4.2.2 The Thellier - Thellier Method

The principle on which the Thelliers' method rests is the law of additivity of partial thermo-remanent magnetization (PTRM) which states that the partial thermo-remanent magnetization (PTRM) acquire in any given temperature interval is independent of that acquired in other temperature intervals. Therefore, each PTRM preserves information about the intensity independent of the rest of the TRM so that one can make several estimates of the intensity. The sum of the PTRM's acquired separately over adjacent temperature subranges is equal to the total TRM acquired all at once over the entire range. That is,

$$J(T_n,T_{n-1}) + \ldots\ldots J(T_3,T_2) + J(T_2,T_1) = J(T_n,T_1)$$

for

$T_c > T_n > T_{n-1} > \_\_\_\_ > T_3 > T_2 > T_1 > T_r$

where $J(T_i,T_{i-1})$ is the TRM gained by cooling from T_i to T_{i-1},T_c is the Curie temperature and Tr is room temperature.

If the NRM of a rock is entirely original TRM, and the TRM spectrum (distribution of TRM with temperature) remains unchanged, comparison of the NRM($J_N = J_n(T_c,T_r)$) and the TRM($J_A = J_a(T_c,T_r)$) produced artificially in the laboratory by a field Fa determines the magnitude of the earth's field Fe at the time and place the rock cooled. When the TRM is linear with field, the relation is : $(J_n/J_a = F_e/F_a)$ - - - - - - - - (1)

This equation was first used by Koenigsberger in 1938.

However, the low-temperature part of the NRM may contain secondary magnetization and changes in the TRM spectrum commonly occur during the heating. That is why the condition required for the equation (1) to get a true measure of the paleo-intensity is not obtained. Thellier's method is design to detect whether the requisite conditions are met and is superior to (1) for rocks in which the additivity law of PTRM is valid.

In this study, paleo-intensity measurements were made using modified Thellier - Thellier (1959) method. Specimens were heated progressively in a series of temperature steps from 30 degree to 600

degree C. Each step consisted of two heatings and coolings, each lasting about two to six hours , to the same temperature, the longer times corresponding to the higher temperature steps. The first heating and cooling was done in zero field; the second heating and cooling was in an applied field of 0.5 Oe. The remanence was measured after each cooling.

In our experiment, the modified Thelliers' method was used. The experimental procedure consists of the following step:

a) The intensity and direction of the NRM vector, J_N is measured at Tr (room temperature).

b) The specimens were heated to Ti > Tr and cooled back to Tr in the absence of a magnetic field (zero field), and the remaining magnetization NRM vector, Dn(Ti,Tr), is measured at Tr.

c) The specimens were reheated to Ti > Tr and cooled back to Tr in a known magnetic field Fa (applied field), which is continuously present throughout the cooling cycle. The magnetization is measured at Tr to obtain the PTRM acquired between Ti and Tr.

$$J(T_i,T_r)=D_n(T_i,T_r)+J_a(T_i,T_r)------(2)$$

where J_a is the PTRM acquired in the temperature interval (T_i,T_r) and in the applied field F_a.

Steps b) and c) are repeated at successively higher temperature until Tc is reached that is the entire NRM has been exhausted.

Ja(Ti,Tr) is obtained by using the vector equation (2). Robert S Coe (1967) pointed out that a rocks behave ideally in the Thelliers' method if Dn(Ti,Tr) and Ja(Ti,Tr) satisfy the linear relation:

$$D_n(T_i,T_r)=J_N-(F_e\ F_a)J_a(T_i,T_r) \text{ - - - - - - - - - (3)}$$

The data for paleo-intensity determination is expressively plotted in the diagrams known as Arai diagram. The Dn versus Ja for each Ti generated for each specimen is plotted in cartesian coordinates in order to get the NRM-TRM curves which are complied in Appendix (B). To have an additional control over the paleo-intensity determination, the evolution of NRM vector during thermal demagnetization, using vector diagrams were studied. Such vector diagrams are shown in Appendix C.

4.2.3 Data and Results

Ninety two NRM-TRM curve (Arai diagrams) and Vector diagrams were drawn for the samples selected for this study, which were form seven different lithostratigraphic units. The majority of NRM-TRM curves deviated from a straight line so much that even a rough estimate of paleo-intensity cannot be made. Coe (1967a; 1967b) discusses the factors or mechanisms which change the NRM-TRM curve from straight line of interest (which cause non-ideal behavior in Thellier's method) in great details. Some of the

many possible causes of such non-ideal behavior include

1. The effect of changes in the original NRM due to the addition of secondary components of magnetization.

2. The effect of non-linearity on the acquisition of TRM . (the original NRM and artificial TRM are not acquired linearly with the applied field).

3. The effect of changes in the state of magnetic interaction in the rock since acquisition of original NRM.

4. The effect of sample self-demagnetization field on the remanence inducing field inside the sample.

5. The effect of the cooling rate on the acquisition of TRM.

6. The effect of changes in the TRM blocking temperature spectrum induced by repeated heating in the laboratory, or the effect of physio-chemical changes in their mineralogy from the time they acquire their NRM to the time of NRM measurement and production of TRM in the laboratory.

Therefore, the first step is to identify which non-ideal mechanisms are operative in each specimen from the shape of the NRM-TRM curves. And then to evaluate their effects so that a reliable paleo-intensity can be obtained.

Consequently, to obtain the paleo-intensity, first the straight line that best fit the data points by the method of least squares was determined. The paleo-intensity values were then calculated from

the relation: $F = - bF_a$

where F_a laboratory field used in the production of artificial TRM and b is the slope of the best-fit line.

4.3 OPAQUE MINERALOGY

In this section, a brief account is given of the minerals of main importance in this study and of their magnetic properties which are necessary background for interpreting the magnetic behavior of rock specimens.

4.3.1 Crystal Chemistry and Magnetism

Ferromagnetic substances in rocks (such as metallic iron and many other iron minerals) carry the information about the paleomagnetic field of the earth, and hence are the most important constituents of rocks in their study for paleomagnetic measurements. In ferromagnetic substances, there is an interaction between the spin magnetic moment in nearby atoms that tend to align in parallel orientation, allowing it to have a magnetization referred to as the spontaneous magnetization, even in the absence of external magnetic field. Spontaneous magnetization is temperature dependent, decreasing with increasing temperature and disappearing at the curie point (Collinson, 1983).

When considering the magnetic minerals we are far more interested in the special type of ferromagnet which characterizes the titanomagnetite series. The titanomagnetite minerals are usually represented by the general formula xFe_2TiO_4 $(1-x)xFe_3O_4$, where x is the mole fraction of ulvospinel in magnetite. This series consists of solid solution or intergrowths of different compositions of the end members, magnetite and ulvospinel. Complete solid solution of magnetite and ulvospinel occurs above 600° C and below this temperature a varying degree of exsolution takes place resulting in a structure of intergrown lamellae. Magnetite-rich to approximately equi-molecular compositions are important as the carriers of NRM in igneous rocks.

The curie temperature decreases almost linearly with increasing x, from 578° for $x=0$ to $-153°$ C for ulvospinel ($x=1$). At $x=0.8$, the curie point is at room temperature. The spontaneous magnetization at room temperature decreases linearly with increasing x, from 90-93 emu gm for pure magnetite to 0 for pure ulvospinel.

Magnetite is a cubic mineral with an inverse spinel mineral structure that has 24 iron ions in one unit cell. Eight are in one group (group A) and have their spins moment aligned in parallel directions. The other 16 (group B) are also parallel to each other. However, group B of iron ions are aligned in opposition to the

group A of ions. The result is that only 8 out of 24 iron ions present actually contribute to the overall properties of magnetite. It is a dark black mineral that is optically isotropic in polished section with a reflectivity of approximately 21%. Magnetite has a Curie temperature of 578° C, when cooled from temperatures above its Curie point in the presence of a magnetic field, it acquires a TRM (Strangway, 1970).

Ulvospinel is the other end member of the titanomagnetite series. The structure of ulvospinel is similar to that of magnetite, except that one of the iron ions is replaced by titanium. The result is that the substance is no longer ferromagnetic but behave like an anti-ferromagnetic material, since there are equal numbers of iron ions on the two sublattices. Ulvospinel is optically isotropic, with a reflectivity slightly less than that of magnetite.

Ilmenite is a rhombohedral mineral and very common in igneous rocks. With slower cooling of titanium-bearing magnetite, the titanium exsolves from the solid solution as ilmenite. This may occur in two forms: first, as discrete crystals or aggregates of ilmenite grains at the margins of the magnetite, and second, as laths in the octahedral (111) planes of the magnetite forming a highly characteristic intergrowth where cooling has been more rapid. Although ilmenite does not play an important role in determining the natural magnetization, it has one important

function in the study; that is to break up larger magnetite grains into smaller ones. In volcanic rocks, the content of titanium is usually high and the iron-titanium oxide minerals formed are in a mixture form of magnetite and ulvospinel. As cooling proceeds, ulvospinel becomes mineralogically unstable and tends to oxidize to form ilmenite and magnetite. Since ilmenite is rhombohedral and is structurally incompatible with the magnetite, an intimate intergrowth of magnetite and ilmenite forms. This material can easily be identified in reflected light. The effect of this is to create a great magnetic stability in the magnetite.

4.3.2 Ore Microscopic Study

In order to understand the mineralogy of the magnetic behavior of samples, polished-sections were prepared for microscopic study. These represent each litho-stratigraphic unit of the Harrat Rahat lava flows and were taken from the same core fragments used for Paleo-intensity determination. Microscopic examination was made in oil immersion at different magnifications (x 20 to x 100) by using a Carl Zeiss D-7082 Oberkochen transmitted and reflected light research microscope. The opaque minerals observed are mainly more or less equi-dimensional titanomagnetite grains and slender elongated laths of ilmenite (Plate 2.A)

These phases of titanomagnetite and ilmenite were identified from every single lava flow sequence examined in the present study.

Plates 1-3 show reflected light photomicrographs of selected samples chosen to show progressive stages of oxidation of titanomagnetite from low to high temperature.

The oxidation stages used in this research are those of Wilson & Watkins (1967) who divided such stages into six progressive classes as follows:

1. Titanomagnetite with no ilmenite exsolution.
2. Titanomagnetite with one or more exsolved ilmenite lamellae in some parts of the grain.
3. Titanomagnetite with abundant oxidation-exsolution lamellae of ilmenite.
4. The sharp, well-defined ilmenite lamellae of class 3 become mottled and distinctly lighter in color, and shows signs of incipient alteration to titanohematite.
5. With increasing oxidation the products become more coarsely crystalline. The characteristic mineral phase at this stage is rutile. Both the ilmenite and the titanomagnetite are oxidized to oriented intergrowths of rutile in a host of titanohematite. Relic areas of titanomagnetite may still persist, and in these cases contain exsolution rods of alumino-spinels.
6. The maximum degree of oxidation is characterized by the high temperature (> 585° C) index mineral pseudo-brookite. The oxidation of titanomagnetite to titanomaghemite may be

Plate 1–3: Reflected light photomicrographs.

Plate 1.A: A titanomagnetite grain containing few pale laths of ilmenite.
(sample No. 13R112 / Madinah)

Plate 1.B: Ilmenite associated with titanomagnetite subdivided by exsolution lamellae of second phase ilmenite set along planes of the titanomagnetite host.
(sample No. 15R137 / Hammah)

Plate 2.A: Whitened hetrogeneous lamellae (I) of "metailmenite" in a titanomagnetite (M) host (Partially crossed polars).
(sample No. 33R068 / Shawahit)

Plate 2.B: Rhombohedral and triangular areas of titanomagnetite (M) which is in the process of being altered to titanohematite (H). The original ilmenite lamella has been transformed first to metailmenite and then to titanohematite.
(sample No. 03R068 / Shawahit)

Plate 3.A: A grain of titanomagnetite with trellis texture of ilmenite lamellea.
(sample No. 16R151 / Hammah)

Plate 3.B: Myrmekitic texture of hematite at the boundary of titanomagnetite grain.
(sample No. 11R004 / Shawahit)

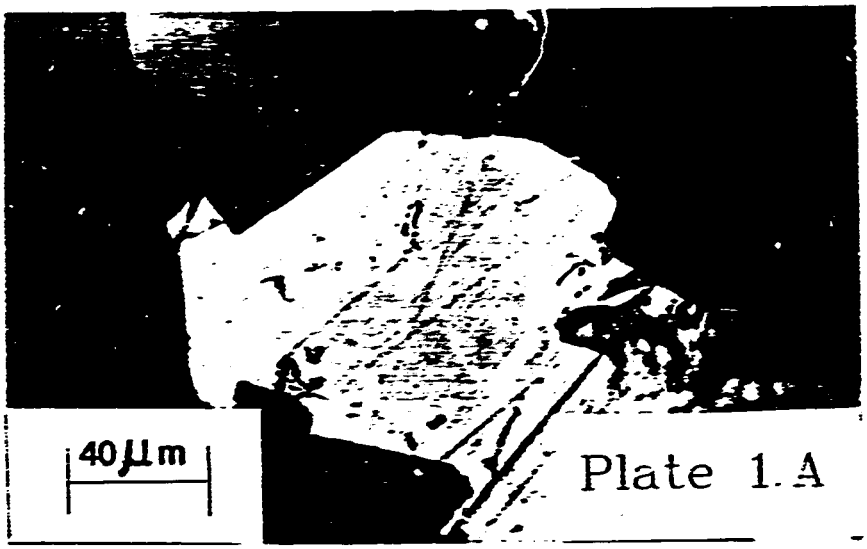

Plate 1.A

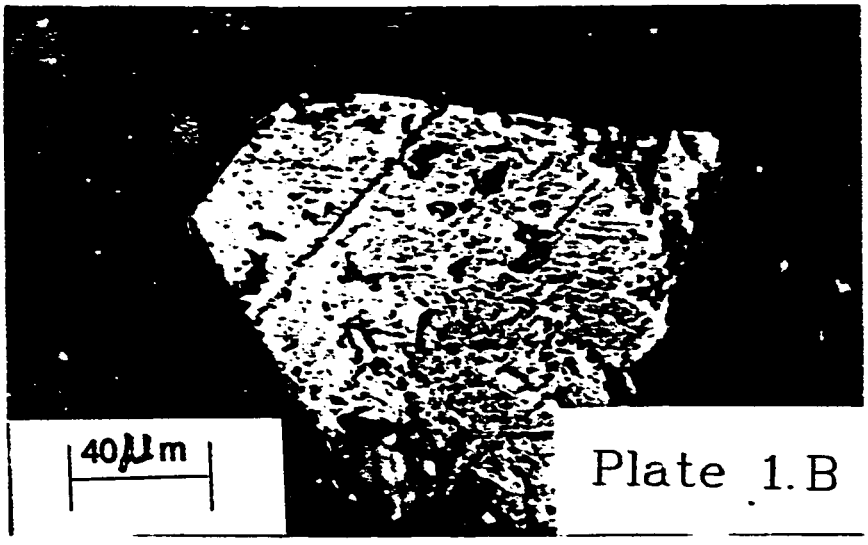

Plate 1.B

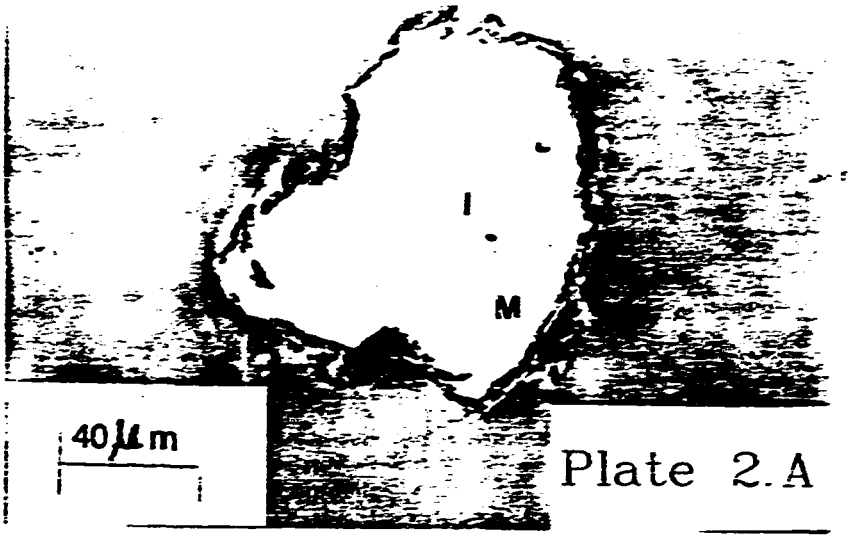

Plate 2.A

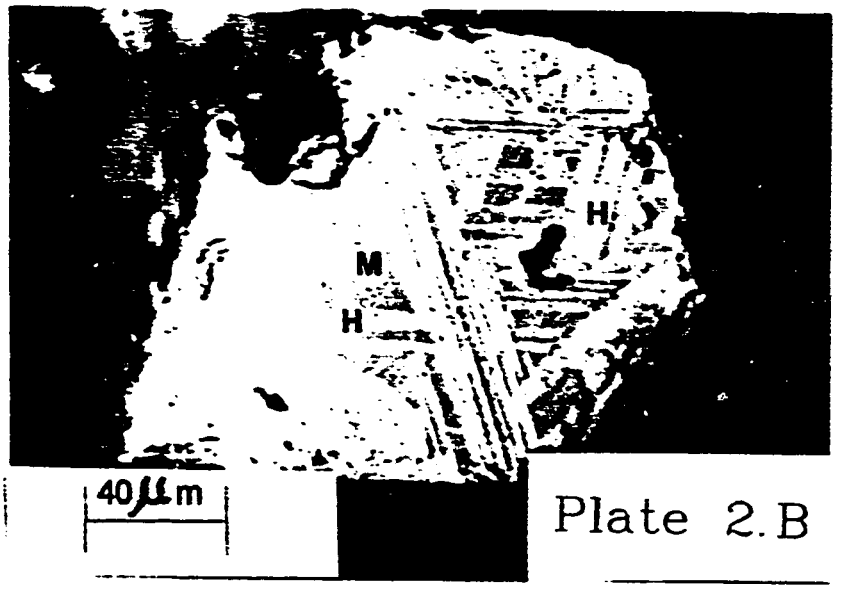

Plate 2.B

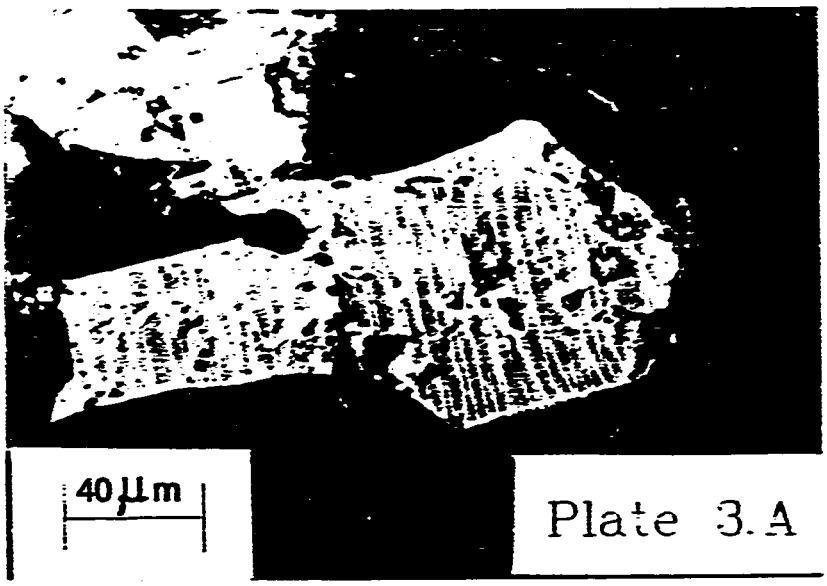

Plate 3.A

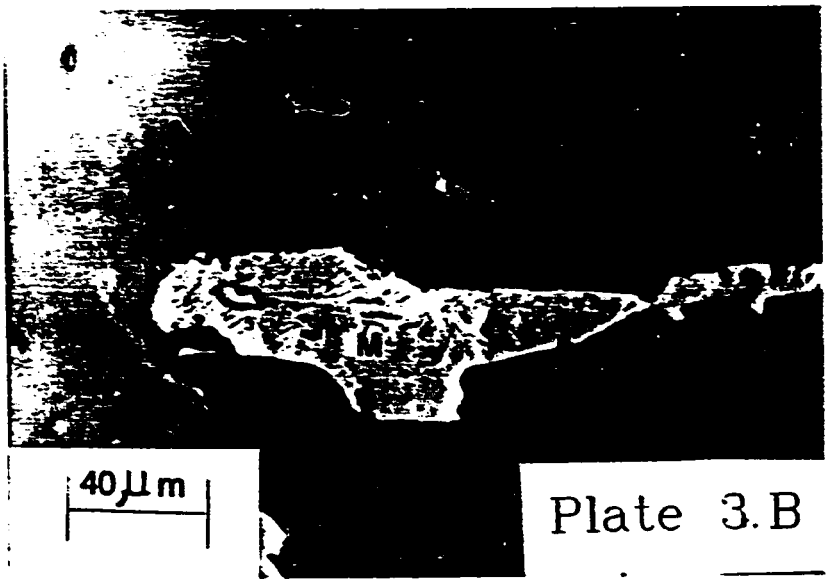

Plate 3.B

superimposed on the high temperature oxidation sequence, but is restricted to homogeneous titanomagnetite or titanomagnetite containing exsolution lamellae of ilmenite. Maghemite inverts to hematite between 590 and 650° C. The oxidation of magnetite to maghemite has been reported to take place at temperatures as low as 200° C. many also form at a lower temperature as weathering product.

Samples from the Madinah Basalt contain homogeneous titanomagnetite and a single or a few lamellae of ilmenite, indicating the class 2 stage of oxidation (Plate I.A). Most of these titanomagnetite grains are relatively smaller in size than those of Shawahit Basalts grain which contain visible grains that range from 20 to 100 micrometer. Their isotropic nature and gray colors with varying light brownish tints suggest that they are titanomagnetite. Ilmenite intergrowths are very rare in these samples and occur only in a few large grains where one or two lamellae of ilmenite are seen in the photomicrographs. The sample numbers 12R100; 54R085; 55R190 & 57R198, all of which are from the Madinah Basalts show no sign of ilmenite intergrowths in the titanomagnetite grains.

Samples from the Hammah Basalt contain titanomagnetite with abundant oxidation-exsolution lamellae of ilmenite, indicating the class 3 stage of temperature oxidation (Plate I.B & 3.A). The grains

are mostly subhedral to euhedral (rhombohedral) with abundant voids in it. The grain size are different from one sample to another. Ilmenite intergrowth are quite common in the titanomagnetite grains of these samples. Exsolution intergrowths are abundant in the large euhedral grains consisting two or three sets of approximately 2 micrometer lamellae of ilmenite in the plane of host titanomagnetite (Plate 1.B).

In one of the polished sections (sample # 16R151) from Hammah, grains of titanomagnetite with the trellis texture of ilmenite lamellae were observed. The trellis texture consists of two sets of numerous thin lamellae of unaltered ilmenite oriented in different planes of titanomagnetite. (Plate 3.A).

Samples from the Shawahit Basalt contain relatively large sized grains of titanomagnetite. The gray color with light brownish pink tint, the isotropic nature and the low to moderate reflectivity of these grains suggest a high content of unexsolved Ti in titanomagnetite. Exsolution intergrowths are very abundant and oxidation to meta-hematite at the boundaries of the crystals are observed in some of the polished sections. Hematite appears white in comparison with magnetite or ilmenite and it is strongly anisotropic. Texturally, ilmenite occurs as fine lamellae, thick laths, or as an irregular composite form in titanomagnetite. Sometimes, all forms can be present in a single titanomagnetite

grain. In most samples from the Shawahit Basalt. (e.g samples Nos. 11R004; 33R058; 33R066) the sharp. well defined ilmenite lamellae of titanomagnetite become mottled and distinctly lighter in color. and hence one cannot identify individual mineral phases because of the submicroscopic and heterogeneous nature of the inversion products. According to Watkin & Haggerty (1967) it has been termed 'meta-ilmenite'. indicating the class 4 stage of oxidation (Plate 2.A). The distinctive penetration or interfingering texture known as Myrmekitic texture of hematite at the boundary of titanomagnetite grain with iddingsite (alter olivine) was observed in one of the samples (11R004) from the Shawahit Basalts (Plate 3.B).

CHAPTER 5

CONCLUSIONS AND RECOMMENDATIONS

The determined pole position for the Pliocene-Pleistocene lies at latitude 86.74° N and longitude 345.49° E with α95 of 6.1.

In the light of the foregoing observations it is concluded that the magnetization was acquired at the time of the rocks formed and that the mean magnetization direction approximate the direction of a geocentric axial dipole field. Therefore, This paleomagnetic pole is considered reliable.

1. Both normal and reversed polarities are observed and their respective mean directions are more or less antipodal (Fig. 4.5). This shows that secular variation has been averaged out and secondary components have successfully been removed.
2. The comparison of cleaned directions (ChRM) obtained by AF (alternating field) and thermal demagnetization are consistent (not significantly different) for the same site. This suggests that the secondary components were removed.
3. The mean directions do not differ significantly from site to site, which indicates the observed mean directions are a record of the remanence at the time of cooling.
4. The number of site-mean VGPs used (23) to calculate a paleomagnetic pole is well above the requirement for reasonable

averaging of geomagnetic secular variations and for estimating dispersion of site-mean. (It is commonly agreed that the number of site-mean VGPs should be 10).

5. The number of samples used are adequate enough to average out orientation and experimental errors and has improved the precision of the mean site remanence direction.

It is suggested that more and more paleomagnetic studies from carefully dated rocks from Cenozoic volcanic flows are needed to be carried out to establish a reliable Cenozoic pole for Arabia. Such a pole is essential for determining the timing and amount of Red Sea rifting and also improve resolution of the rotational history of Arabia with respect to Africa.

A total of ninety two NRM-TRM curve (Arai diagrams) and Vector diagrams were drawn for the samples selected for paleo-intensity study, which were form seven different lithostratigraphic units. The majority of NRM-TRM curves deviated from a straight line so much that even a rough estimate of paleo-intensity could not be made.

In Paleo-intensity experiment, it would be of great practical importance to develop a set of petrological, mineralogical and magnetic criteria to aid in the selection of specimens suitable for the experiment. Specimens should be selected to have NRMs with minimum secondary remanence components. Preferentially, specimens to have more oxidized titanomagnetite minerals because such specimens are less susceptible to

further physio-chemical changes during laboratory heating. In paleo-intensity experiment, if non-ideal behavior is observed (as in our case), it is not sufficient to assume that the non-ideal behavior is due to chemical or mineral alteration of the specimen. Further experiments should be conducted to determine its sources. It would also be desirable to examine polished section from each specimen before and after the experiment so that comparison of the opaque minerals before and after heating could reveal the relationship between the ideal behavior of rock specimens and their opaque mineralogy.

REFERENCES

Ade-Hall, J.M.; Reynolds, P.H.; Dagley, P.; Musset, A.E; Hubbard, T.P and Klitzsch, E. (1974): Geophysical studies of North Africa Cenozoic volcanic areas I: Haruj Assuad. Libya. Canadian Jour. of Earth Sciences. v.11. p. 998-1000.

Abokhodair, A.A and Shebl, H.T. (1989): Paleo-intensity by Thelliers' Technique: A New Reliability Criterion. J.K.A.U. Earth Sci. vol 3. Special Issue 1st Saudi Symp. on Earth Sci., Jeddah, 1989.

Banerjee, S. K. (1989): Physics of Rock Magnetism. Geomagnetism Vol. 3 Edited by J.A. Jacobs. p.1-30. Academic Press. Harcourt Brace Jovanovich. Publishers London.

Basahel, M.H. (1981): A paleomagnetic study of the Shumaysi formation. M.S thesis, Faculty of Earth Sciences. King Abdulaziz University , Jeddah, Saudi Arabia.

Blakely, R.J. (1987): Geomagnetism and Paleomagnetism. Reviews of Geophysics, v.25, No. 5. p.895-899. June 1987.

Bobier, C., & Robin, C., (1969): Etude paleomagnetique du massif eruptif de Cavallo (nord-Constantinois. Algerie). Comptes Rendus de l'Academie des Sciences de Paris, v. 269, ser. D. p. 134-137.

Brock, A., Gibson, I.L., & Gracci, P. (1970): The paleomagnetism of the Ethiopian flood basalt succession near Addis Ababa. Geophy.

Journal of the Royal Astro. Soc. v.19. p.485-494.

Camp. V.E., Roobol. M.J., and Hooper. P.R.(1991): The Arabian continental alkali basalt province: Part II. Evolution of Harrats Khaybar, Ithnayn, and Kura. Kingdom of Saudi Arabia. Geological Society of America Bulletin. v. 103. p.363-391.25 figs., 5 tables. March 1991.

Camp. V.E., and Roobol. M.J. (1987): Geologic map of the Cenozoic lava field of Harrat Rahat. Saudi Arabian Deputy Ministry for Mineral Resources Geoscience Open-file report DGMR-OF-07-9.

Coe.R.S. (1967a): Paleo-intensities of the Earth's magnetic field determined from Tertiary and quaternary Rocks. J. Geophys. Res., 72. 3247-3262.

Coe.R.S. (1967): The determination of Paleo-intensities of the Earth's magnetic field with emphasis on mechanisms which could cause non-ideal behavior in Thellier's method. J.Geomagn. Geoelectr.,19. 157-535.

Coleman. R.G., Gregory. R.T., and Brown. G.F., (1983): Cenozoic volcanic rocks of Saudi Arabia. Saudi Arabian Deputy Ministry Mineral Resources Open-file report USGS-OF-03-93. 82p.

Collinson. D.W. (1983): Methods in Rock Magnetism and Paleomagnetism Techniques and Instrumentation. Chapman and

Hall. 503p.

Dunlop, D.J., (1979): On the use of Zijiderveld vector diagrams in multicomponent paleomagnetic studies. Phys. Earth Planet. Intererior. 20 (1979) p. 12-24.

Hailwood, E.A. (1989): Magnetostratigraphy. Geological Society Special Report No.19. Blackwell Scientific Publications. 84p.

Hailwood, E.A. (1975): The Paleomagnetism of Triassic and Cretaceous Rocks from Morocco. Geophys. J. R. Soc. v.41. p.219-235.

Hussain, A.G., Schulta, A., Soffel, H. & Fahim, M., (1976): Magnetization and paleomagnetism of Abu Zaabal and Abu Rawash basalts. Egypt. Helw. Instr. Geophys. Bull., 134, 1-15.

Hussain, A.G., Schulta, A. & Soffel H. (1979): Paleomagnetism of the basalt of Wadi Abu Tereifiya, Mandisha and dioritic dykes of Wadi Abu Tereifiya, Mandisha and dioritic dykes of Wadi Abu Shihat, Egypt. Geophys. J. R. ast. Soc., 56, 55-61.

Hussain, A.G. and Bakor, A.R.(1989): Petrography and Paleomagnetism of the Basalts, southwest Harrat Rahat, Saudi Arabia. Geophys. J. Int. v.99, p.687-698.

Irving, E. (1964): Paleomagnetism and its Applications to Geological and Geophysical Problems. John Wiley & Sons Inc., New York, 399p.

Kellogg, K.S., and R.L. Reynolds (1980): Paleomagnetic Study of the As Sarat Volcanic Fields, Southwestern Saudi Arabia. Open File Report U.S.G.S. -OF- 02-65.

Kellogg, K.S and Beckmann, G.E.J.(1981): Paleomagnetic Investigations of Upper Proterozoic Rocks in the Eastern Arabian Shield, Saudi Arabia. Open File Report 81-675 (IR) SA-36, 31p.

Kellogg, K.S and Blank, H.R. (1982): Paleomagnetic Evidence Bearing on Tertiary Tectonics of the Tihamat Asir Coastal Plain, Southwestern Saudi Arabia. Open File Report U.S.G.S. -OF- 02-65.

Khodair, A.A and Coe, R.S (1975): Determination of Geomagnetic Paleointensities in Vacuum. Geophys. J.R. astr. Soc. 42, 107-115, 1975.

Levi, S. (1977): The effect of magnetite particle size on paleo-intensity determinations of the geomagnetic field. Phys. of the Earth and Planetary Interiors, 13, 245-259.

McCallum, I.S (1987): Petrology of the Igneous Rocks. Reviews of Geophysics, v.25, No. 5, p.1021-1042, June 1987.

McElhinny, M. W.(1973) : Paleomagnetism and Plate Tectonics. Cambridge University Press.

McElhinny, M. W. & Cowley, J A (1977): Paleomagnetic direction and Pole positions-XIV. Pole numbers 14/1 to 14/574. R. Astr. Soc.,

Geophys. J. 49,313-356.

Moufti, M.R.H (1985): The Geology of Harrat Al Madinah volcanic field, Harrat Rahat, Saudi Arabia. Ph.D., thesis, Department of Environmental Science, University of Lancaster.

Nagata, T.(1961): Rock Magnetism. Maruzem Company Ltd. Tokyo.350 p.

Parkinson, W.D (1983): Introduction to Geomagnetism. Scottish Academic Press Ltd, Edinburgh. 433p.

Patel, J.P., & Gracii, P., (1972): Paleomagnetic studies of Kipiti Phonolite of Kenya. Earth & Planetary Science Letters, v.16, p.213-218.

Patel, J.P., & Raja, P.K.S (1979): Paleomagnetic results from the Narosura and Magadi volcanics of Kenya. Phys. Earth planet Inter., 19, 7-14.

Piper, J.D.A.(1989): Paleomagnetism. Geomagnetism Vol. 3 Edited by J.A. Jacobs, p.30-161, Academic Press, Harcourt Brace Jovanovich, Publishers London.

Piper, J.D.A. & Richardson, A. (1972): The paleomagnetism of the Gulf of Guinea volcanic province, West Africa. Geophy. Journal of the Royal Astro. Soc. v.29, p.147-171.

Pouchan, P., & Roche, A (1971): Etude paleomagnetique de formations volcanique du Territoire des Afars et Issas. Comptes Rendus de l'Academie des Sciences de Paris. v. 272. ser. D. p. 531-534.

Reilly, T.A, Raja, P.K.S., Mussett, A.E., and Brock, A. (1976) The paleomagnetism of Late Cenozoic volcanic rocks from Kenya and Tanzania. Geophy. Journal of the Royal Astro. Soc. v.45. p.483-494.

Robert, N. and Piper, J.D.A.(1989): A description of the Behavior of the Earth's Magnetic Field. Geomagnetism Vol. 3 Edited by J.A. Jacobs, p.161-260, Academic Press, Harcourt Brace Jovanovich, Publishers London.

Ron Day (1977) : TRM and Its Variation with Grain Size. Adv. Earth Planet. Sci., 1, 1-33, 1977.

Salis, J. Sebastien and Bonhommet, N (1989): Paleointensity of the Geomagnetic Field from Dated Lavas of the Chaine des Puys, France 1.7-12 Thousand Years Before Present. J. of Geophysical Research, v.94, no. B11, p.15,771-15,784.

Sallomy, J.T. & Krs, M.(1980): A paleomagnetic study of some igneous rock from Jordan, Proc. Evolution Mineralization of the Arabian-Nubian Shield, FES Bull., 3, 155-164.

Schult, A. & Soddel, H (1973): Paleomagnetism of Tertiary basalts

from Libya. Geophys. J. R. ast. Soc., 32, 373-380.

Schult, A. (1974): Paleomagnetism of Tertiary Volcanic rocks from the Ethiopian Southern and Danakil block, J. Geophys., 40, 203-212.

Shaw, J., (1974): A new method for determining ancient geomagnetic field strengths: application to five historic lavas. Geophys. J.R. ast. Soc., 39, 133-141.

Sherwood, G.J (1989): MATZIJ- A Basic program to determine paleomagnetic remanence directions using Principal component analysis. Computers & Geosciences, v 15, no.7, p.1173-1182.

Skiba, W.J., Gilboy, C.F.,and Smith J.W.(1986): Explanatory Notes to the Geologic Map to the Rabigh Quadrangle, Sheet 22 D, Kingdom of Saudi Arabia. Complied by Colin R. Ramsay.

Stacey, F.D and Banerjee, S.K (1974): The Physical Principles of Rock Magnetism. Developments in Solid Earth Geophysics. Elsevier Scientific Publishing Co., 195 p.

Strangway, D.W.(1970): History of the Earth's Magnetic Field. McGraw-Hill Book Co., New York, 168 p.

Tarling, D. H.(1983): Paleomagnetism: Principles and Applications in Geology, Geophysics and Archaeology. Champan and Hall, London, 379p.

Thellier, E.(1938): Sur l'amantation des terres cuites et ses applications geophysiques. Ann. Inst. Phys. Globe, 16, 157-302.

Thellier, E., and O.Thellier, (1959): Sur l'intensit'e du champ magne'tique terrestre dans le pass'e historique et g'eologique. Ann. G'eophys..15,285-376.

Van Zijl, J.S.V., Graham K.W.T., and Hales, A.L.(1962): The Paleomagnetism of the Stormberh lavas of South Africa. Parts 1 & 2, Geophys. J.R. ast. Soc., 7, 23-39; 169-182.

Wilson, R. L., (1961): Paleomagnetism in northern Ireland. Part 1. The Thermal Demagnetization of Natural Magnetic Moments in rocks. Geophys. J. R. ast. Soc., 5, 45-58.

Watkins, N.D and Haggerty, S.E. (1967): Primary Oxidation Variation and Petrogenesis in a Single Lava. Contr. Mineral. and Petrol. 15, 251-271.

Yousif, I.A., and G.E.J. Beckmann (1981) : A Paleomagnetic Study of some Tertiary and Cretaceous Rocks in Western Saudi Arabia: Evidence on the Movement of the Arabian Plate. KAU Faculty of Earth Sciences, Bull 4. p.89-106.

Zijderveld, J.D.A., (1967): A.C. Demagnetization of Rocks: Analysis of results. In D.W. Collinson, K.M. Creer and S.K. Runcorn (Editors), Methods in Paleomagnetism. Elsevier, Amsterdam, pp.245-286.

Appendix A

This Appendix contains a brief discription of the sample localities.

Measurement (Y,Z) are made with respect to specimen coordinate axes.

Y = Azimuth from the North

Z = Angle of Hade

Locality # 1

Sample site # 1

Longitude : 40 21 00

Latitude : 23 15 41

Sample number	Y	Z
11P001	124	42
11R01	0.0	0.0
11R002	79	40
11R003	78	80
11R004	158	38
11R005	90	25
11R006	131	21
11R007	77	78
11R008	100	45
11R009	121	29
11R010	130	59
11R011	303	15
11R012	223	49
11R013	340	22
11R014	268	58

Locality # 1

Sample site # 2

Longitude : 40 09 00

Latitude : 23 18 13

Sample number	Y	Z
12R092	188	54
12R10	0.0	0.0
12R093	113	44
12R094	7	54
12R095	127	39
12R096	110	45
12R097	4	35
12R098	349	44
12R099	85	42
12R100	345	25
12R101	170	35

SAMPLES CHART FOR CENTRAL HARRAT RAHAT

Locality # 1

Sample site # 3

Longitude : 40 18 97

Latitude : 23 17 54

Sample number	Y	Z
13R102	79	34
13R103	358	40
13R104	124	60
13R11	0.0	0.0
13R105	165	60
13R106	14	22
13R12	0.0	0.0
13R107	310	30
13R108	115	16
13R109	328	15
13R13	0.0	0.0
13R14	0.0	0.0
13R110	344	59
13R111	76	53
13R112	65	54
13R113	27	72
13R114	80	56
13R15	0.0	0.0

SAMPLES CHART FOR CENTRAL HAMRAT RAHAT

Locality	# 1
Sample site	# 4
Longitude	: 40 18 09
Latitude	: 23 17 24

Sample number	Y	Z
14R115	295	30
14R116	294	26
14R117	334	39
14R118	74	29
14R119	305	32
14R120	353	61
14R121	356	66
14R122	355	58
14R123	93	76
14R124	353	30
14R125	215	44
14R126	51	85
14R127	32	58
14R128	29	45
14R129	24	71
14R130	17	56
14R131	39	96
14R132	30	54

SAMPLES CHART FOR CENTRAL MARKAT KHAT

Locality	# 1
Sample site	# 5
Longitude	: 40 15 88
Latitude	: 23 16 63

Sample number	Y	Z
15R133	270	54
15R134	326	73
15R135	330	30
15R136	249	47
15R137	141	29

SAMPLES CHART FOR CENTRAL HARRAT RAHAT

Locality	# 1
Sample site	# 6
Longitude	: 40 15 /6
Latitude	: 23 17 11

Sample number	Y	Z
16R138	170	52
16R139	195	48
16R140	183	48
16R141	172	52
16R142	141	43
16R143 (lost)	199	43
16R144	155	52
16R145	200	59
16R146	223	58
16R147	200	78
16R148	205	84
16R149	111	69
16R150	260	67
16R151	108	58
16R15	0.0	0.0
16R16	0.0	0.0

SAMPLES CHART FOR CENTRAL HARRAT RAHAT

Locality	# 1
Sample site	# 7
Longitude	: 40 11 47
Latitude	: 23 15 72

Sample number	Y	Z
17R152	20	40
17R17	0.0	0.0
17R18	0.0	0.0
17R19	0.0	0.0
17R153	319	86
17R154	73	71
17R155	106	34
17R156	93	53
17R20	0.0	0.0
17R21	0.0	0.0
17R22	0.0	0.0

SAMPLES CHART FOR CENTRAL HARRAT RAHAT

Locality	# 2
Sample site	# 1
Longitude	: 40 28 e.'
Latitude	: 22 52 e2

Sample number	Y	Z
21R015	350	39
21R016	330	25
21R017	195	24
21R018	80	33
21R019	302	22
21R03	U.0	U.0
21R020	50	24
21R021	290	24
21R022	44	24
21R023	124	44
21R024(lost mark)	290	17

SAMPLES CHART FOR CENTRAL HARBOR BASIN

Locality	# 2
Sample site	# 2
Longitude	: 40 28 08
Latitude	: 22 52 34

Sample number	Y	Z
22R025	152	30
22R026	160	35
22R04	0.0	0.0
22R027	108	31
22R028	93	38
22R05	0.0	0.0
22R029	85	38
22R06	0.0	0.0
22R030	220	34
22R031	344	30
22R032	301	53
22R033	350	50
22R034	121	54
22R035	214	25
22R036	146	42
22R07	0.0	0.0

SAMPLES CHART FOR CENTRAL HAMAT KAHAT

Locality	# 2
Sample site	# 3
Longitude	: 40 28 38
Latitude	: 22 52 22

Sample number	Y	Z
23R037	85	39
23R038	56	30
23R039	55	50
23R040	29	35
23R041	206	32
23R042	345	36
23R043	122	37
23R044(lost)	150	32

SAMPLES CHART FOR CENTRAL HARRAT HANAT

Locality	# 3
Sample site	# 1
Longitude	: 40 19 07
Latitude	: 22 35 58

Sample number	Y	Z
31R045	138	39
31R046	164	53
31R047	194	40
31R048	110	54
31R049	108	75
31R050	70	50
31R051	39	47
31R052	72	49
31R053	171	54

SAMPLES CHART FOR CENTRAL HARRAT KHAT

Locality # 3

Sample site # 3

Longitude : 40 21 62

Latitude : 22 38 84

Sample number	Y	Z
33R060	170	30
33R061	210	56
33R062	188	51
33R063	216	78
33R064	224	56
33R065	240	70
33R066	225	64
33R067	258	60
33R068	305	60
33R069	192	80

SAMPLES CHART FOR CENTRAL HARRAT RAHAT

Locality	# 4
Sample site	# 1
Longitude	: 40 24 26
Latitude	: 22 50 03

Sample number	Y	Z
41R070	305	40
41R071	33	42
41R072	315	39
41R073	46	54
41R074	15	56
41R075	95	46

SAMPLES CHART FOR CENTRAL MAKRAI RAHAI

Locality	# 4
Sample site	# 2
Longitude	: 40 22 05
Latitude	: 22 50 03

Sample number	Y	Z
42R076	170	46
42R077	126	45
42R078	30	54
42R079	15	30
42R080	57	60
42R081	90	54
42R082	255	40
42R08	U.O	U.O
42R09	U.O	U.U
42R083	260	29
42R084	50	56

SAMPLES CHART FOR CENTRAL MARKAT PARAT

Locality # 4

Sample site # 3

Longitude : 40 11 03

Latitude : 22 50 24

Sample number	Y	Z
43R085	5	47
43R086	310	46
43R087	214	47
43R088	43	54
43R089	75	38
43R090	320	48
43R091	45	47

SAMPLES CHART FOR CENTRAL HARRAT RAHAT

Locality # 5

Sample site # 1

Longitude : 39 54 11

Latitude : 23 18 94

Sample number	Y	Z
SIR157	200	35
SIR158	135	40
SIR159	175	30
SIR23	0.0	0.0
SIR160	203	25

SAMPLES CHART FOR CENTRAL HARRAT HARAT

Locality # 5

Sample site # 2

Longitude : 39 53 23

Latitude : 23 19 08

Sample number	Y	X
52R161	6	50
52R162	270	87
55R163	334	88
52R164	28	89
52R165	307	85
52R166	298	88
52R167	6	77
52R24	0.0	0.0

SAMPLES CHART FOR CENTRAL HARRAT RAHAT

Locality	# 5
Sample site	# 3
Longitude	: 39 56 47
Latitude	: 23 15 68

Sample number	Y	Z
53R168	145	40
53R169	314	29
53R170	205	16
53R25	U.0	U.0
53R171	121	52
53R172	82	30
53R173	155	36
53R174	118	17
53R175	41	19
53R176	262	30

SAMPLES CHART FOR CENTRAL HARRAT RAHAT

Locality	# 5
Sample site	# 4
Longitude	: 39 55 73
Latitude	: 23 16 56

Sample number	Y	Z
54R177	117	54
54R26	0.0	0.0
54R178	119	10
54R179	140	25
54R27	0.0	0.0
54R180	154	16
54R181	160	28
54R182	344	33
54R183	97	10
54R28	0.0	0.0
54R184	359	50
54R29	0.0	0.0
54R185	128	35

SAMPLES CHART FOR CENTRAL HARRAT RAHAT

Locality # 5

Sample site # 5

Longitude : 39 57 05

Latitude : 23 15 14

Sample number	Y	Z
55R186	216	39
55R187	252	40
55R188	259	36
55R30	0.0	0.0
55R189	343	32
55R190	352	44
55R31	0.0	0.0

SAMPLES CHART FOR CENTRAL HARRAT KHAI

Locality # 5

Sample site # 6

Longitude : 39 57 02

Latitude : 23 14 69

Sample number	Y	Z
56R191	10	53
56R192	51	39
56R32	U.D	U.D
56R193	45	22
56R33	U.D	U.D
56R194	352	72
56R195	140	26
56R196	196	90
56R34	U.D	U.D
56R35	U.D	U.D
56R36	U.D	U.D

SAMPLES CHART FOR CENTRAL HARRAT RAHAT

Locality # 5

Sample site # 7

Longitude : 39 57 64

Latitude : 23 9 25

Sample number	Y	Z
S7R197	111	61
S7R37	U.O	U.O
S7R199	72	63
S7R38	U.O	U.O
S7R200	188	25
S7R201	54	47
S7R202	148	23

Appendix B
NRM–TRM Curves

This Appendix contains 92 NRM–TRM curves obtained by Thellies' experiment. The number appearing next to each data point indecates the temperature of the paired heating steps.

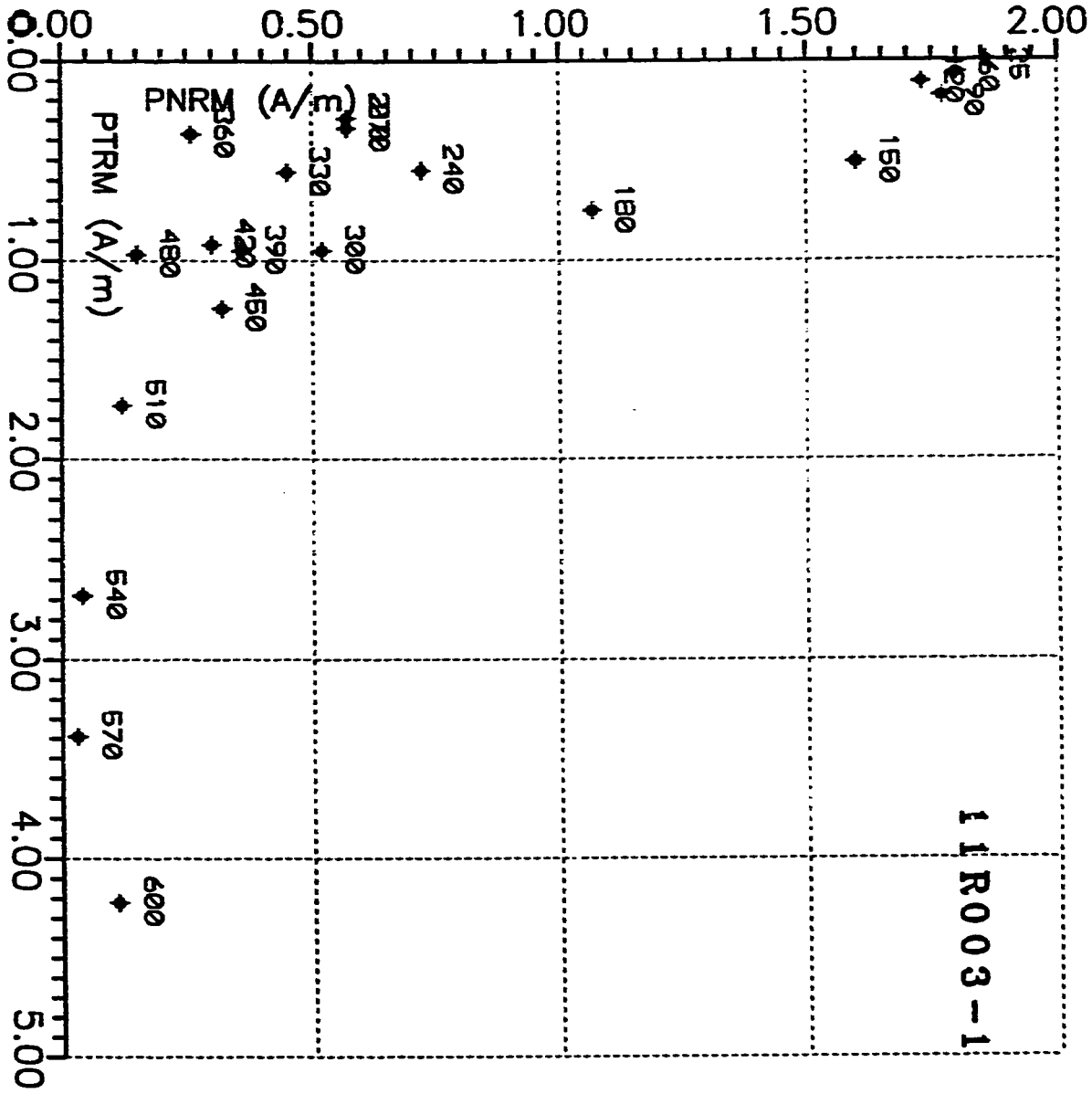
0.00
0.50
1.00
1.50
2.00
PNRM (A/m)
PTRM (A/m)
0.00
1.00
2.00
3.00
4.00
5.00
150
180
240
300
330
360
390
420
450
480
510
540
570
600
11R003-1

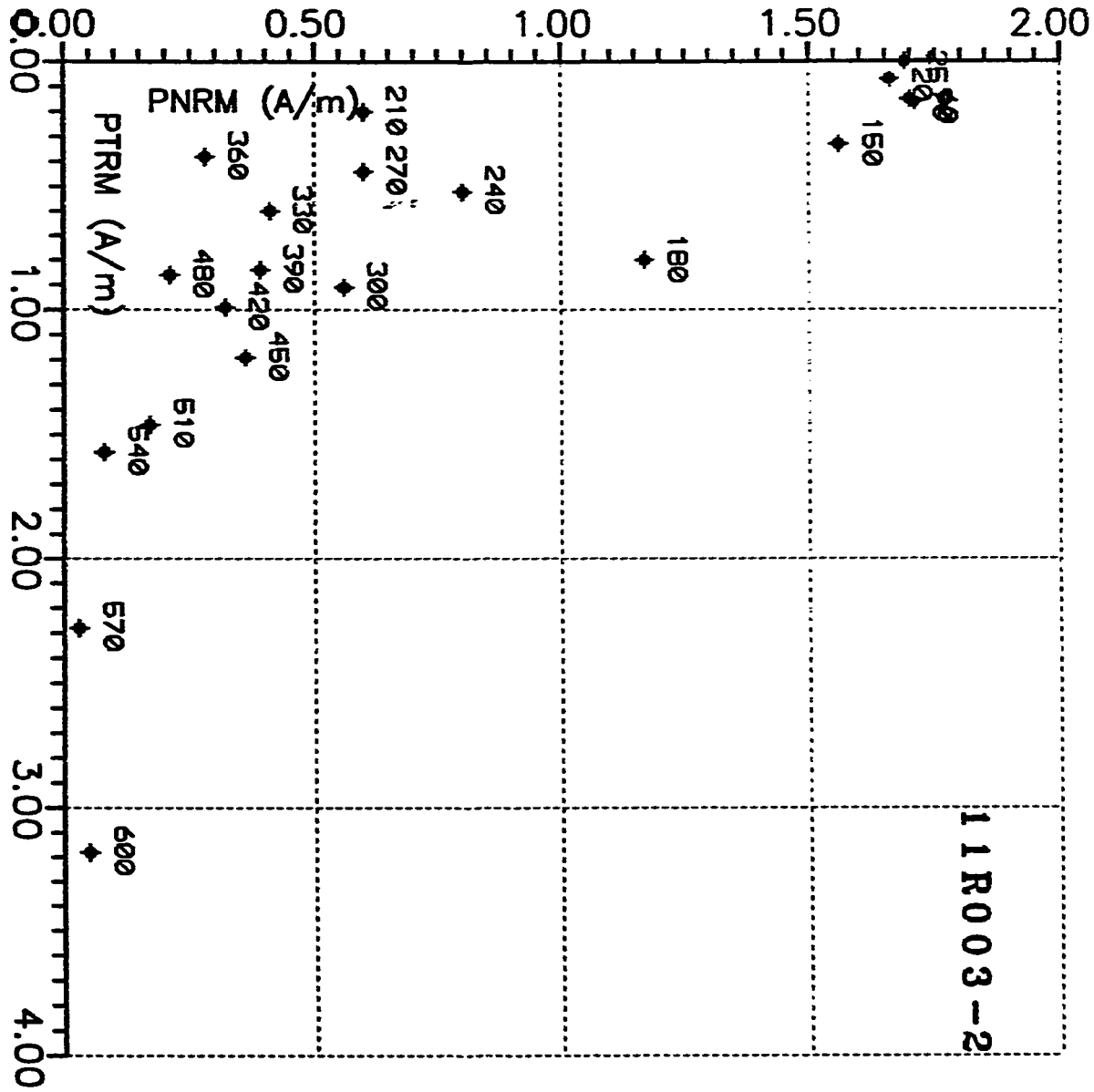
0.00
0.50
1.00
1.50
2.00
PNRM (A/m)
PTRM (A/m)
0.00
1.00
2.00
3.00
4.00
150
180
210
240
270
300
330
360
390
420
450
480
510
540
570
600
11R003-2

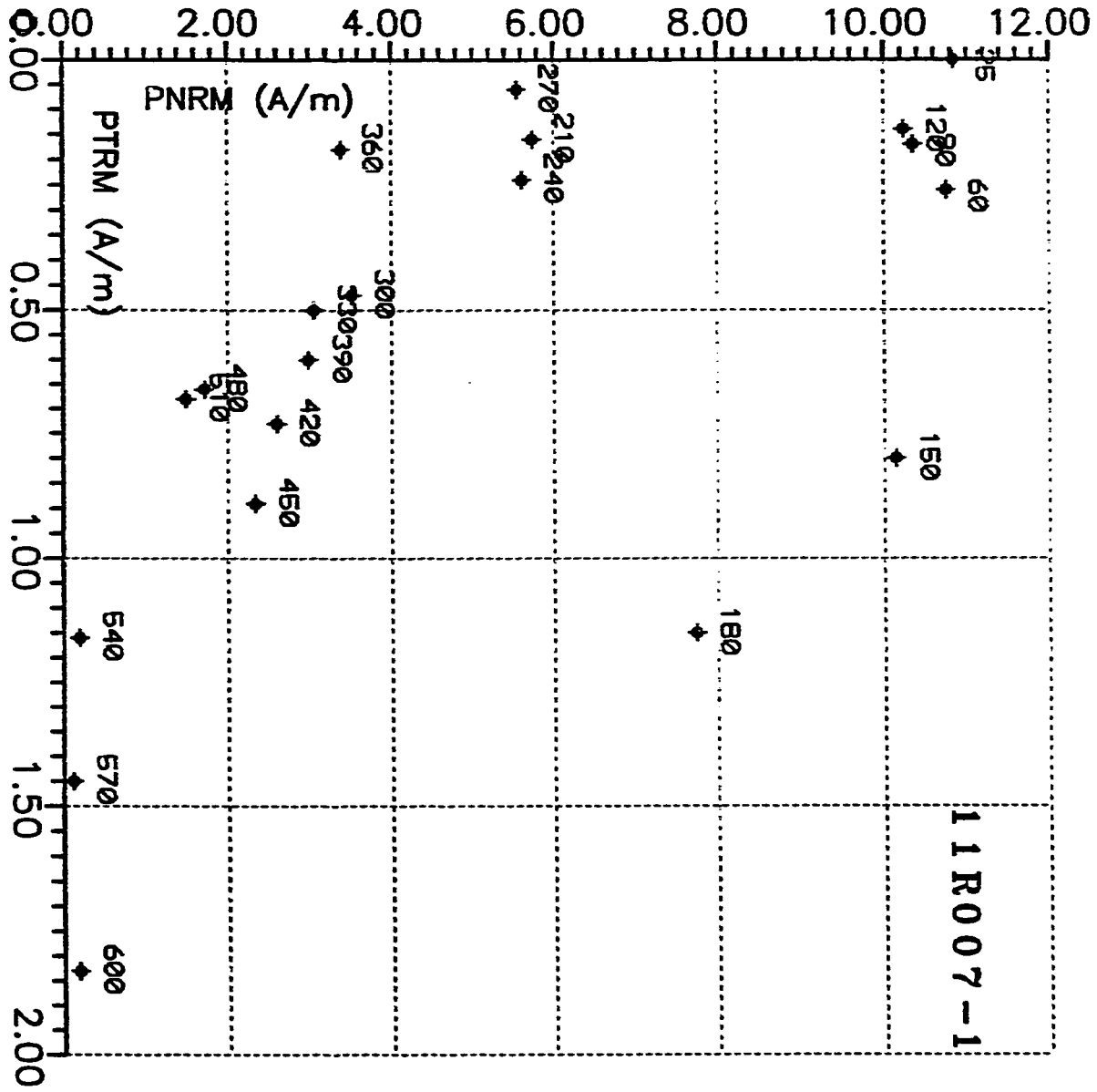
PNRM (A/m)
PTRM (A/m)
0.00
2.00
4.00
6.00
8.00
10.00
12.00
0.50
1.00
1.50
2.00
11R007-1

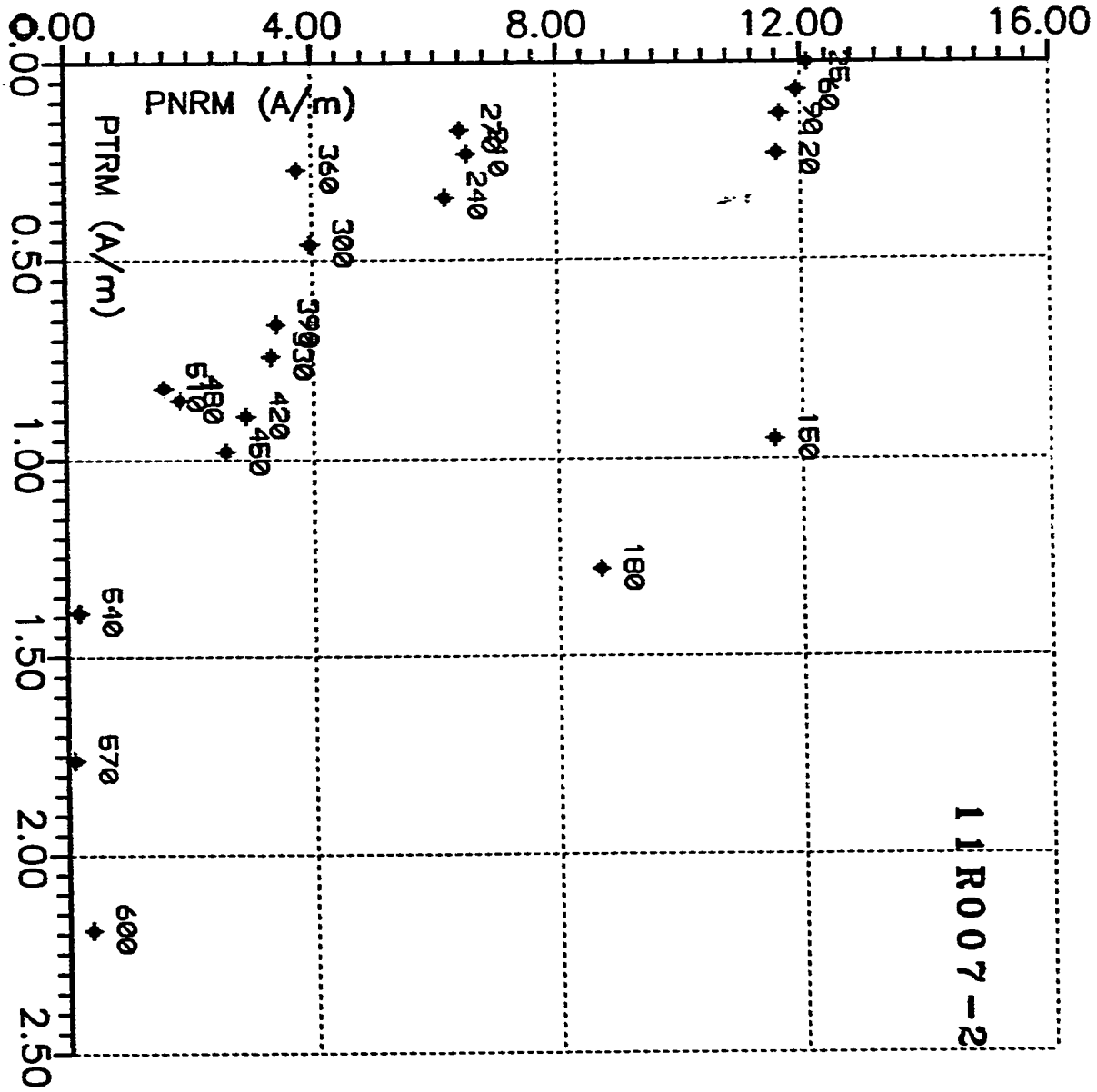
PNRM (A/m)
PTRM (A/m)
0.00
4.00
8.00
12.00
16.00
0.50
1.00
1.50
2.00
2.50
11R007-2

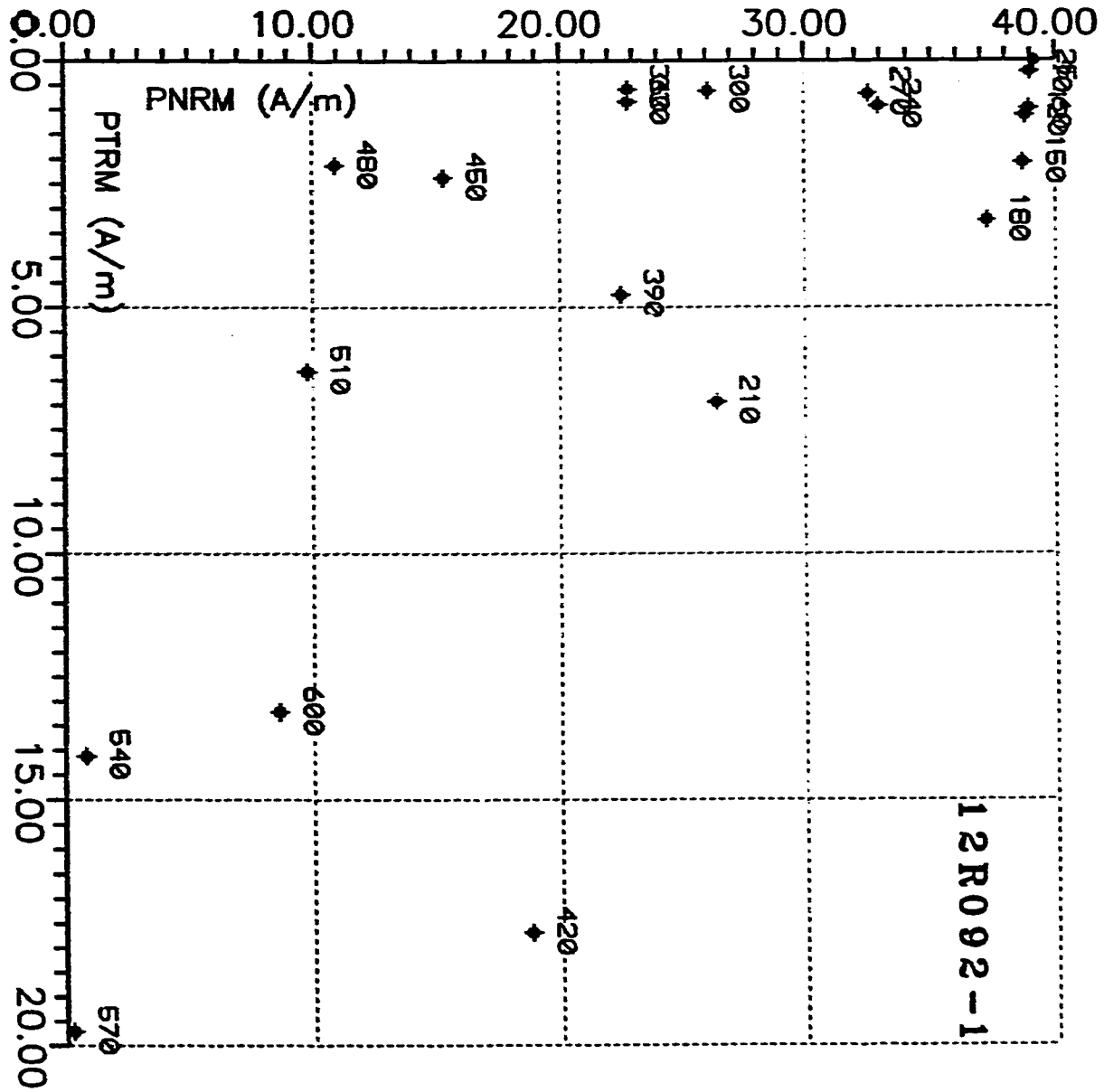
0.00
10.00
20.00
30.00
40.00
PNRM (A/m)
PTRM (A/m)
0.00
5.00
10.00
15.00
20.00
480
450
390
510
210
600
540
420
570
180
300
240
12R092-1

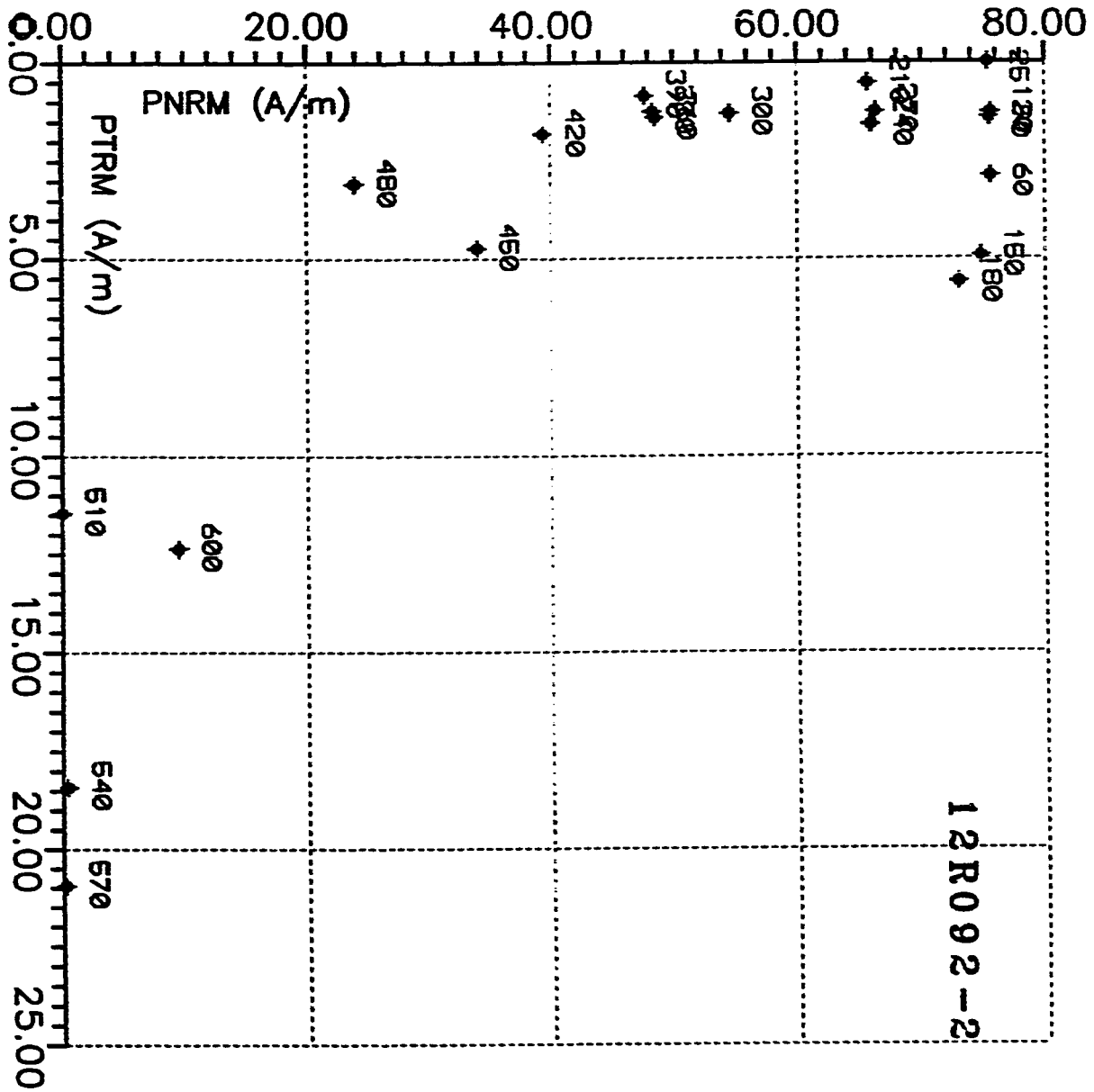
0.00
20.00
40.00
60.00
80.00
PNRM (A/m)
PTRM (A/m)
0.00
5.00
10.00
15.00
20.00
25.00
300
420
480
450
60
180
510
600
540
570
12R092-2

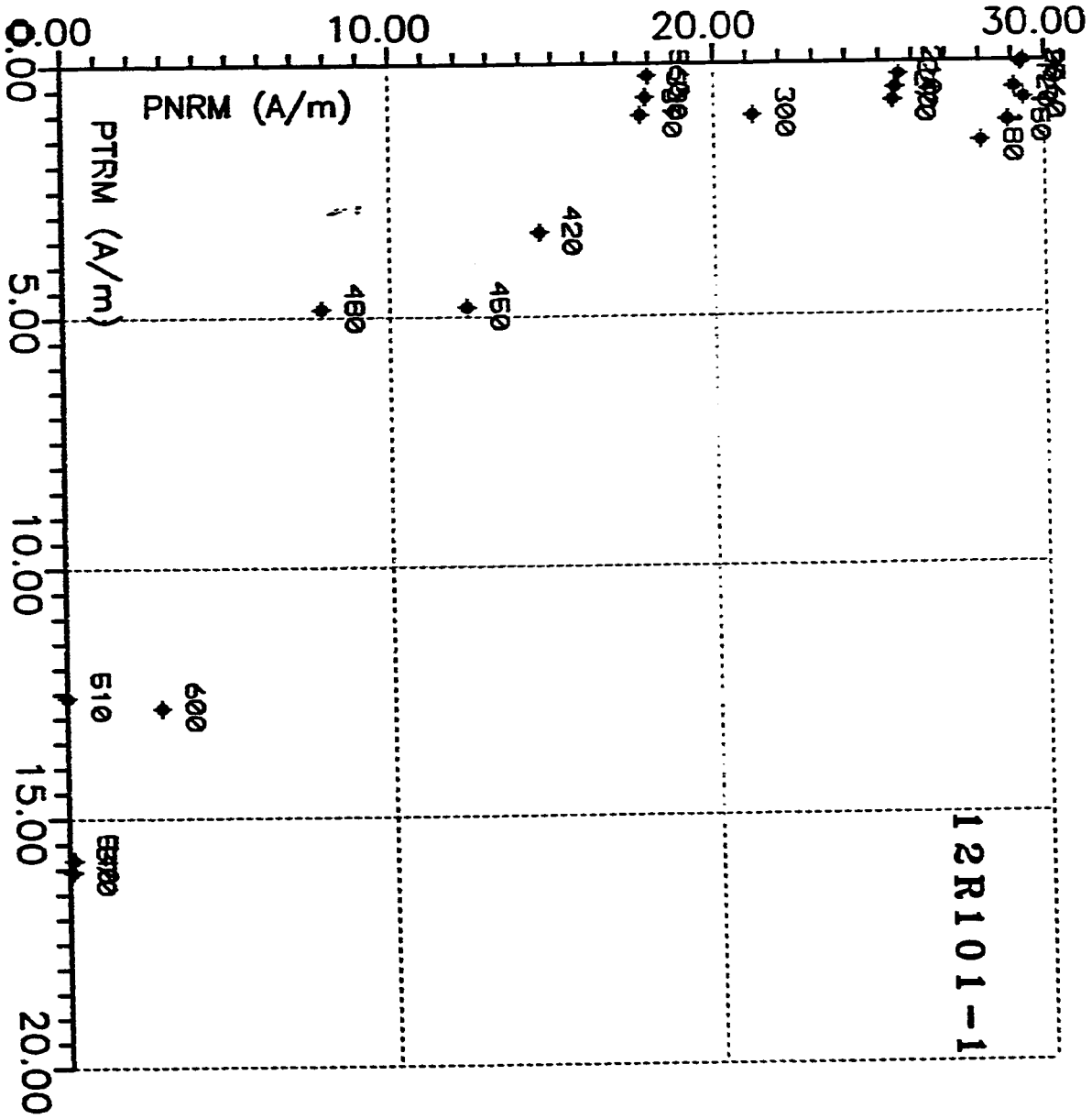
0.00
10.00
20.00
30.00
PNRM (A/m)
PTRM (A/m)
0.00
5.00
10.00
15.00
20.00
300
420
480
450
510
600
12R101-1

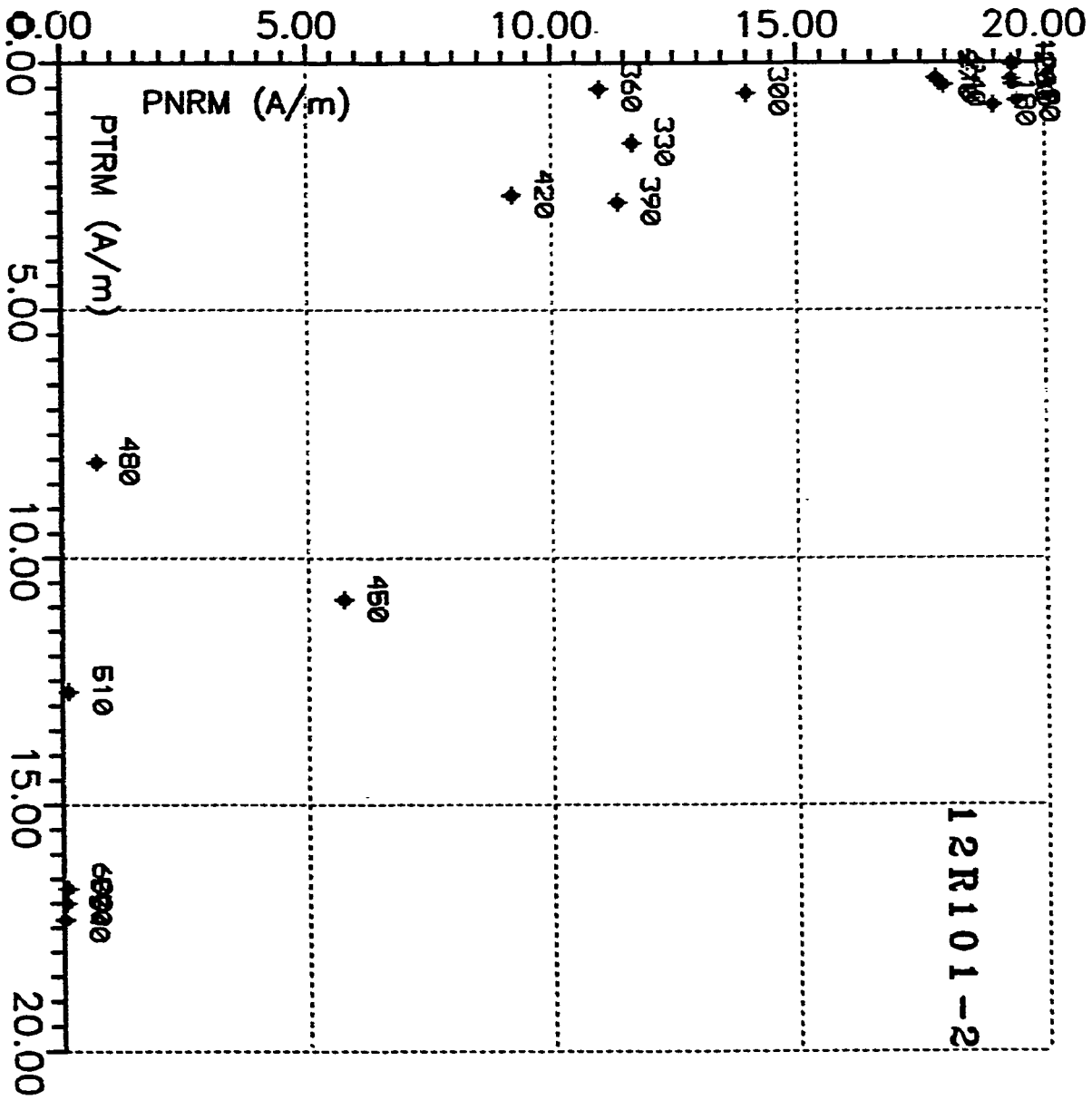
0.00
5.00
10.00
15.00
20.00
PNRM (A/m)
PTRM (A/m)
300
330
360
390
420
450
480
510
12R101-2

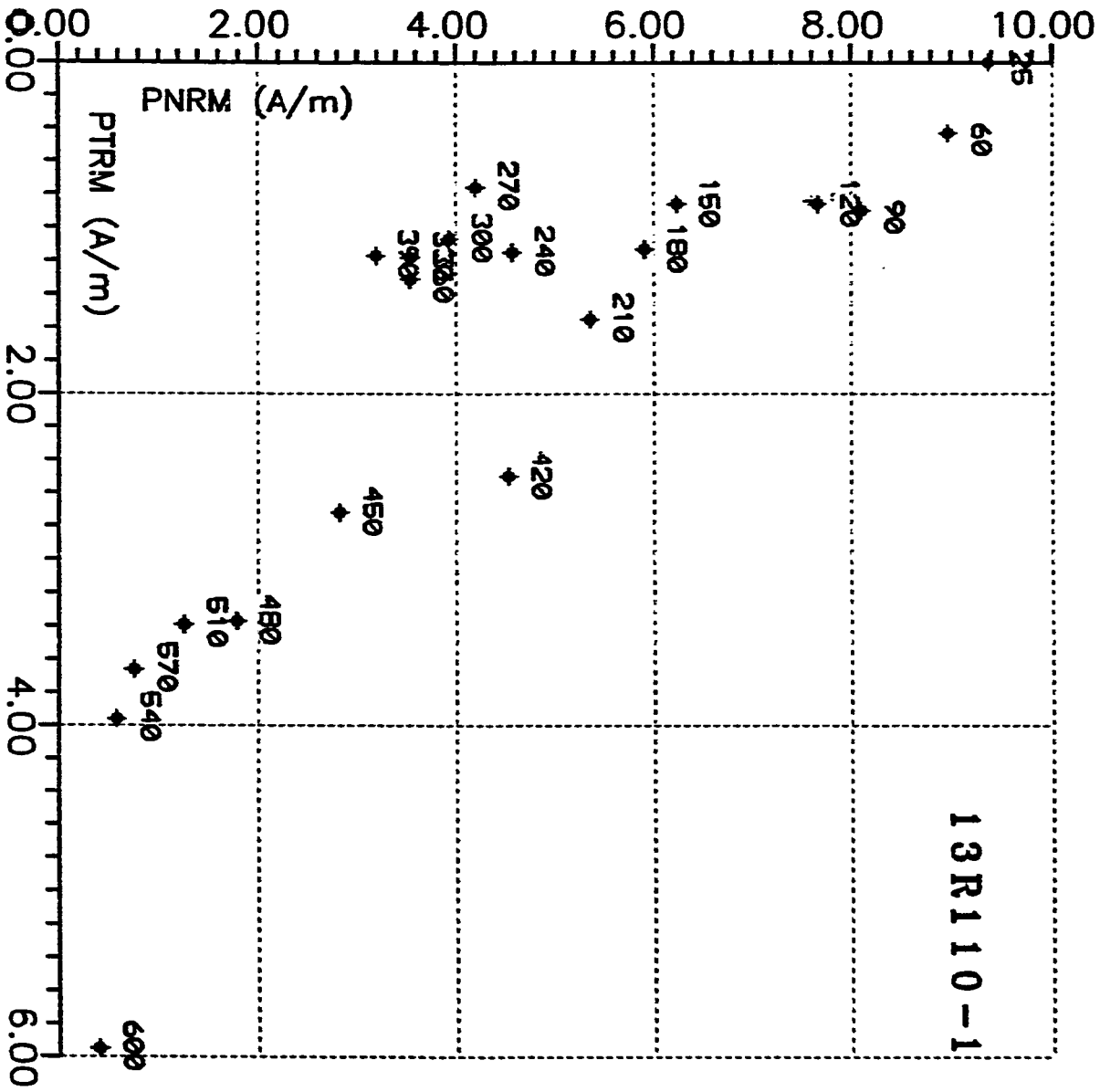
0.00
2.00
4.00
6.00
8.00
10.00
PNRM (A/m)
PTRM (A/m)
13R110-1

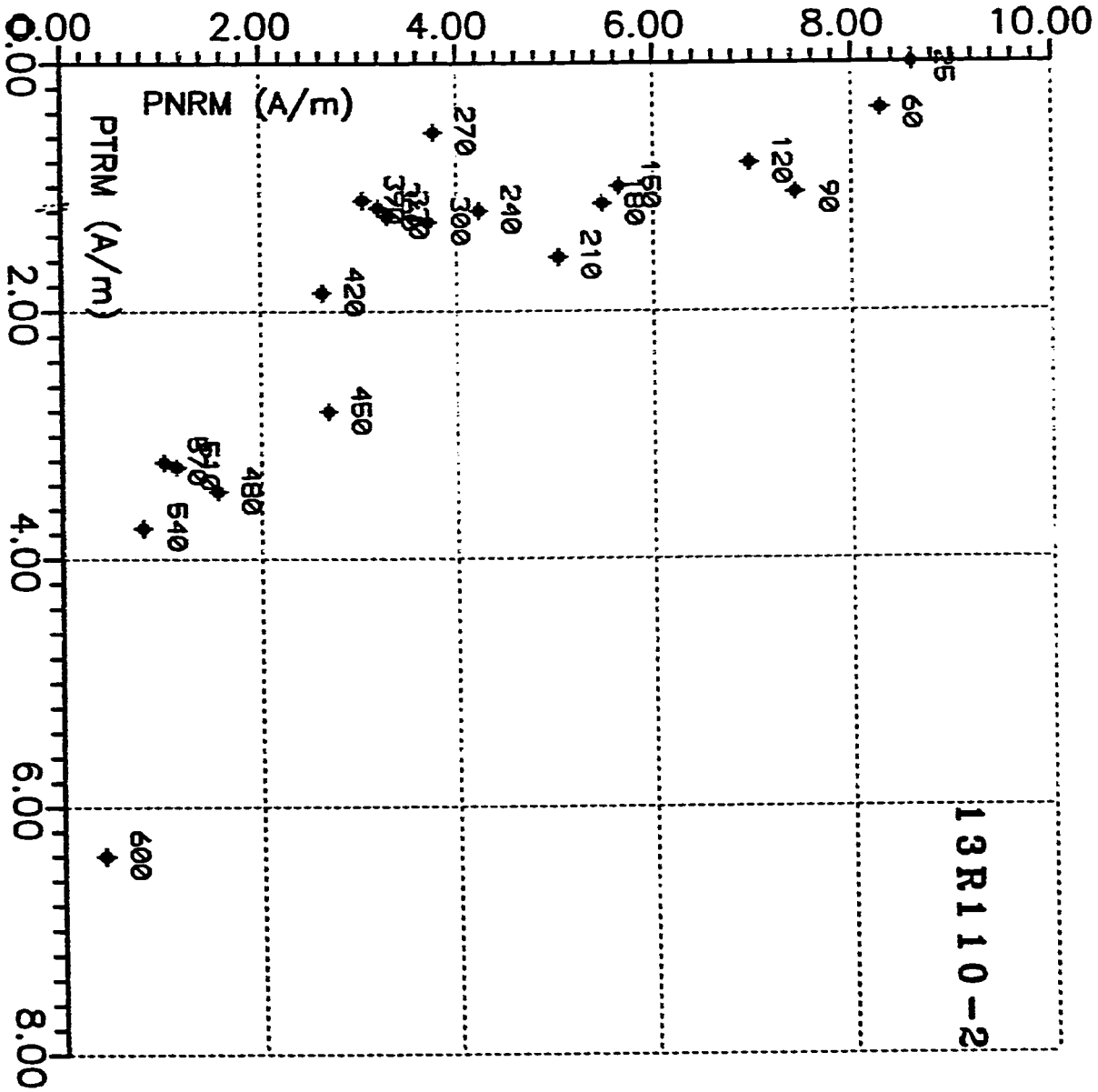
0.00
2.00
4.00
6.00
8.00
10.00
PNRM (A/m)
PTRM (A/m)
15
60
90
120
150
180
210
240
270
300
420
450
480
540
600
13R110-2

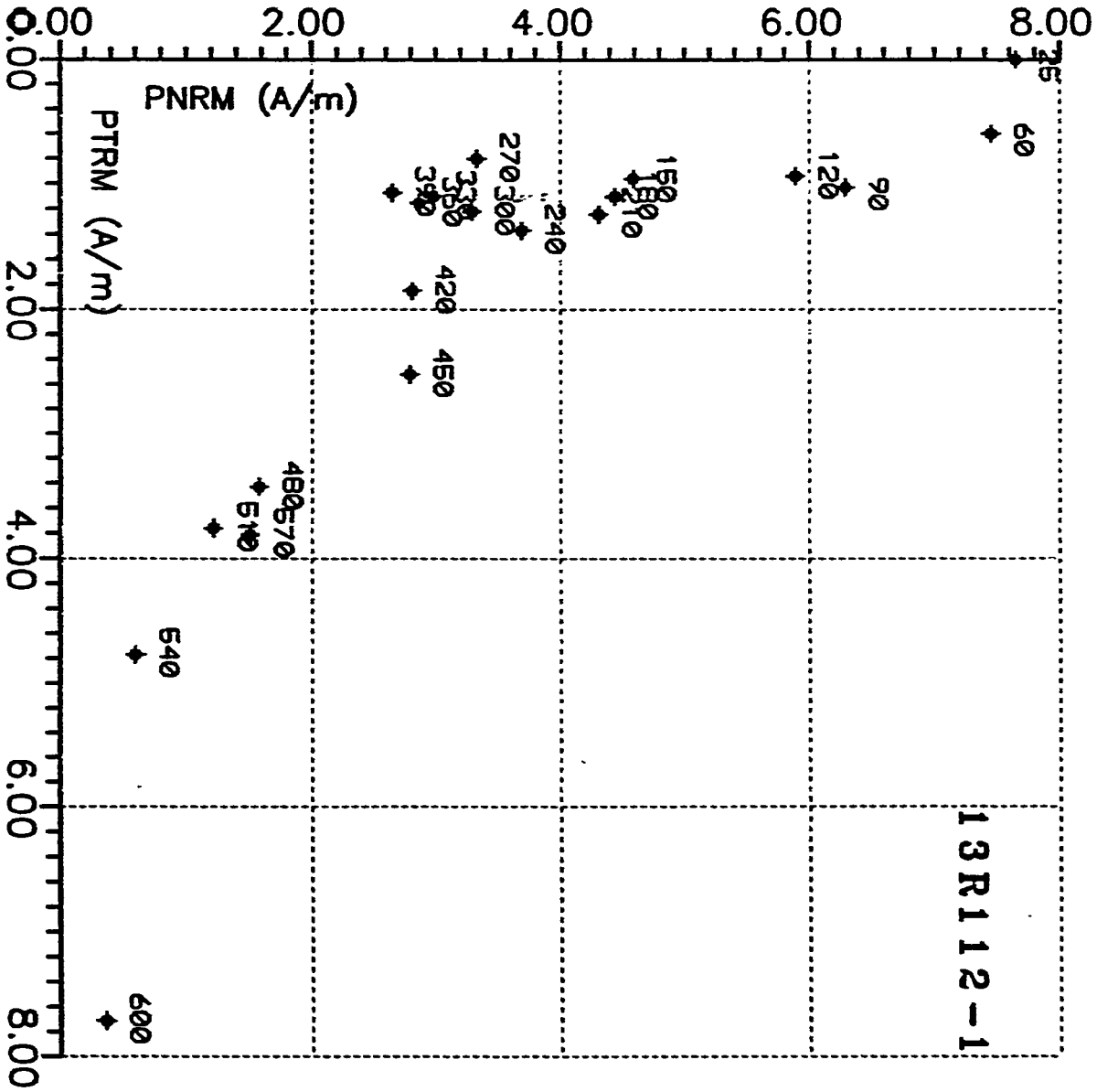
0.00
2.00
4.00
6.00
8.00
PNRM (A/m)
PTRM (A/m)
25
60
90
120
150
180
210
240
270
300
330
360
390
420
450
480
510
540
570
600
13R112-1

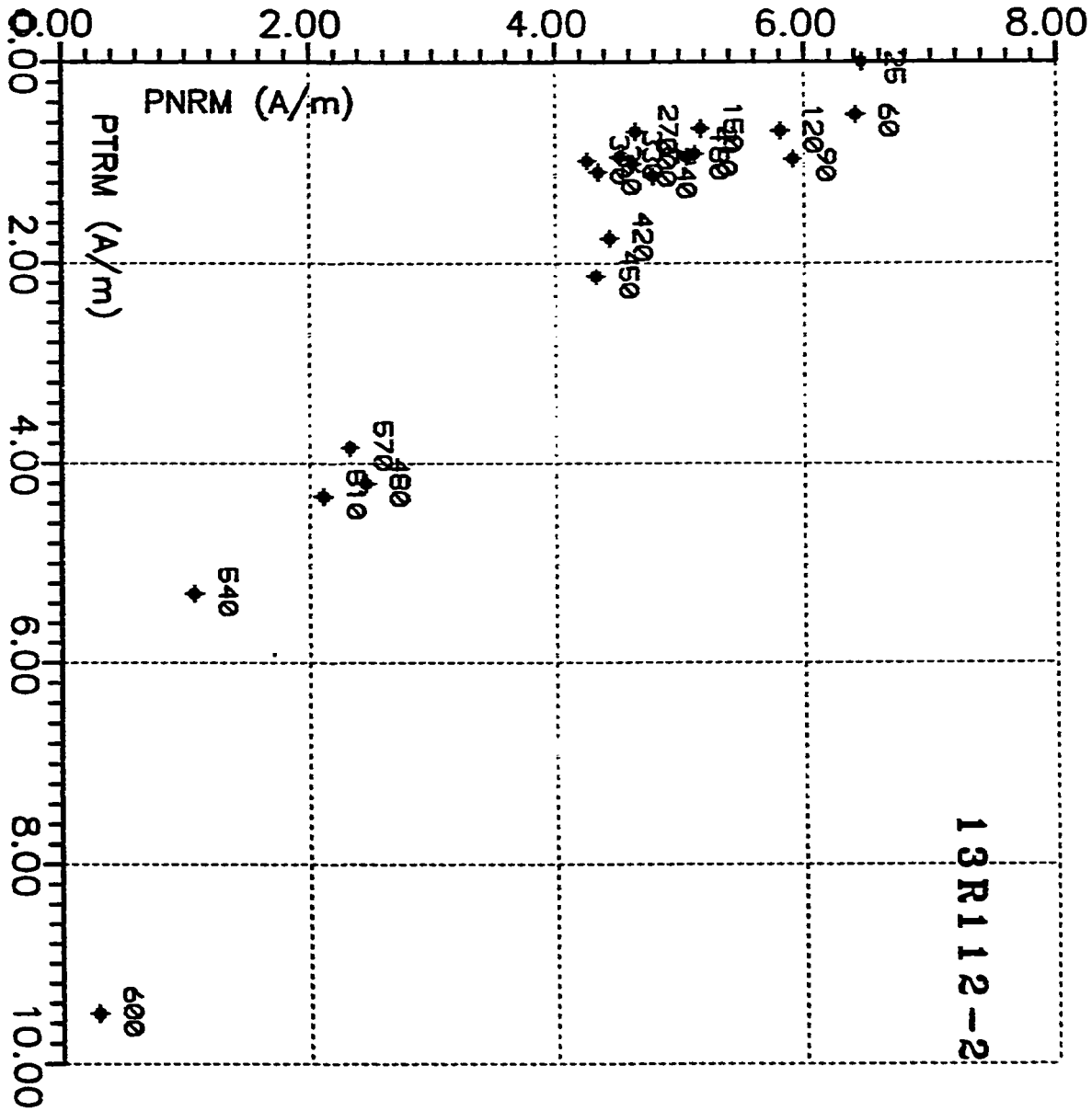
0.00
2.00
4.00
6.00
8.00
PNRM (A/m)
PTRM (A/m)
0.00
2.00
4.00
6.00
8.00
10.00
13R112-2

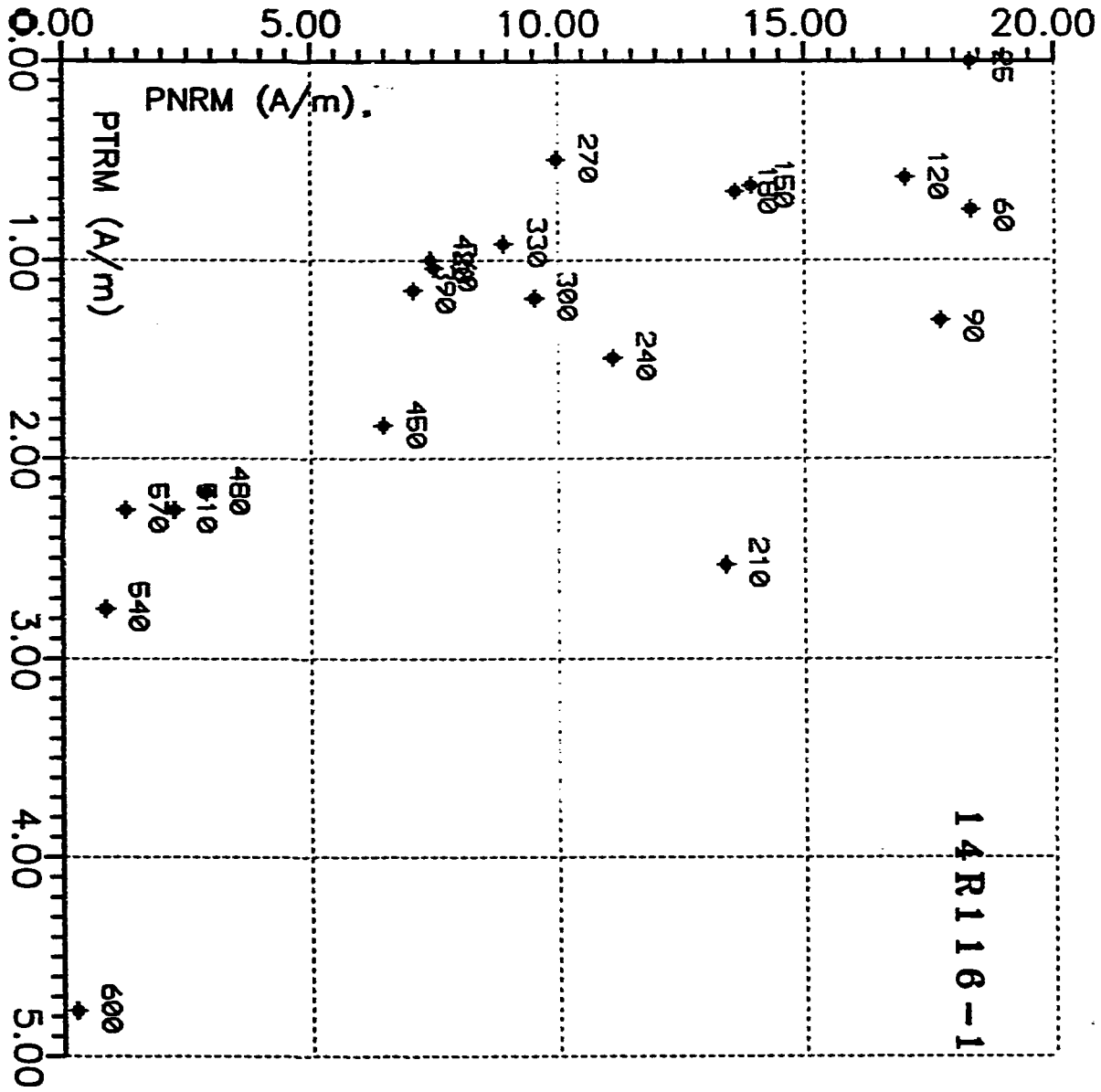
0.00
5.00
10.00
15.00
20.00
PNRM (A/m).
PTRM (A/m)
0.00
1.00
2.00
3.00
4.00
5.00
25
60
120
150
180
270
330
300
90
240
450
210
480
510
570
540
600
14R116-1

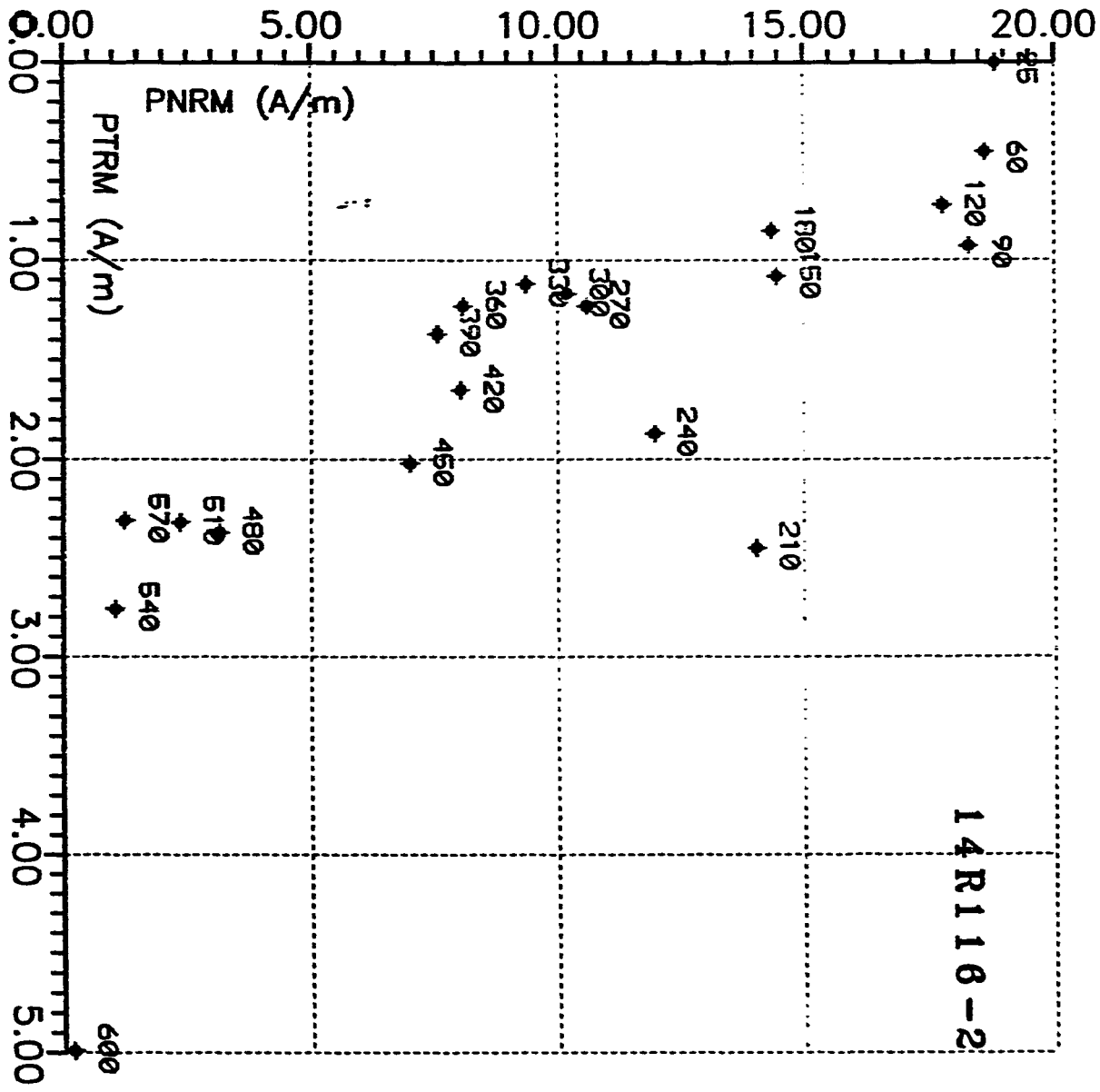
0.00
5.00
10.00
15.00
20.00
PNRM (A/m)
PTRM (A/m)
0.00
1.00
2.00
3.00
4.00
5.00
45
60
120
90
100
150
330
300
270
360
390
420
240
450
480
510
570
540
210
600
14R116-2

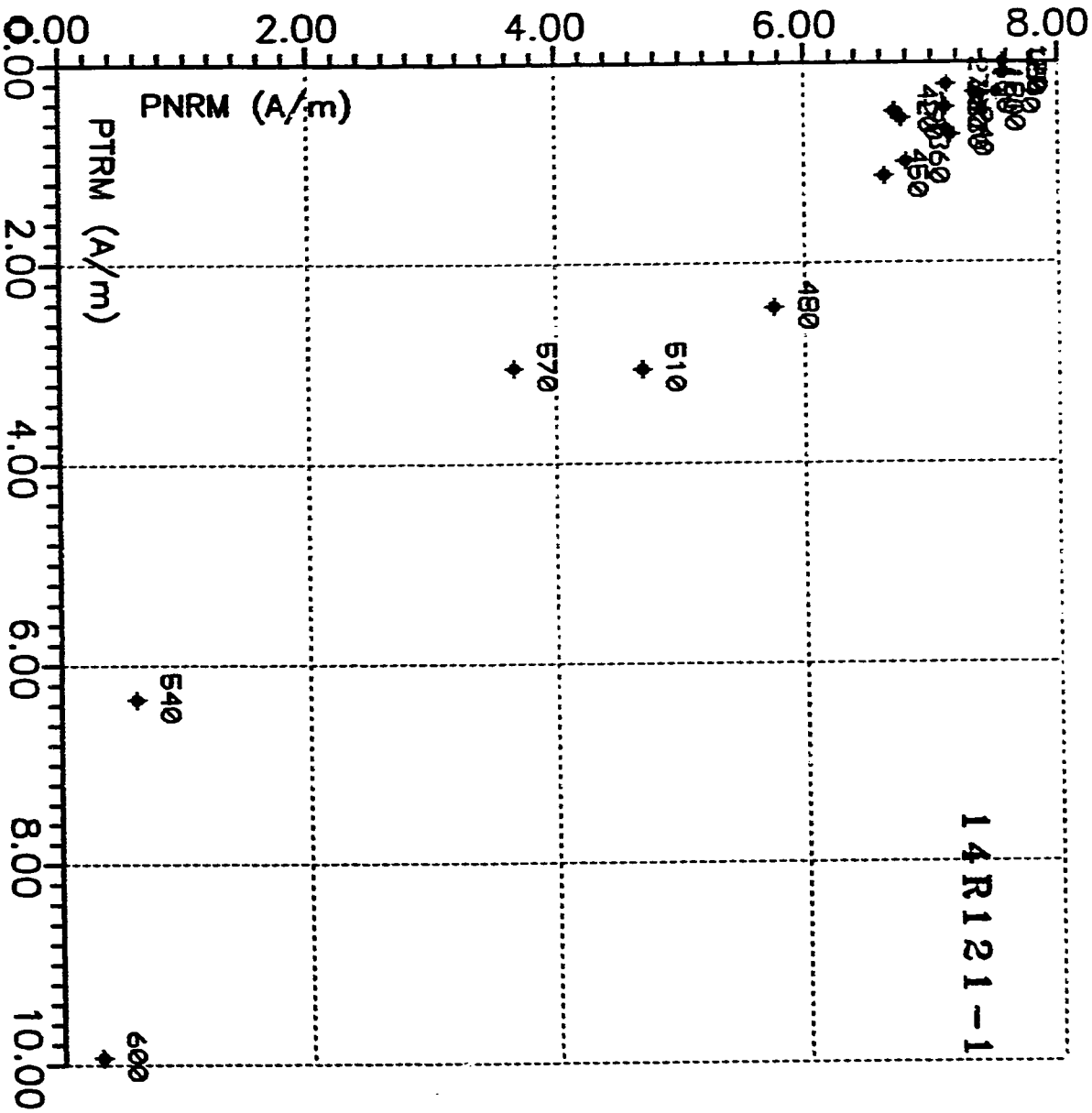
0.00
2.00
4.00
6.00
8.00
PNRM (A/m)
PTRM (A/m)
0.00
2.00
4.00
6.00
8.00
10.00
480
510
570
540
600
14R121-1

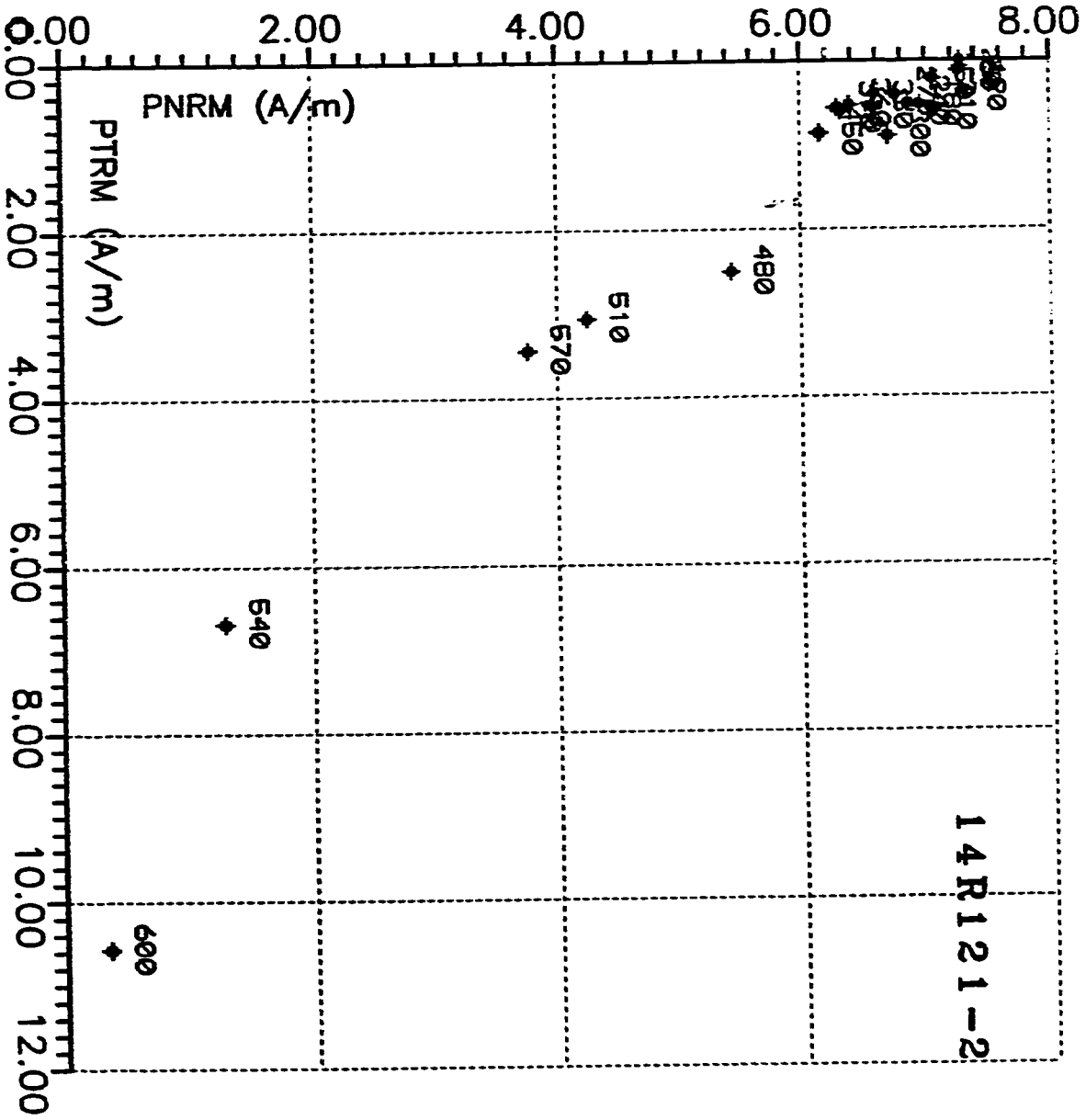
0.00
2.00
4.00
6.00
8.00
PNRM (A/m)
PTRM (A/m)
0.00
2.00
4.00
6.00
8.00
10.00
12.00
480
510
570
540
600
14R121-2

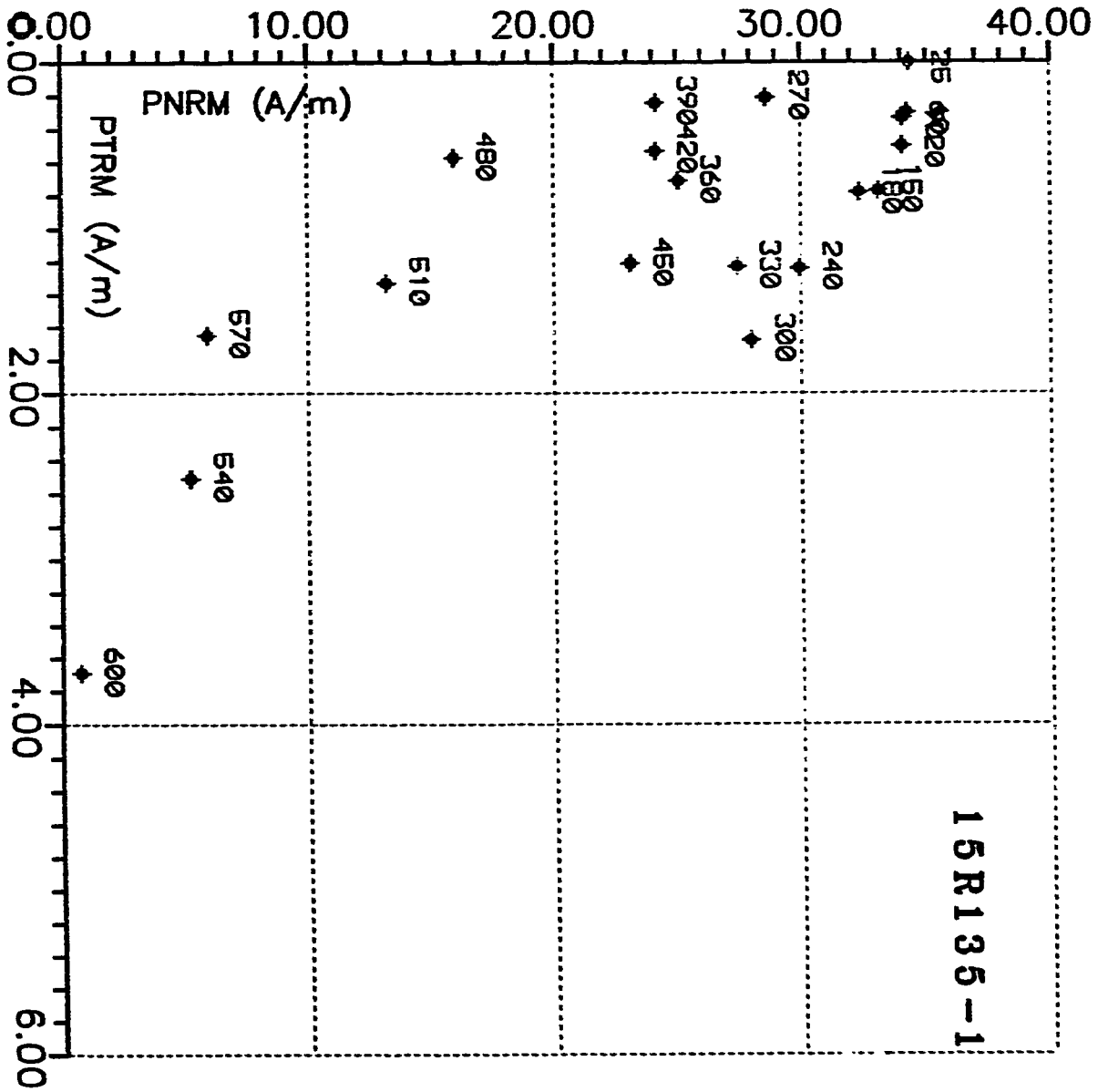
0.00
10.00
20.00
30.00
40.00
PNRM (A/m)
PTRM (A/m)
0.00
2.00
4.00
6.00
25
270
390
420
360
480
150
180
450
330
240
510
570
300
540
600
15R135-1

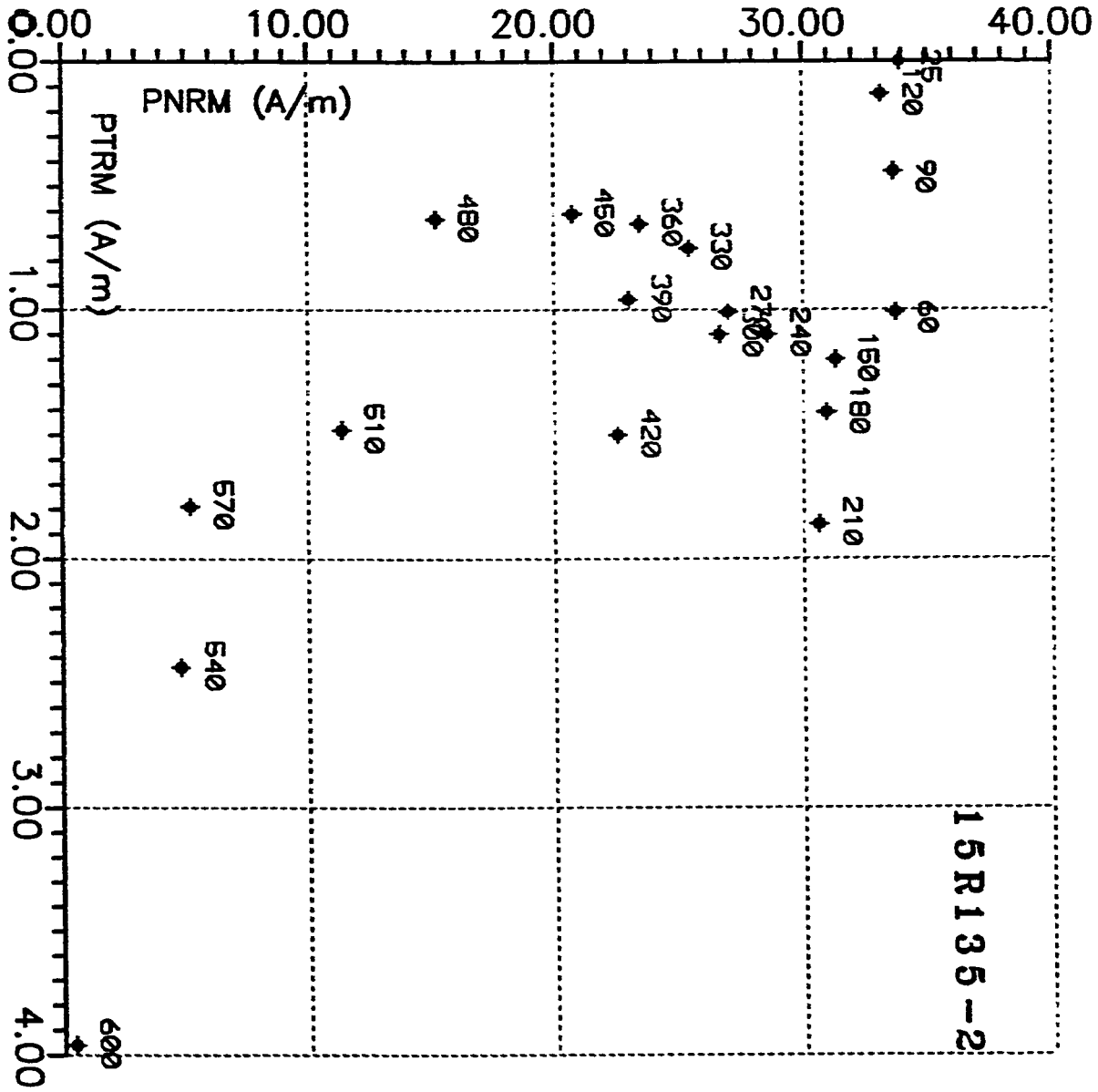
0.00
10.00
20.00
30.00
40.00
PNRM (A/m)
PTRM (A/m)
0.00
1.00
2.00
3.00
4.00
15
120
90
480
450
360
330
390
270
300
240
60
150
180
510
420
210
570
540
600
15R135-2

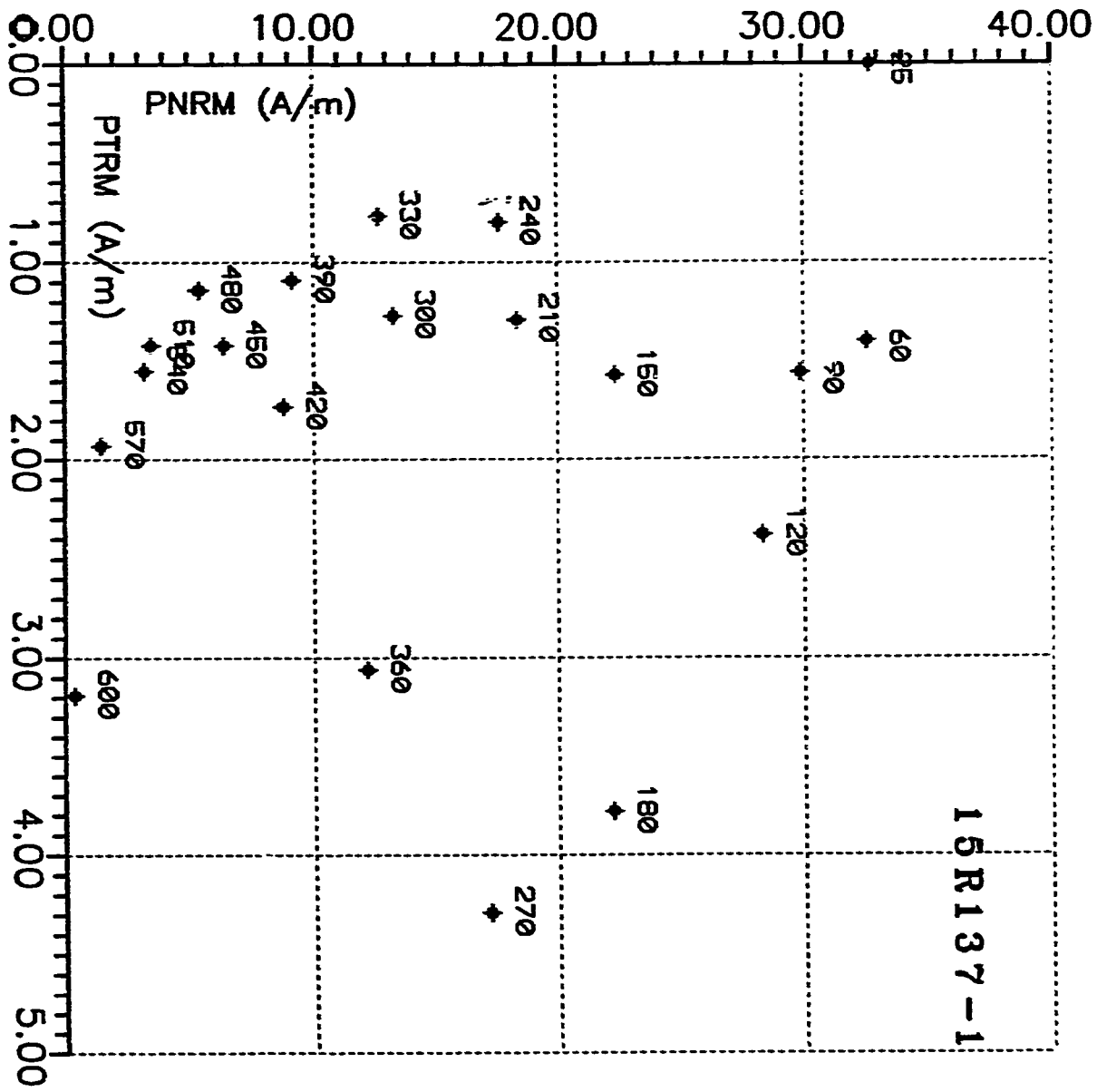
0.00
10.00
20.00
30.00
40.00
PNRM (A/m)
0.00
1.00
2.00
3.00
4.00
5.00
PTRM (A/m)
35
60
90
120
150
180
210
240
270
300
330
360
390
420
450
480
510
540
570
600
15R137-1

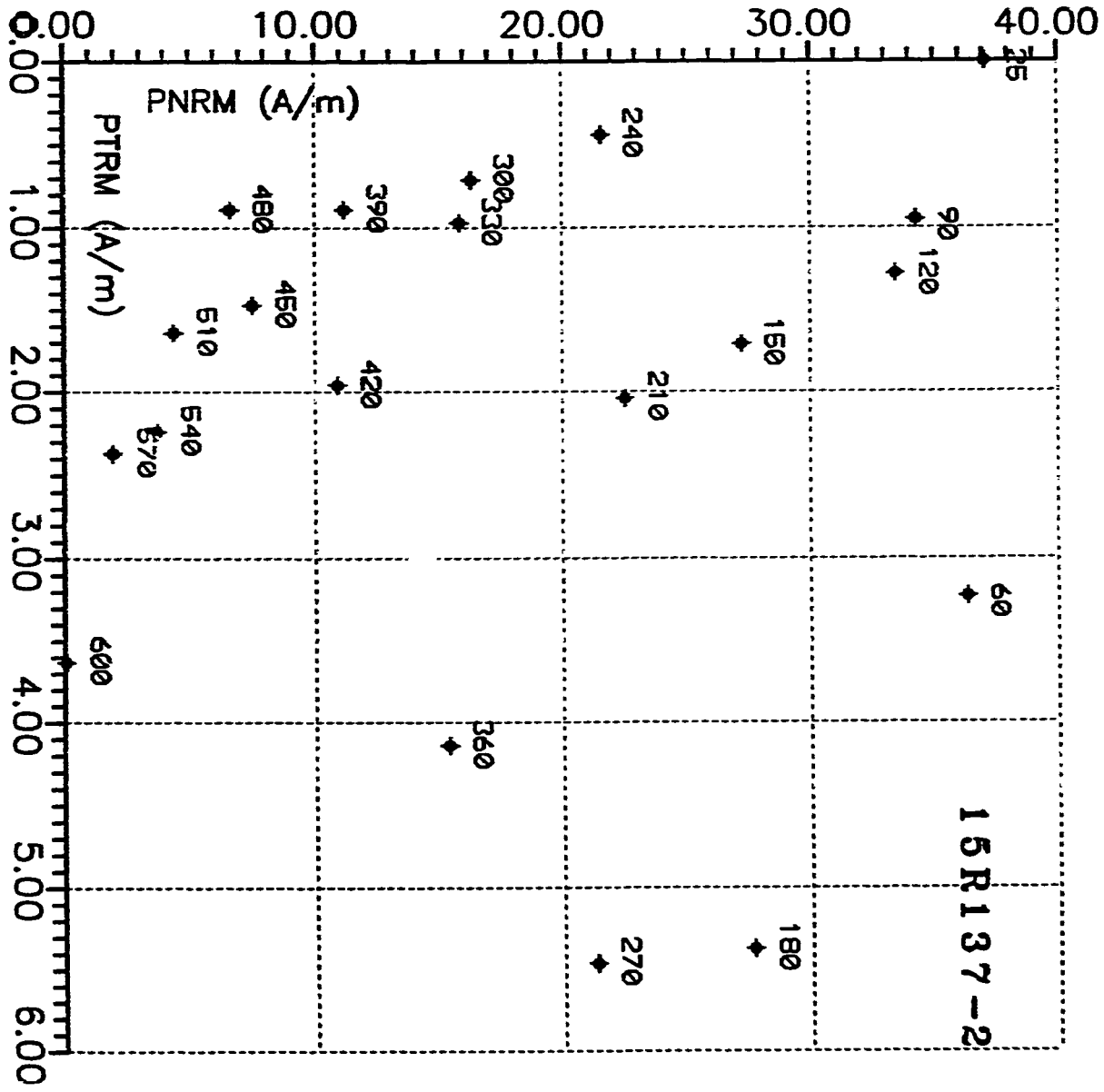
0.00
10.00
20.00
30.00
40.00
PNRM (A/m)
PTRM (A/m)
0.00
1.00
2.00
3.00
4.00
5.00
6.00
25
240
300
330
390
480
90
120
450
510
150
420
210
540
570
60
600
360
270
180
15R137-2

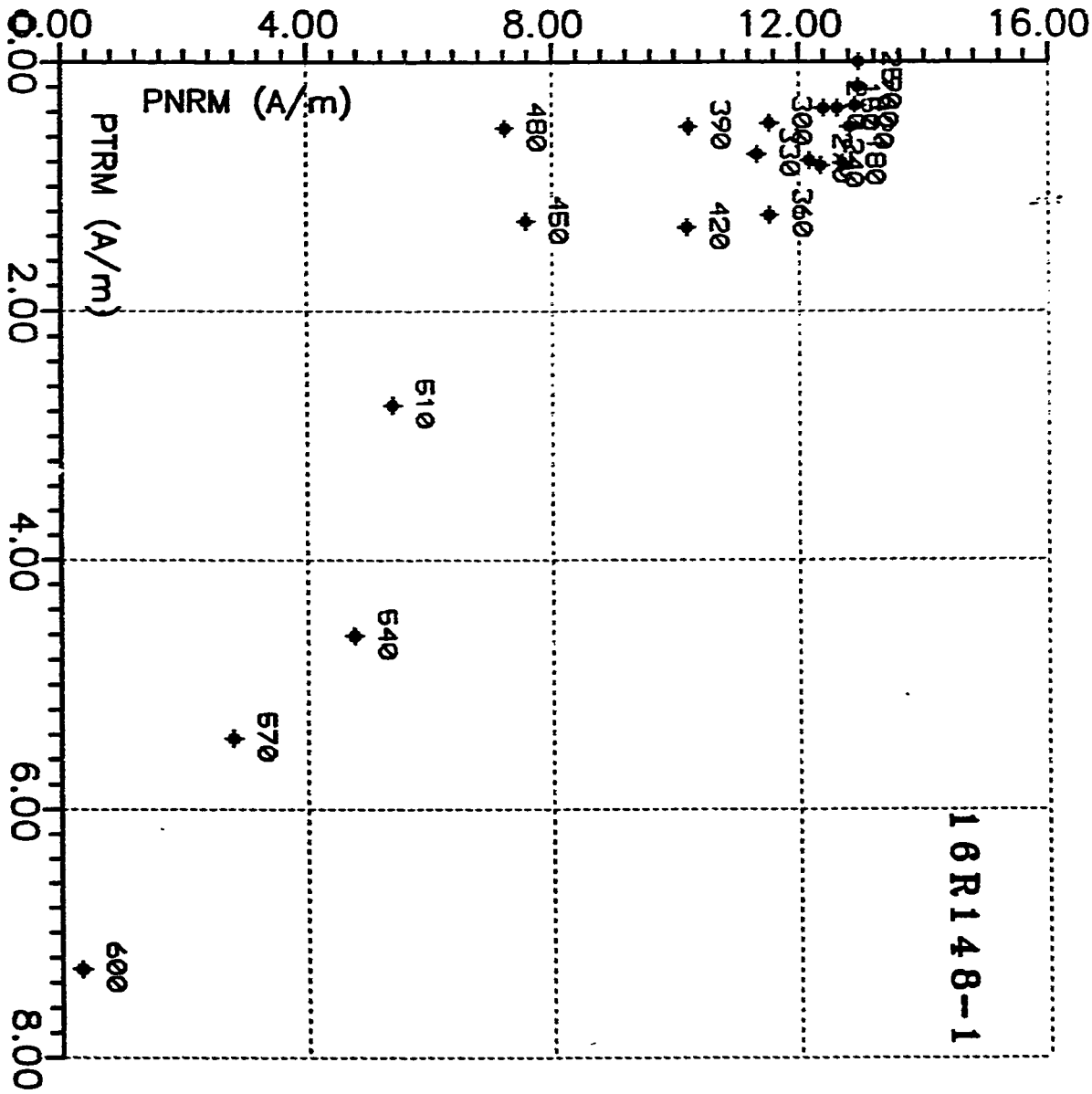
0.00
4.00
8.00
12.00
16.00
PNRM (A/m)
PTRM (A/m)
0.00
2.00
4.00
6.00
8.00
480
450
390
420
360
510
540
570
600
16R148-1

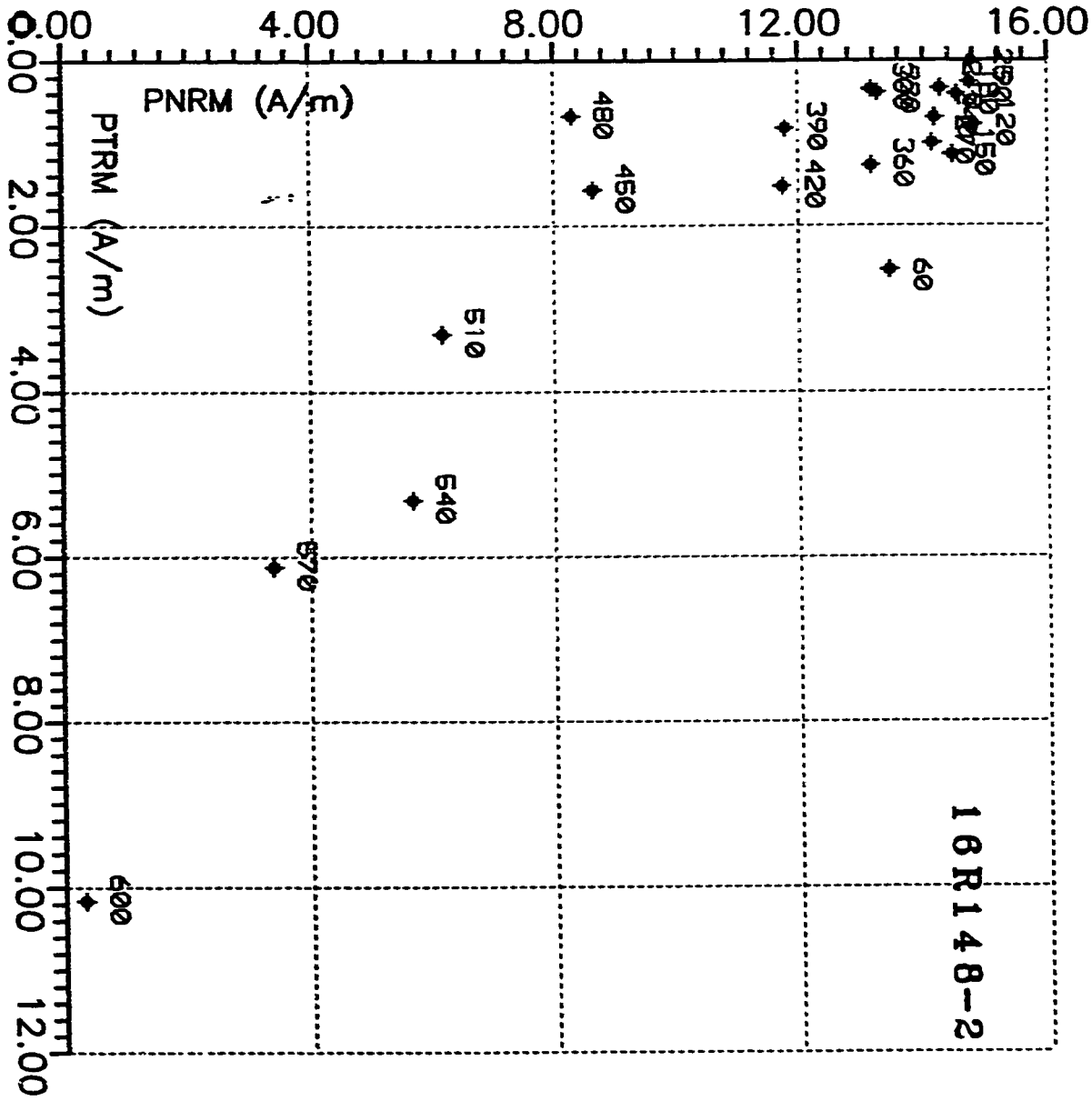
0.00
4.00
8.00
12.00
16.00
PNRM (A/m)
PTRM (A/m)
0.00
2.00
4.00
6.00
8.00
10.00
12.00
480
450
390
420
360
60
510
540
570
600
16R148-2

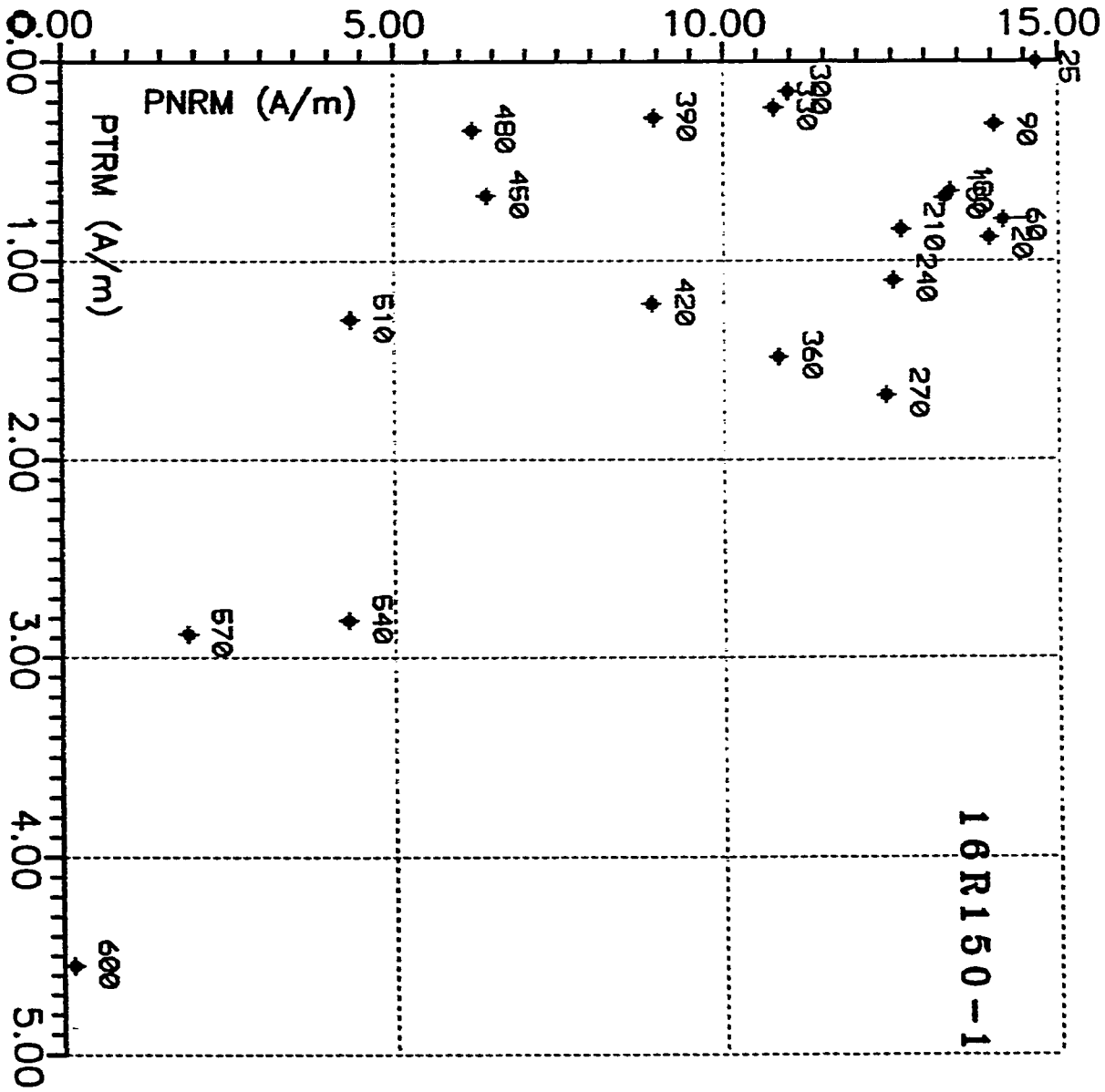
0.00
5.00
10.00
15.00
PNRM (A/m)
PTRM (A/m)
0.00
1.00
2.00
3.00
4.00
5.00
25
90
120
210
240
300
330
390
420
450
480
510
540
570
600
360
270
16R150-1

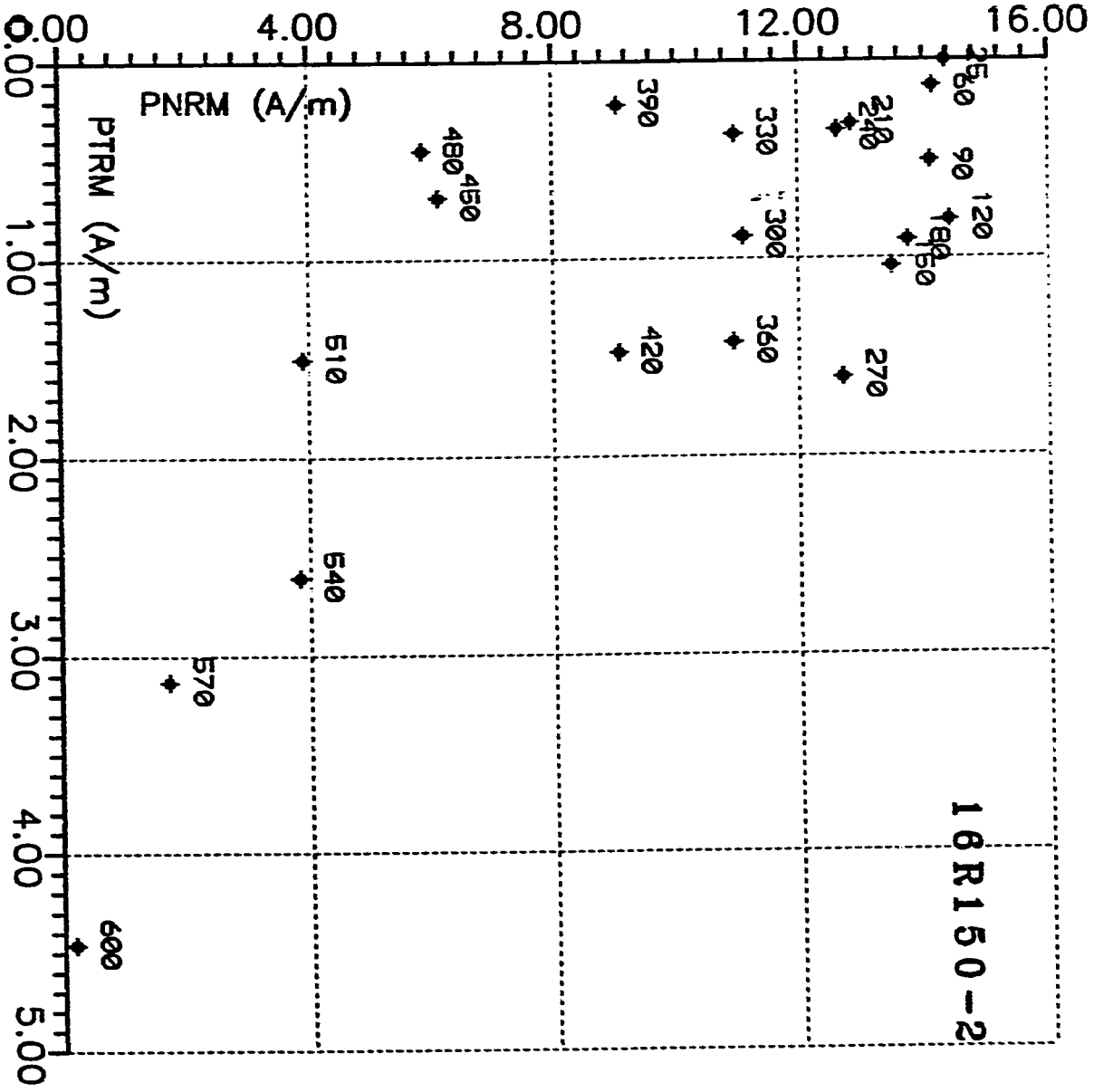
0.00
4.00
8.00
12.00
16.00
PNRM (A/m)
PTRM (A/m)
0.00
1.00
2.00
3.00
4.00
5.00
60
90
120
150
210
240
270
300
330
360
390
420
450
480
510
540
570
600
16R150-2

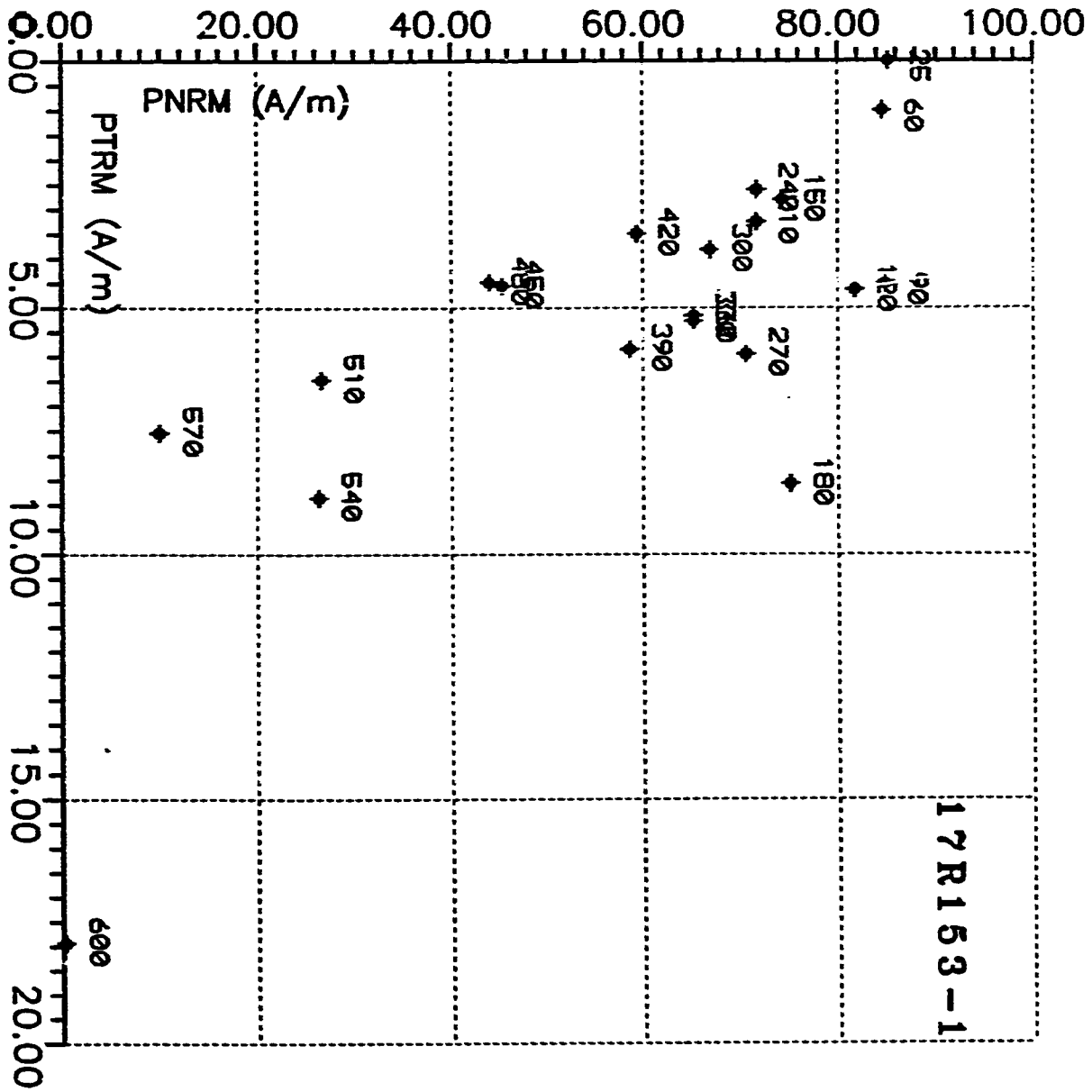
0.00
20.00
40.00
60.00
80.00
100.00
PNRM (A/m)
PTRM (A/m)
0.00
5.00
10.00
15.00
20.00
25
60
90
120
150
180
210
240
270
300
330
360
390
420
450
480
510
540
570
600
17R153-1

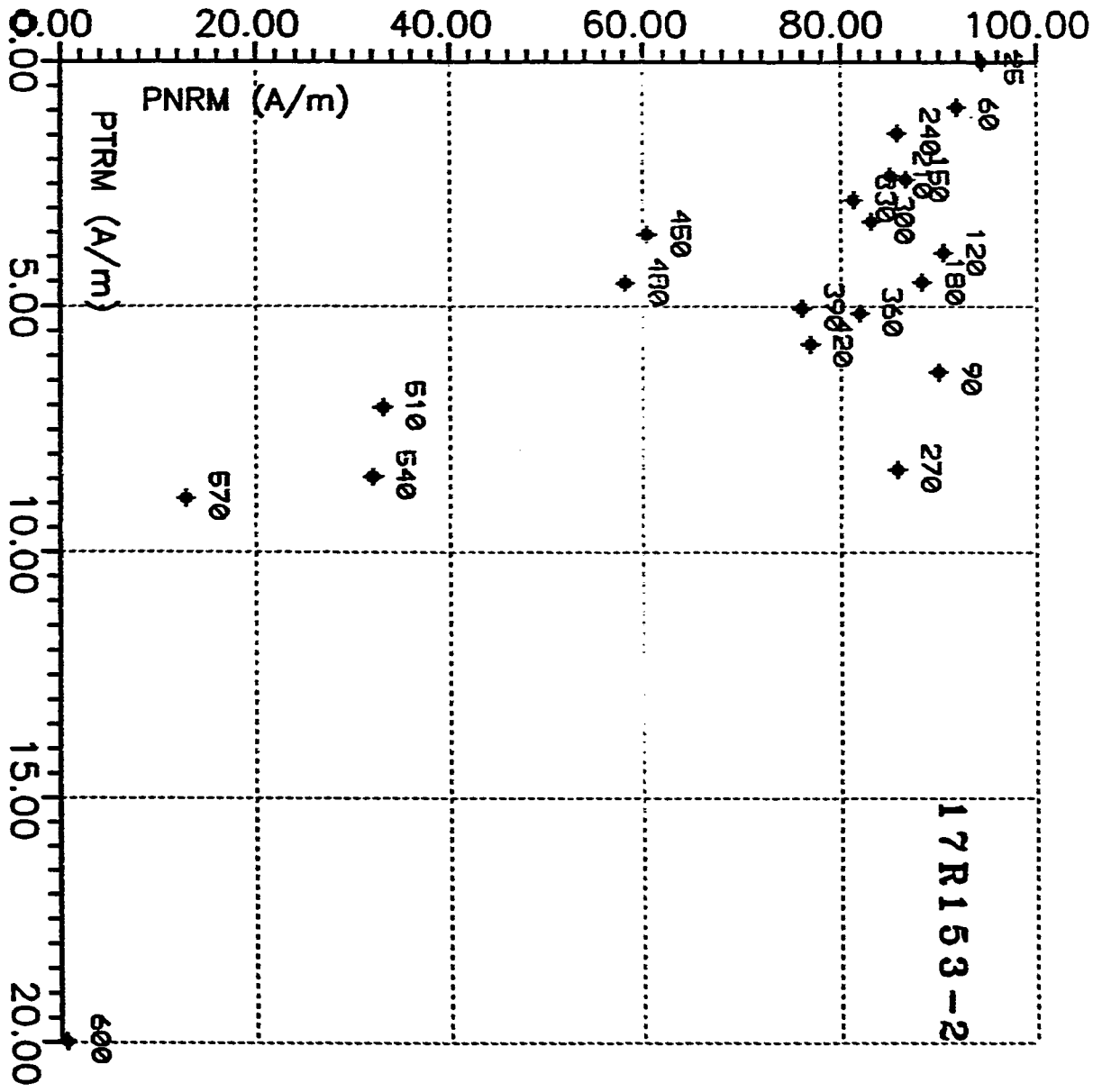
0.00
20.00
40.00
60.00
80.00
100.00
PNRM (A/m)
PTRM (A/m)
0.00
5.00
10.00
15.00
20.00
45
60
240
150
300
120
180
450
480
390
420
360
90
270
510
540
570
600
17R153-2

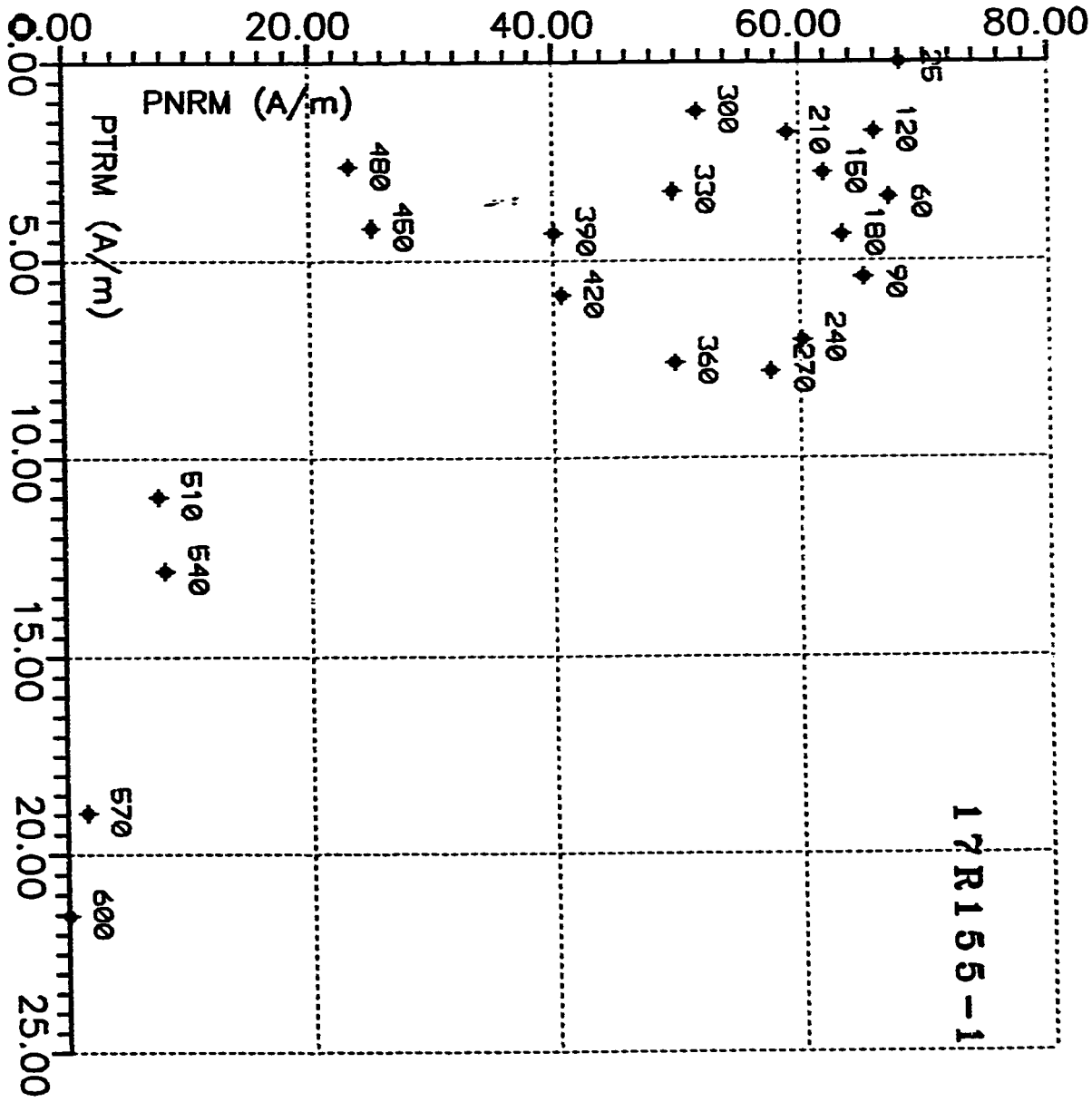
0.00
20.00
40.00
60.00
80.00
PNRM (A/m)
PTRM (A/m)
0.00
5.00
10.00
15.00
20.00
25.00
25
120
60
300
210
150
180
90
330
480
450
390
420
240
360
270
510
540
570
600
17R155-1

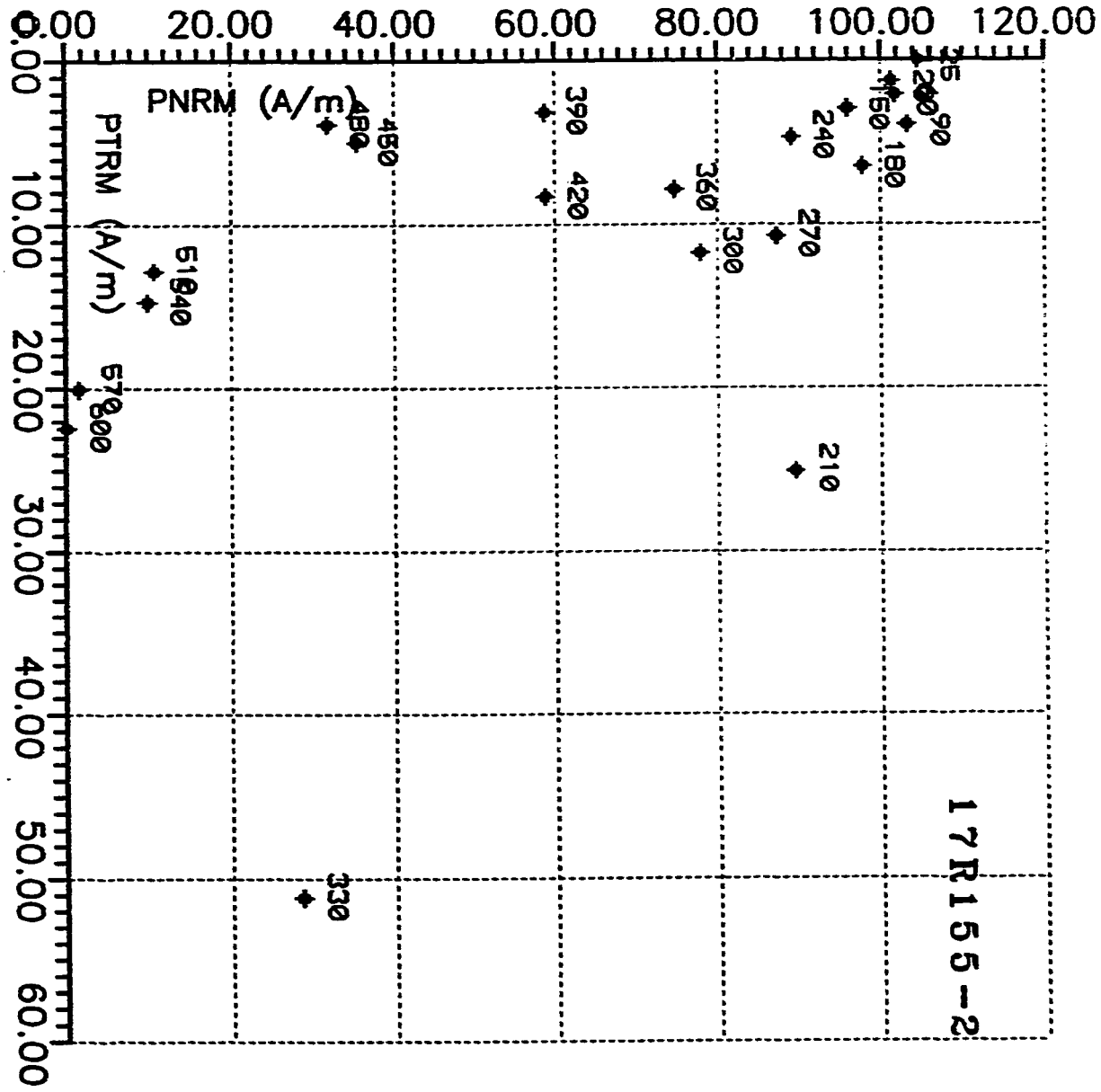
0.00
20.00
40.00
60.00
80.00
100.00
120.00
PNRM (A/m)
PTRM (A/m)
0.00
10.00
20.00
30.00
40.00
50.00
60.00
90
150
180
240
270
300
360
390
420
450
480
210
330
510
540
570
600
17R155-2

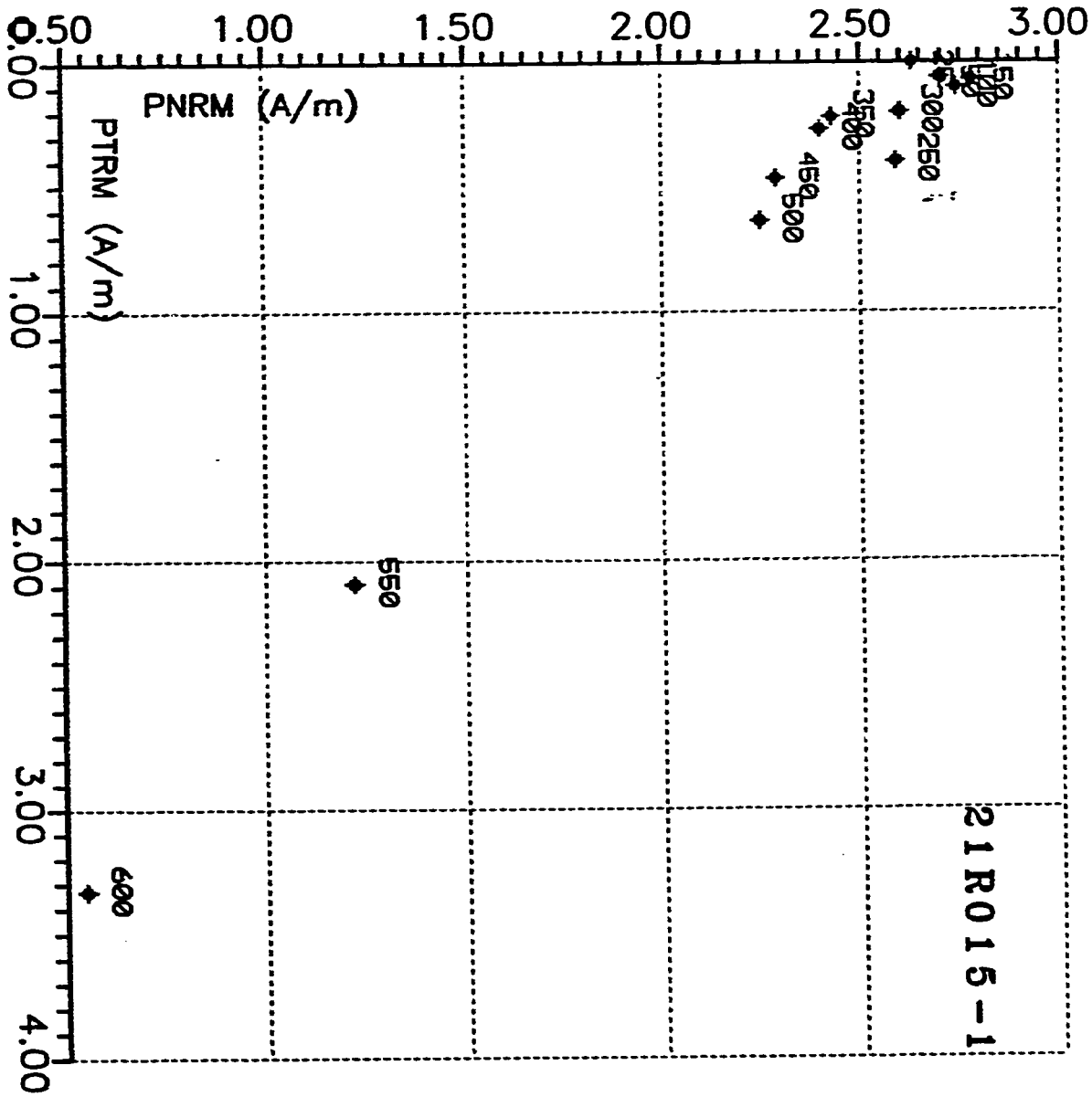
0.50
1.00
1.50
2.00
2.50
3.00
PNRM (A/m)
PTRM (A/m)
0.00
1.00
2.00
3.00
4.00
550
600
21R015-1

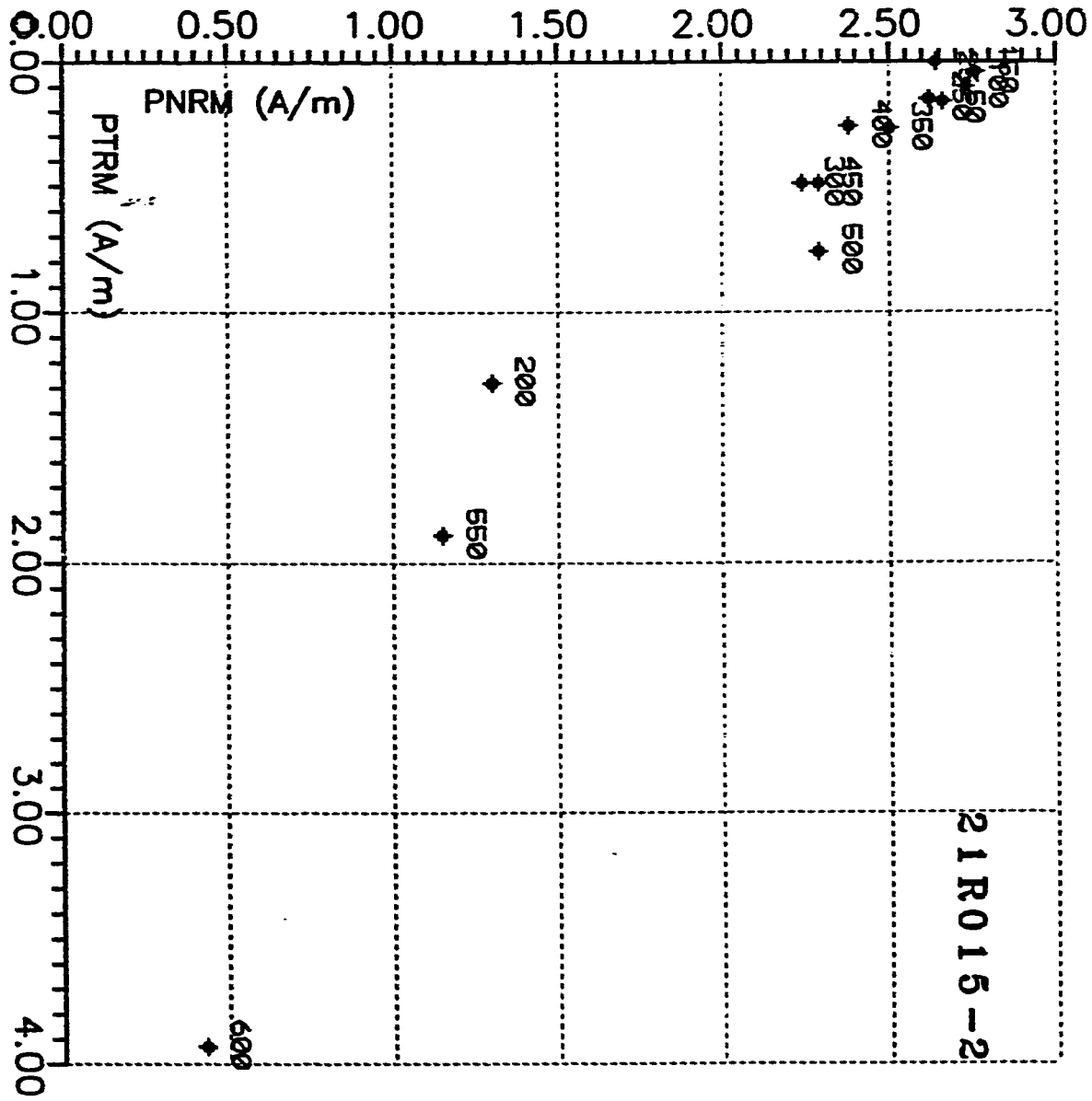
0.00
0.50
1.00
1.50
2.00
2.50
3.00
PNRM (A/m)
PTRM (A/m)
1.00
2.00
3.00
4.00
350
400
450
500
200
550
600
21R015-2

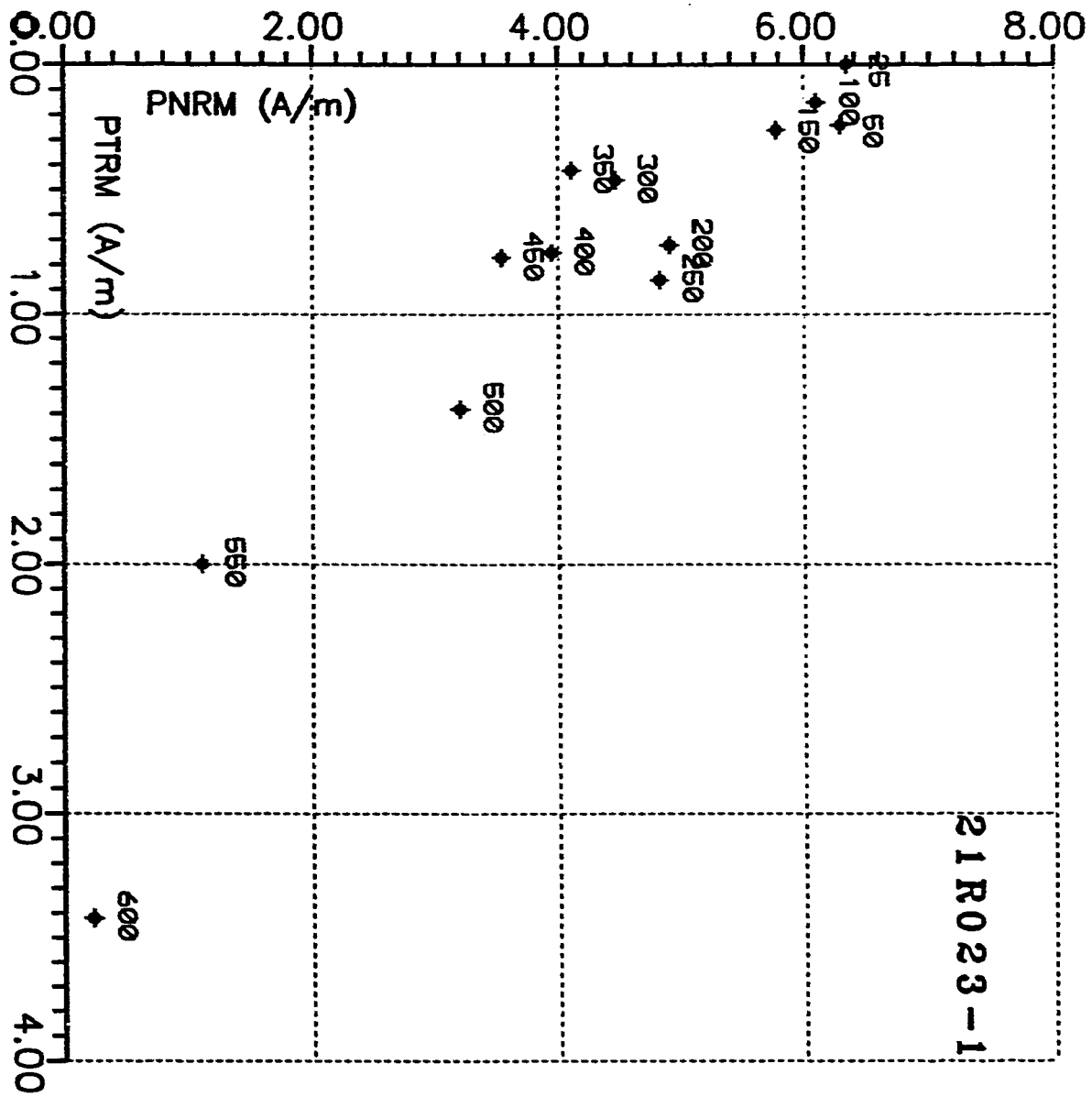
0.00
2.00
4.00
6.00
8.00
PNRM (A/m)
PTRM (A/m)
0.00
1.00
2.00
3.00
4.00
25
50
100
150
300
350
400
450
200
250
500
550
600
21R023-1

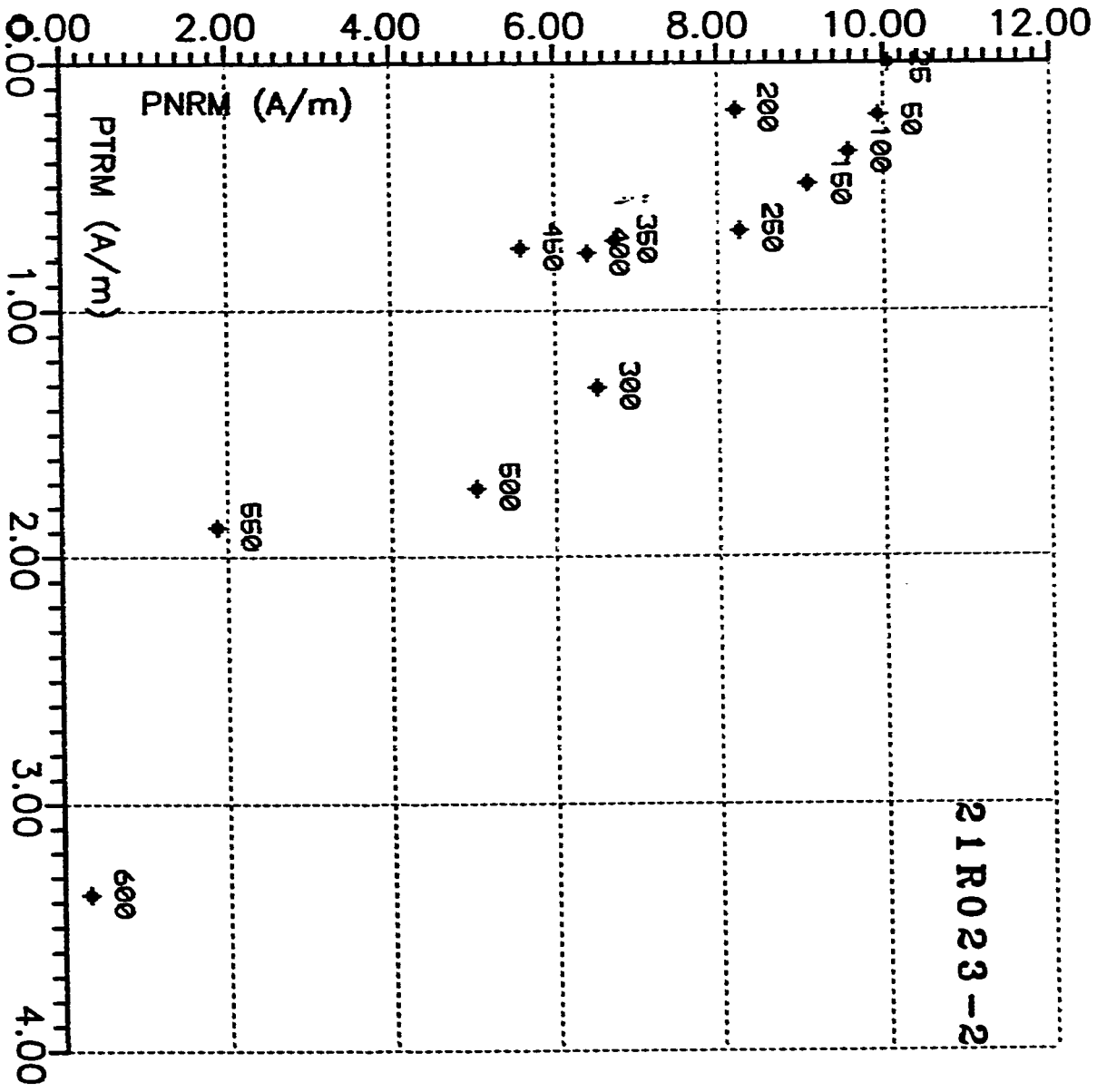
0.00
2.00
4.00
6.00
8.00
10.00
12.00
PNRM (A/m)
PTRM (A/m)
0.00
1.00
2.00
3.00
4.00
25
50
100
150
200
250
350
400
450
300
500
550
600
21R023-2

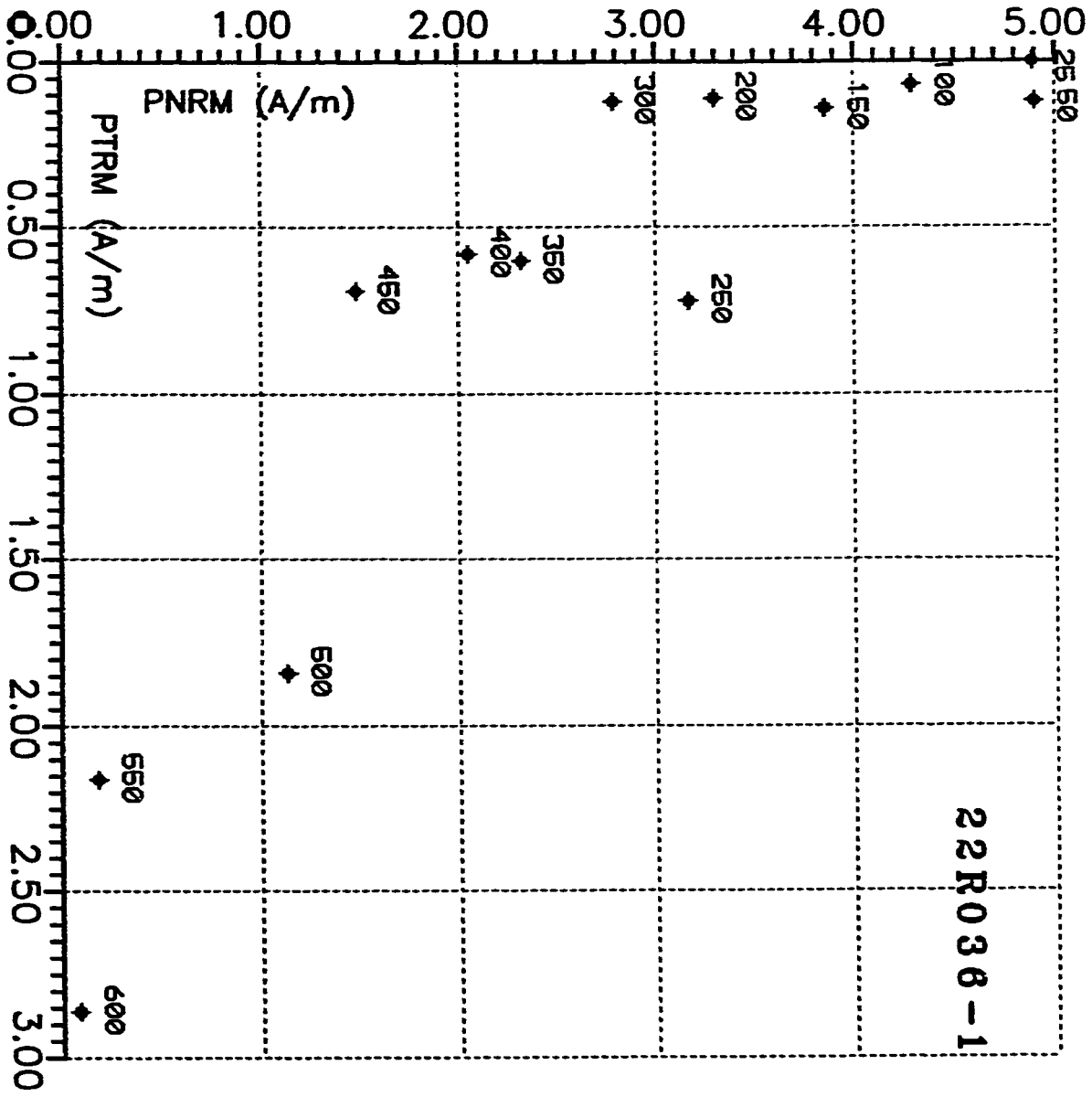
0.00
1.00
2.00
3.00
4.00
5.00
PNRM (A/m)
0.00
0.50
1.00
1.50
2.00
2.50
3.00
PTRM (A/m)
25.50
100
150
200
300
250
350
400
450
500
550
600
22R036-1

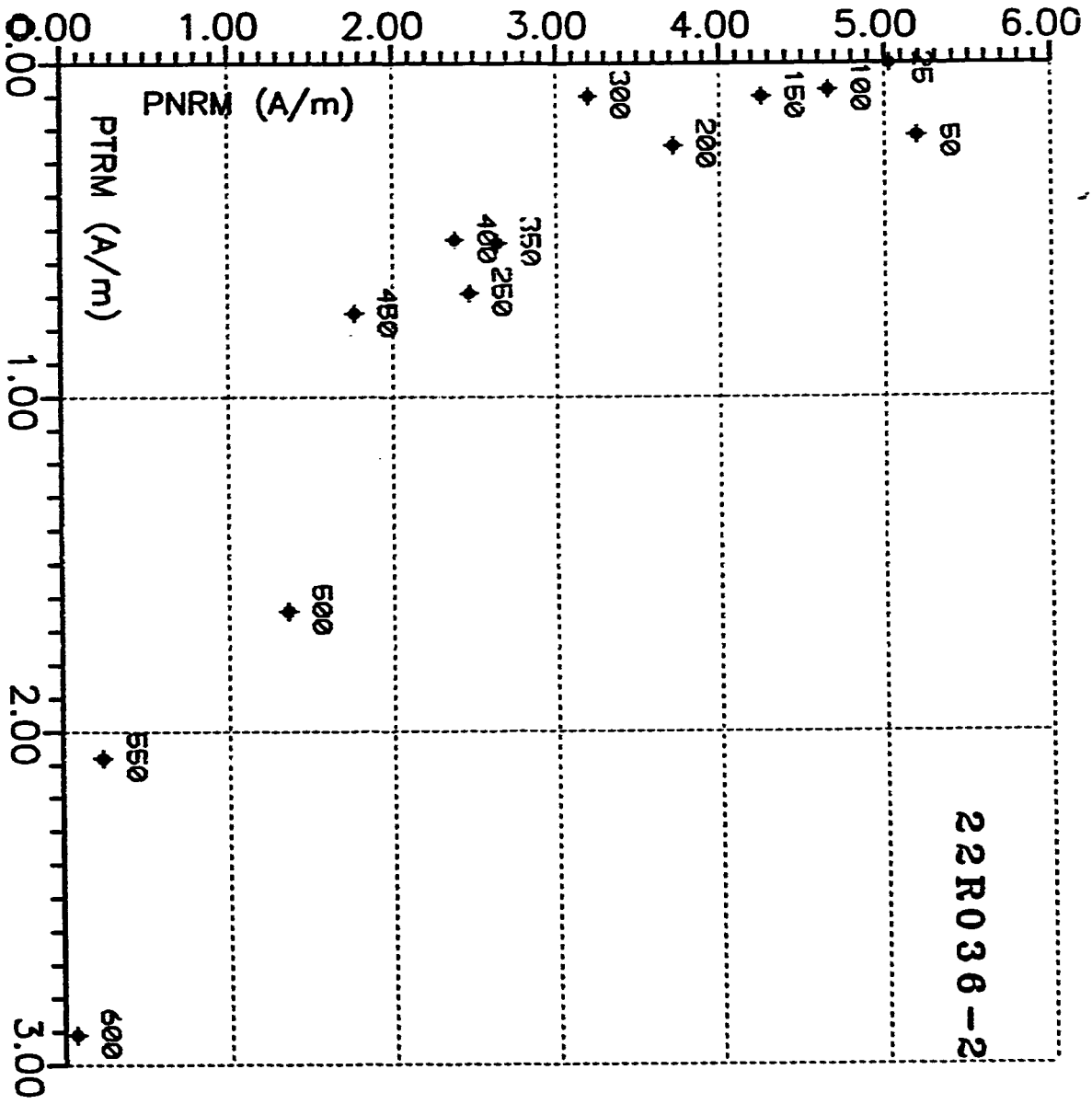
0.00
1.00
2.00
3.00
4.00
5.00
6.00
PNRM (A/m)
PTRM (A/m)
0.00
1.00
2.00
3.00
25
50
100
150
200
300
350
400
250
450
500
550
600
22R036-2

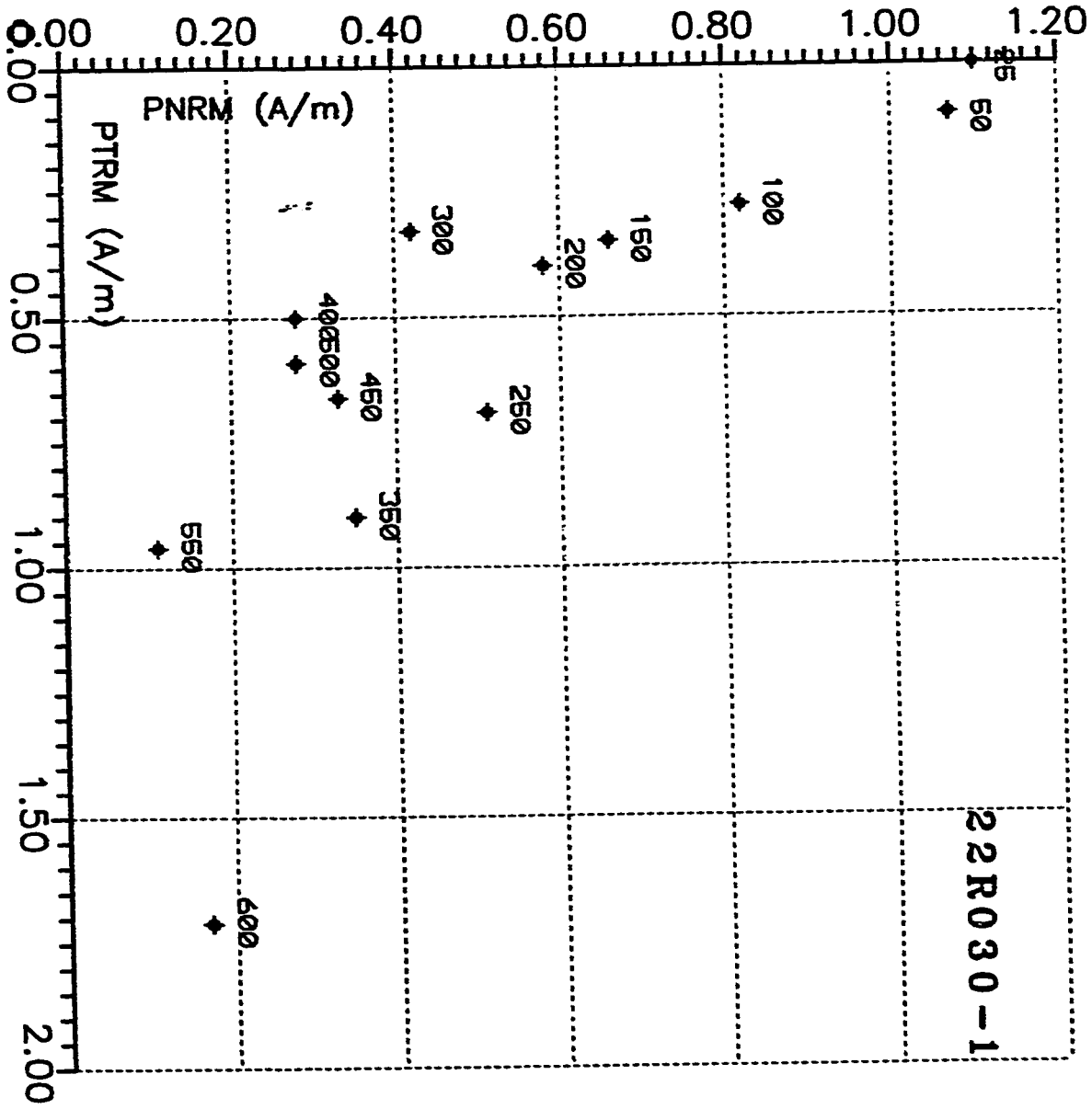
0.00
0.20
0.40
0.60
0.80
1.00
1.20
PNRM (A/m)
0.00
0.50
1.00
1.50
2.00
PTRM (A/m)
25
50
100
150
200
300
400
500
450
250
350
550
600
22R030-1

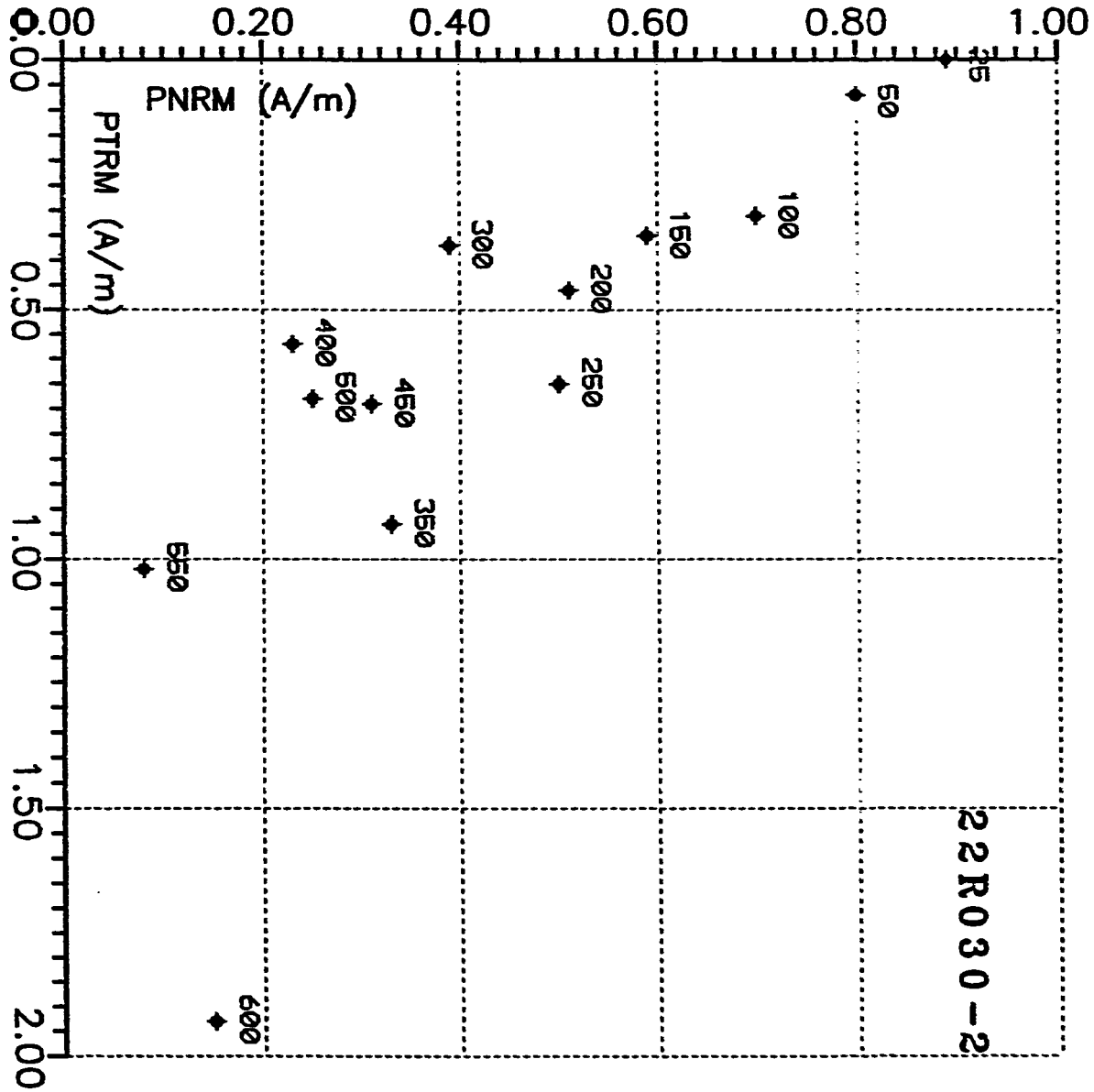
0.00
0.20
0.40
0.60
0.80
1.00
0.00
0.50
1.00
1.50
2.00
PNRM (A/m)
PTRM (A/m)
25
50
100
150
300
200
400
500
450
250
350
550
600
22R030-2

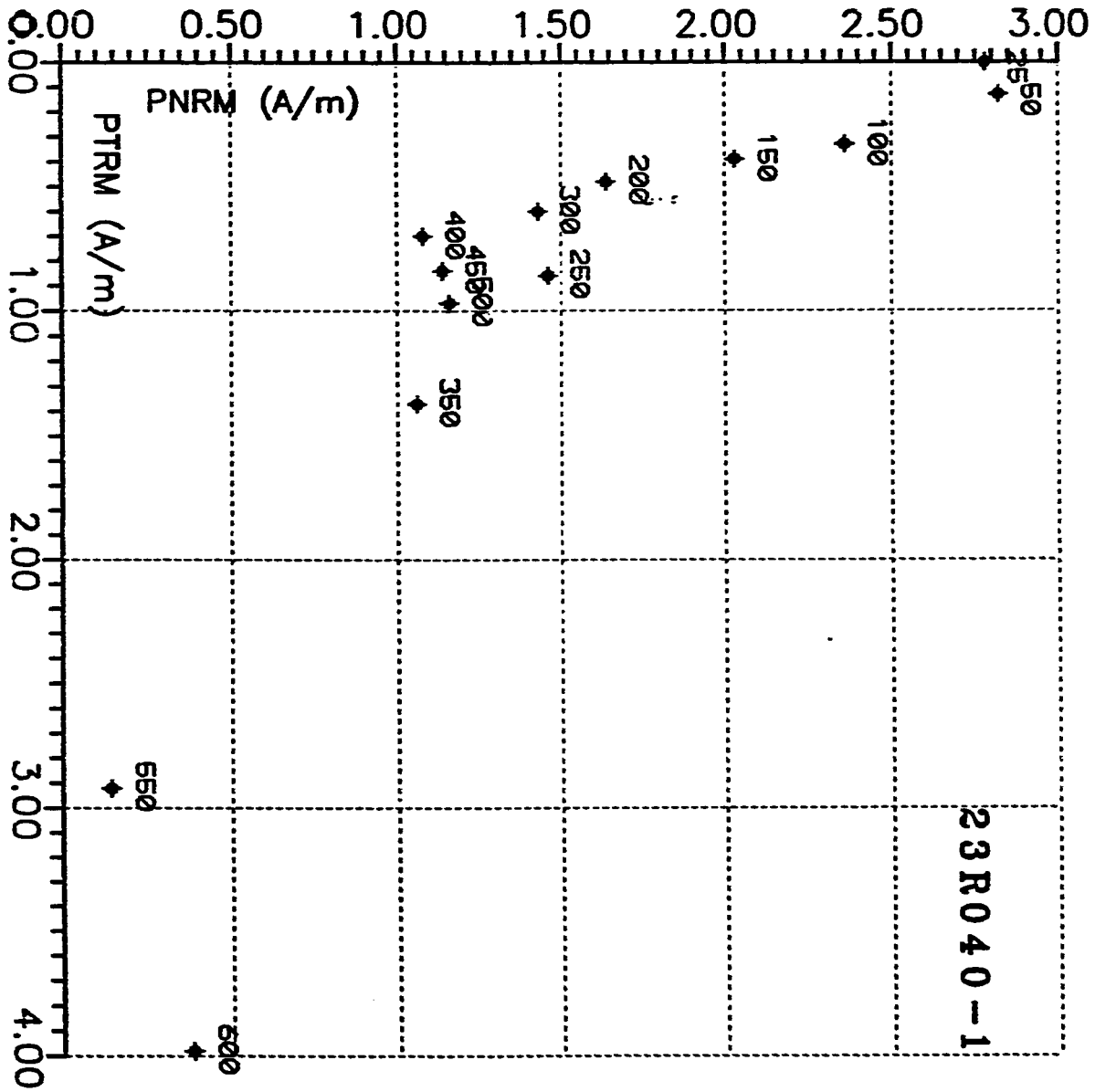
0.00
0.50
1.00
1.50
2.00
2.50
3.00
PNRM (A/m)
PTRM (A/m)
0.00
1.00
2.00
3.00
4.00
50
100
150
200
250
300
350
400
450
500
550
600
23R040-1

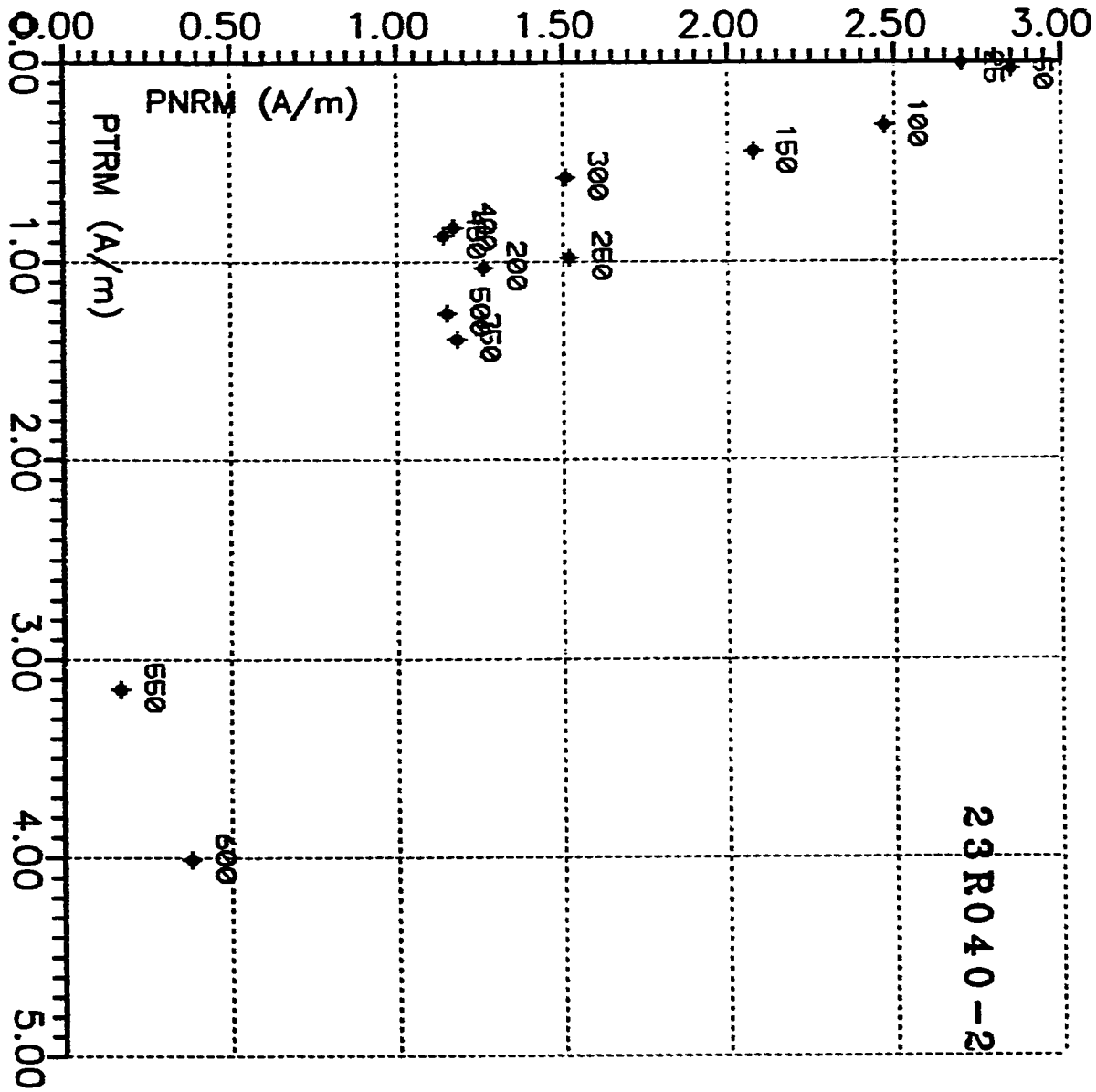
0.00
0.50
1.00
1.50
2.00
2.50
3.00
PNRM (A/m)
PTRM (A/m)
0.00
1.00
2.00
3.00
4.00
5.00
50
100
150
300
250
200
550
600
23R040-2

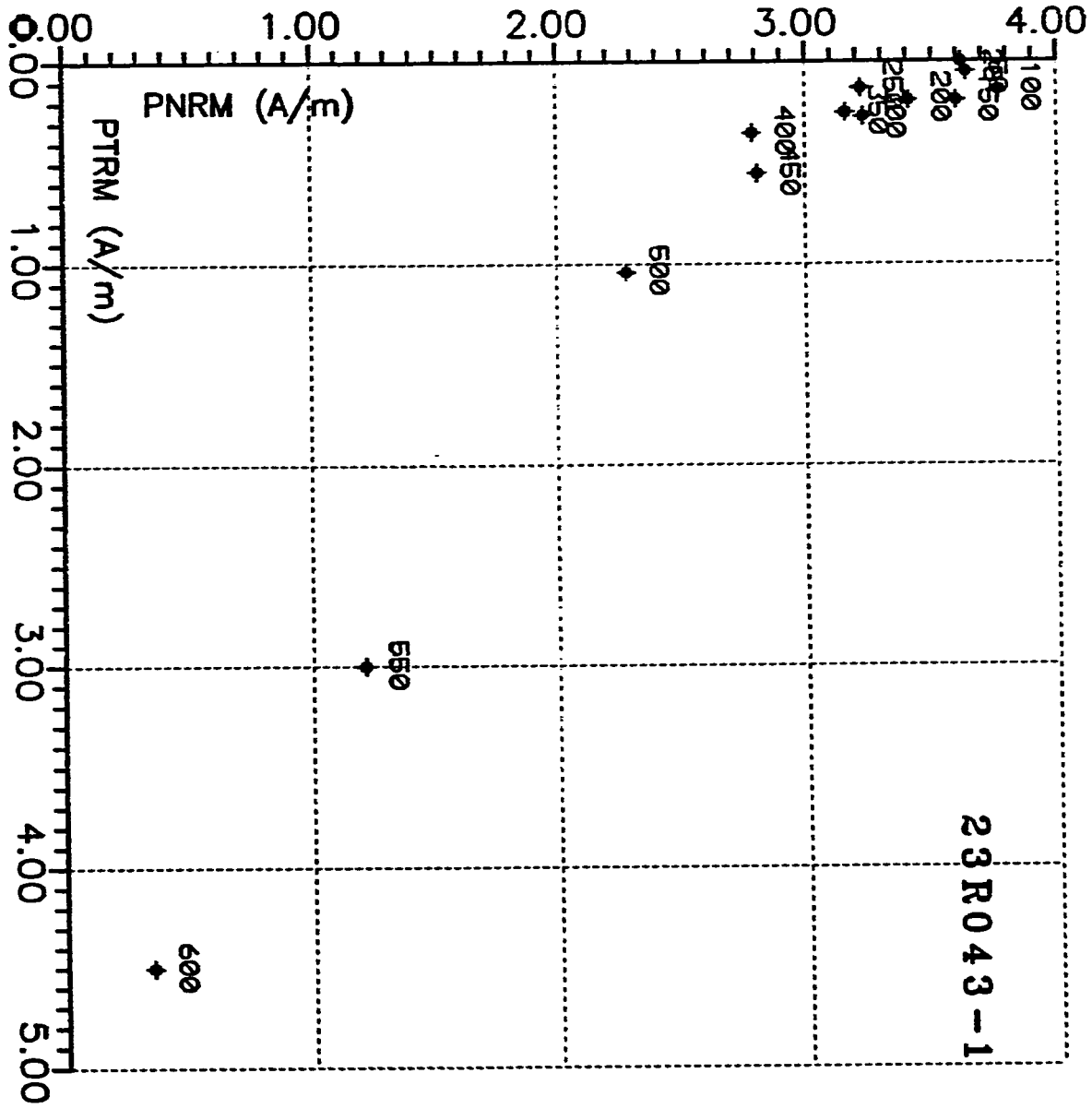
0.00
1.00
2.00
3.00
4.00
PNRM (A/m)
PTRM (A/m)
0.00
1.00
2.00
3.00
4.00
5.00
100
200
400
500
550
600
23R043-1

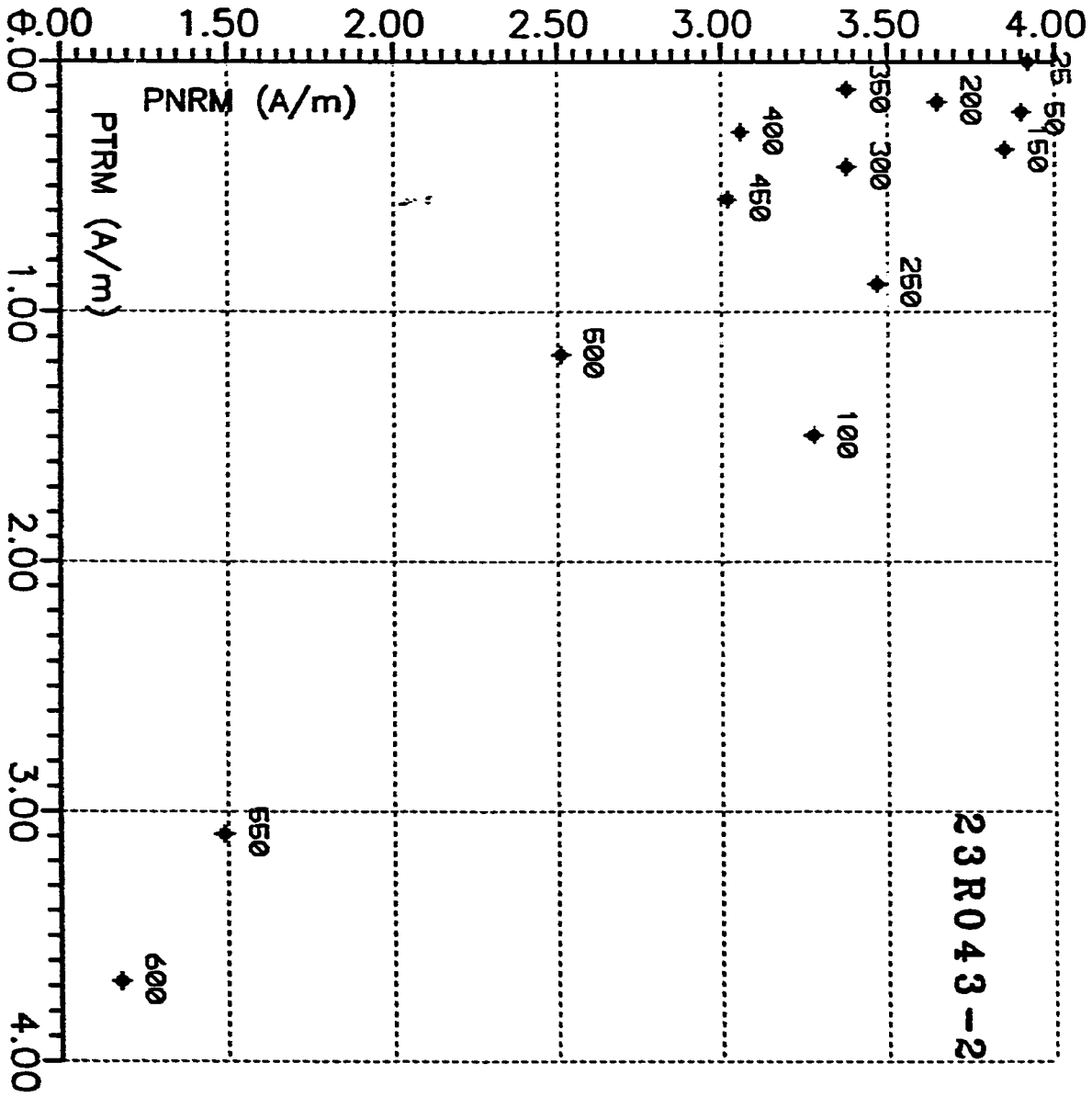
0.00
1.50
2.00
2.50
3.00
3.50
4.00
PNRM (A/m)
PTRM (A/m)
1.00
2.00
3.00
4.00
25
50
50
200
350
300
400
450
250
500
100
550
600
23R043-2

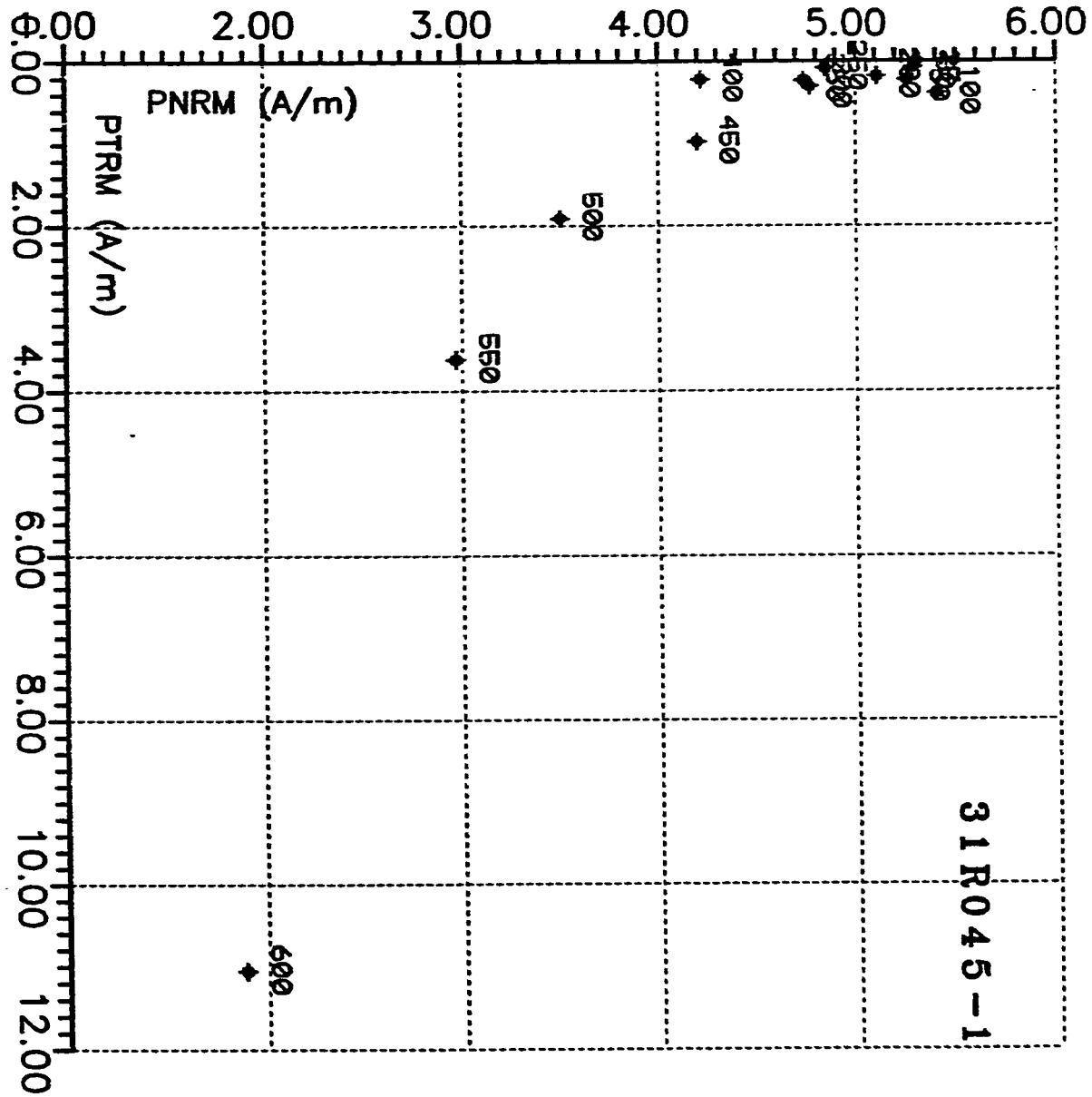
0.00
2.00
3.00
4.00
5.00
6.00
PNRM (A/m)
PTRM (A/m)
0.00
2.00
4.00
6.00
8.00
10.00
12.00
450
500
550
600
31R045-1

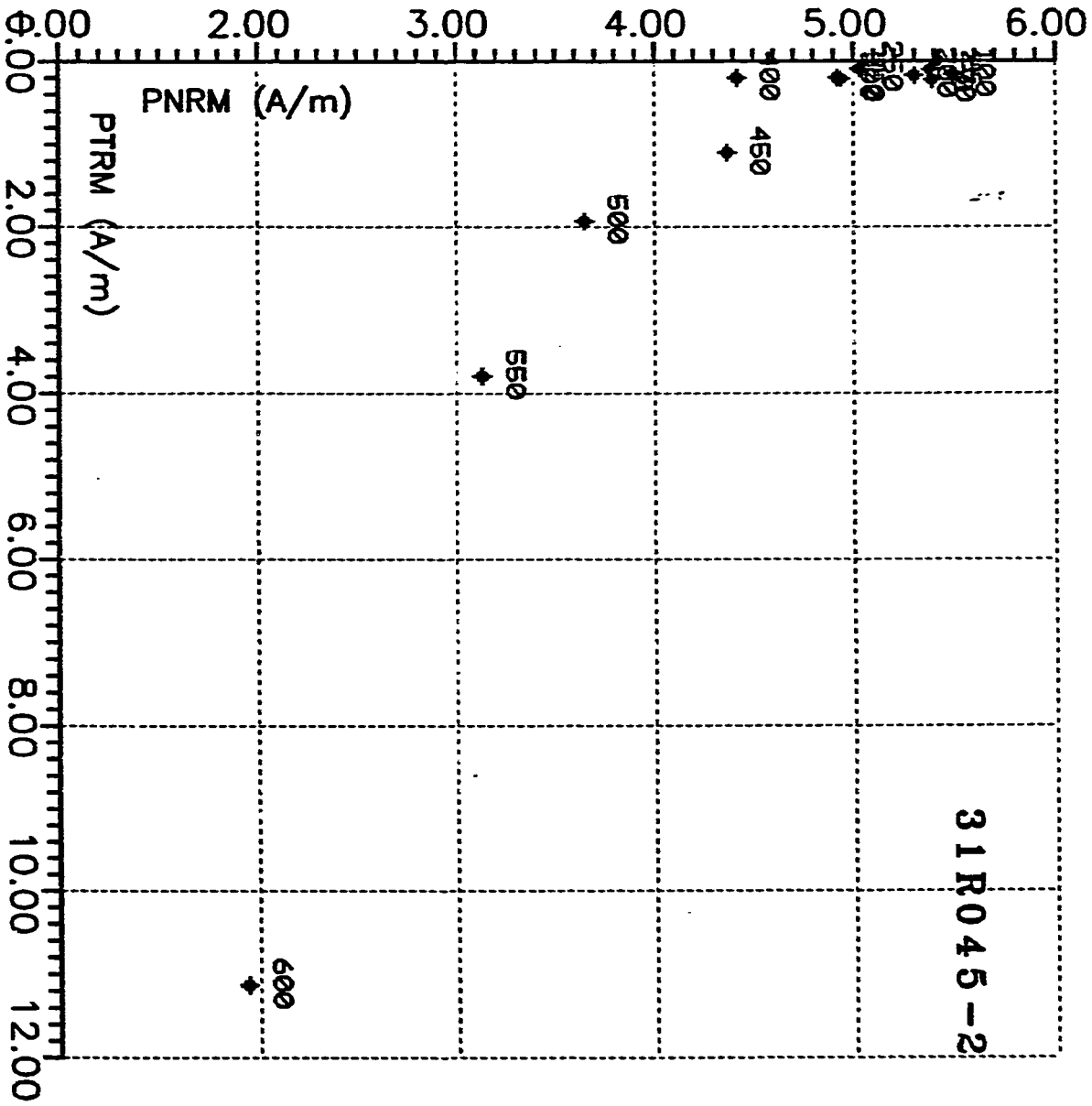
0.00
2.00
3.00
4.00
5.00
6.00
PNRM (A/m)
PTRM (A/m)
0.00
2.00
4.00
6.00
8.00
10.00
12.00
450
500
550
600
31R045-2

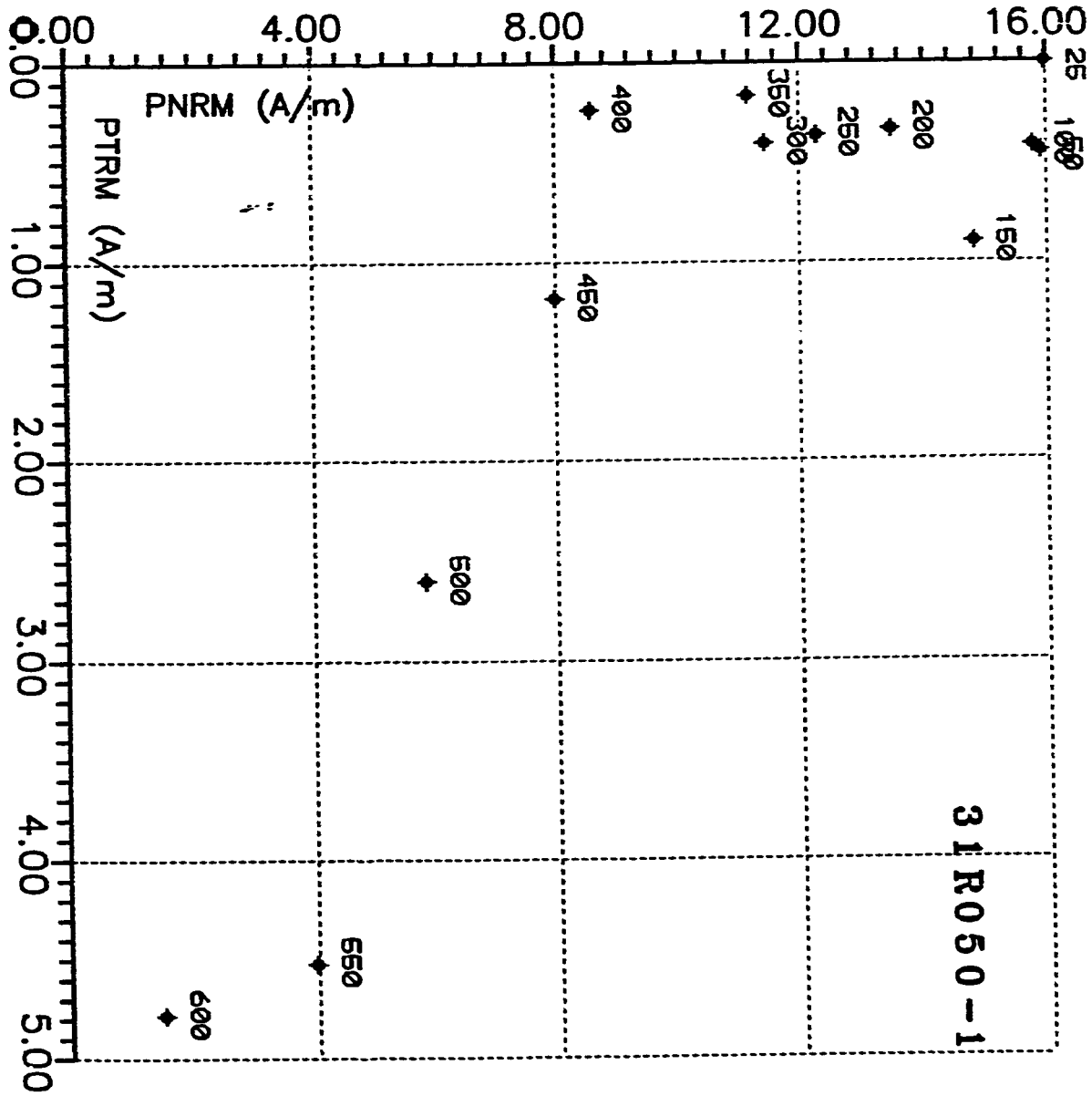
0.00
4.00
8.00
12.00
16.00
PNRM (A/m)
0.00
1.00
2.00
3.00
4.00
5.00
PTRM (A/m)
25
100
150
200
250
300
350
400
450
500
550
600
31R050-1

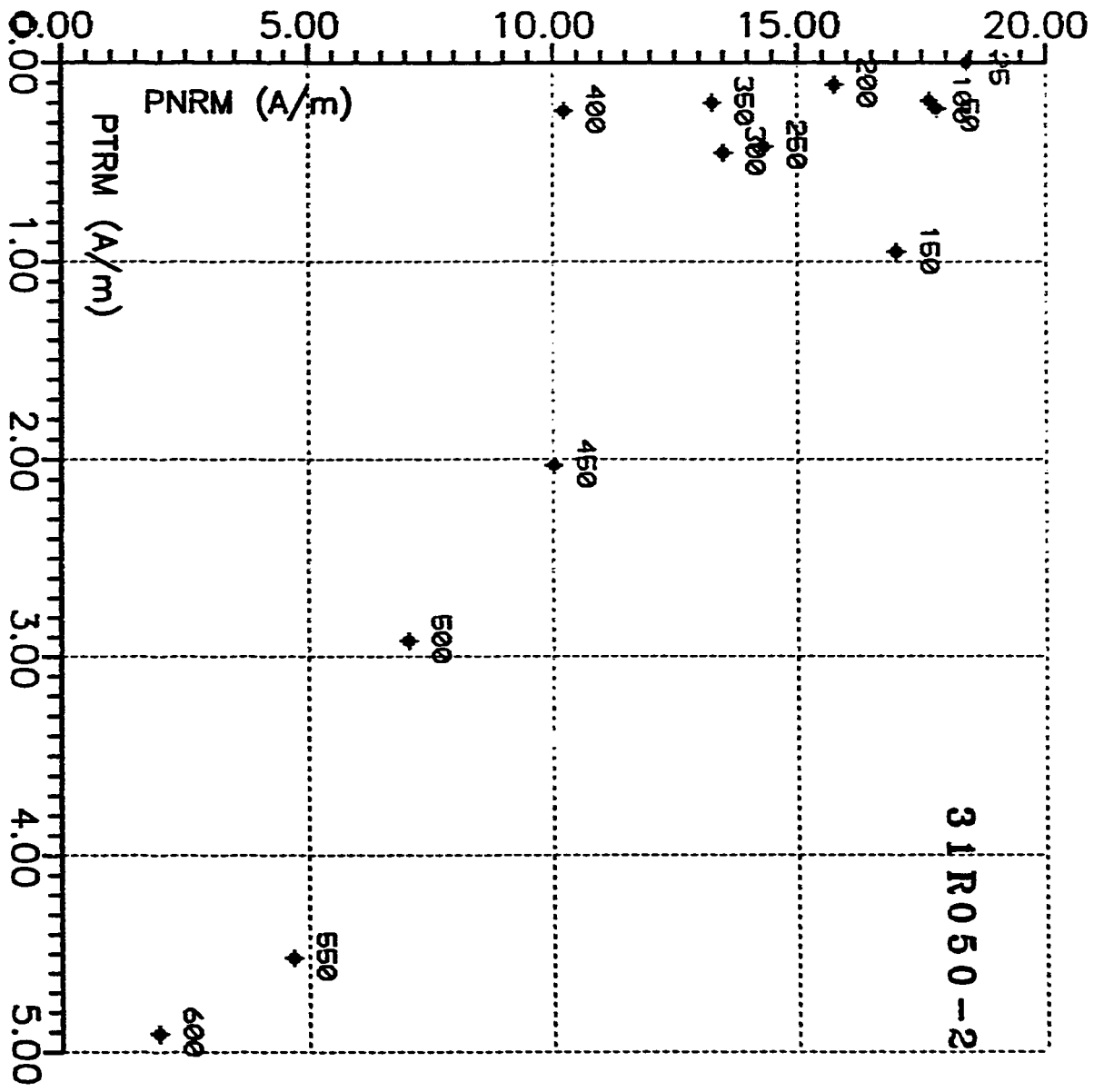
0.00
5.00
10.00
15.00
20.00
PNRM (A/m)
PTRM (A/m)
0.00
1.00
2.00
3.00
4.00
5.00
100
150
200
250
300
350
400
450
500
550
600
31R050-2

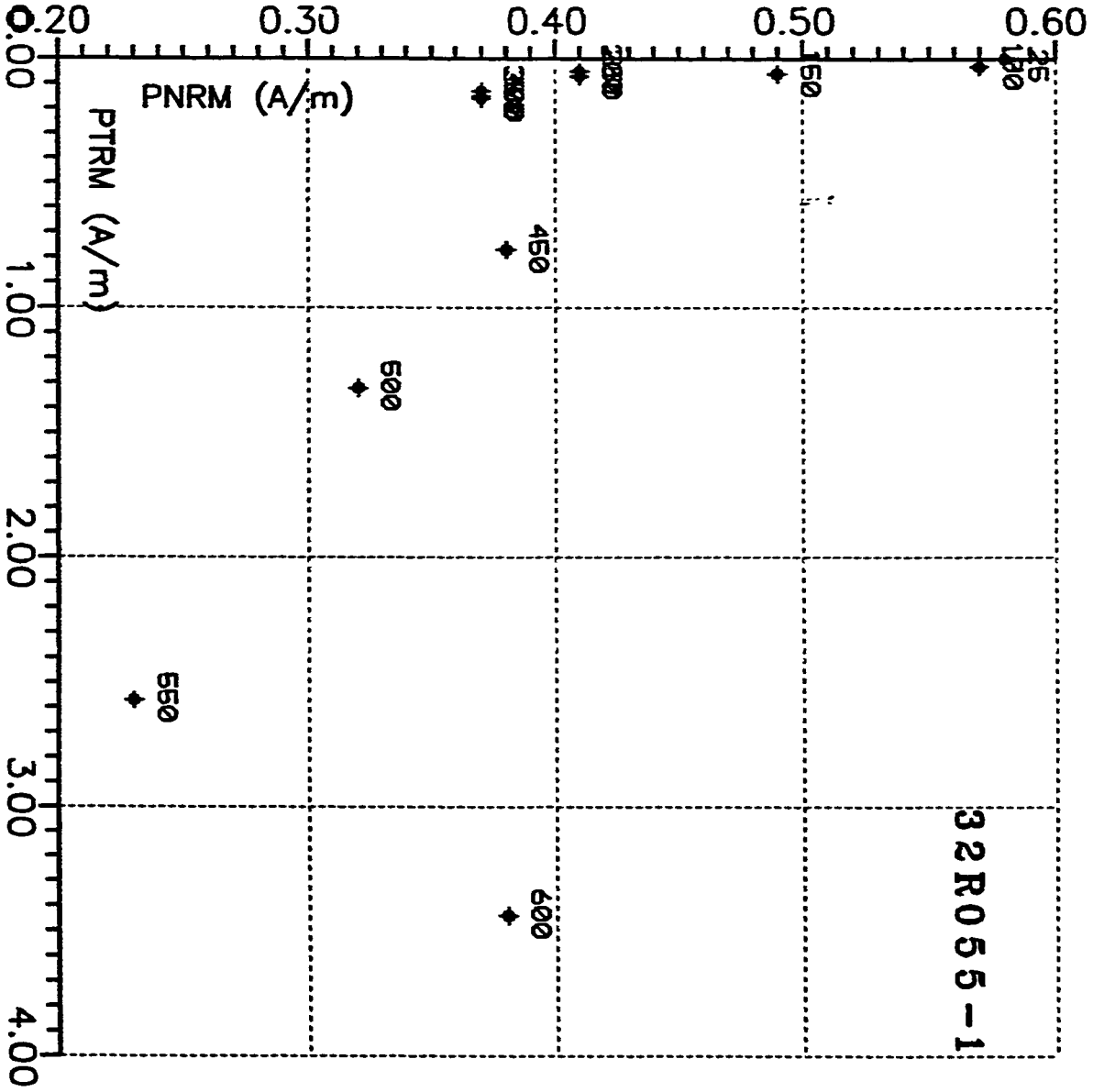
0.20
0.30
0.40
0.50
0.60
PNRM (A/m)
0.00
1.00
2.00
3.00
4.00
PTRM (A/m)
450
500
550
600
32R055-1

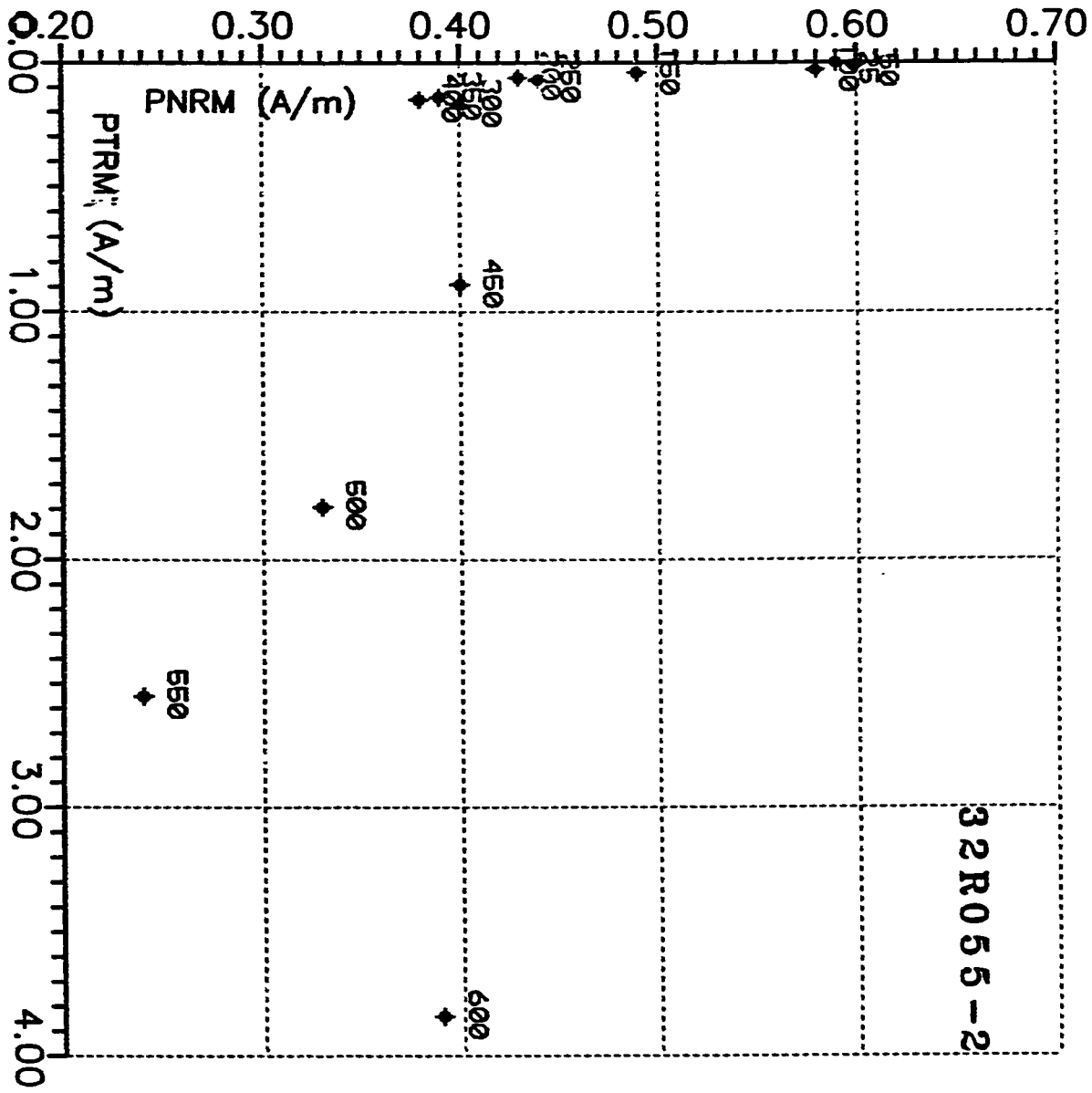
0.20
0.30
0.40
0.50
0.60
0.70
PNRM (A/m)
PTRM (A/m)
0.00
1.00
2.00
3.00
4.00
450
500
550
600
32R055-2

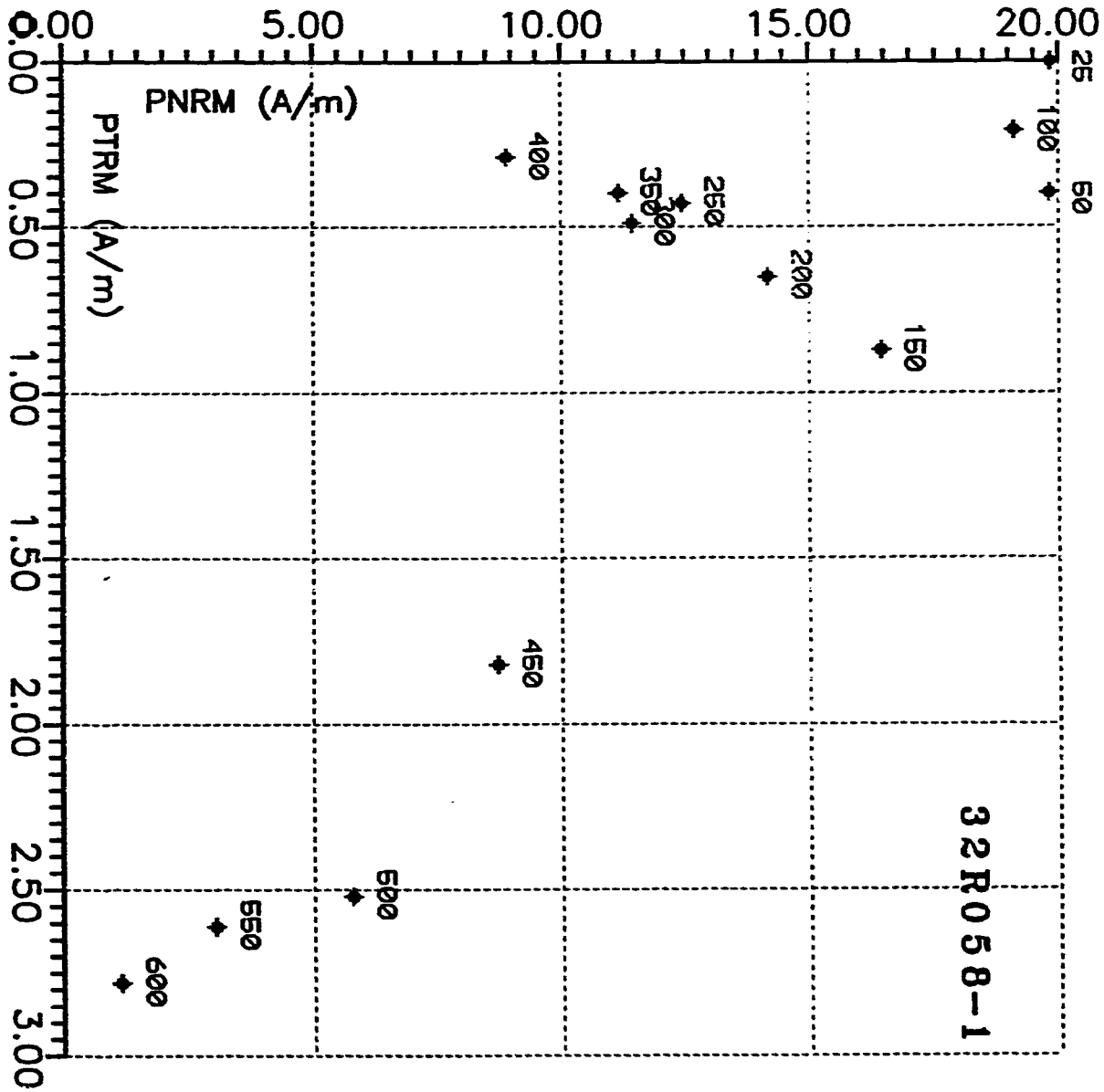
0.00
5.00
10.00
15.00
20.00
PNRM (A/m)
0.00
0.50
1.00
1.50
2.00
2.50
3.00
PTRM (A/m)
25
100
50
400
350
300
250
200
150
450
500
550
600
32R058-1

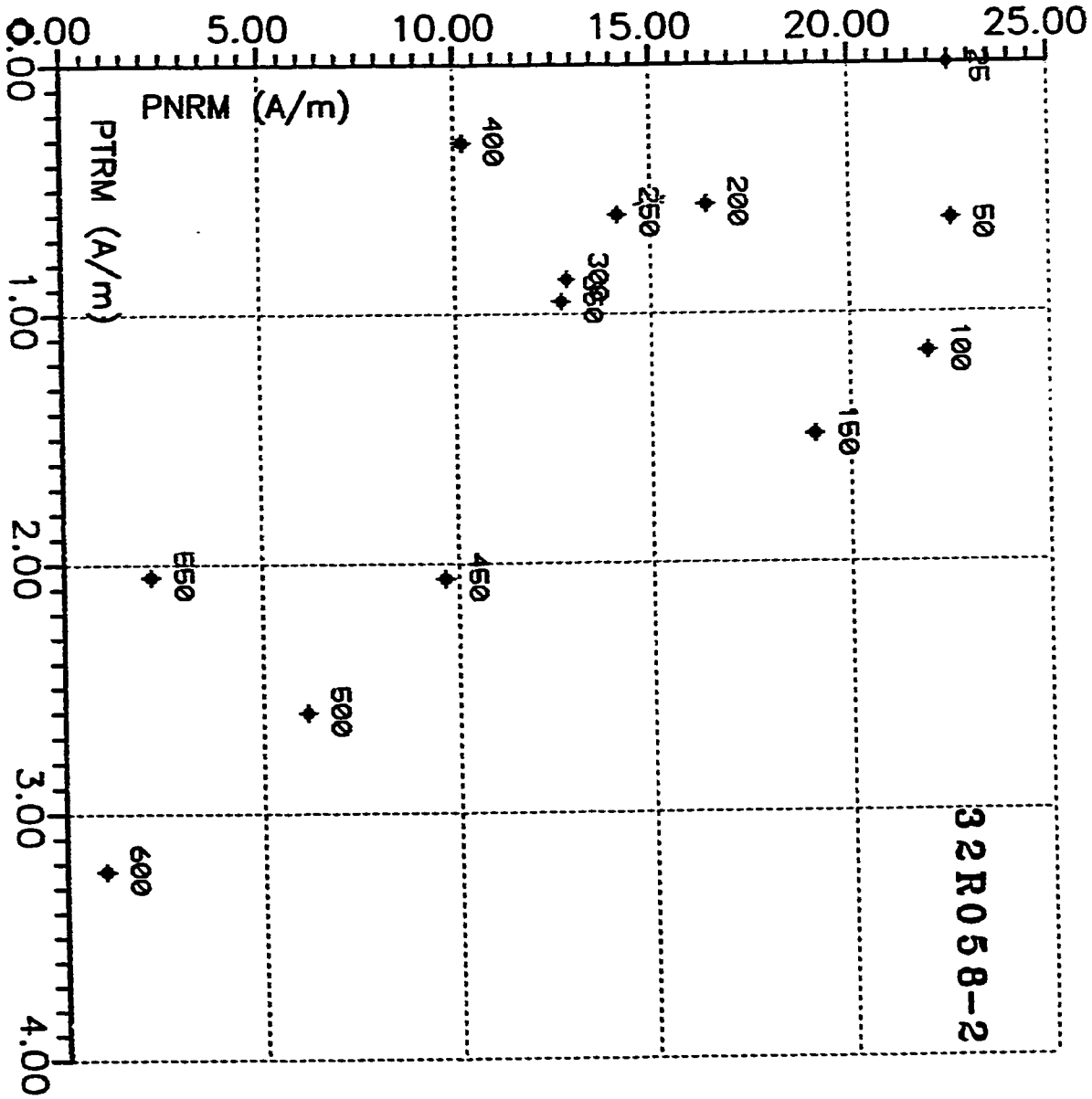
0.00
5.00
10.00
15.00
20.00
25.00
PNRM (A/m)
PTRM (A/m)
0.00
1.00
2.00
3.00
4.00
25
50
100
150
200
250
300
350
400
450
500
550
600
32R058-2

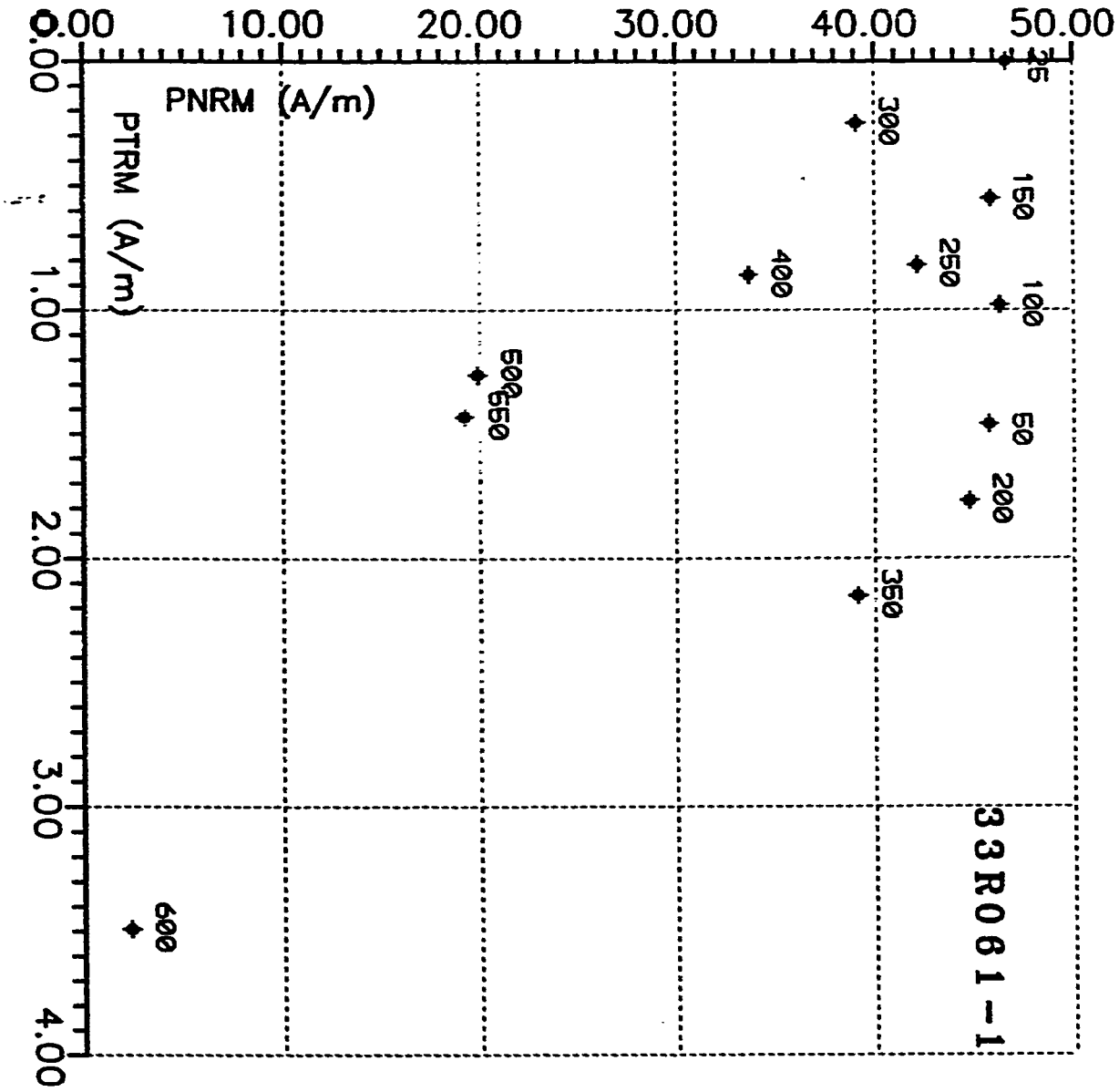
0.00
10.00
20.00
30.00
40.00
50.00
PNRM (A/m)
PTRM (A/m)
0.00
1.00
2.00
3.00
4.00
25
300
150
250
100
400
500
550
50
200
350
600
33R061-1

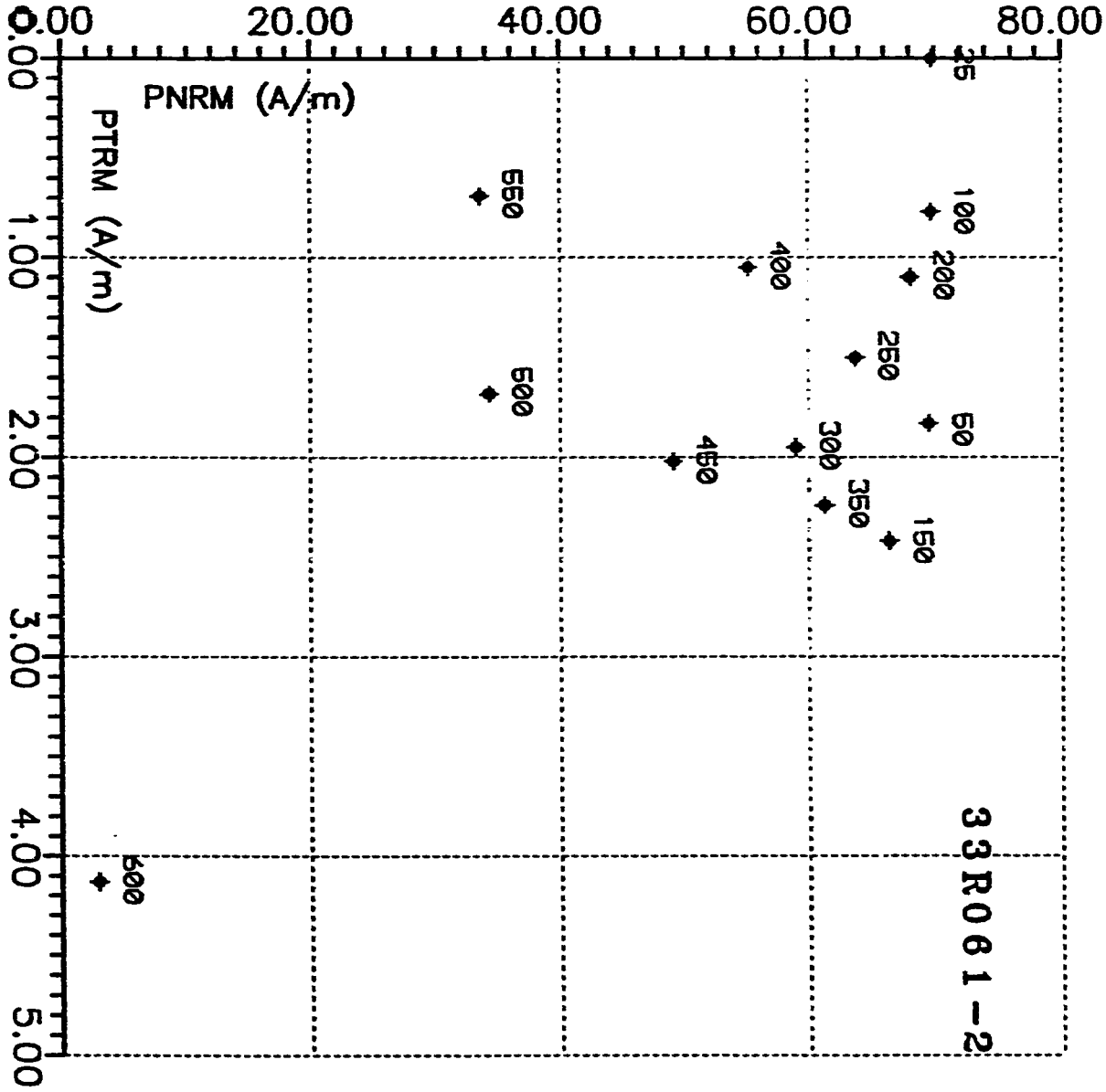
0.00
20.00
40.00
60.00
80.00
PNRM (A/m)
PTRM (A/m)
0.00
1.00
2.00
3.00
4.00
5.00
25
100
200
400
250
550
50
600
300
450
350
150
500
33R061-2

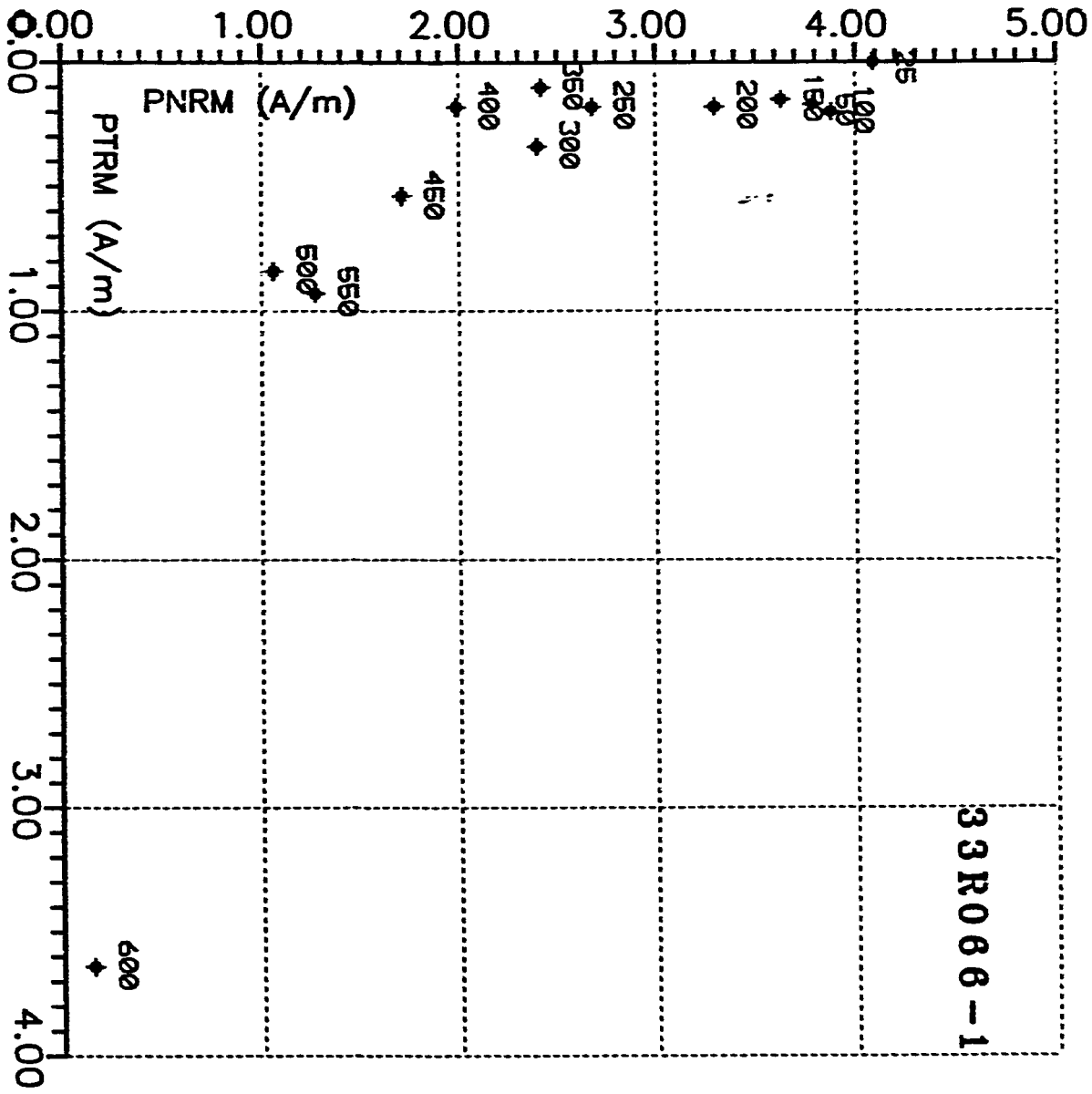
0.00
1.00
2.00
3.00
4.00
5.00
PNRM (A/m)
PTRM (A/m)
25
100
150
200
250
300
350
400
450
500
550
600
33R066-1

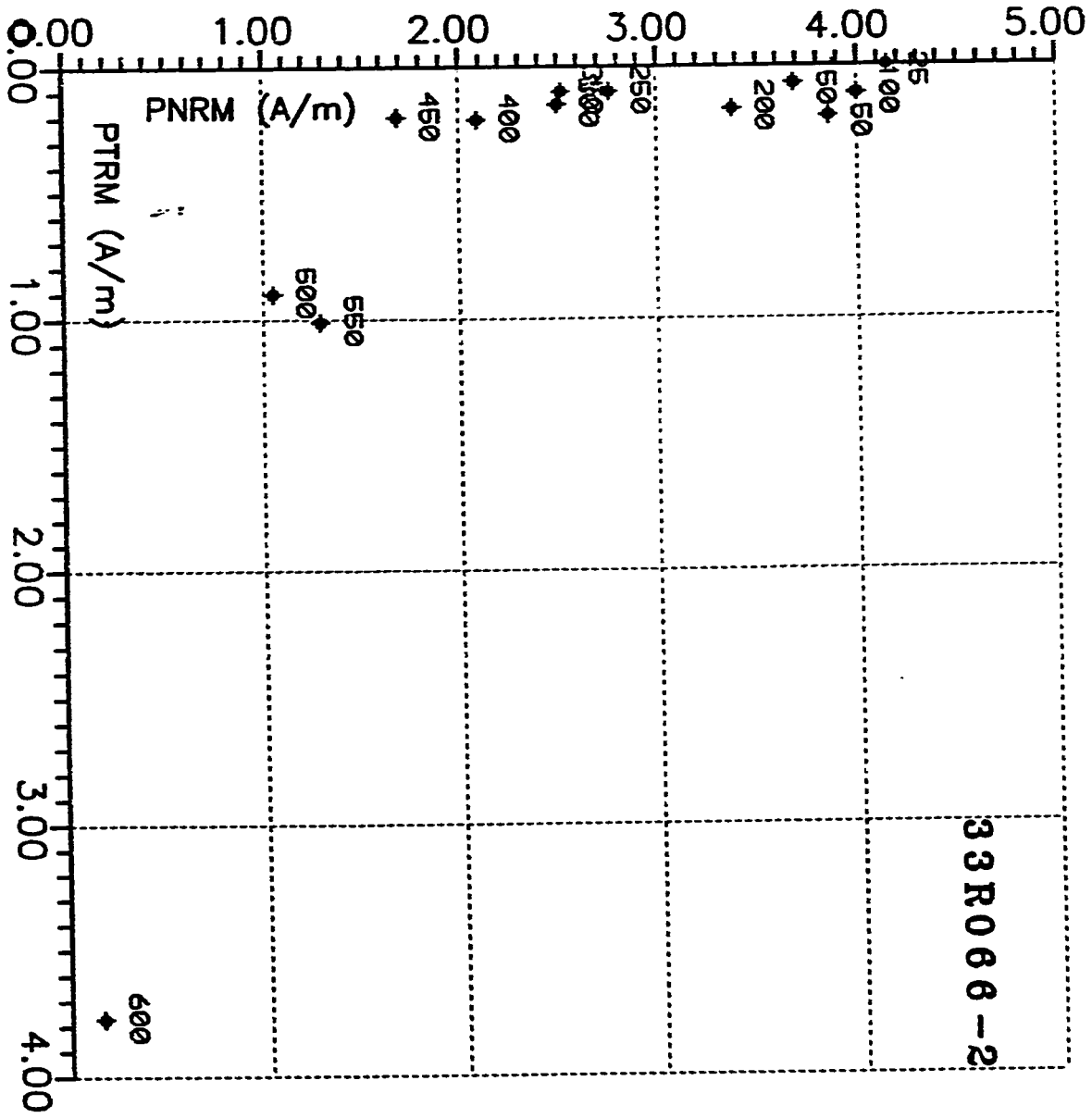
0.00
1.00
2.00
3.00
4.00
5.00
PNRM (A/m)
PTRM (A/m)
450
400
250
200
50
100
500
550
600
33R066-2

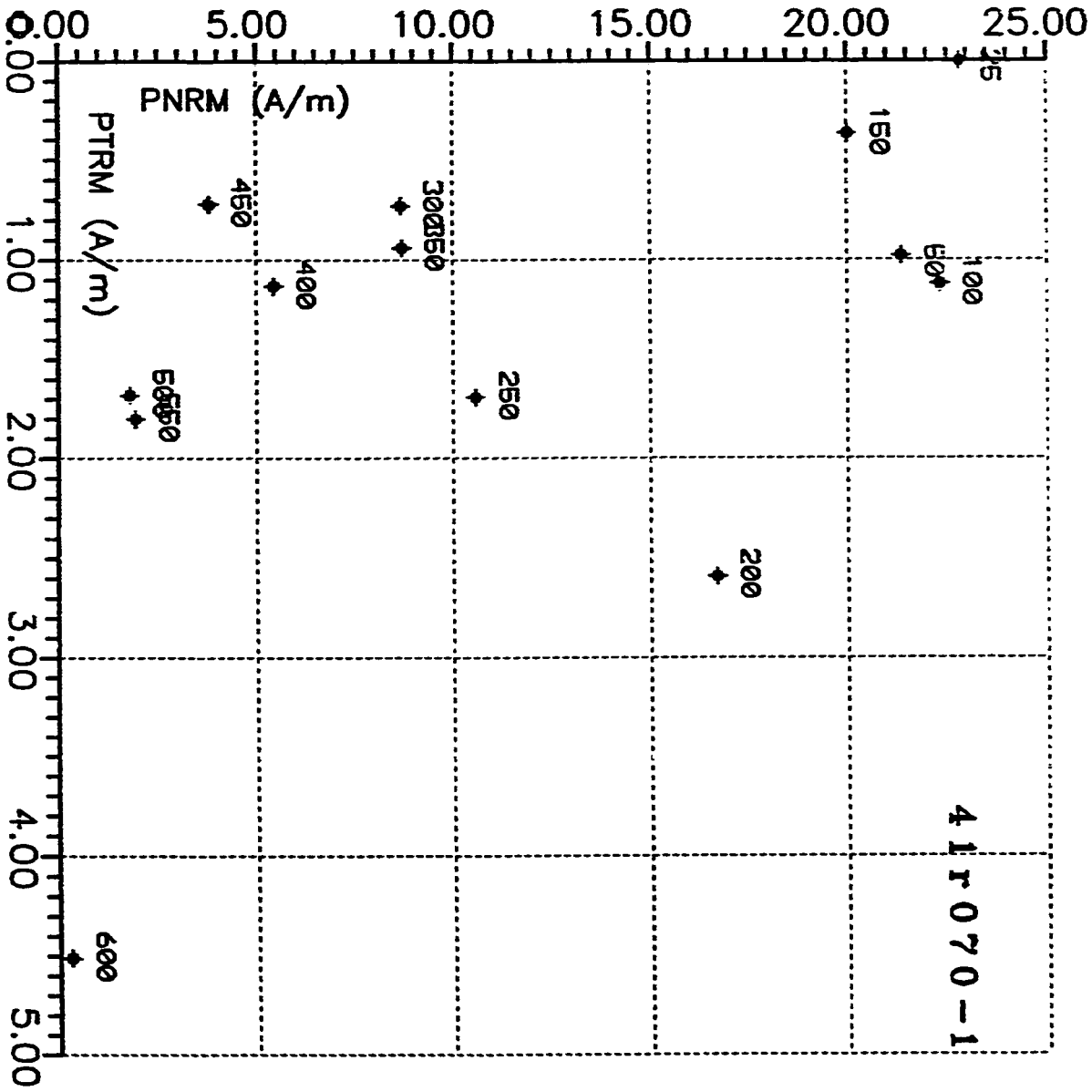
0.00
5.00
10.00
15.00
20.00
25.00
PNRM (A/m)
PTRM (A/m)
0.00
1.00
2.00
3.00
4.00
5.00
35
150
100
250
200
600
41r070-1

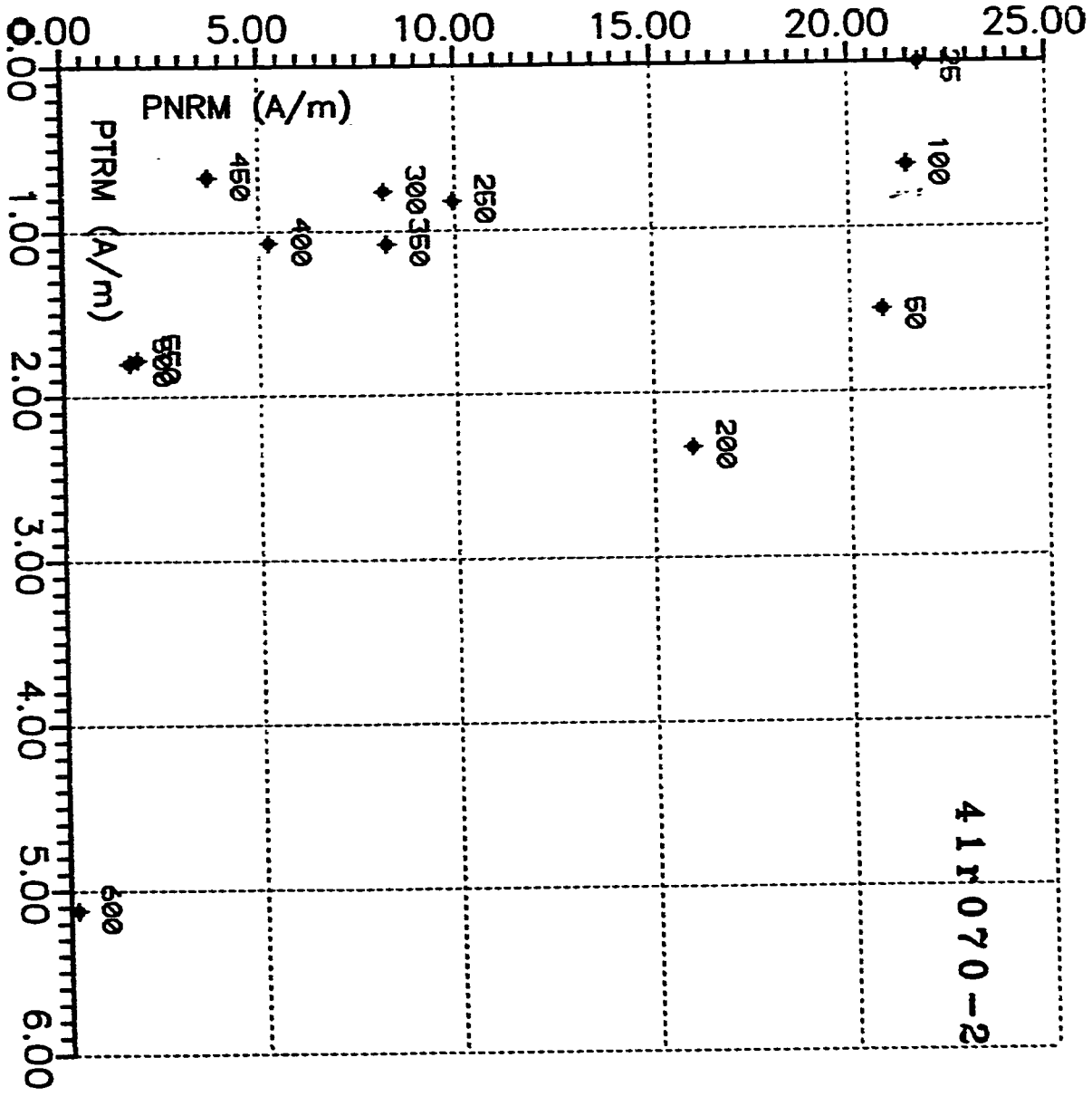
0.00
5.00
10.00
15.00
20.00
25.00
PNRM (A/m)
PTRM (A/m)
0.00
1.00
2.00
3.00
4.00
5.00
6.00
450
400
300
350
250
550
600
100
50
200
41r070-2

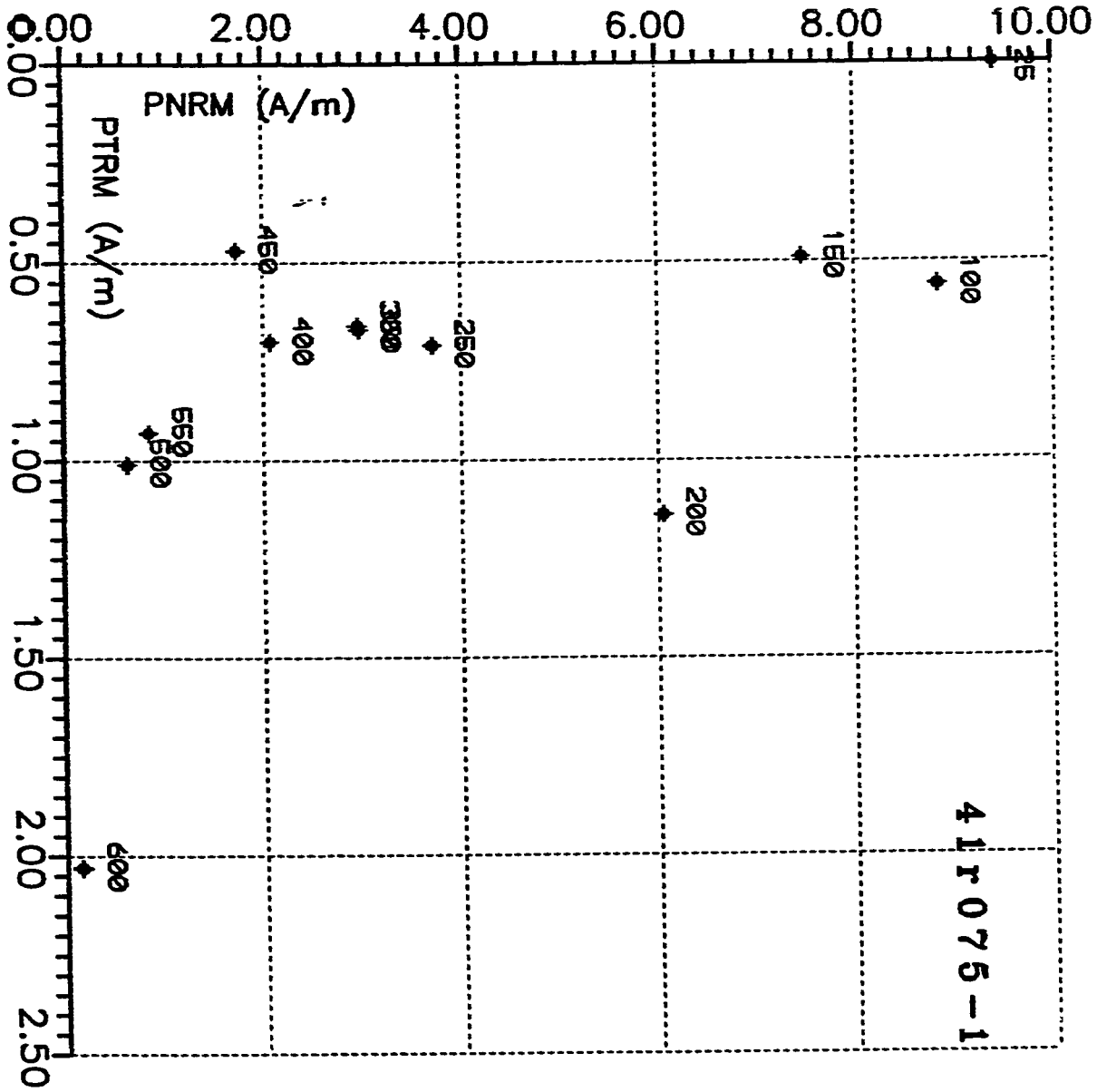
0.00
2.00
4.00
6.00
8.00
10.00
PNRM (A/m)
PTRM (A/m)
0.00
0.50
1.00
1.50
2.00
2.50
25
100
150
200
250
300
400
450
500
550
600
41r075-1

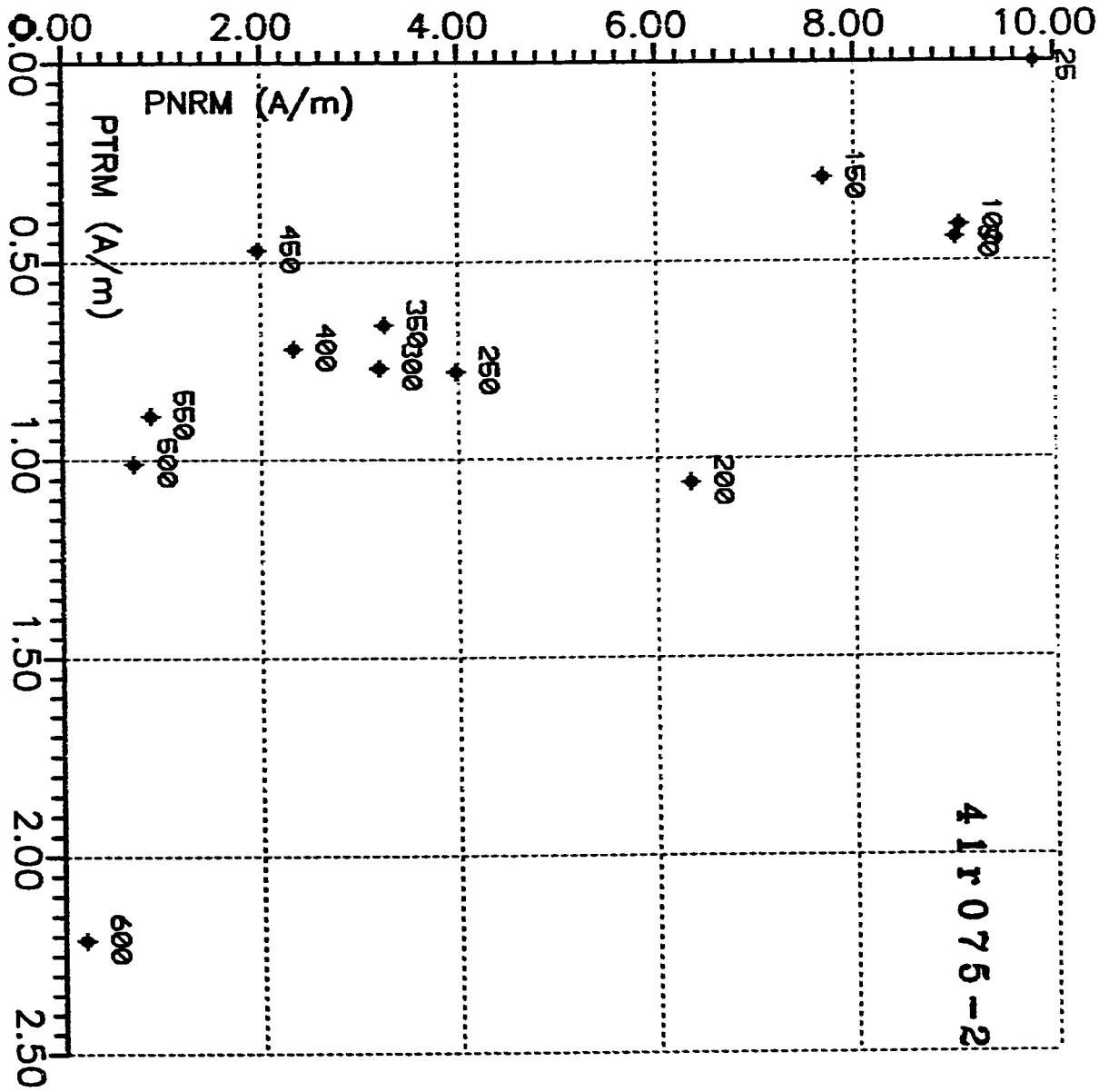
0.00
2.00
4.00
6.00
8.00
10.00
PNRM (A/m)
PTRM (A/m)
0.00
0.50
1.00
1.50
2.00
2.50
25
150
1000
450
350
300
400
250
550
600
200
600
41r075-2

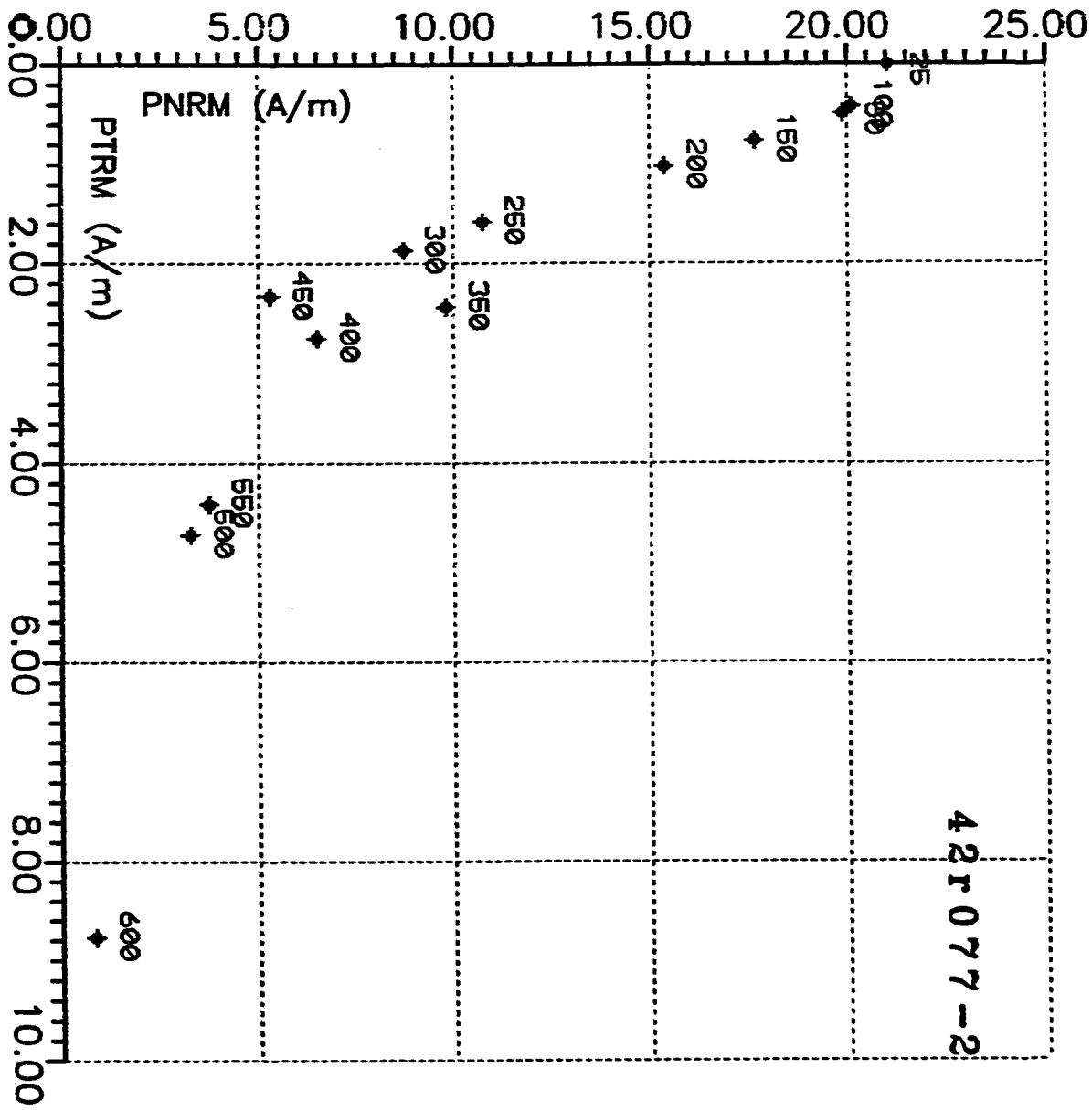
0.00
5.00
10.00
15.00
20.00
25.00
PNRM (A/m)
PTRM (A/m)
0.00
2.00
4.00
6.00
8.00
10.00
25
100
150
200
250
300
350
400
450
550
600
600
42r077-2

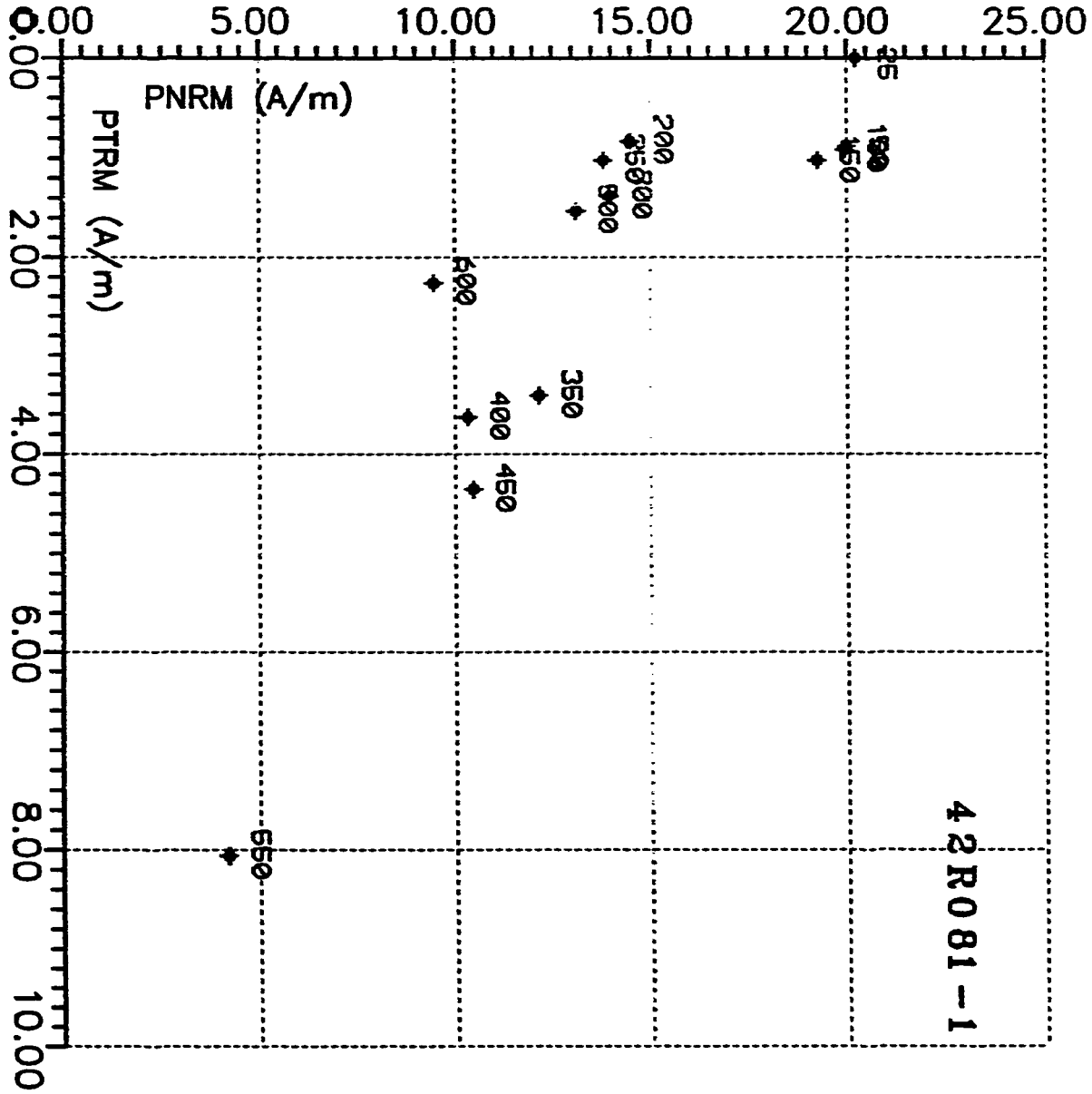
0.00
5.00
10.00
15.00
20.00
25.00
PNRM (A/m)
PTRM (A/m)
0.00
2.00
4.00
6.00
8.00
10.00
600
350
400
450
550
42R081-1

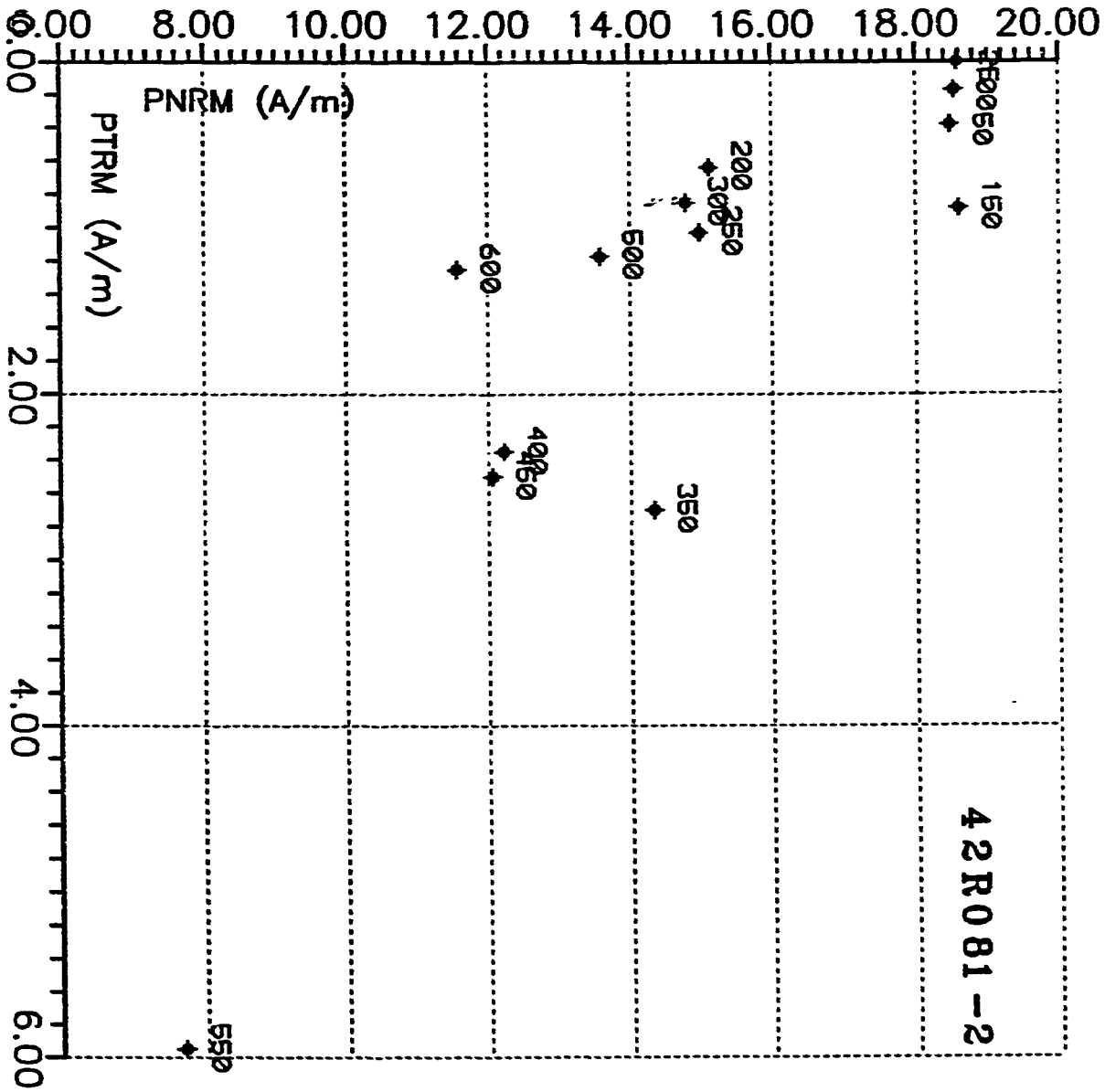
6.00
8.00
10.00
12.00
14.00
16.00
18.00
20.00
PNRM (A/m)
PTRM (A/m)
0.00
2.00
4.00
6.00
150
200
250
300
350
400
450
500
550
600
42R081-2

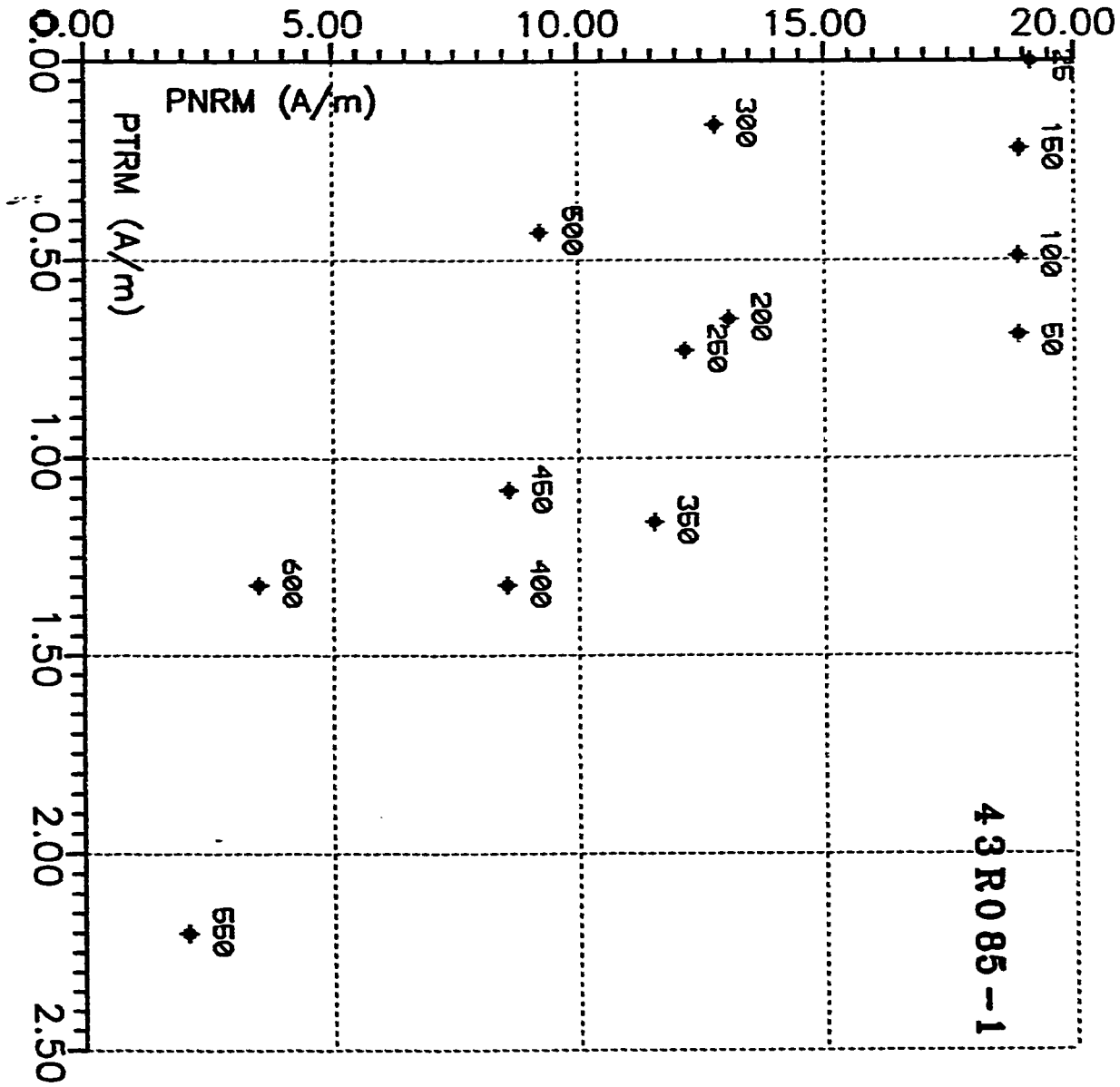
0.00
5.00
10.00
15.00
20.00
PNRM (A/m)
0.00
0.50
1.00
1.50
2.00
2.50
PTRM (A/m)
35
150
100
50
300
500
200
250
450
350
400
600
550
43R085-1

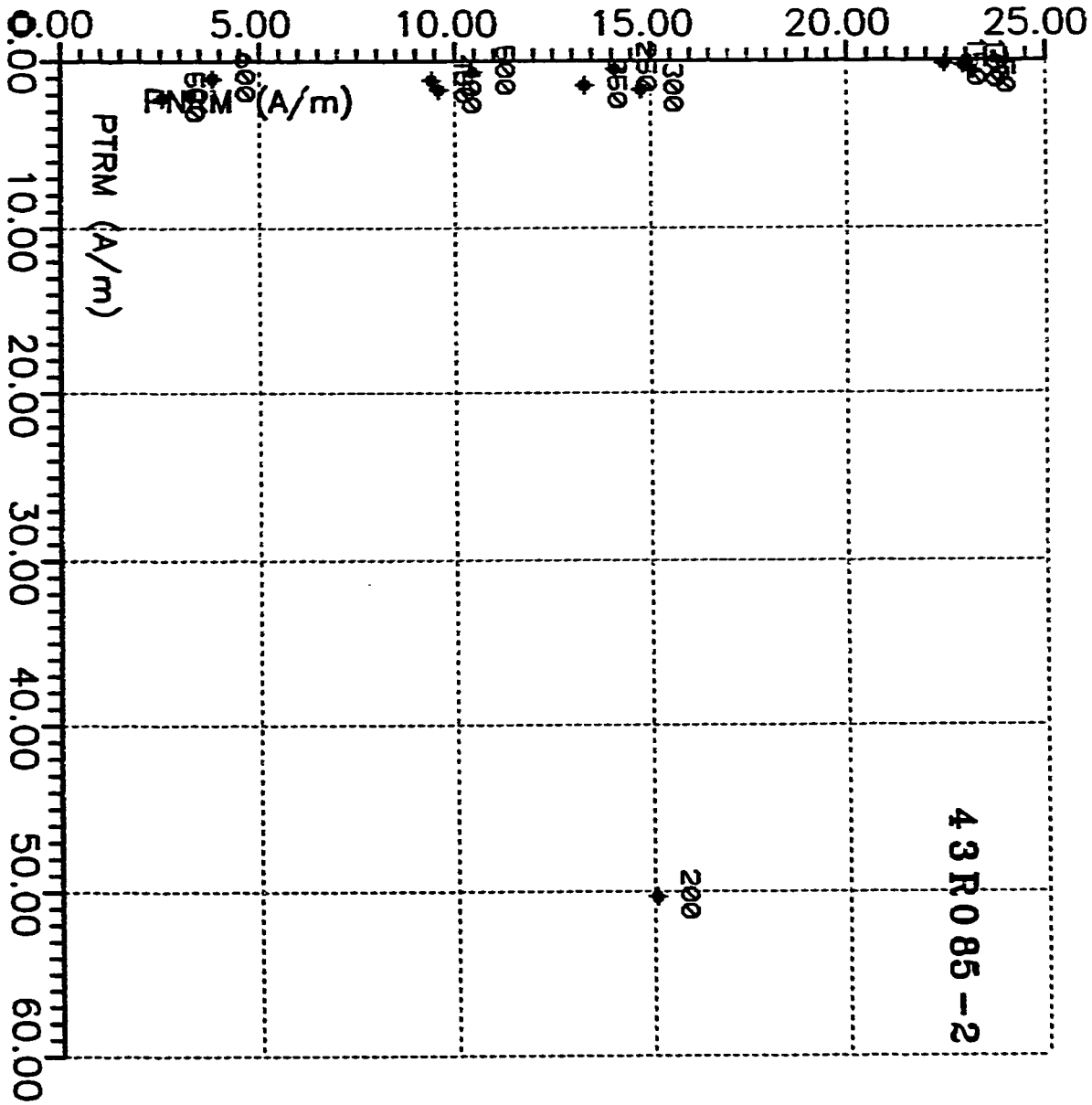
0.00
5.00
10.00
15.00
20.00
25.00
PNRM (A/m)
PTRM (A/m)
0.00
10.00
20.00
30.00
40.00
50.00
60.00
200
43R085-2

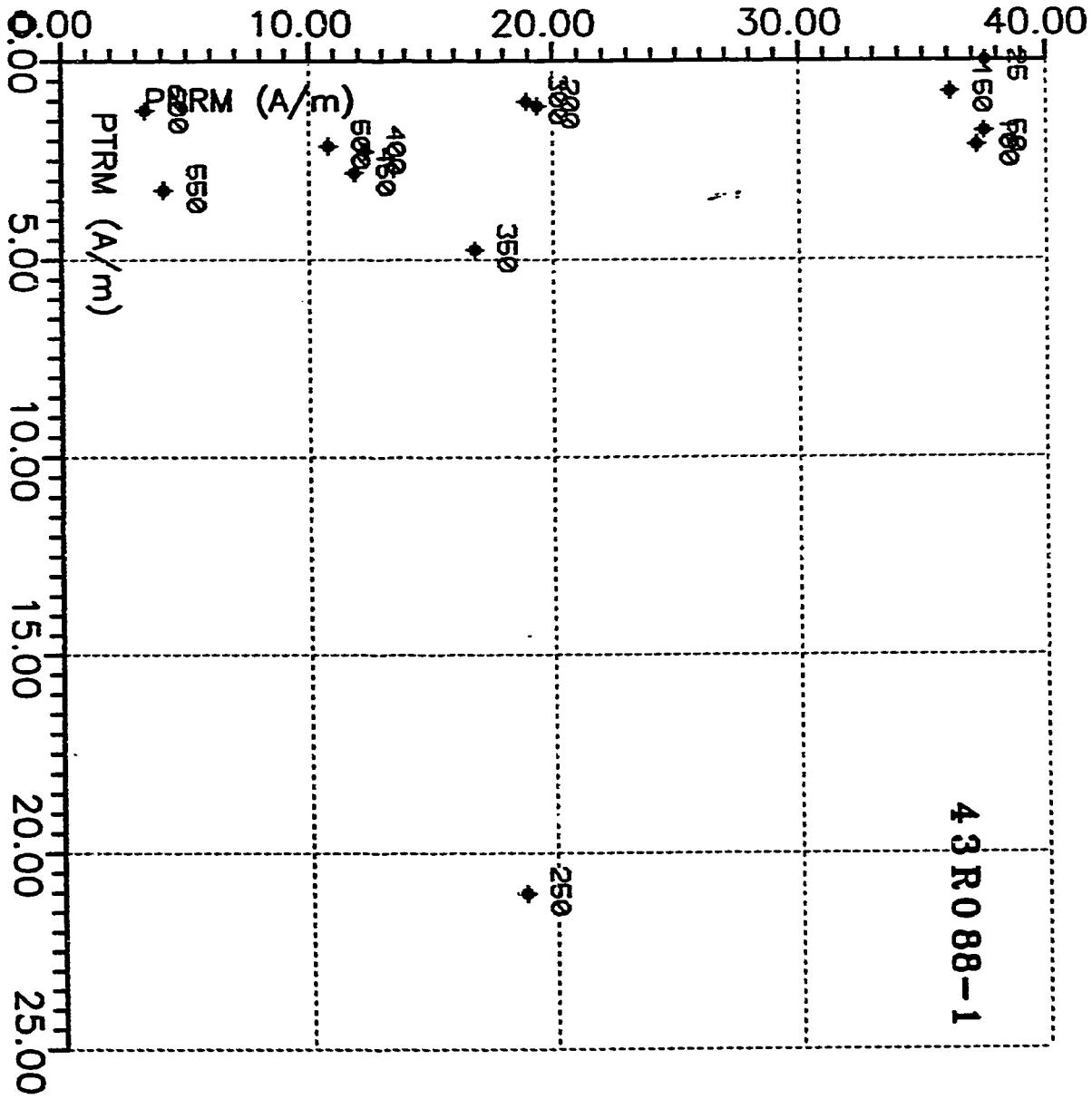
0.00
10.00
20.00
30.00
40.00
0.00
5.00
10.00
15.00
20.00
25.00
PTRM (A/m)
PTRM (A/m)
650
350
250
43R088-1

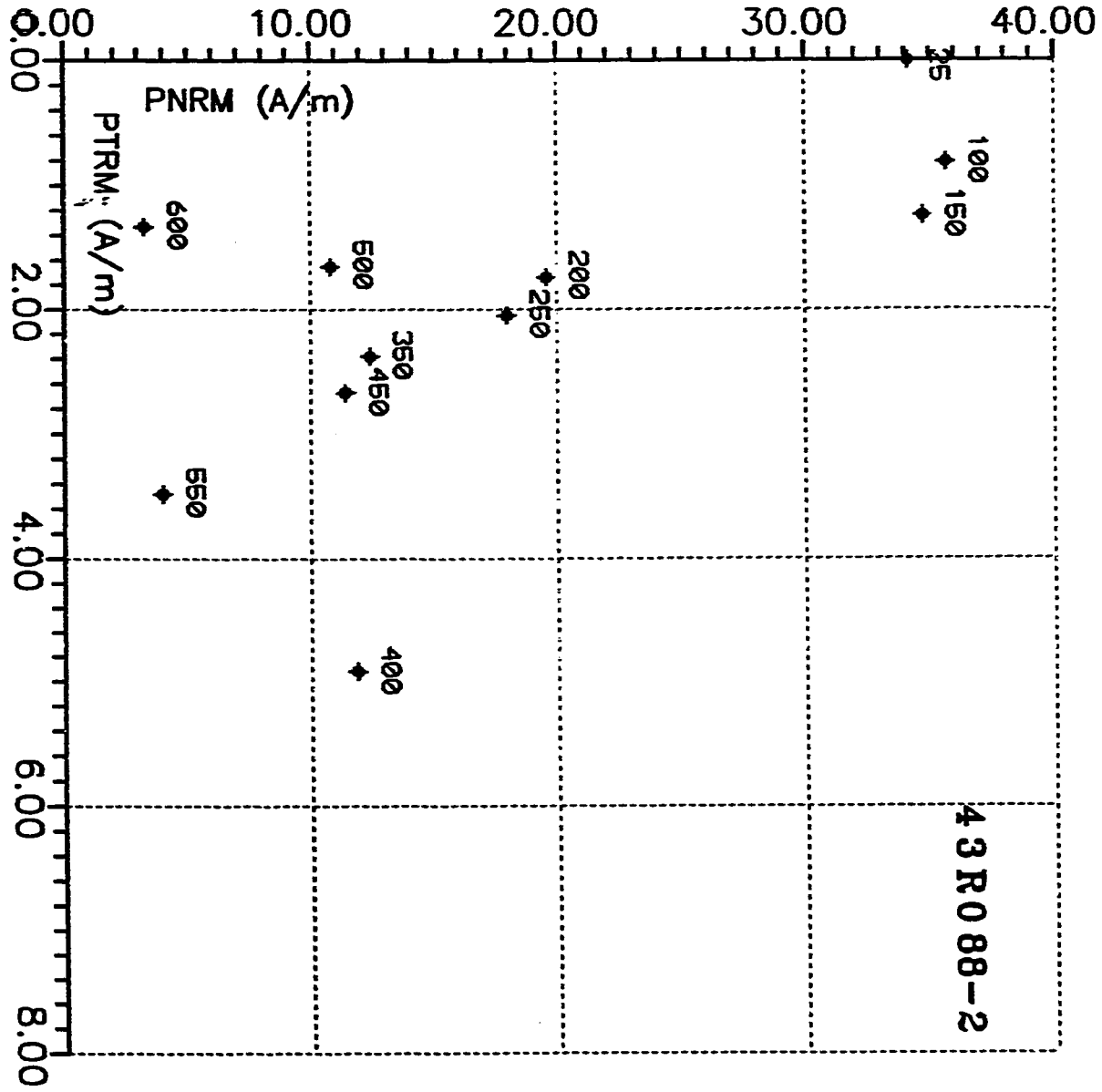
0.00
10.00
20.00
30.00
40.00
PNRM (A/m)
PTRM (A/m)
0.00
2.00
4.00
6.00
8.00
25
100
150
200
250
350
450
500
600
550
400
43R088-2

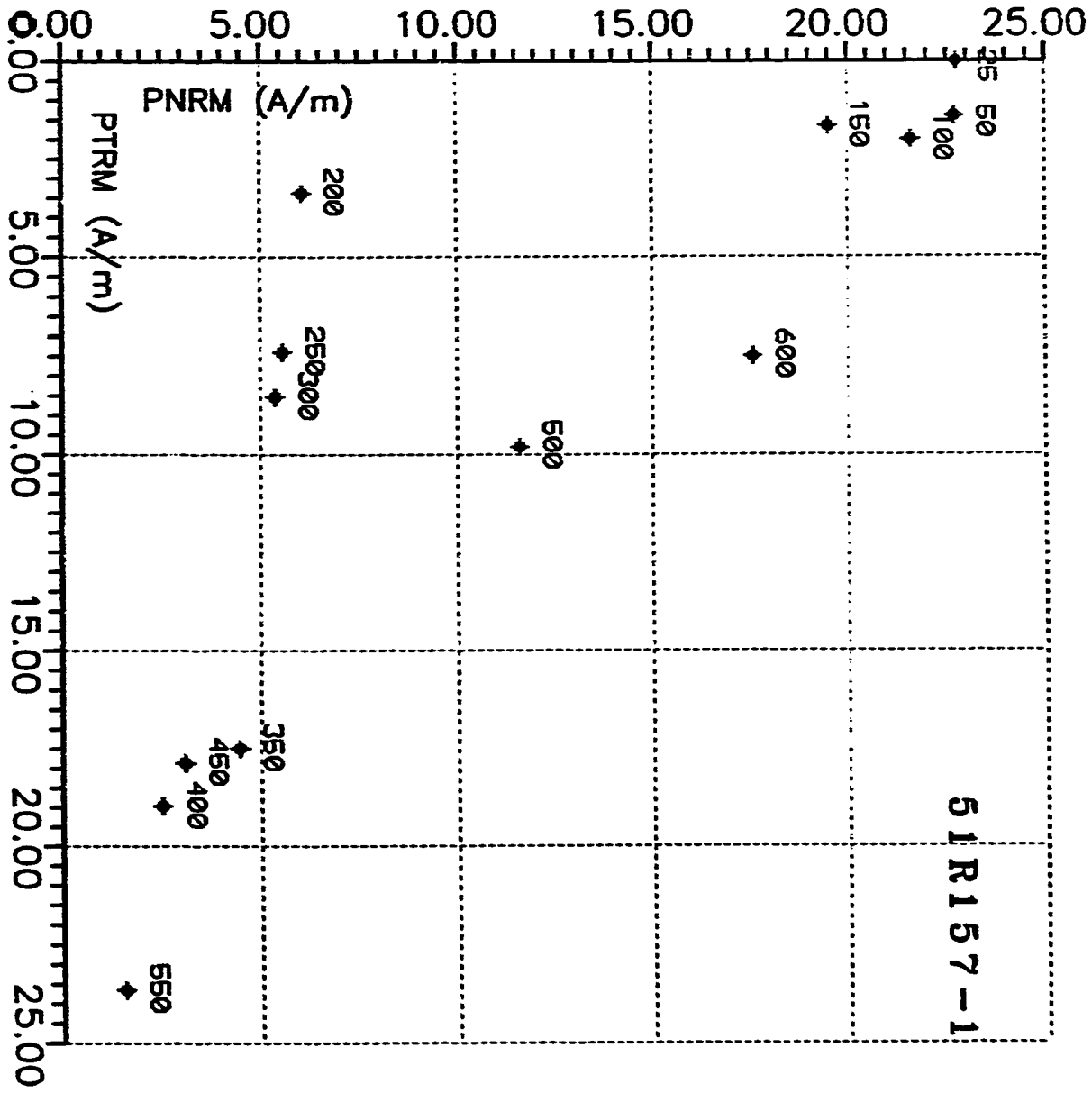
0.00
5.00
10.00
15.00
20.00
25.00
PNRM (A/m)
PTRM (A/m)
25
50
100
150
200
250
300
600
500
350
450
400
550
51R157-1

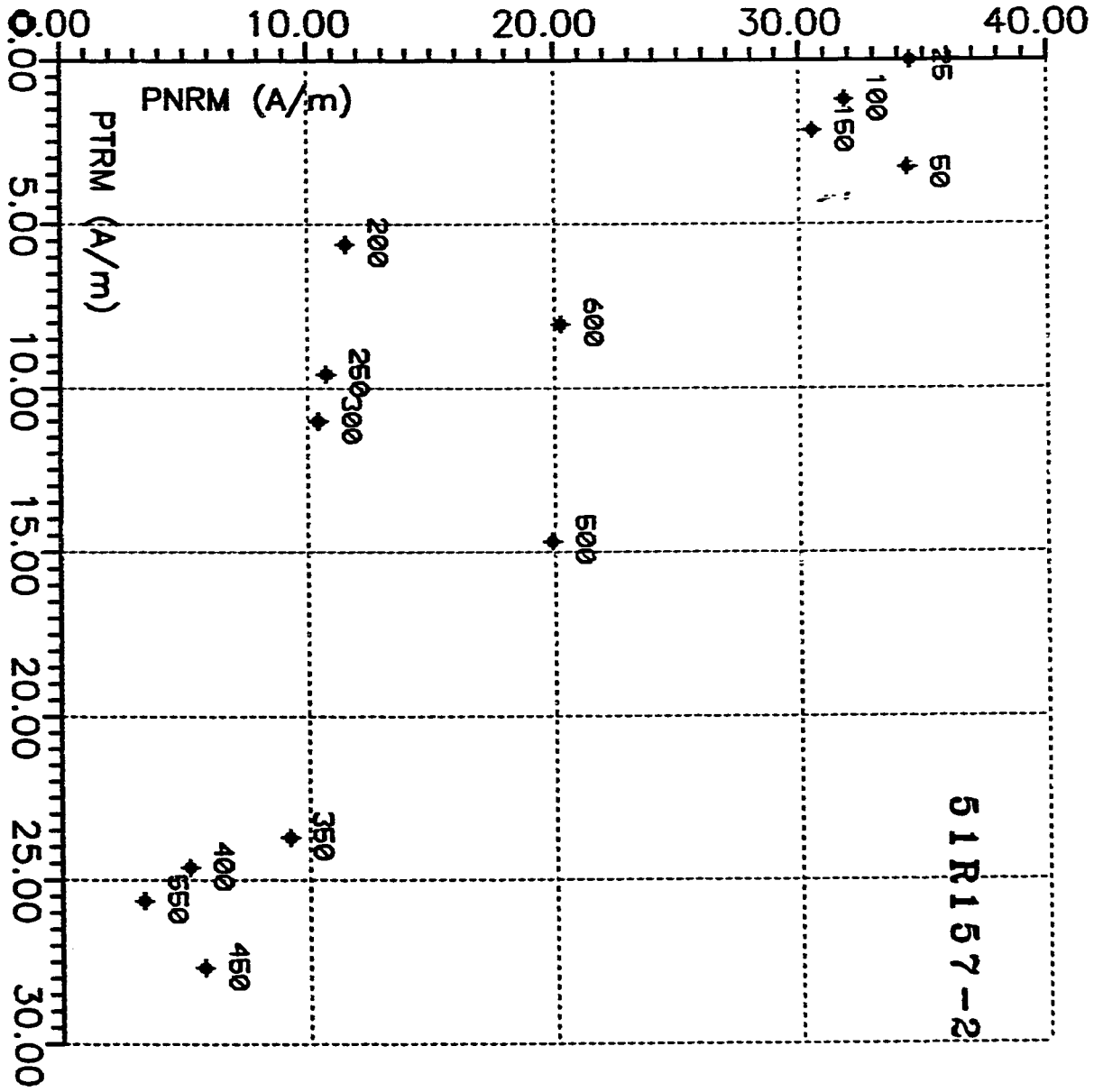
0.00
10.00
20.00
30.00
40.00
PNRM (A/m)
PTRM (A/m)
0.00
5.00
10.00
15.00
20.00
25.00
30.00
25
50
100
150
200
250
300
350
400
450
500
550
600
51R157-2

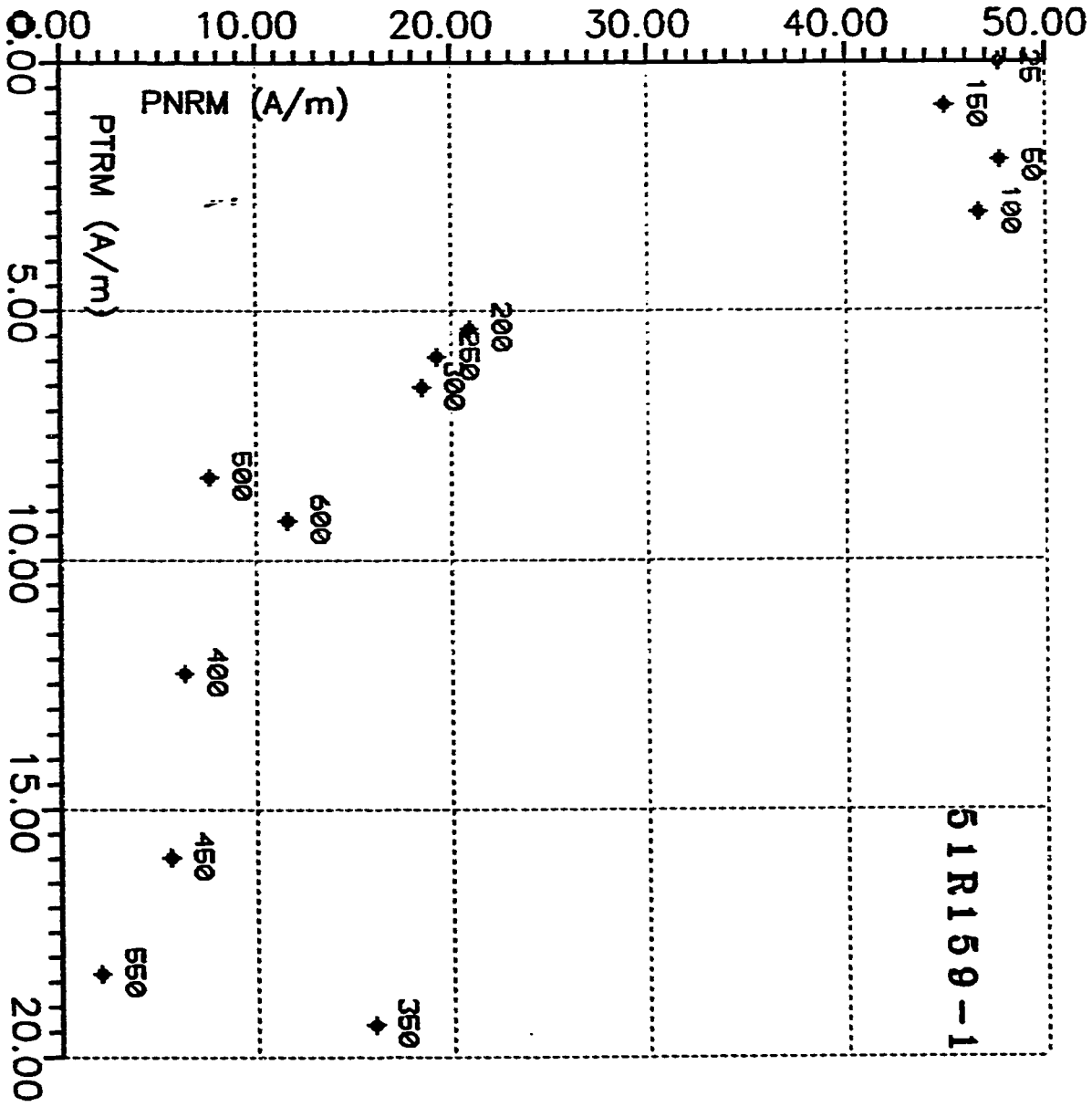
0.00
10.00
20.00
30.00
40.00
50.00
PNRM (A/m)
PTRM (A/m)
0.00
5.00
10.00
15.00
20.00
25
150
50
100
200
250
300
500
600
400
450
550
350
51R159-1

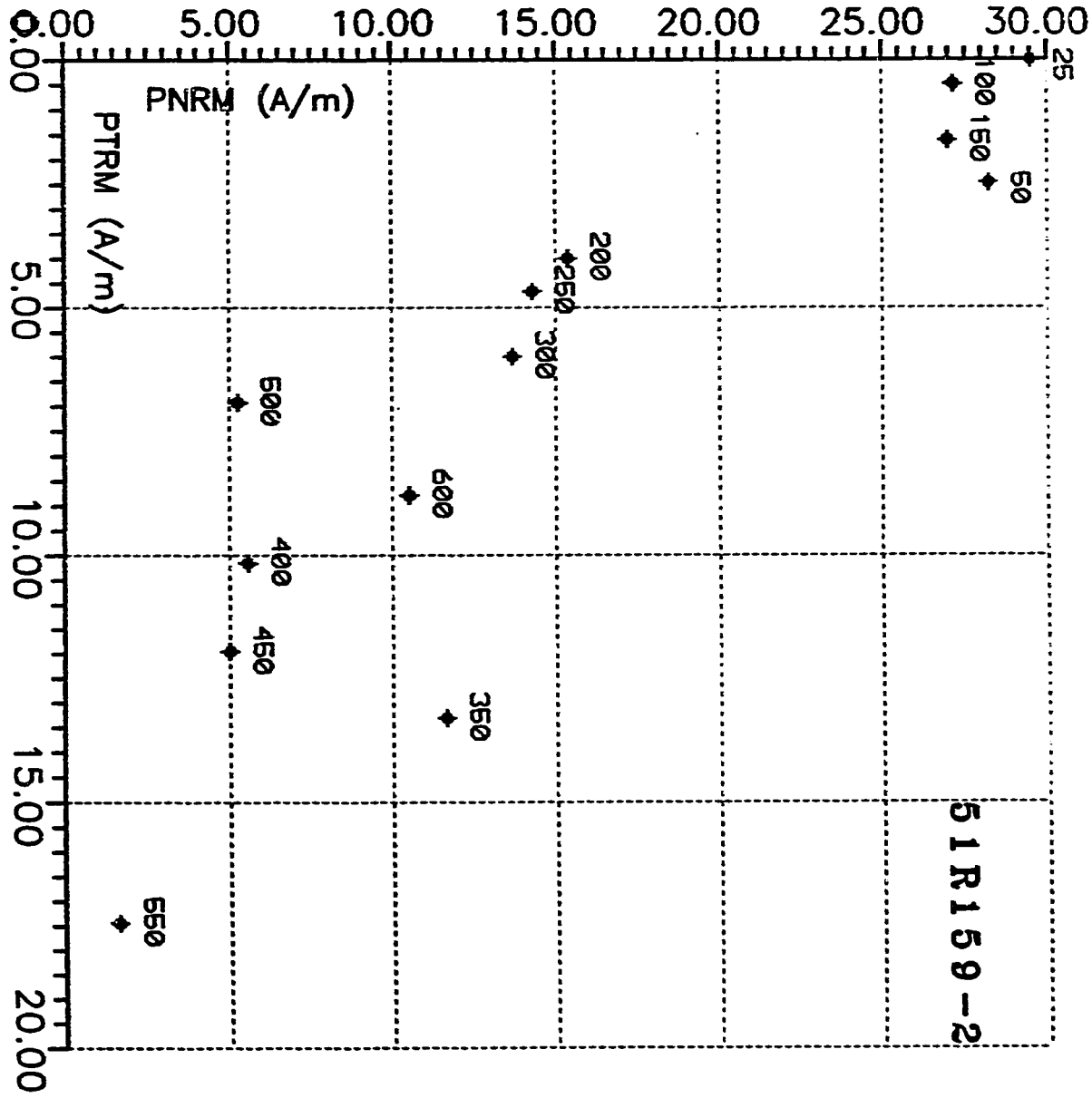
0.00
5.00
10.00
15.00
20.00
25.00
30.00
PNRM (A/m)
PTRM (A/m)
0.00
5.00
10.00
15.00
20.00
25
100
150
50
200
250
300
500
600
400
450
350
550
51R159-2

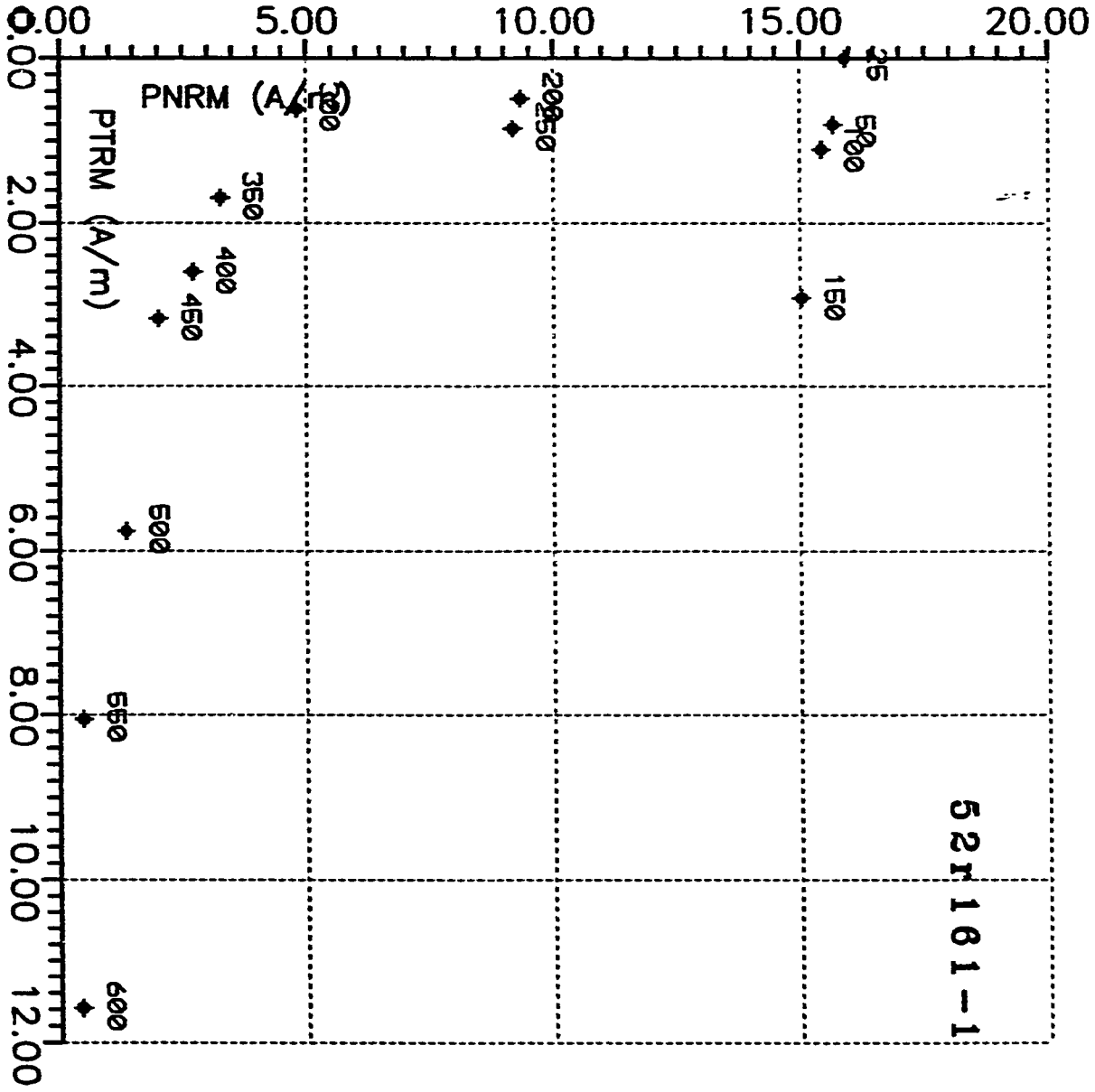
0.00
5.00
10.00
15.00
20.00
PNRM (A/m)
PTRM (A/m)
0.00
2.00
4.00
6.00
8.00
10.00
12.00
100
200
250
25
500
350
400
450
150
500
550
600
52r161-1

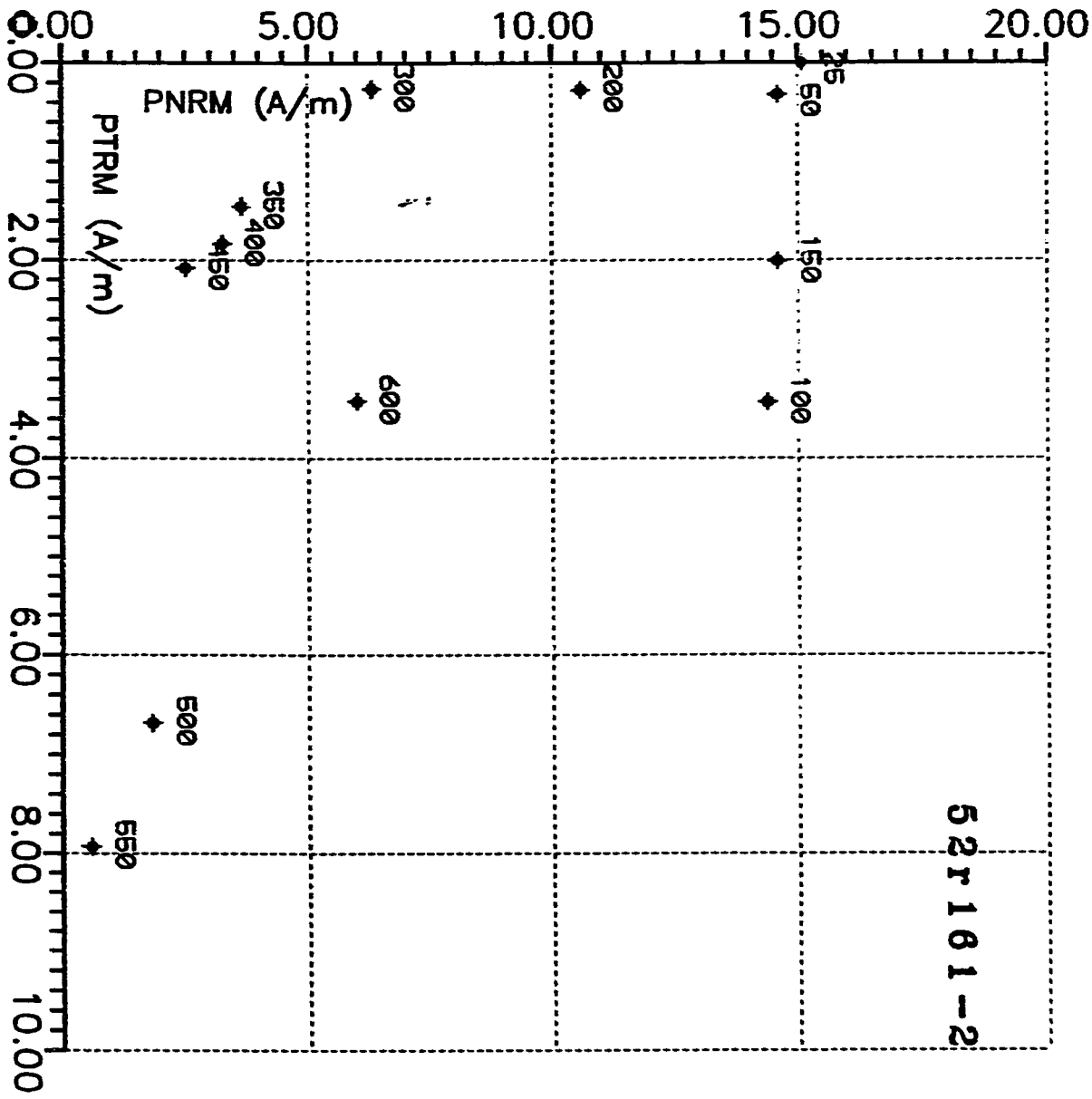
0.00
5.00
10.00
15.00
20.00
0.00
2.00
4.00
6.00
8.00
10.00
PNRM (A/m)
PTRM (A/m)
300
200
25
50
350
400
450
150
600
100
500
550
52r161-2

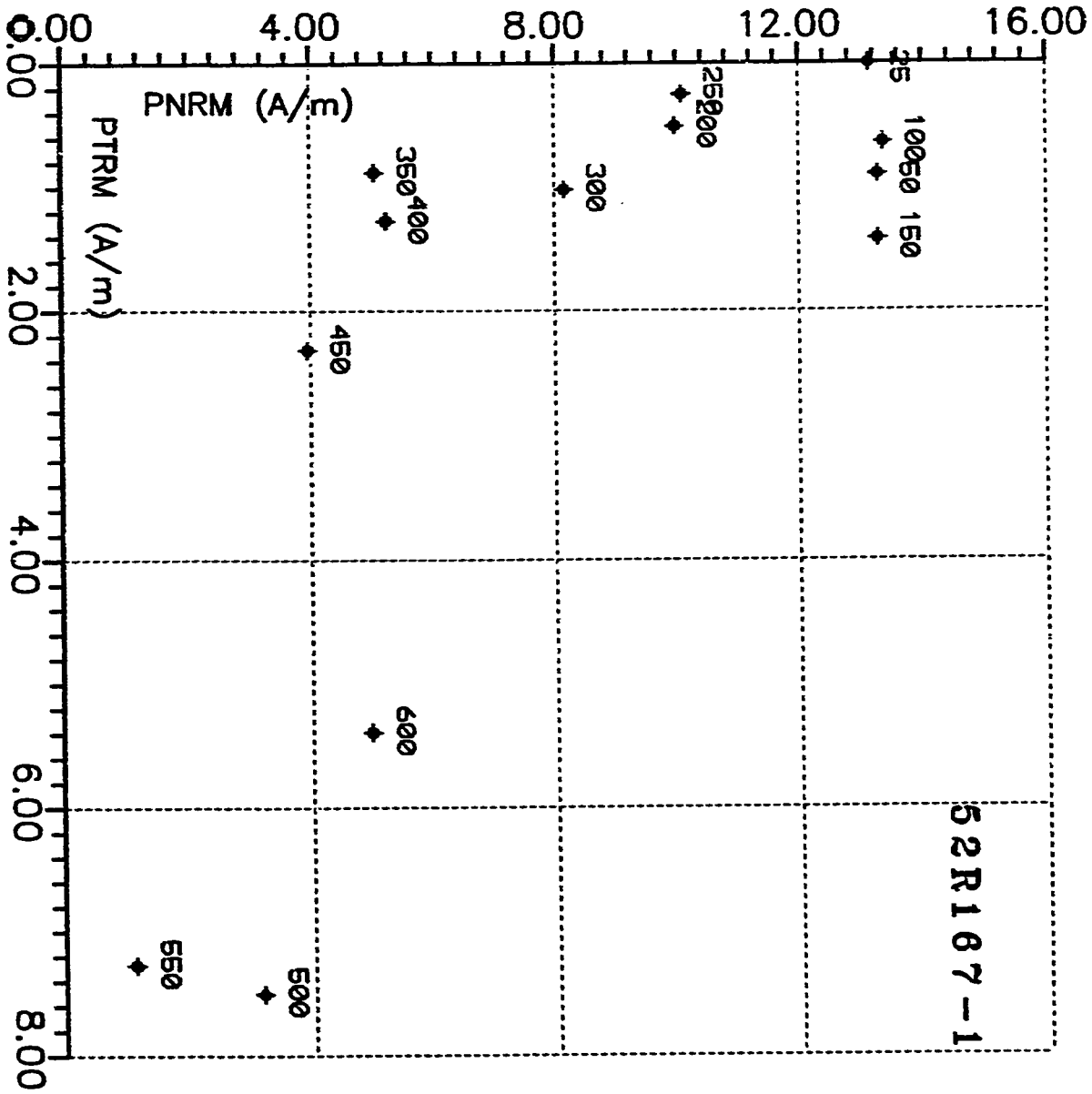
0.00
4.00
8.00
12.00
16.00
PNRM (A/m)
PTRM (A/m)
0.00
2.00
4.00
6.00
8.00
25
100
50
150
250
200
350
400
300
450
600
550
500
52R167-1

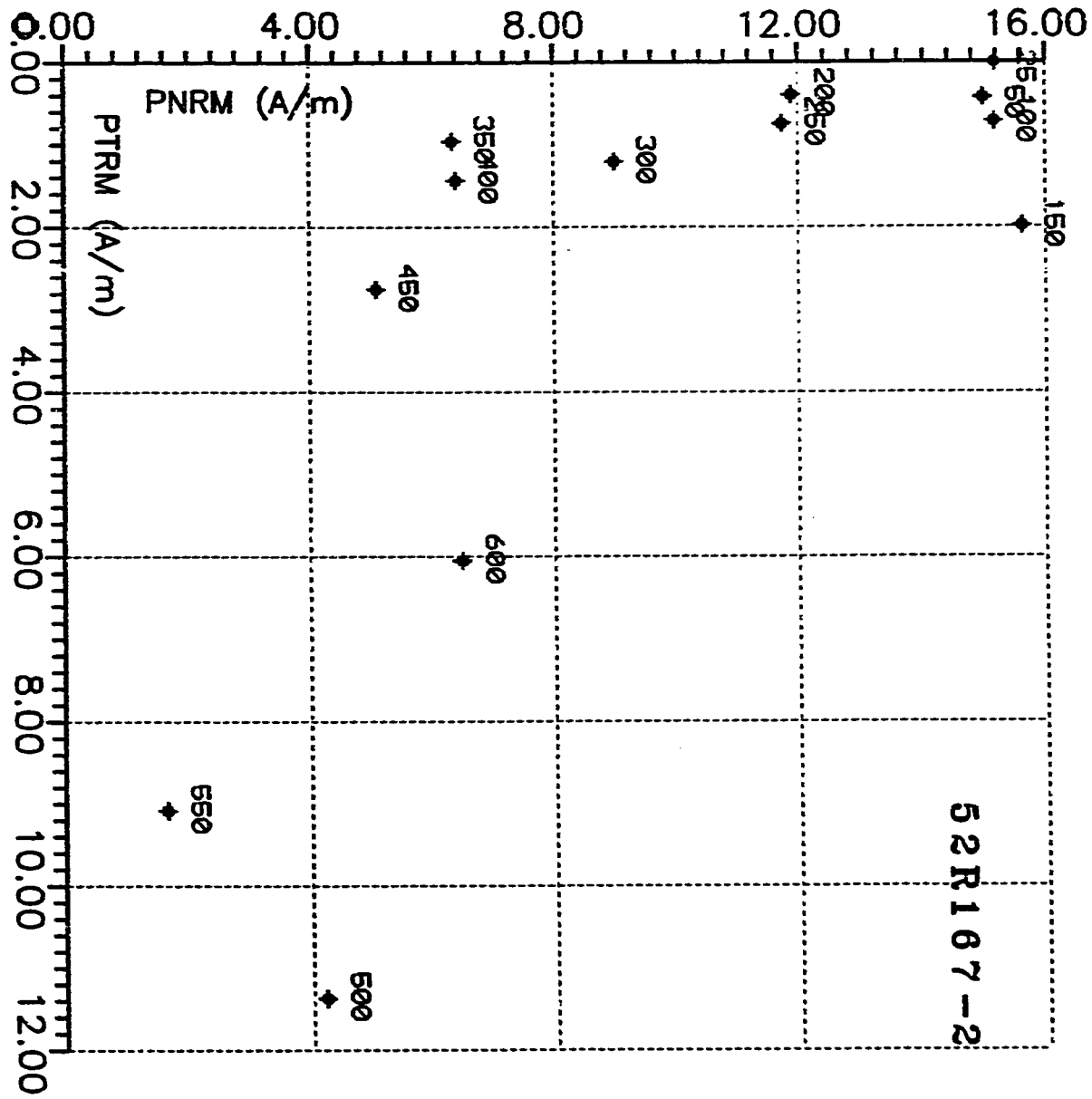
0.00
4.00
8.00
12.00
16.00
PNRM (A/m)
PTRM (A/m)
0.00
2.00
4.00
6.00
8.00
10.00
12.00
150
200
250
300
350
400
450
500
550
600
52R167-2

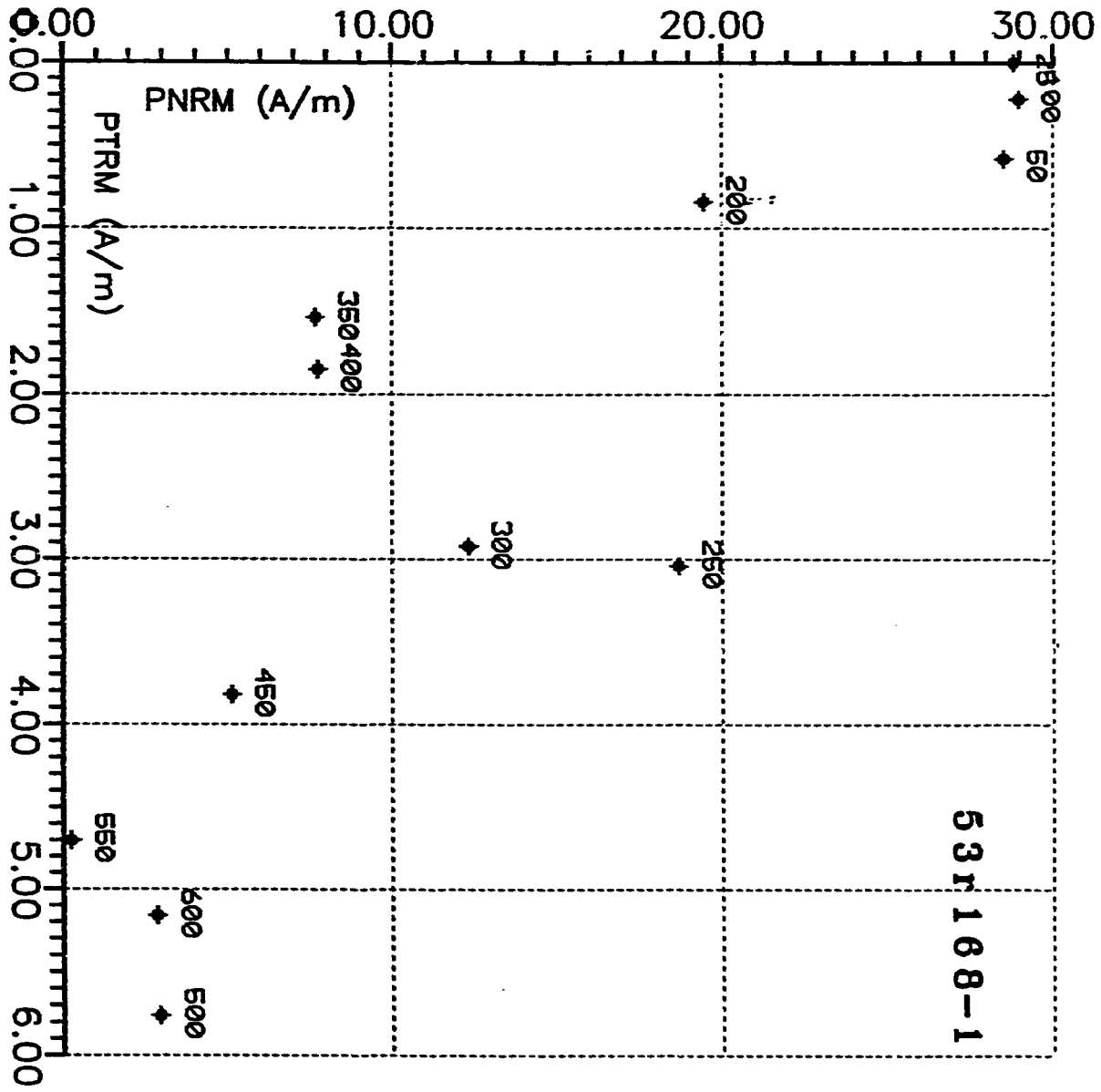
0.00
10.00
20.00
30.00
PNRM (A/m)
PTRM (A/m)
0.00
1.00
2.00
3.00
4.00
5.00
6.00
50
200
350
400
300
250
450
550
600
500
53r168-1

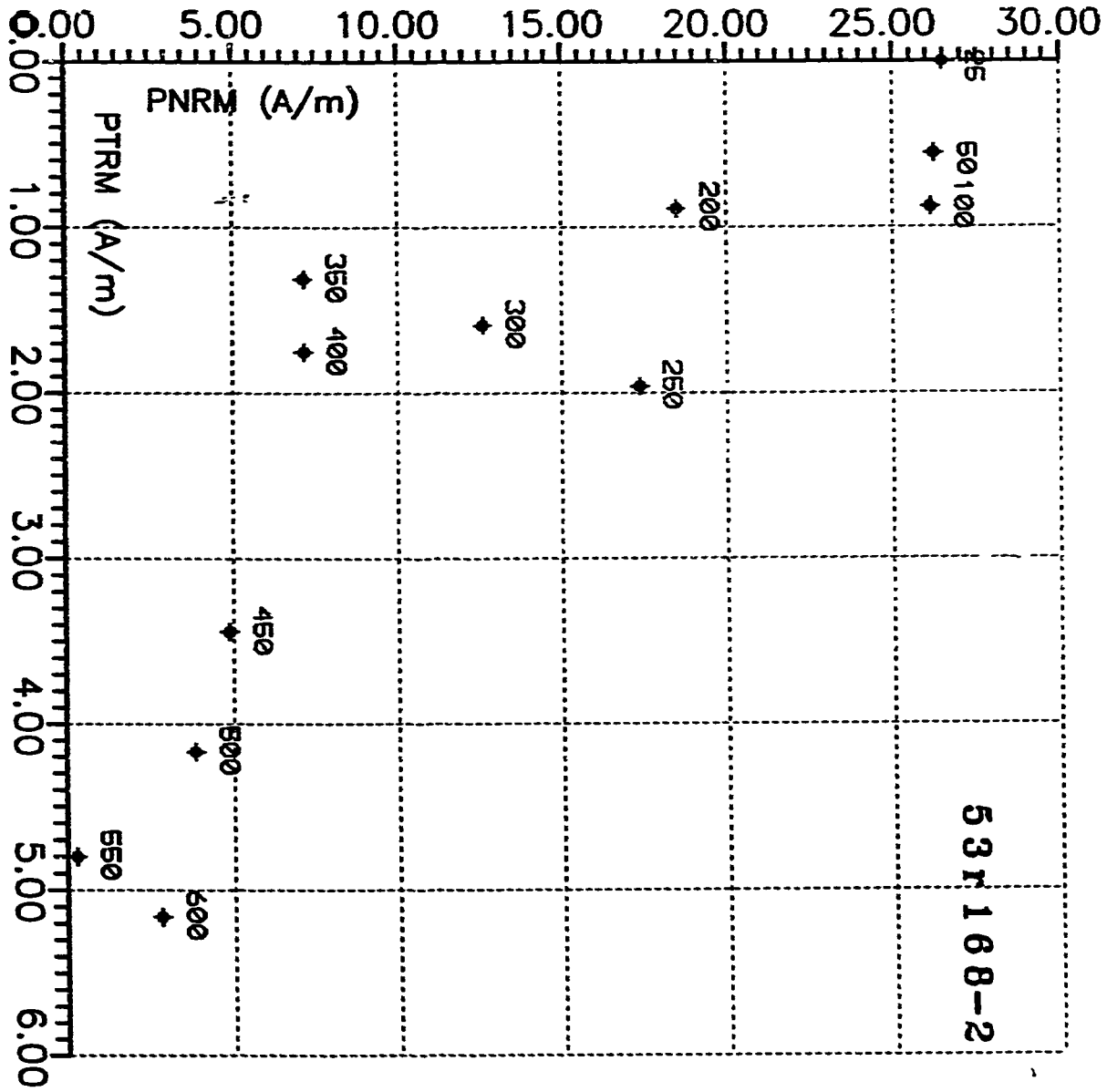
0.00
5.00
10.00
15.00
20.00
25.00
30.00
PNRM (A/m)
PTRM (A/m)
0.00
1.00
2.00
3.00
4.00
5.00
6.00
50
100
200
250
300
350
400
450
500
550
600
53r168-2

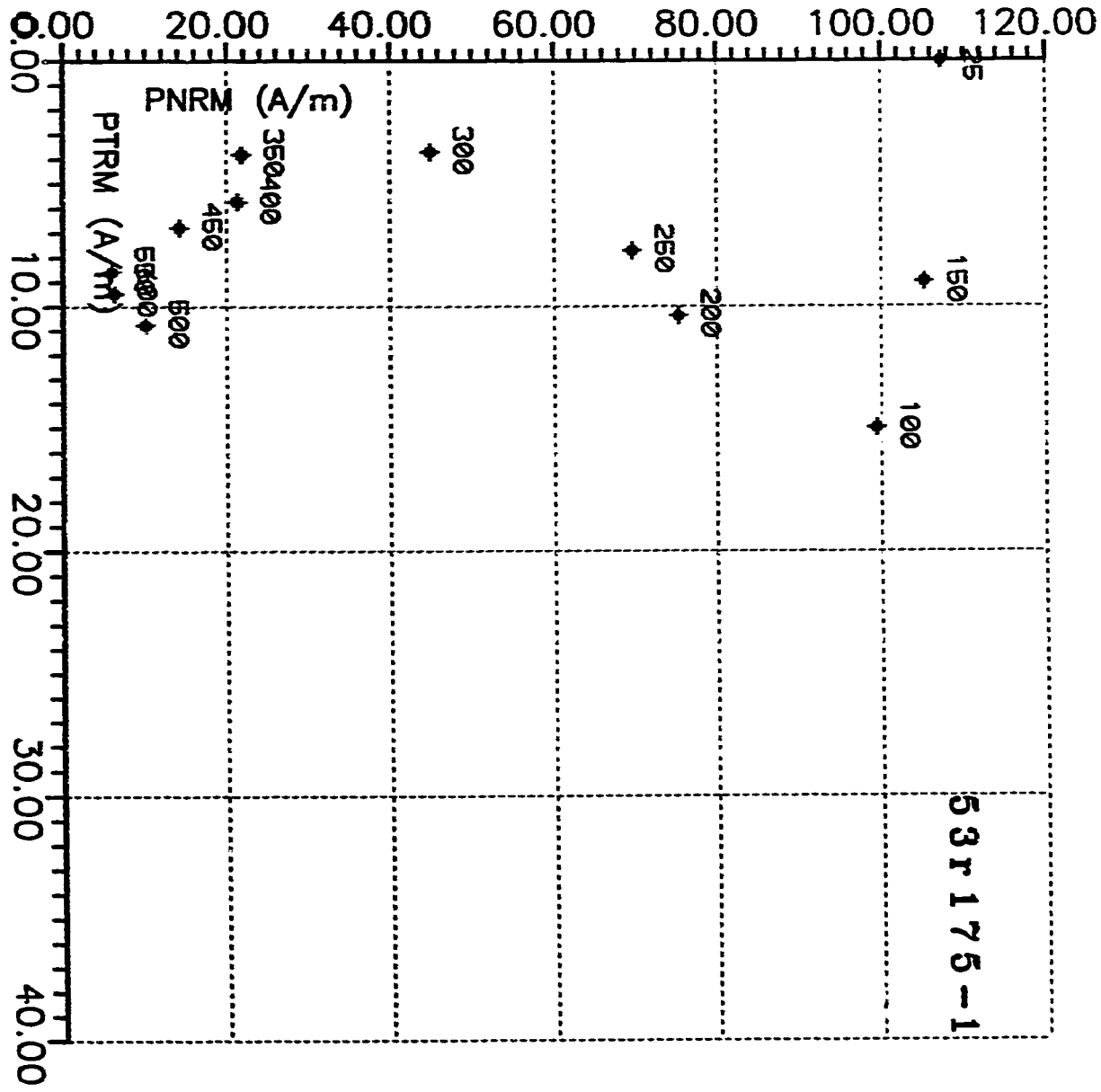
0.00
20.00
40.00
60.00
80.00
100.00
120.00
PNRM (A/m)
PTRM (A/m)
0.00
10.00
20.00
30.00
40.00
25
150
100
200
250
300
350
400
450
500
53r175-1

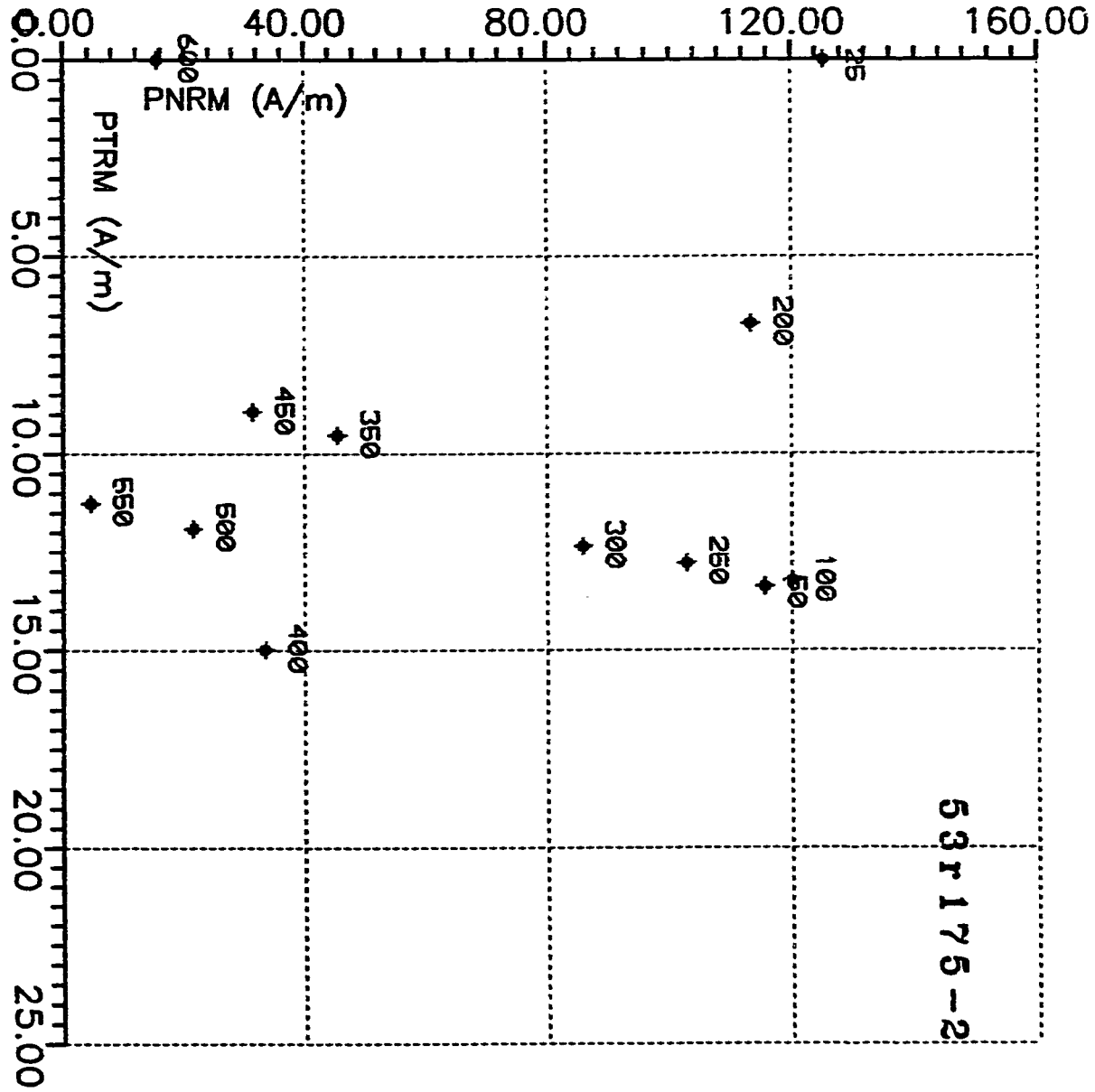
0.00
40.00
80.00
120.00
160.00
PNRM (A/m)
0.00
5.00
10.00
15.00
20.00
25.00
PTRM (A/m)
600
25
200
450
350
550
500
300
250
100
50
400
53r175-2

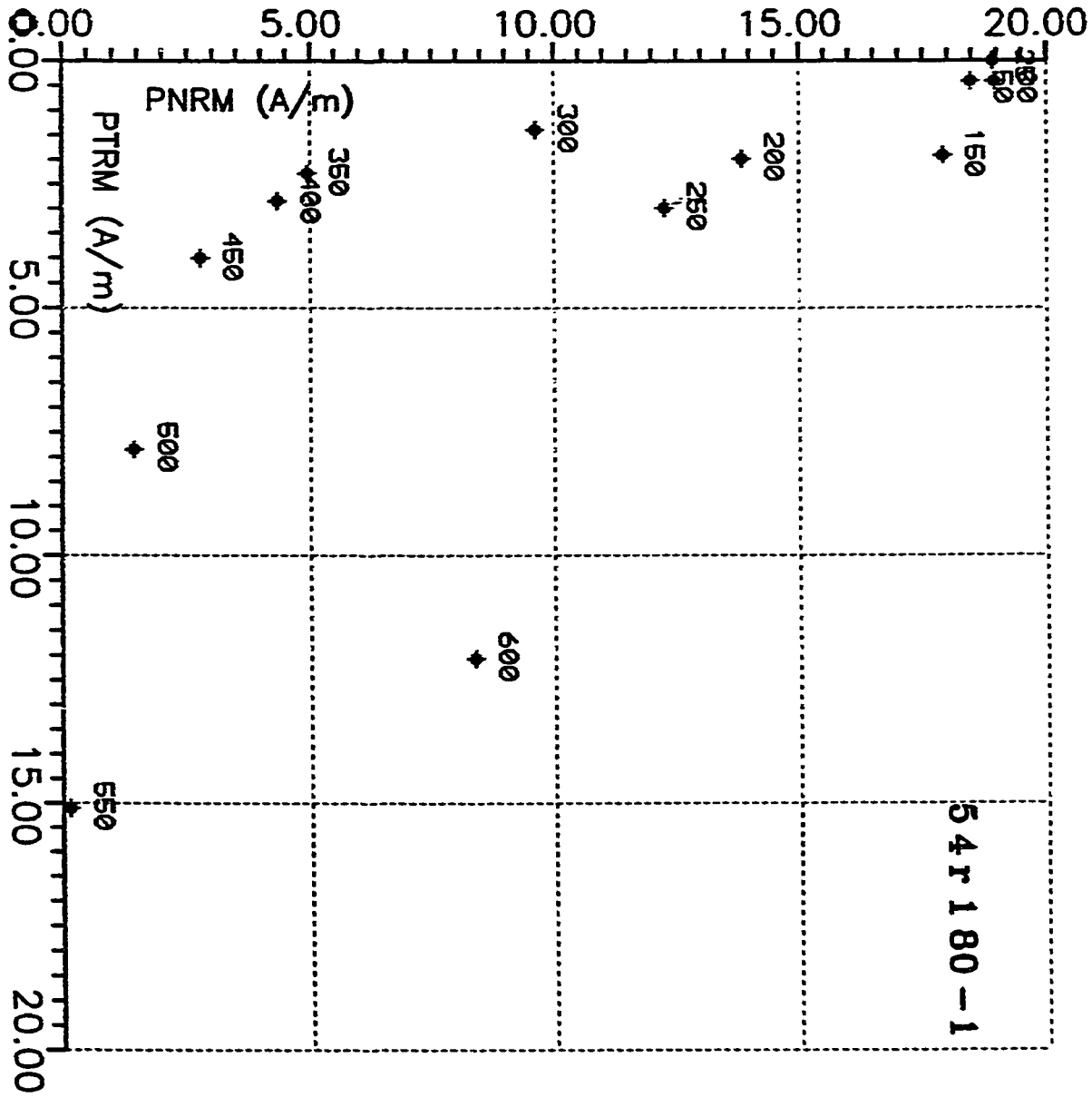
0.00
5.00
10.00
15.00
20.00
PNRM (A/m)
PTRM (A/m)
150
200
250
300
350
400
450
500
600
550
54r180-1

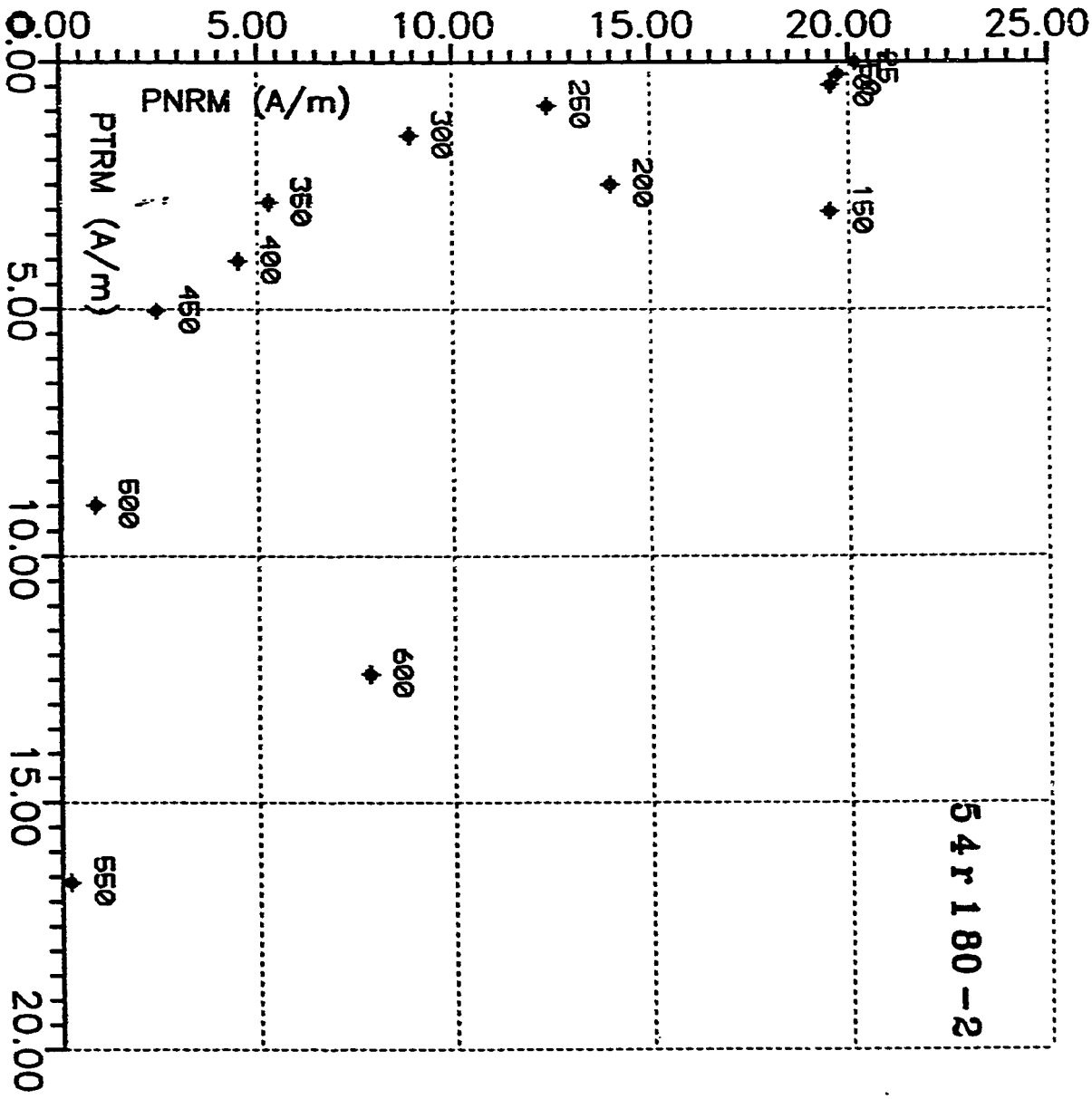
0.00
5.00
10.00
15.00
20.00
25.00
PNRM (A/m)
PTRM (A/m)
350
300
250
200
150
400
450
500
600
550
54r180-2

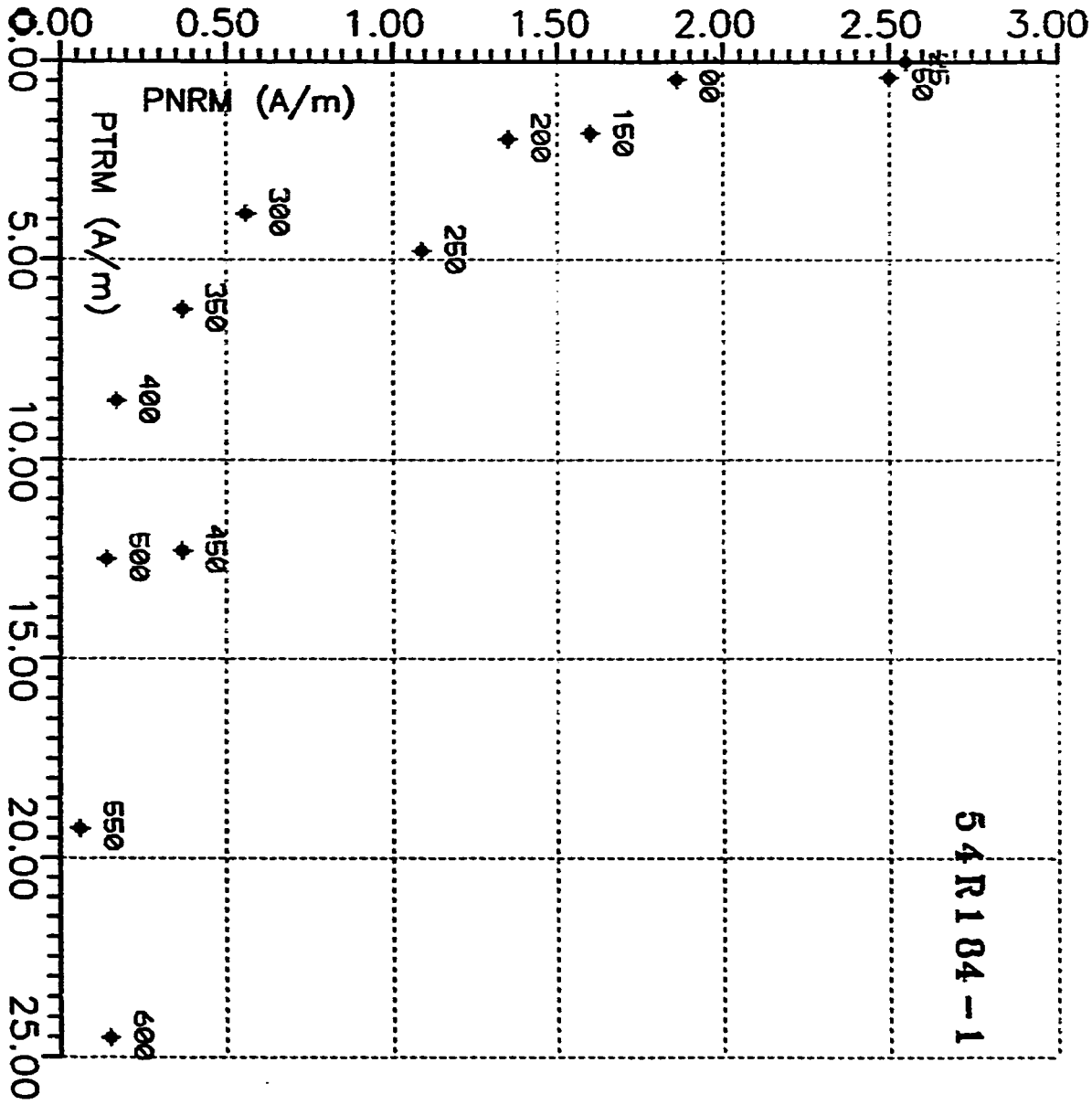
0.00
0.50
1.00
1.50
2.00
2.50
3.00
PNRM (A/m)
PTRM (A/m)
0.00
5.00
10.00
15.00
20.00
25.00
000
050
100
150
200
250
300
350
400
450
500
550
600
54R184-1

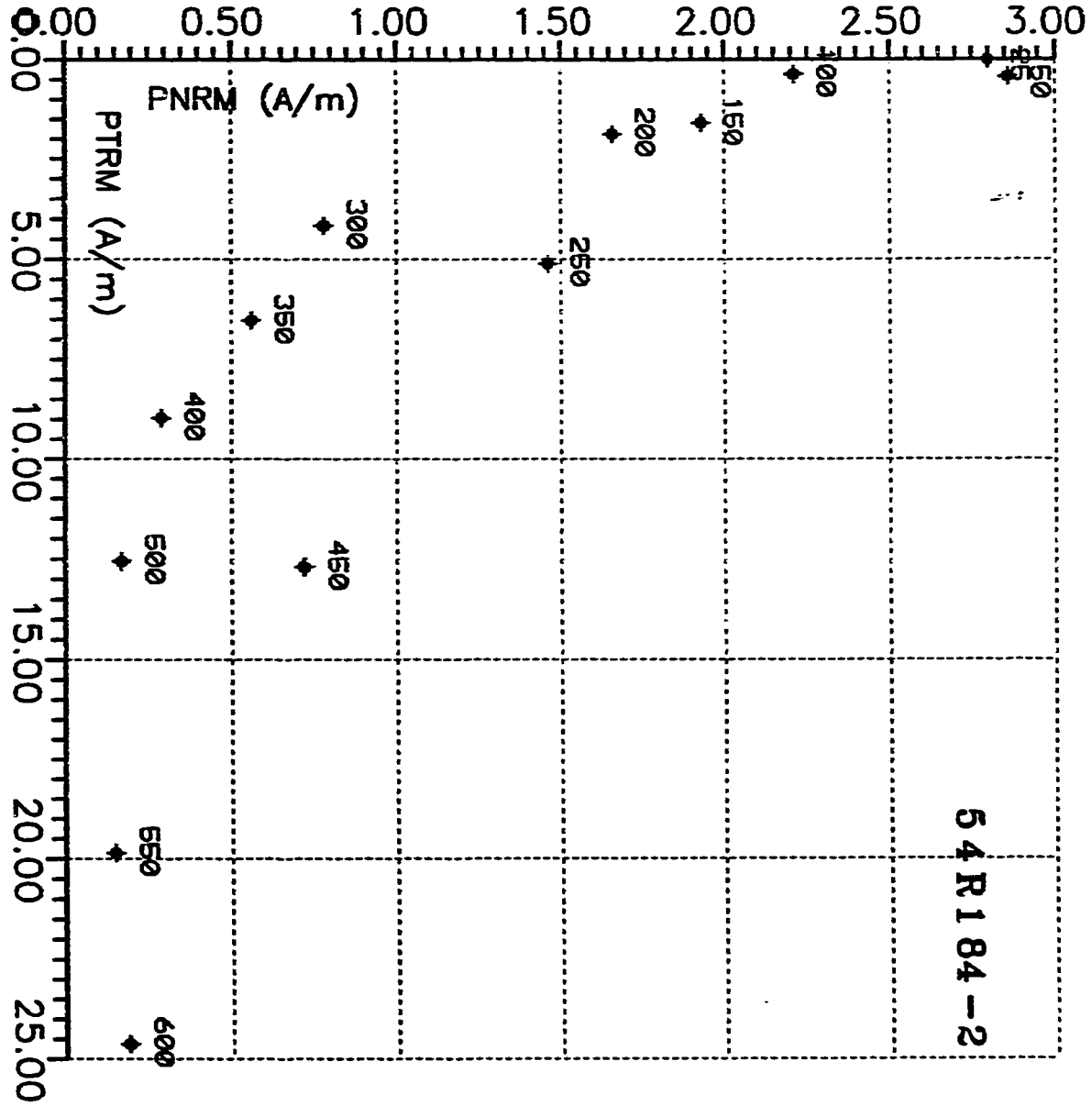
0.00
0.50
1.00
1.50
2.00
2.50
3.00
PNRM (A/m)
PTRM (A/m)
0.00
5.00
10.00
15.00
20.00
25.00
50
100
150
200
250
300
350
400
450
500
550
600
54R184-2

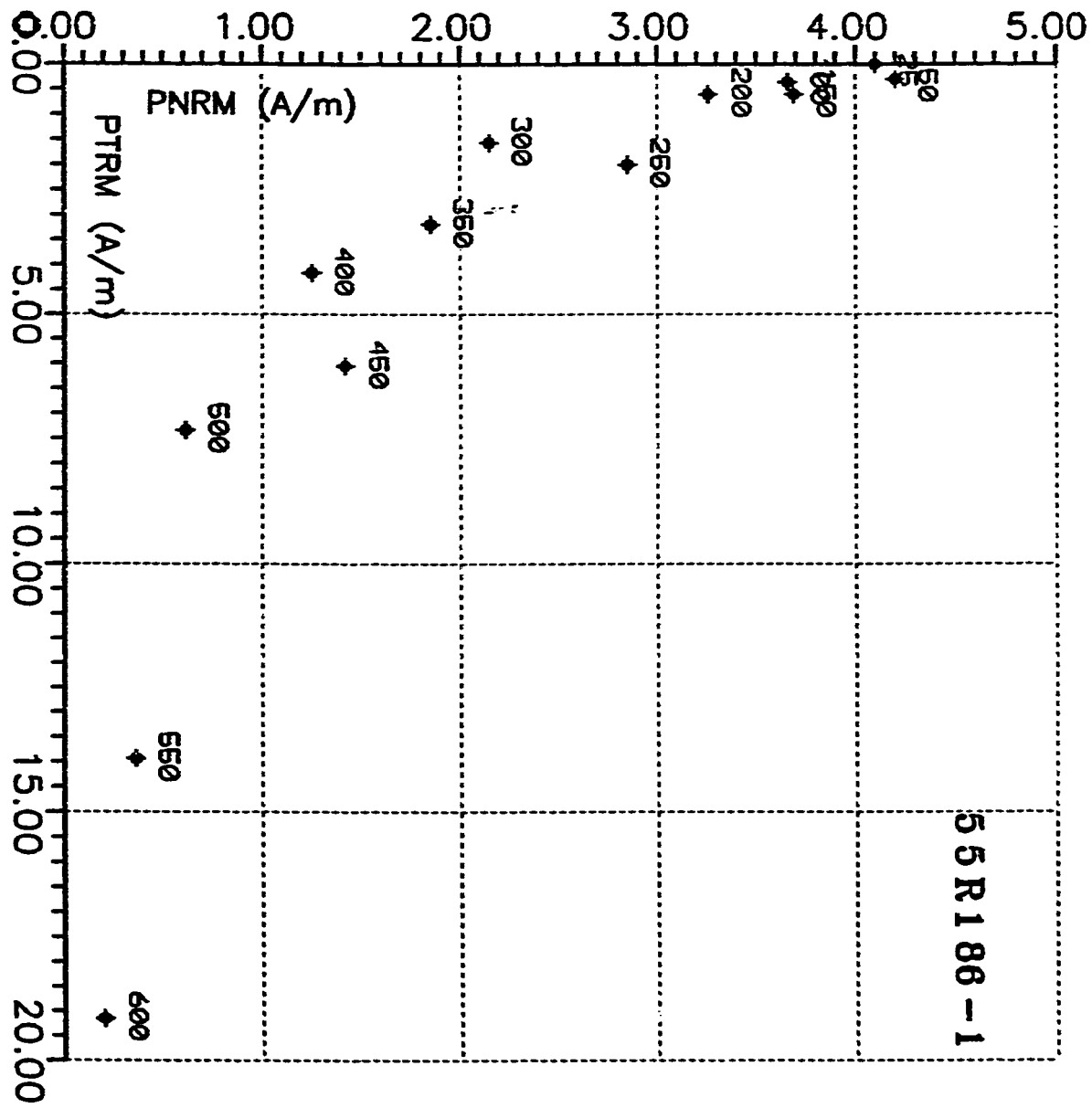
0.00
1.00
2.00
3.00
4.00
5.00
PNRM (A/m)
PTRM (A/m)
0.00
5.00
10.00
15.00
20.00
550
600
55R186-1

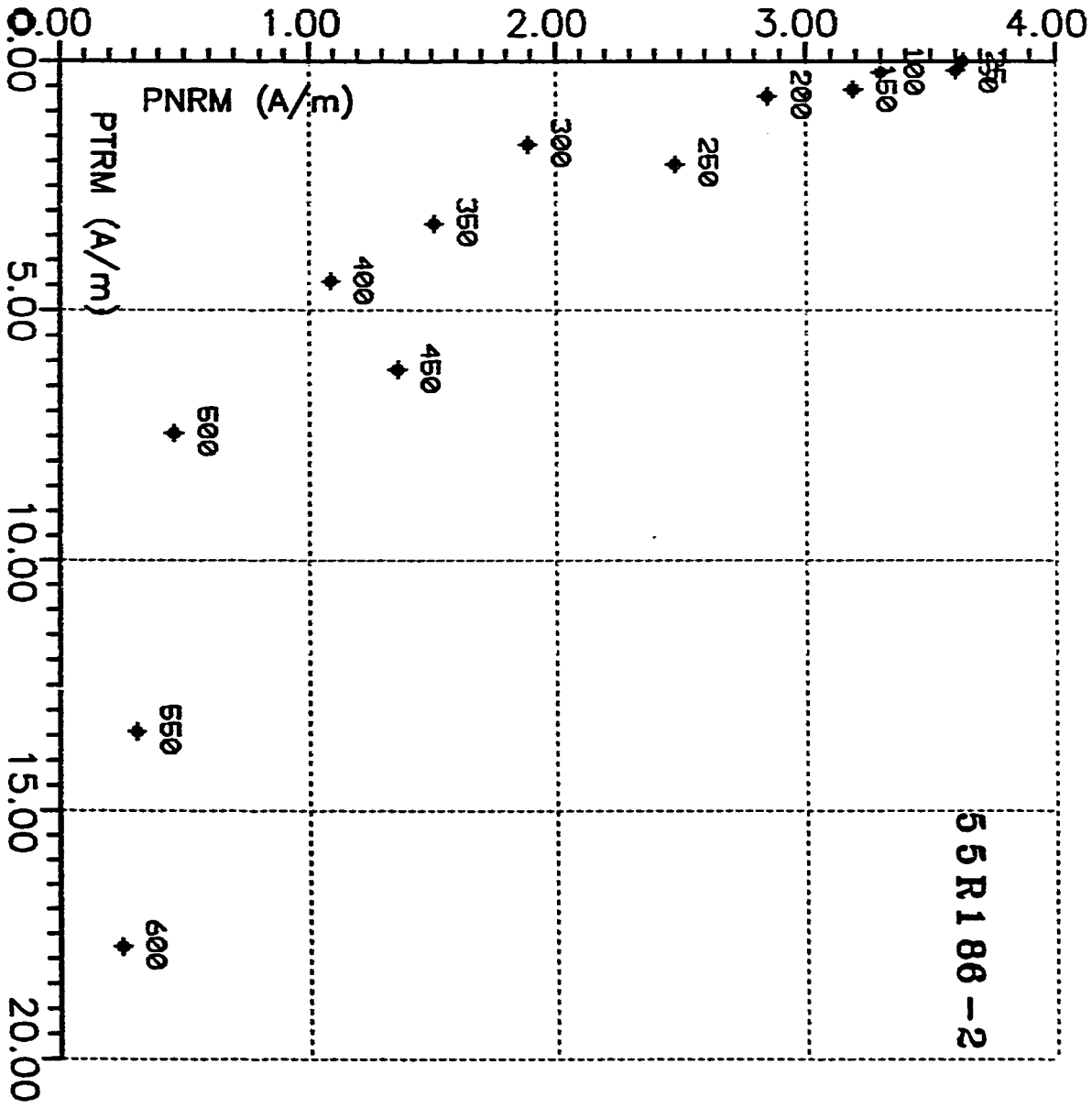
0.00
1.00
2.00
3.00
4.00
PNRM (A/m)
PTRM (A/m)
0.00
5.00
10.00
15.00
20.00
50
100
150
200
250
300
350
400
450
500
550
600
55R186-2

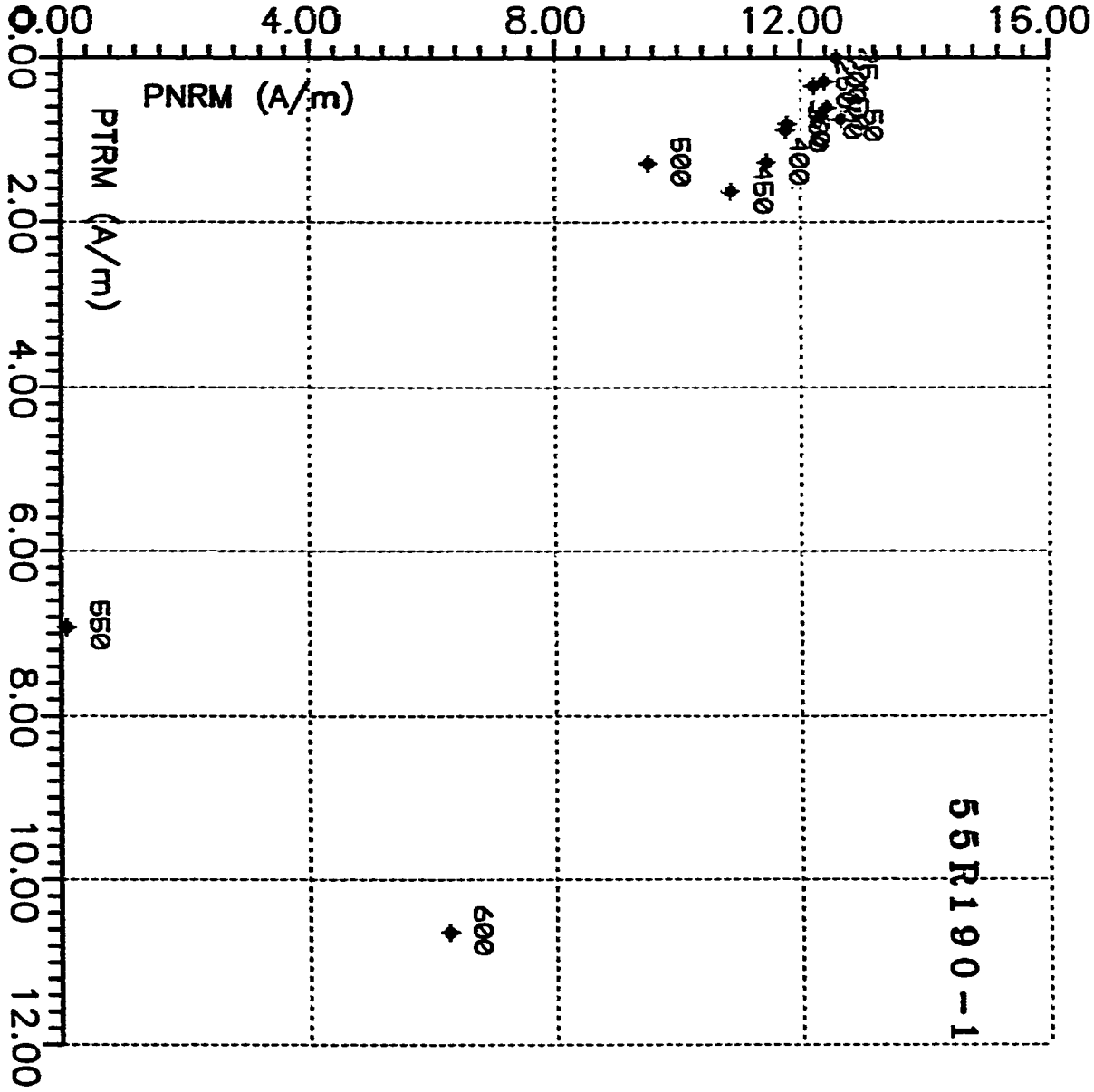
0.00
4.00
8.00
12.00
16.00
PNRM (A/m)
PTRM (A/m)
0.00
2.00
4.00
6.00
8.00
10.00
12.00
500
450
100
550
600
55R190-1

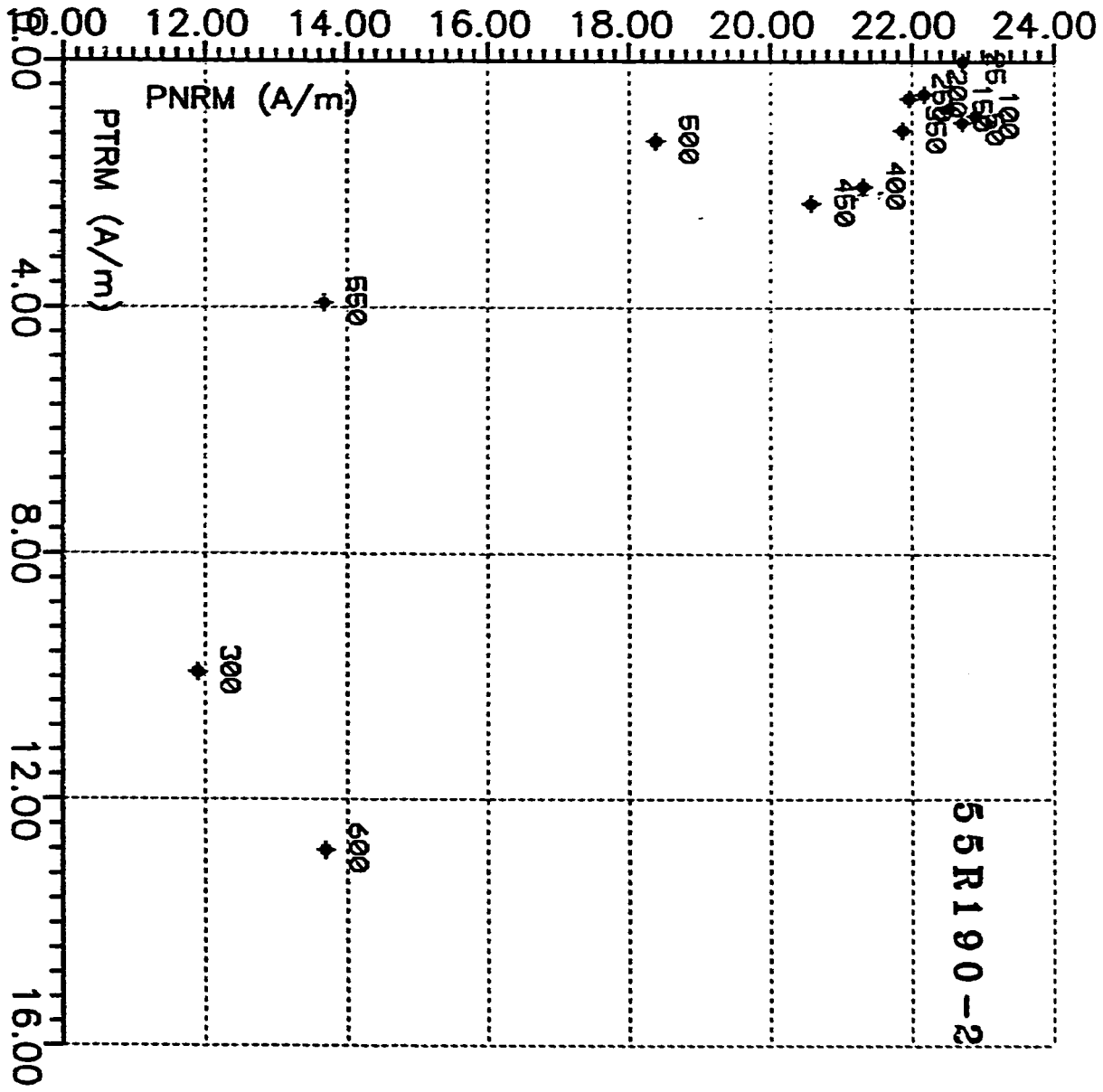
10.00
12.00
14.00
16.00
18.00
20.00
22.00
24.00
4.00
8.00
12.00
16.00
PNRM (A/m)
PTRM (A/m)
100
150
200
250
350
400
450
500
550
300
600
55R190-2

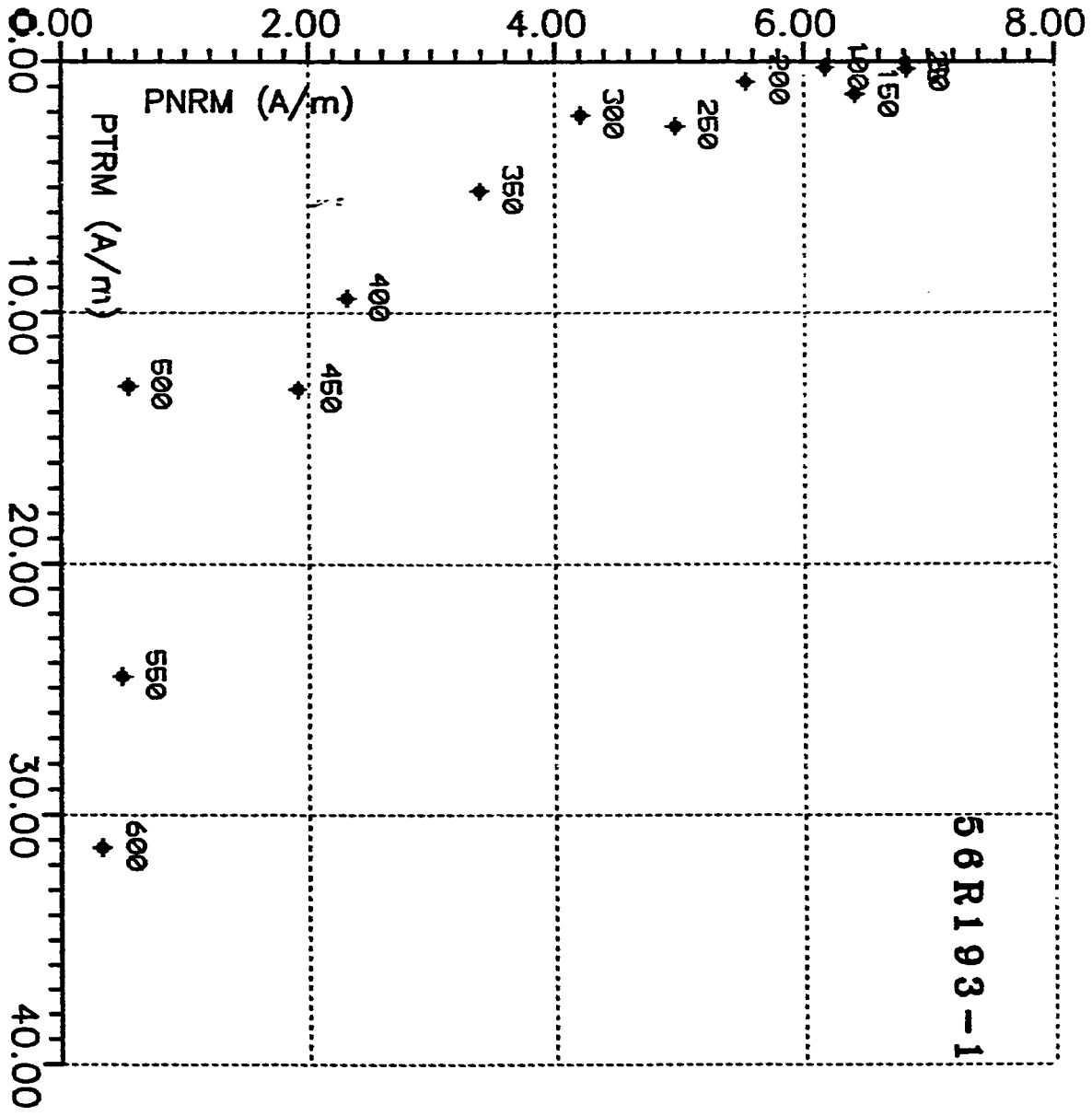
0.00
2.00
4.00
6.00
8.00
PNRM (A/m)
PTRM (A/m)
0.00
10.00
20.00
30.00
40.00
100
150
200
250
300
350
400
450
500
550
600
56R193-1

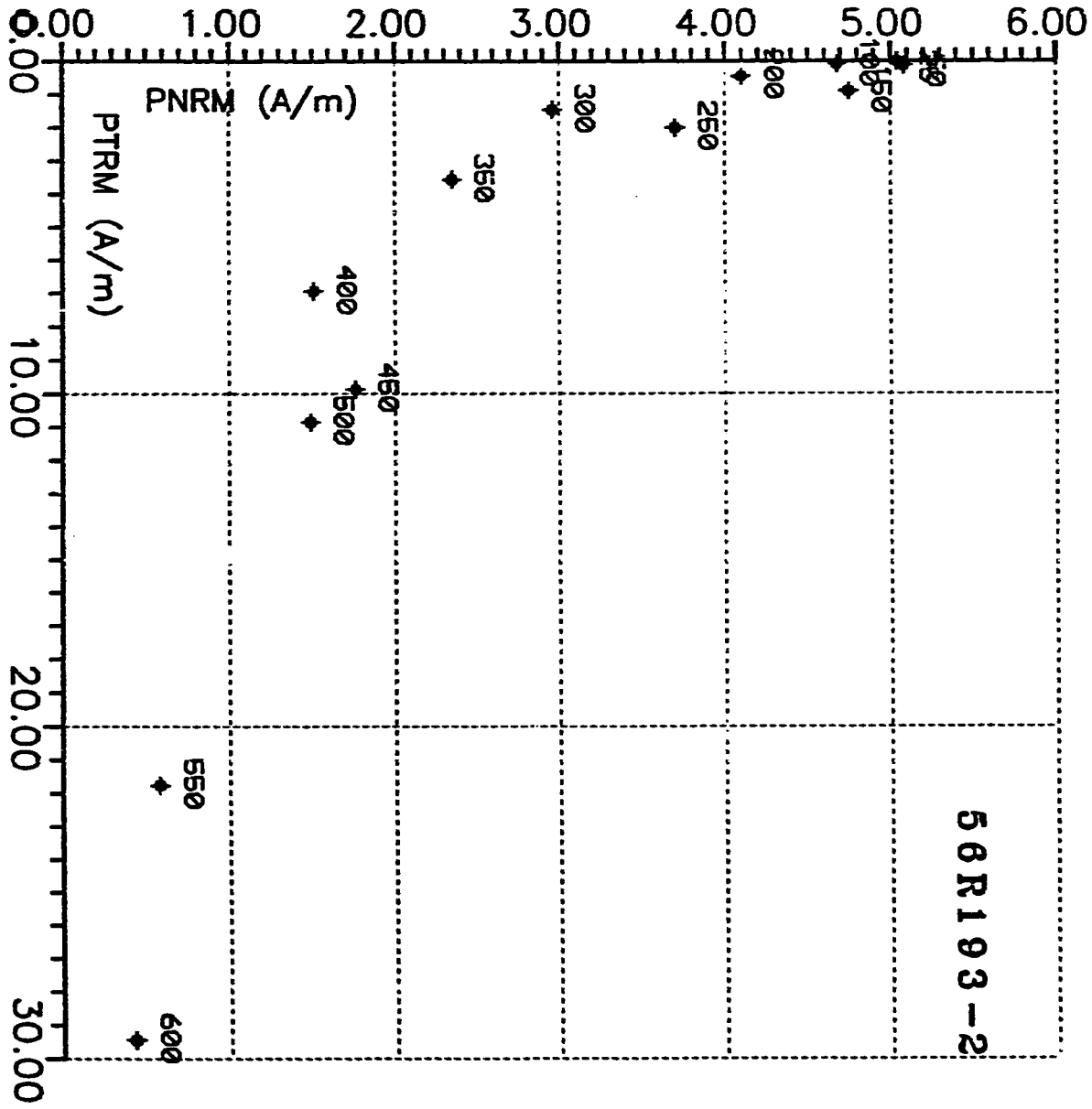
0.00
1.00
2.00
3.00
4.00
5.00
6.00
0.00
10.00
20.00
30.00
PNRM (A/m)
PTRM (A/m)
300
250
350
400
450
500
550
600
56R193-2

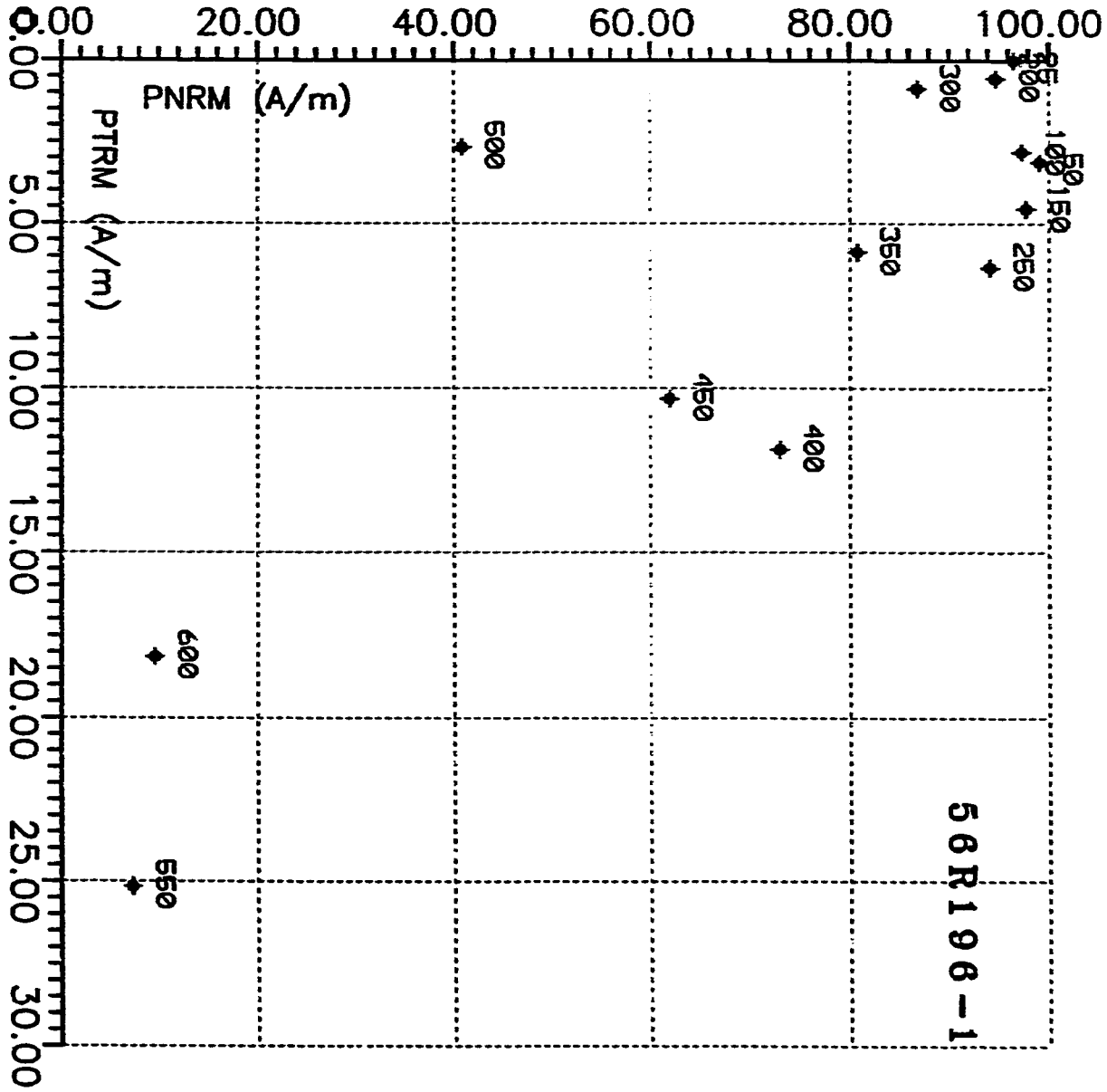
0.00
20.00
40.00
60.00
80.00
100.00
PNRM (A/m)
PTRM (A/m)
0.00
5.00
10.00
15.00
20.00
25.00
30.00
500
300
250
350
150
400
600
550
56R196-1

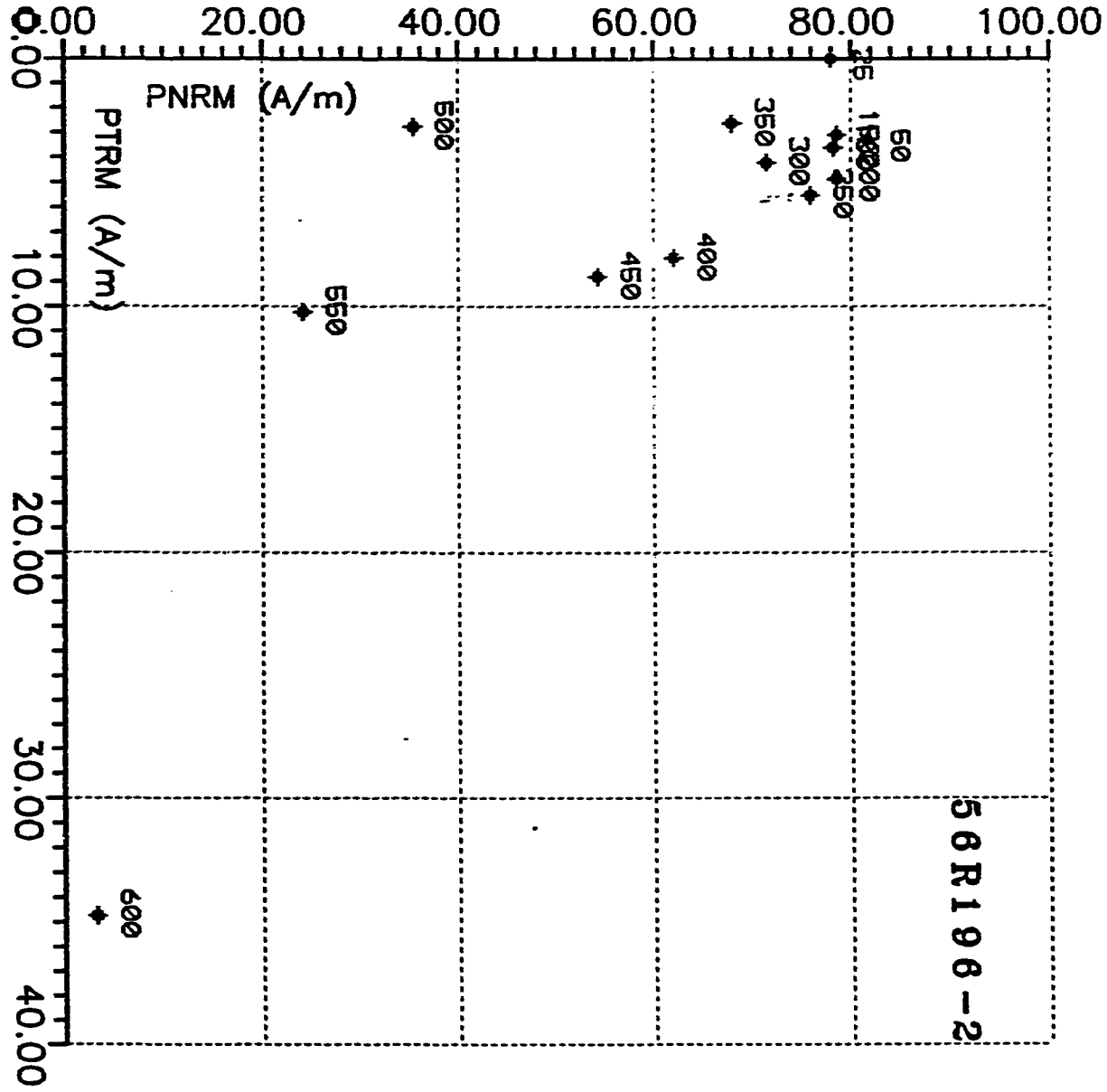
0.00
20.00
40.00
60.00
80.00
100.00
PNRM (A/m)
PTRM (A/m)
0.00
10.00
20.00
30.00
40.00
500
350
300
250
50
400
450
550
600
56R196-2

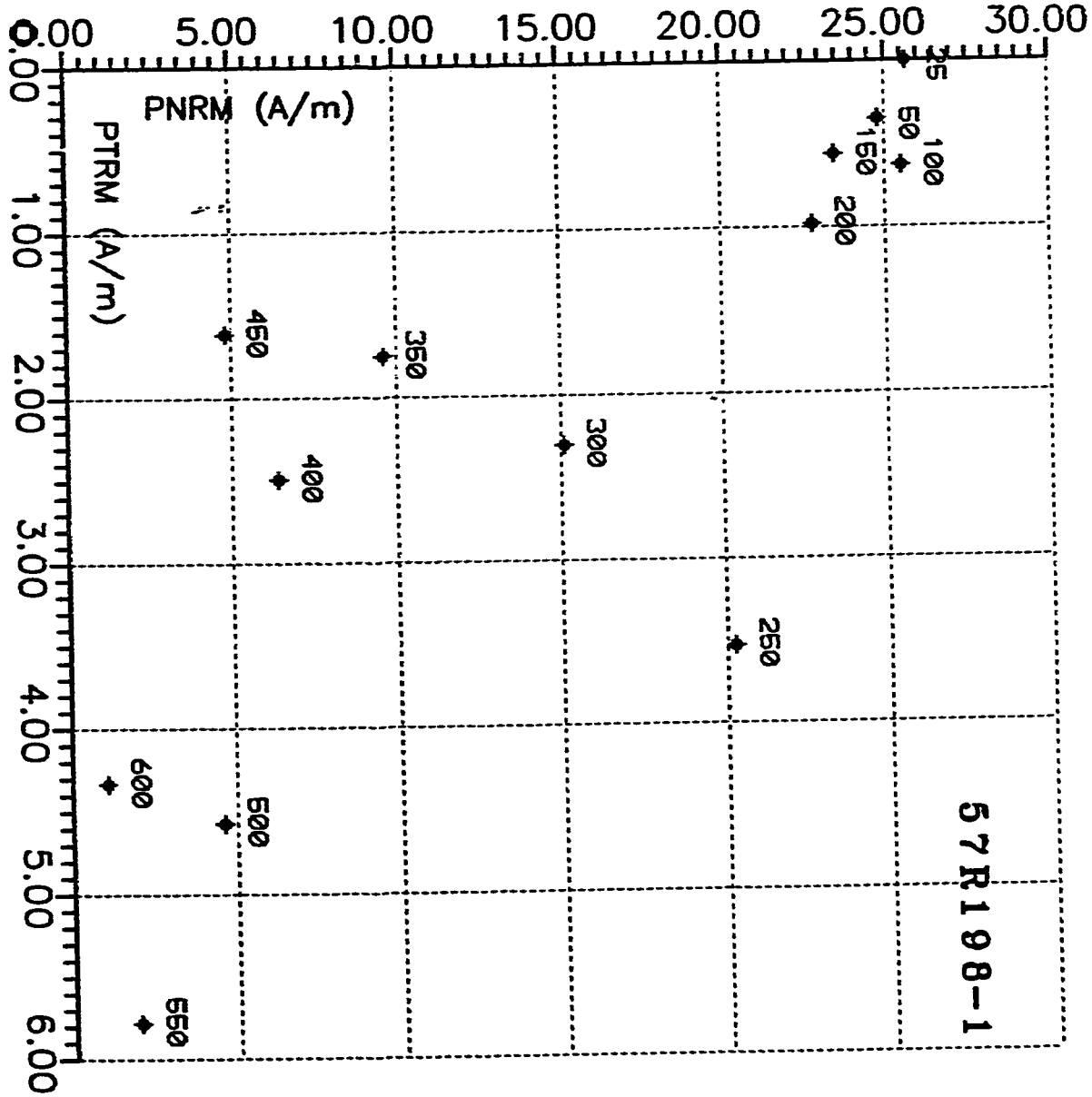
0.00
5.00
10.00
15.00
20.00
25.00
30.00
PNRM (A/m)
PTRM (A/m)
0.00
1.00
2.00
3.00
4.00
5.00
6.00
25
50
100
150
200
250
300
350
400
450
500
600
650
57R198-1

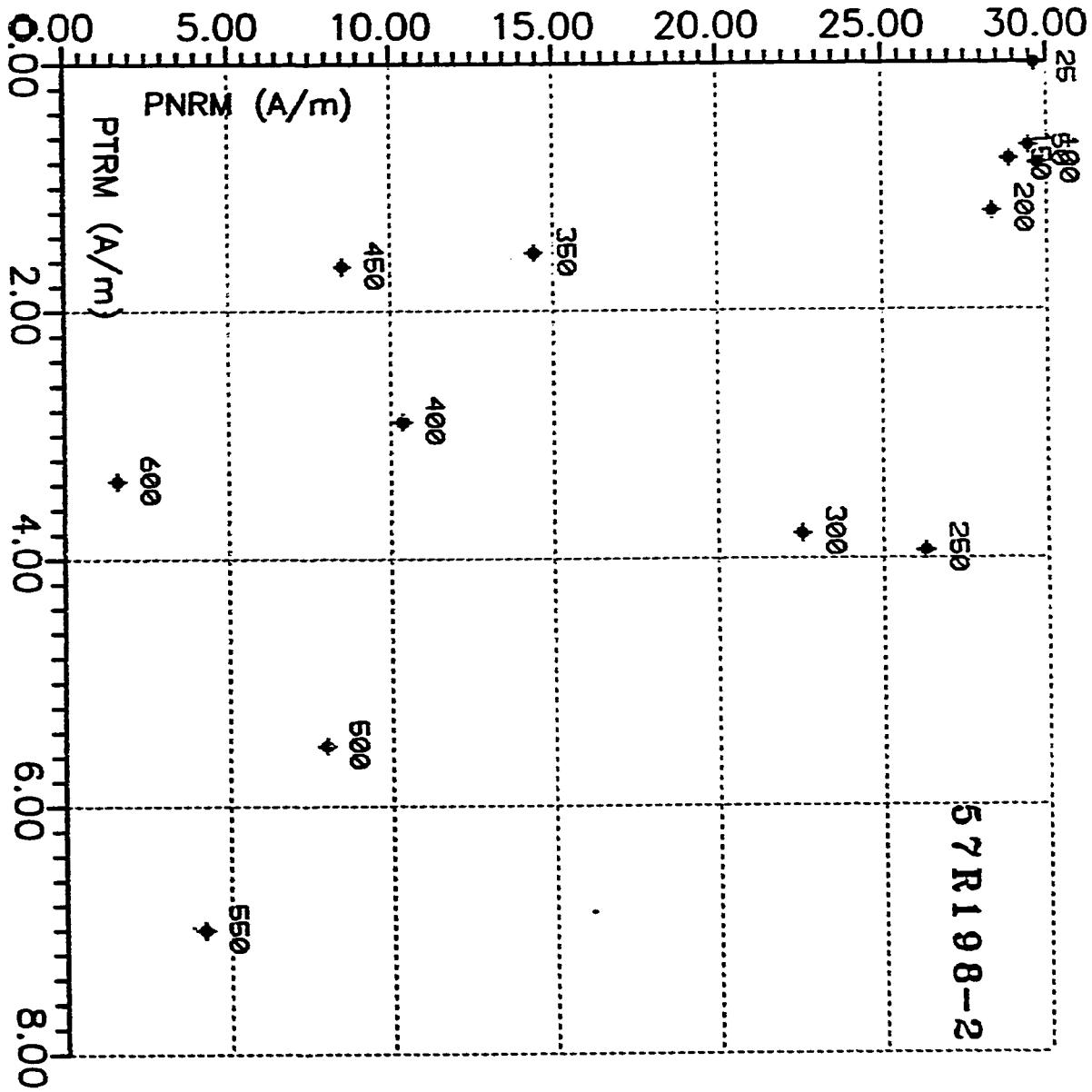
0.00
5.00
10.00
15.00
20.00
25.00
30.00
PNRM (A/m)
PTRM (A/m)
0.00
2.00
4.00
6.00
8.00
25
100
150
200
350
450
400
600
300
250
500
550
57R198-2

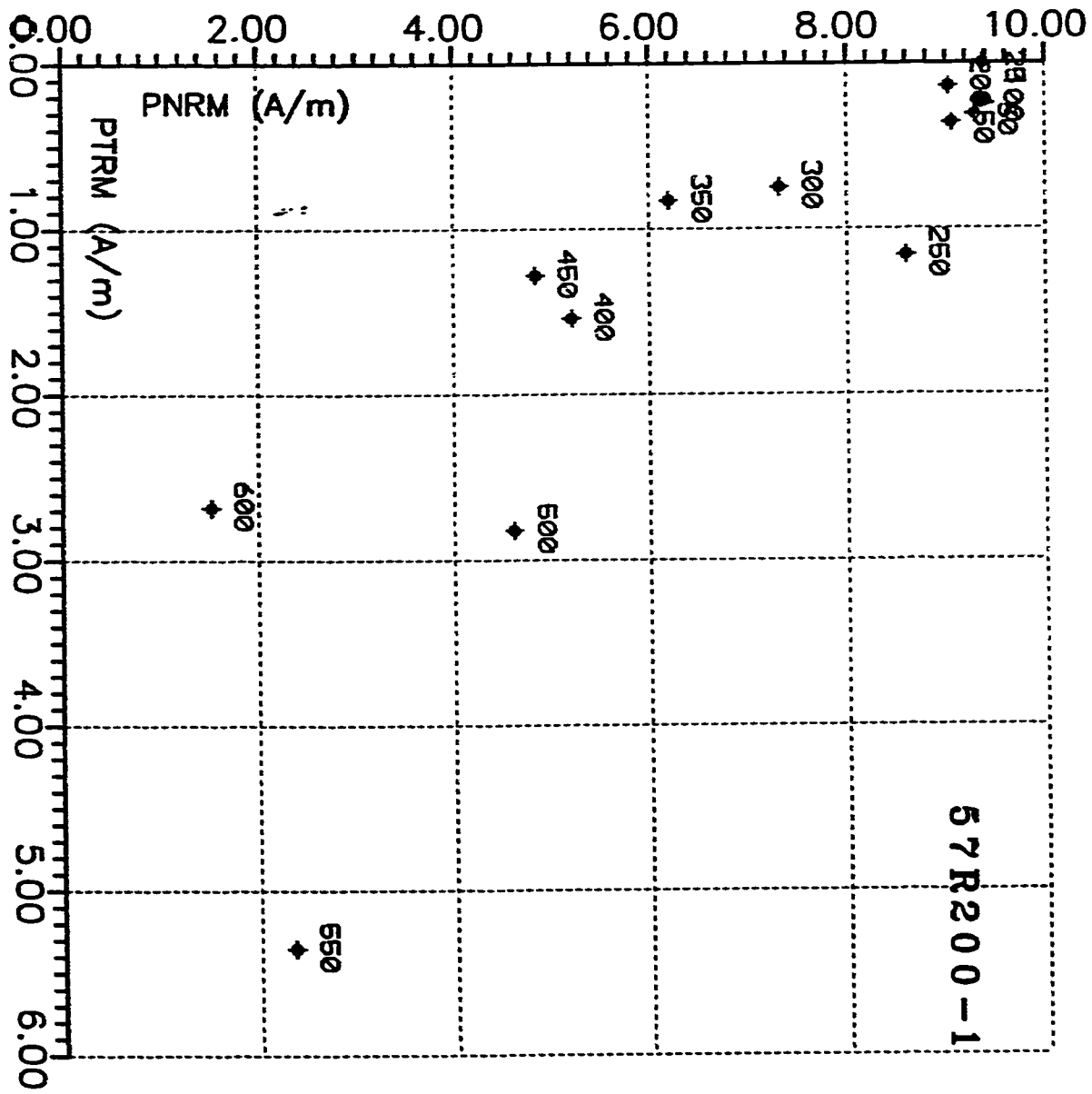
0.00
2.00
4.00
6.00
8.00
10.00
PNRM (A/m)
PTRM (A/m)
0.00
1.00
2.00
3.00
4.00
5.00
6.00
250
300
350
400
450
500
600
650
57R200-1

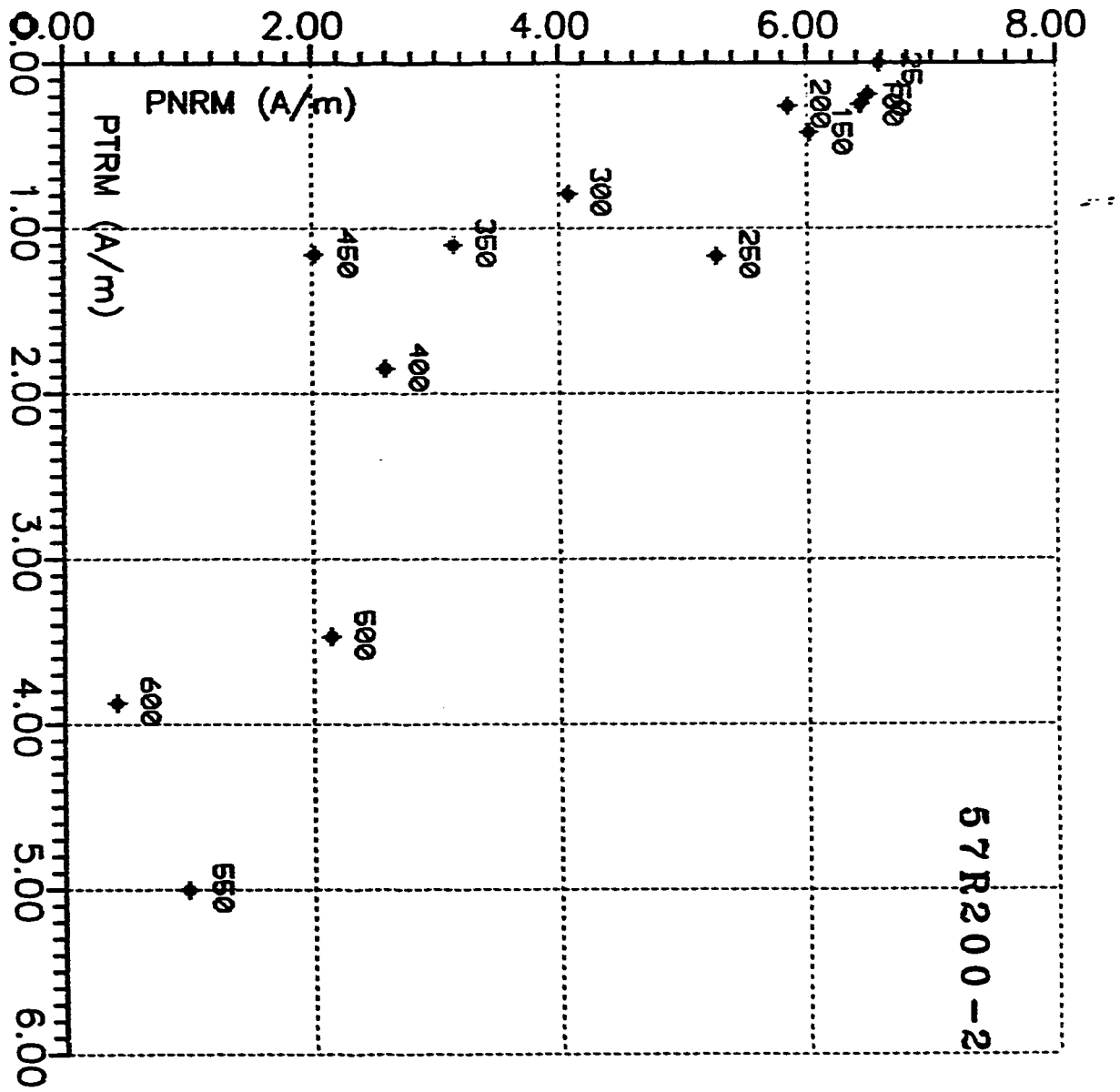
0.00
2.00
4.00
6.00
8.00
PNRM (A/m)
PTRM (A/m)
0.00
1.00
2.00
3.00
4.00
5.00
6.00
25
100
150
200
300
250
350
450
400
500
600
550
57R200-2

Appendix C

This Appendix contains sets of vector diagrams representing the behavior of remanent magnetization during Thermal demagnetization.

Horizontal projection

Vertical projcetion

Temperature= degree C

Locality 1, Site 1 (Tw2)

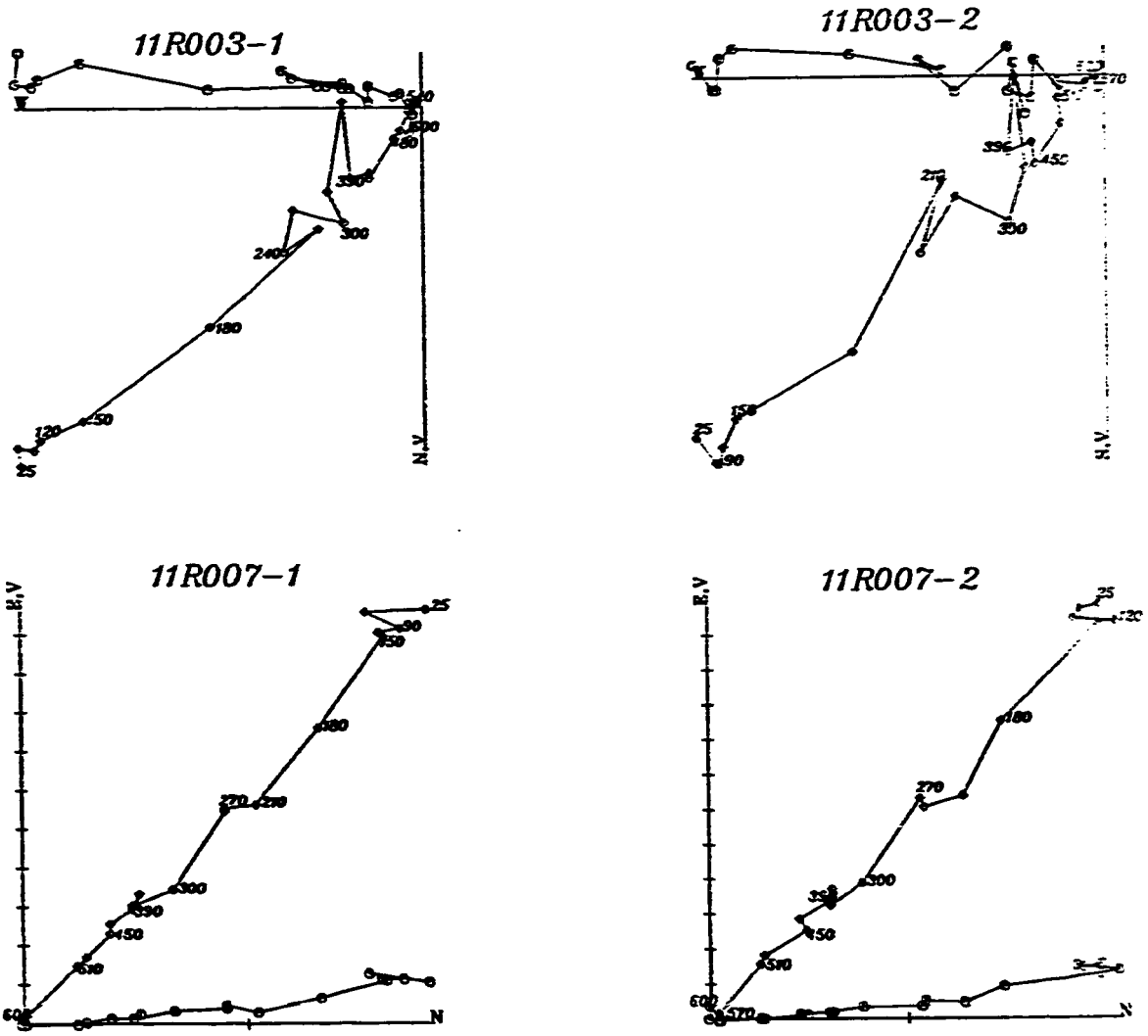

Sets of vector diagrams representing the behavior of remanent magnetization during thermal demagnetization.

Locality 1, Site 2 (Qm2)

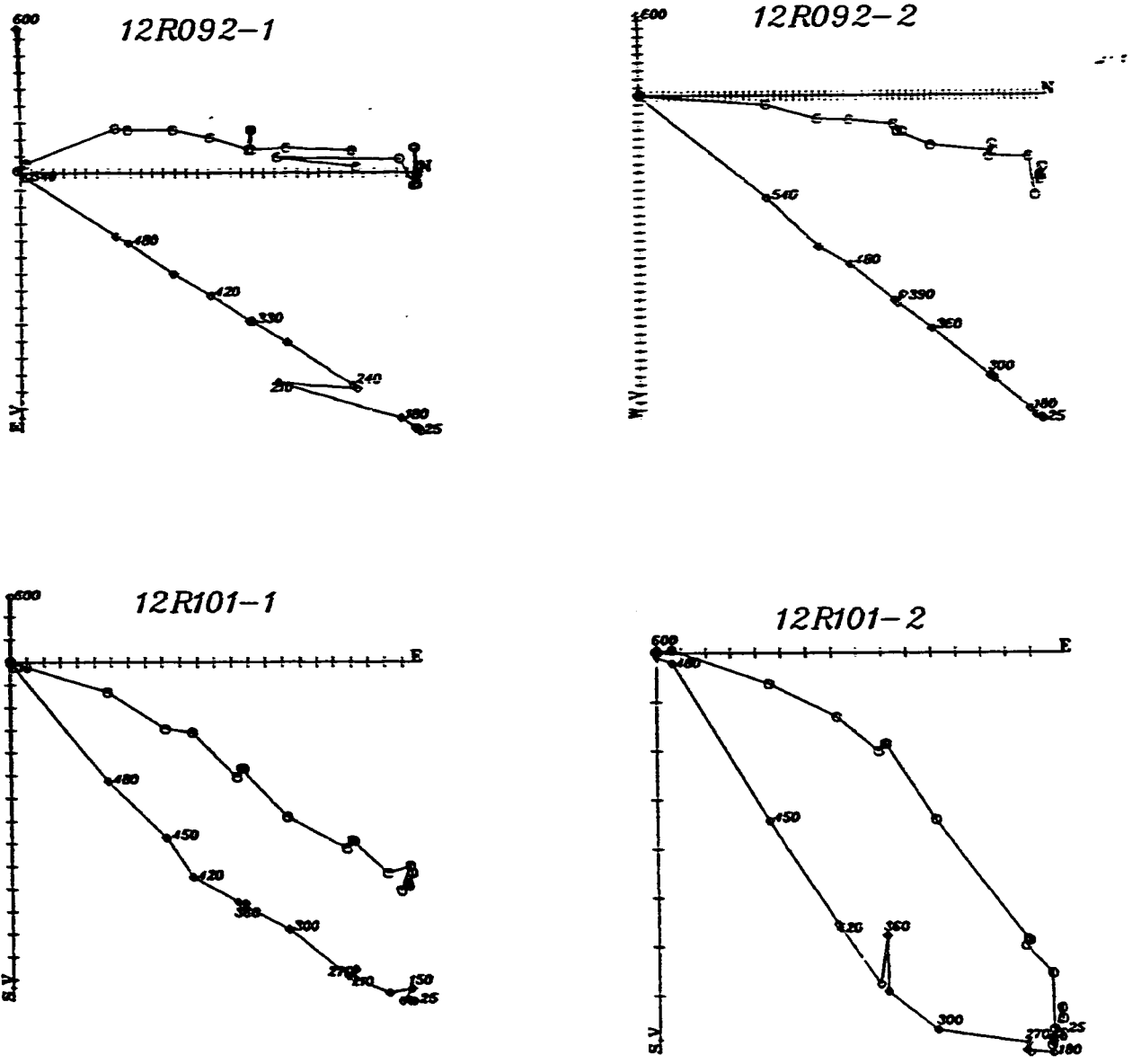

Sets of vector diagrams representing the behavior of remanent magnetization during thermal demagnetization.

Locality 1, Site 3 (Qm1)

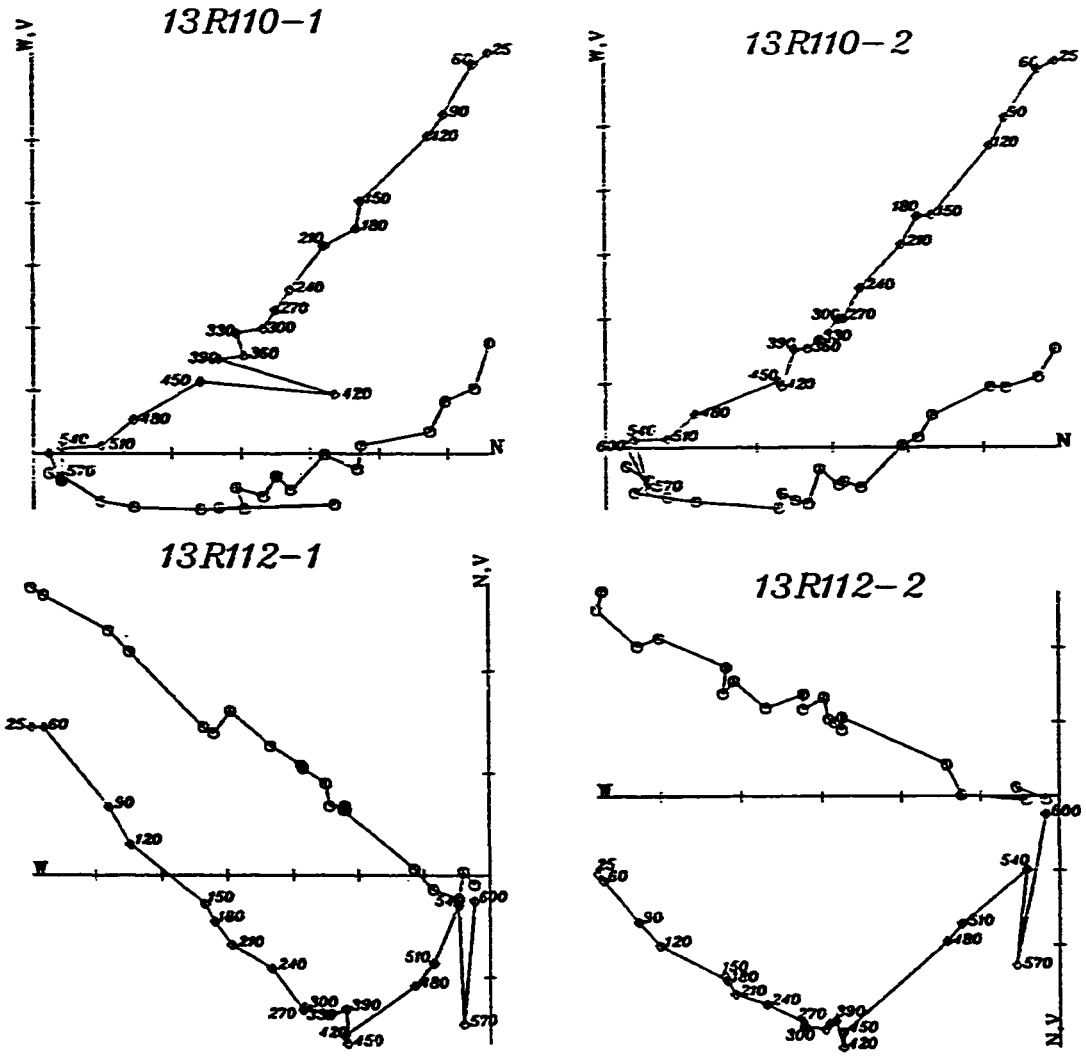

Sets of vector diagrams representing the behavior of remanent magnetization during thermal demagnetization.

Locality 1, Site 4 (Qm1)

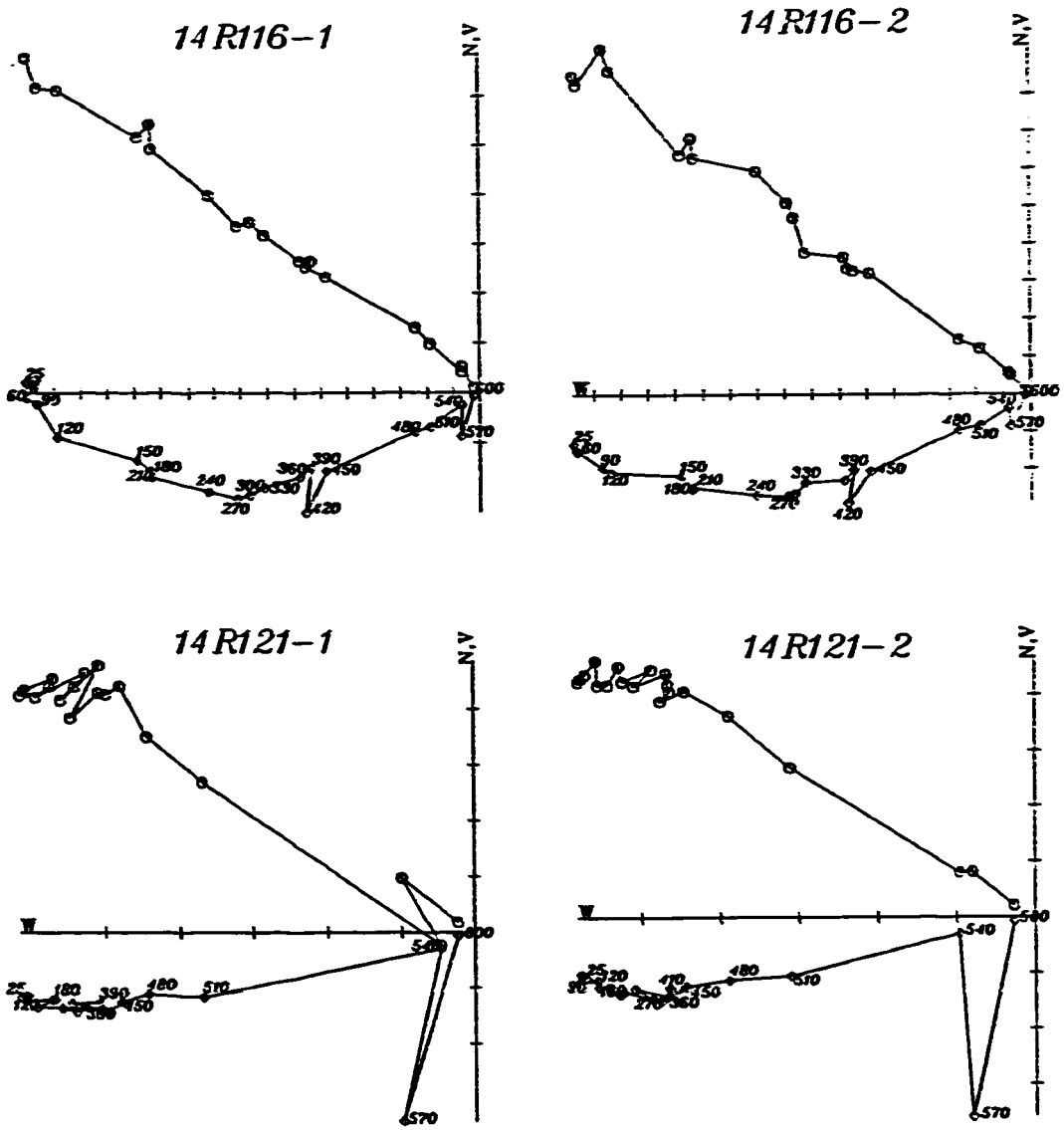

Sets of vector diagrams representing the behavior of remanent magnetization during thermal demagnetization.

Locality 1, Site 5 (Th)

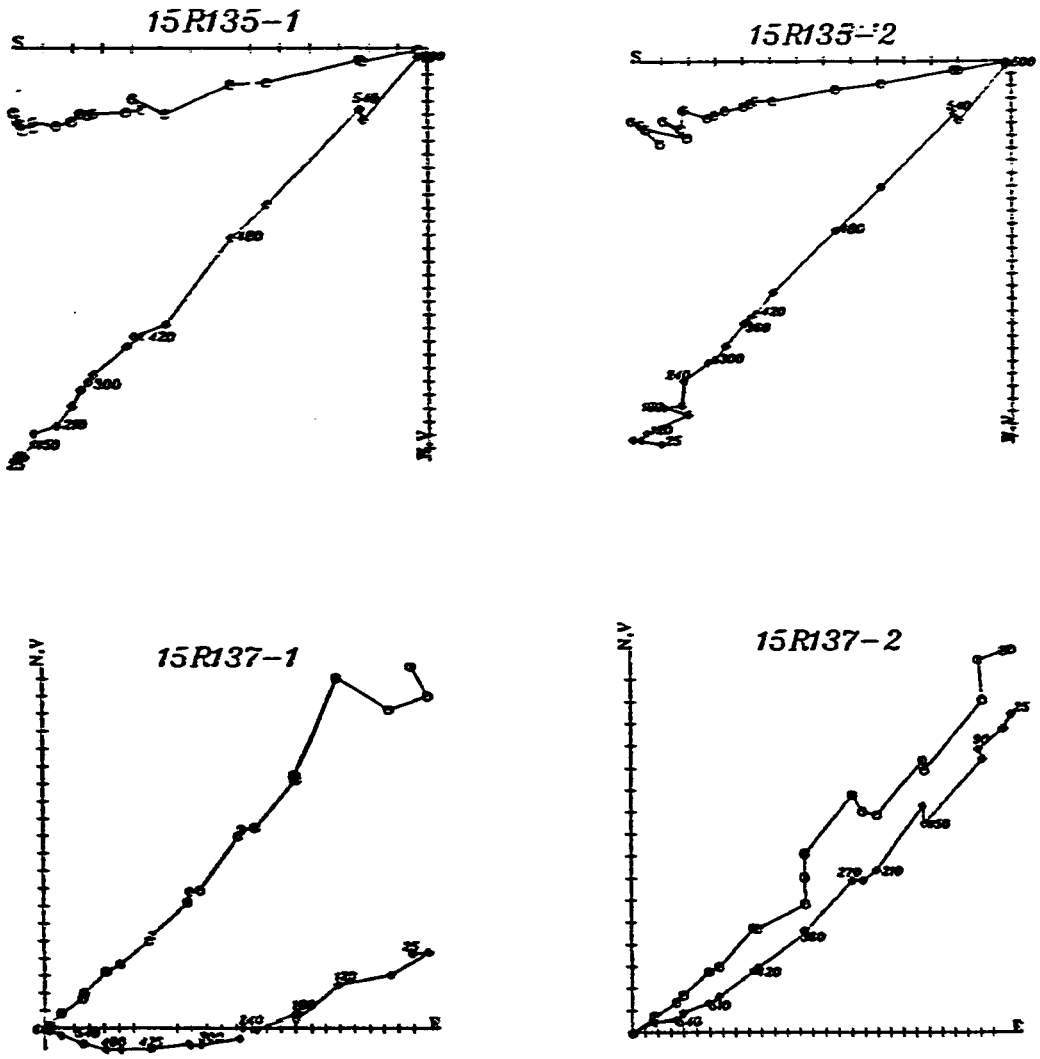

Sets of vector diagrams representing the behavior of remanent magnetization during thermal demagnetization.

Locality 1, Site 6 (Th)

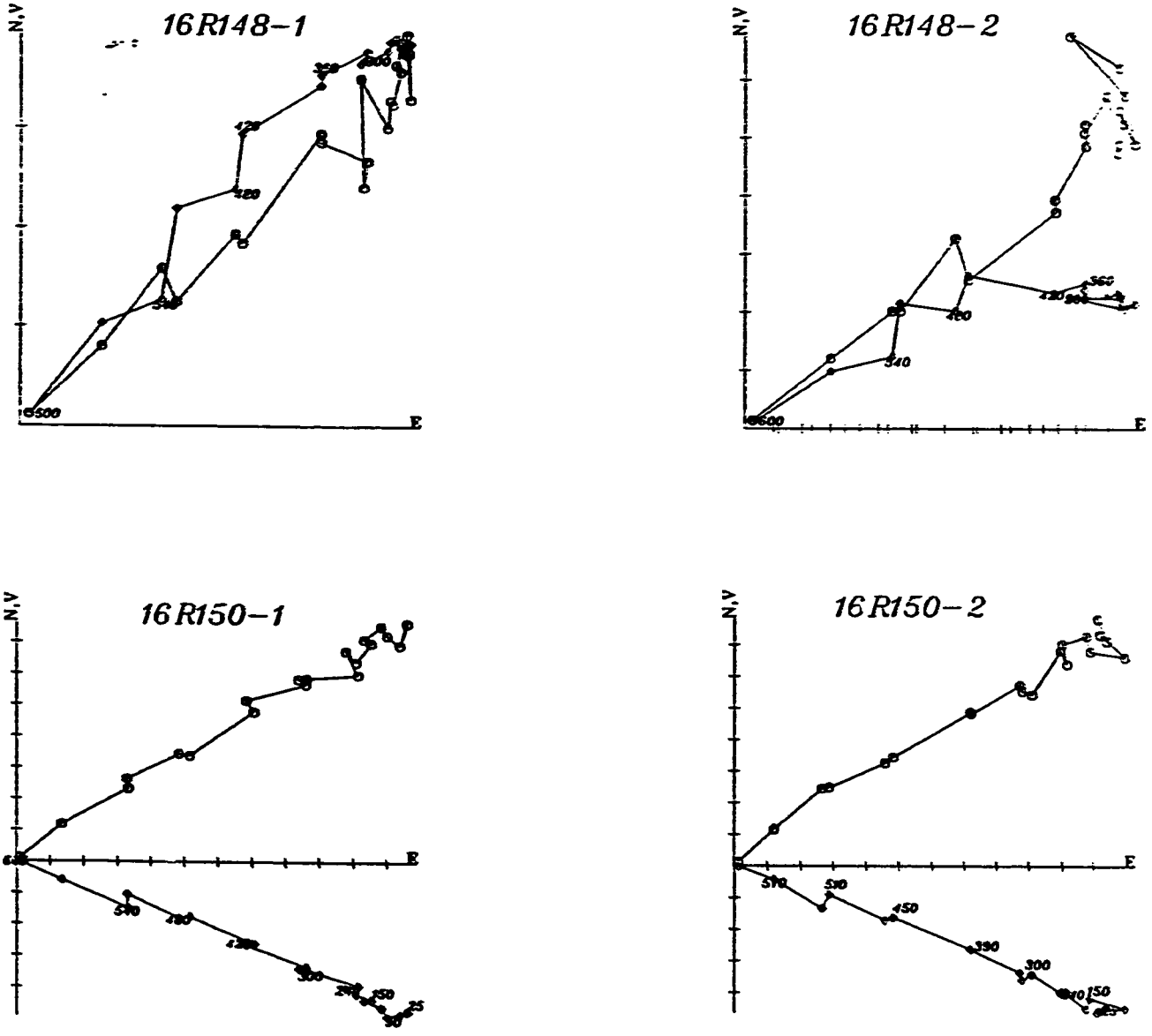

Sets of vector diagrams representing the behavior of remanent magnetization during thermal demagnetization.

Locality 1, Site7 (Qm2)

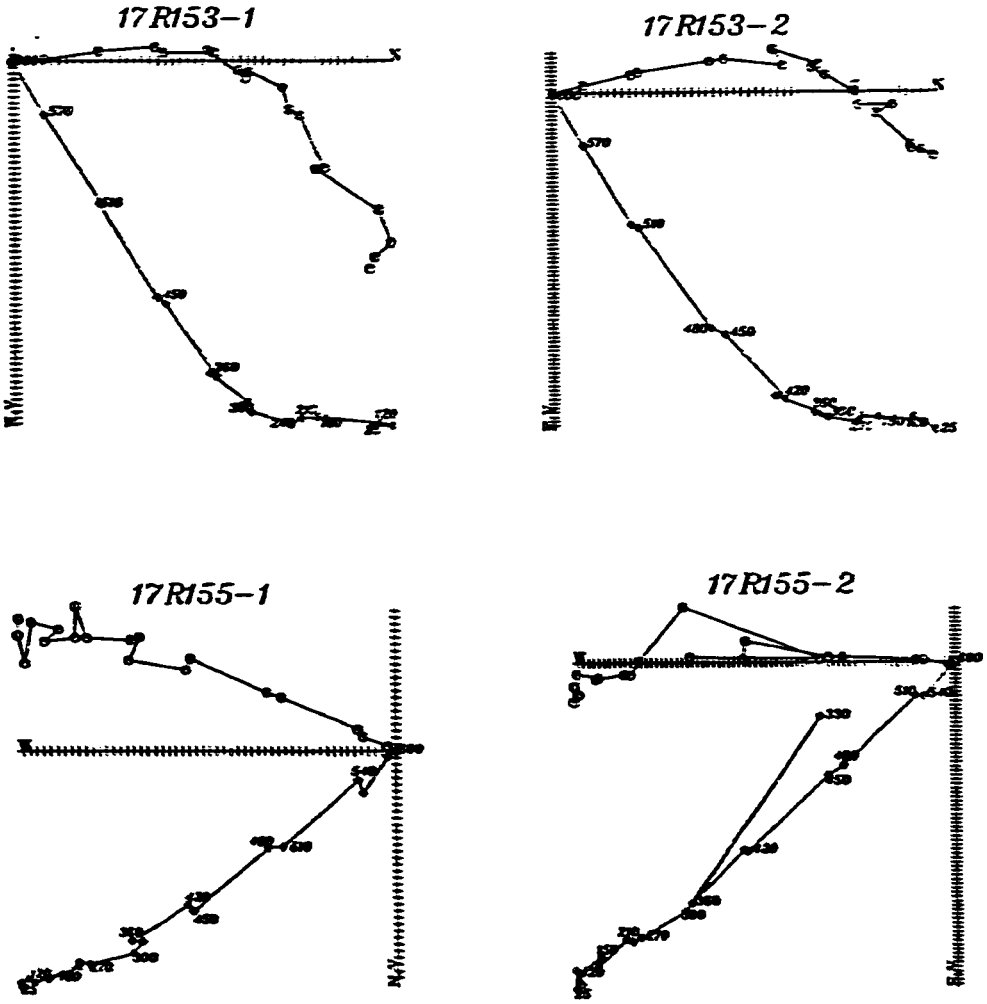

Sets of vector diagrams representing the behavior of remanent magnetization during thermal demagnetization.

Locality 2, Site 1 (Tw1)

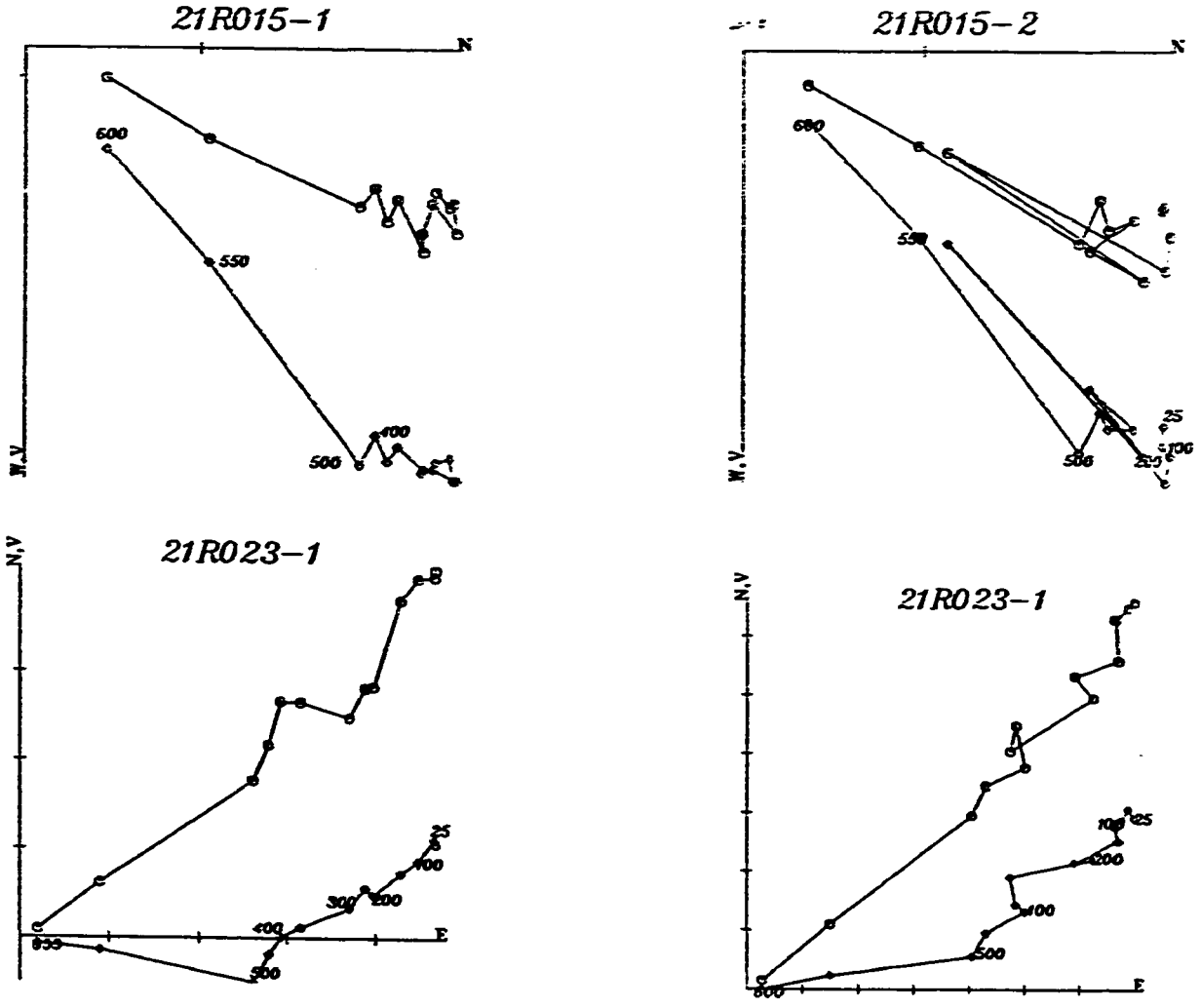

Sets of vector diagrams representing the behavior of remanent magnetization during thermal demagnetization.

Locality 2, Site 2, (Tw1)

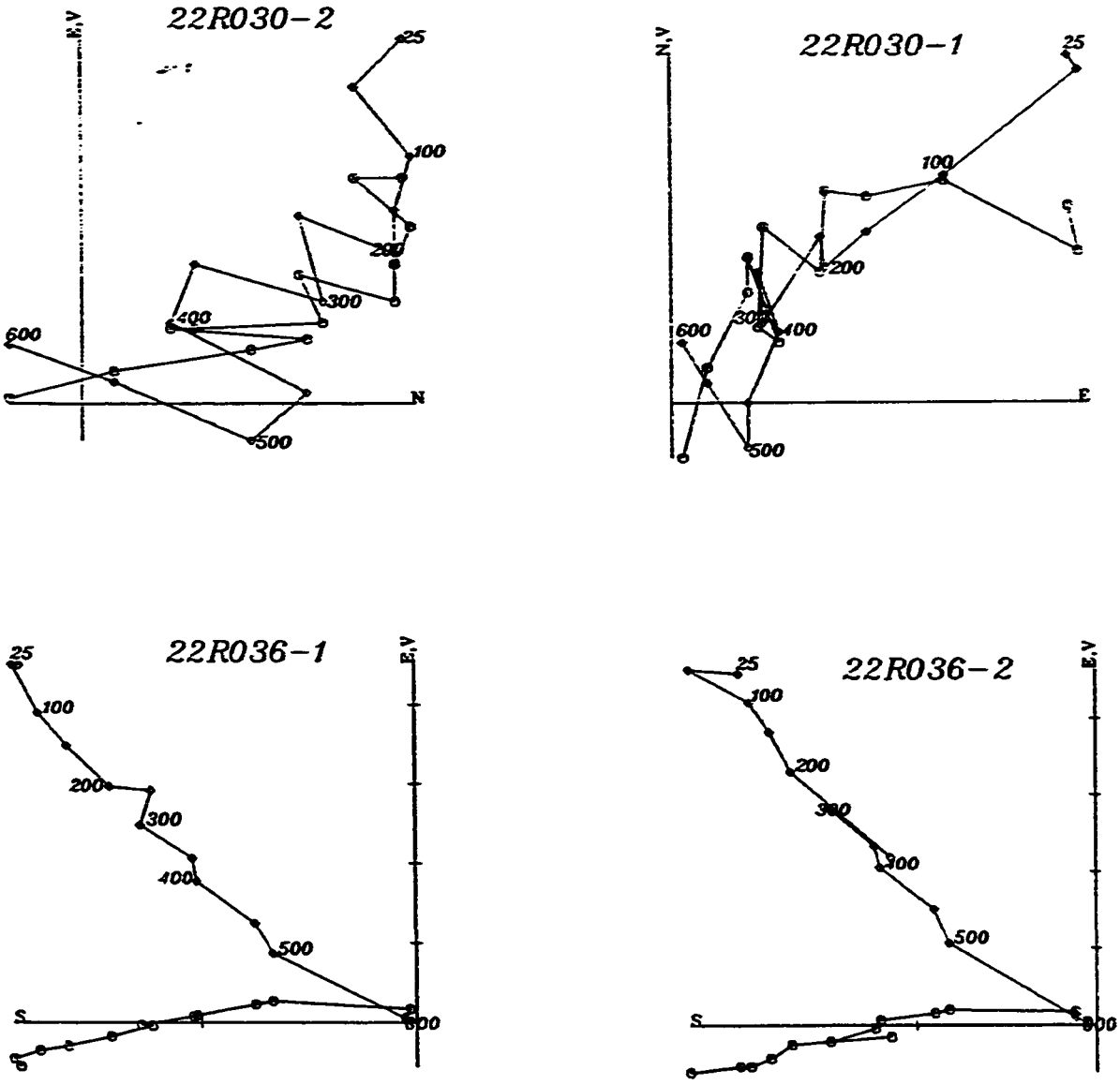

Sets of vector diagrams representing the behavior of remanent magnetization during thermal demagnetization.

Locality 2, Site 3 (Tw1)

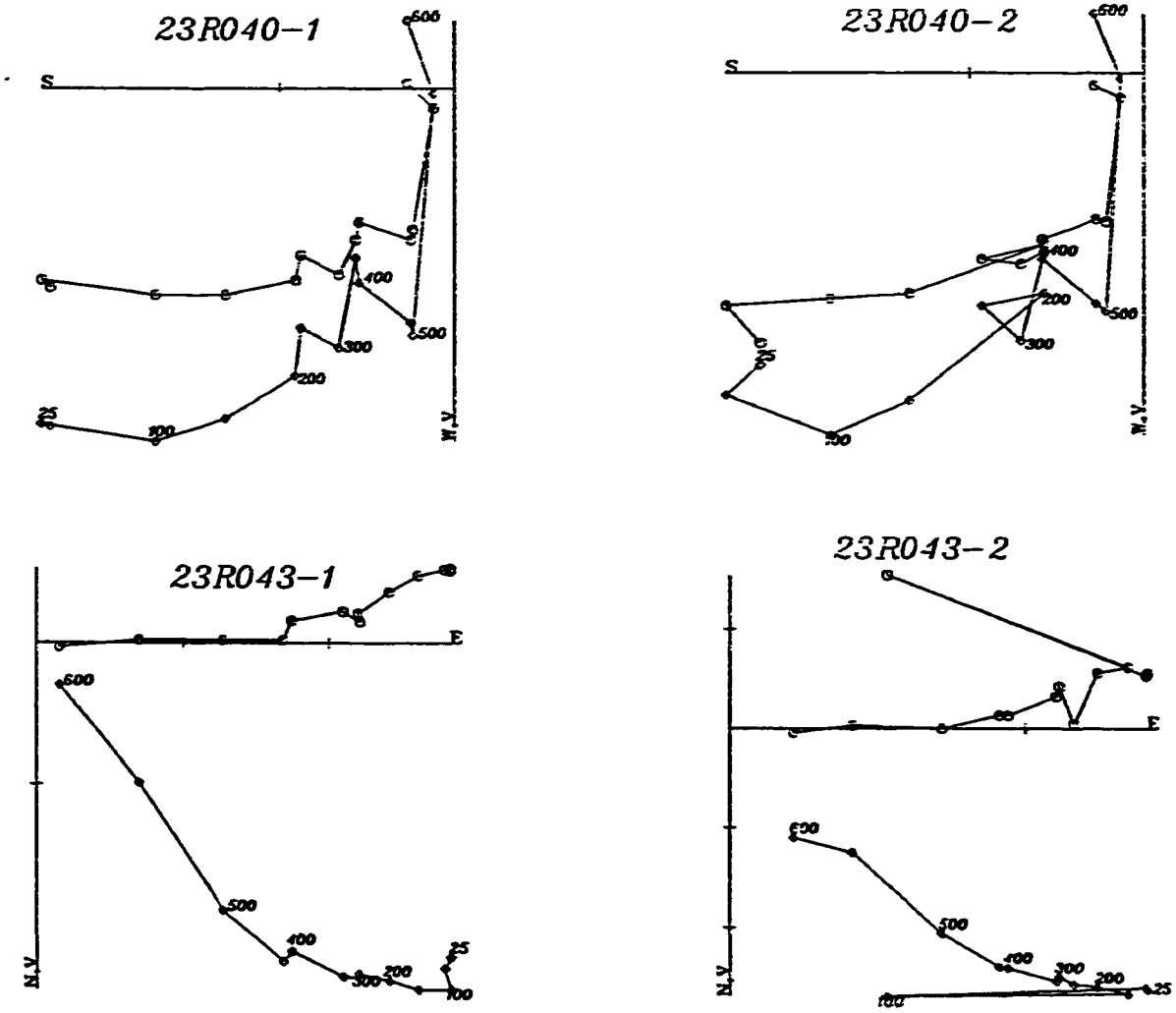

Sets of vector diagrams representing the behavior of remanent magnetization during thermal demagnetization.

Locality 3, Site 1 (Tw1)

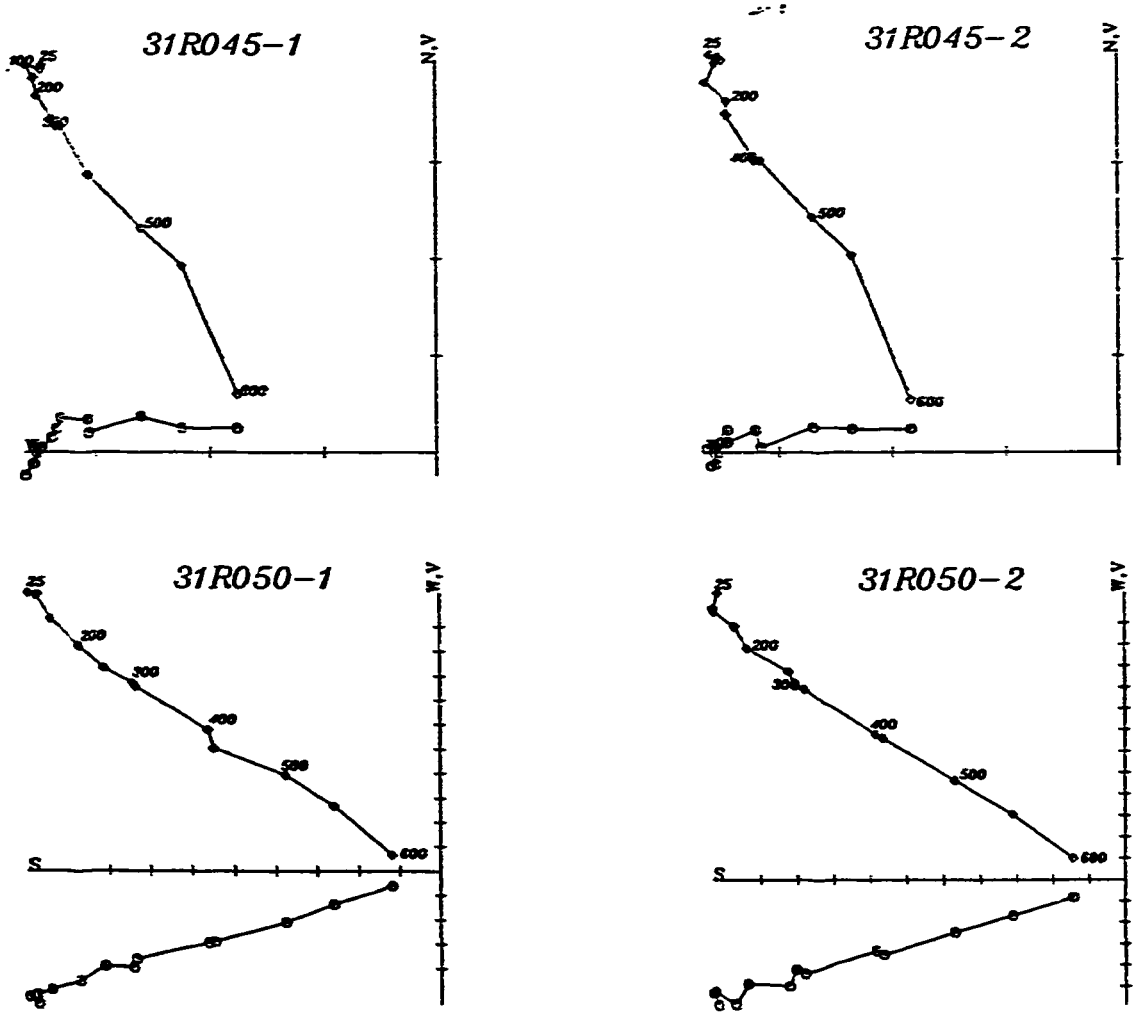

Sets of vector diagrams representing the behavior of remanent magnetization during thermal demagnetization.

Locality3, Site2 (Tw1)

32R055-1

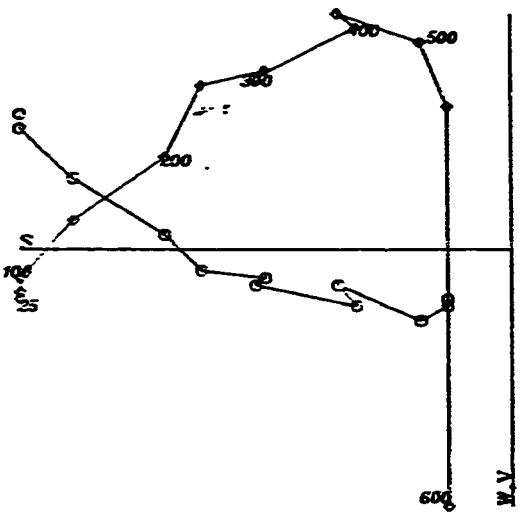

32R055-2

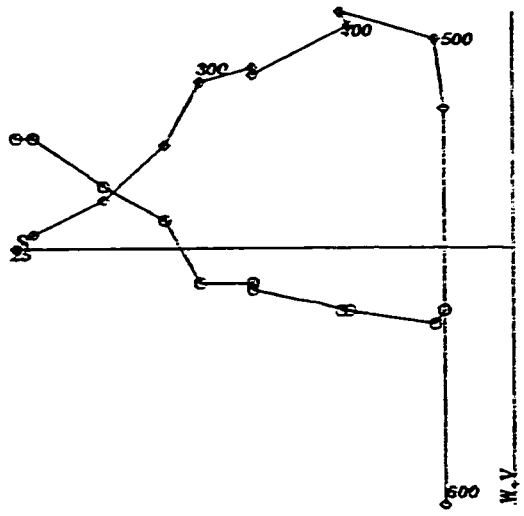

32R058-1

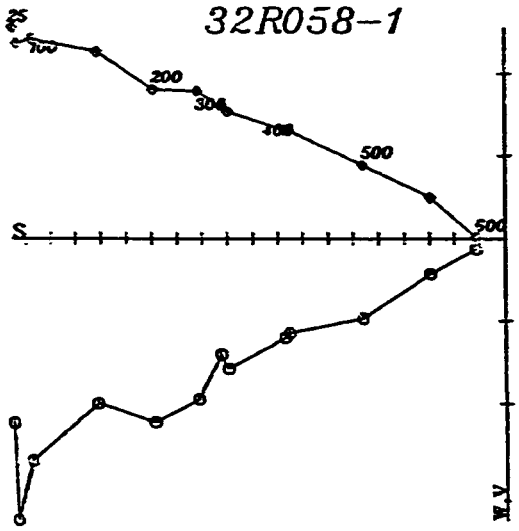

32R058-2

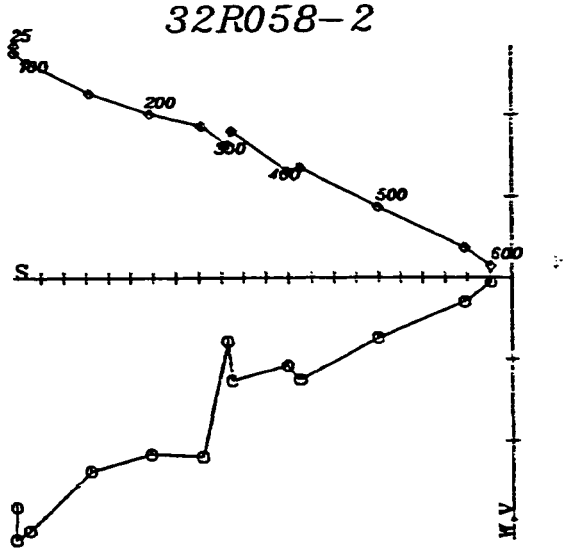

Sets of vector diagrams representing the behavior of remanent magnetization during thermal magnetization.

Locality 3, Site 3 (Tw1)

33R061-1

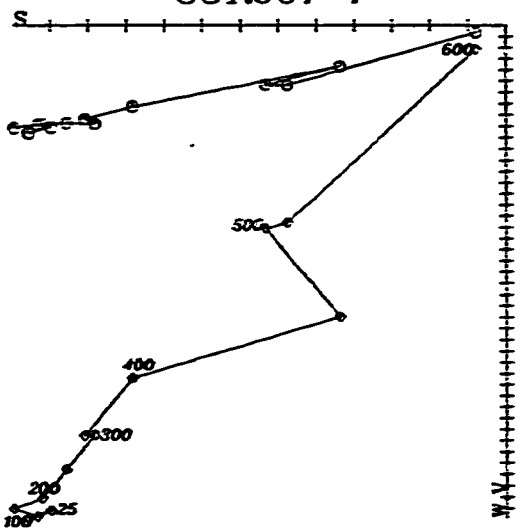

33R061-2

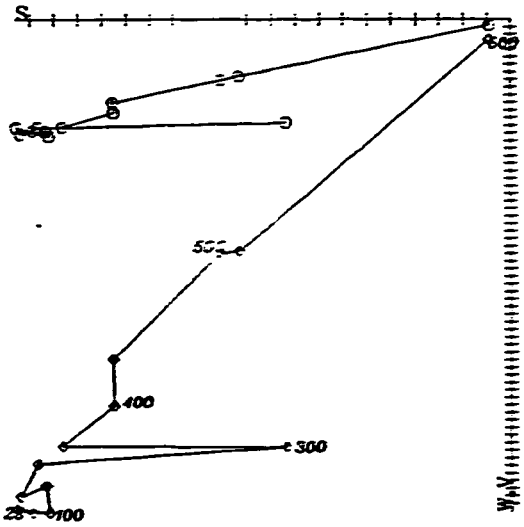

33R066-1

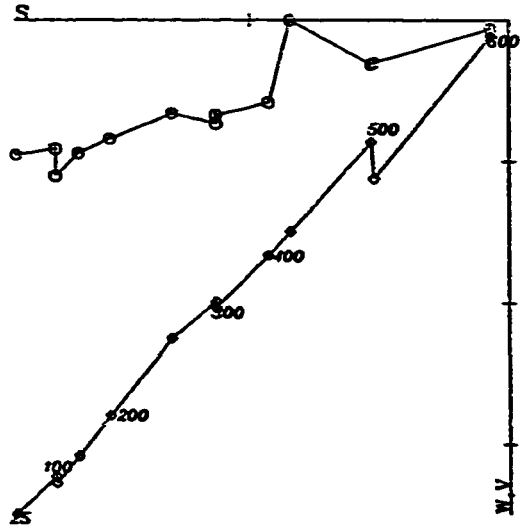

33R066-2

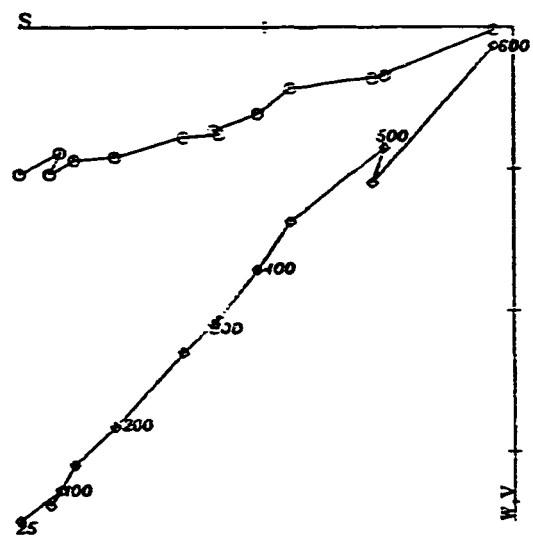

Sets of vector diagrams representing the behavior of remanent magnetization during thermal magnetization.

Locality 4, Site 1 (Th)

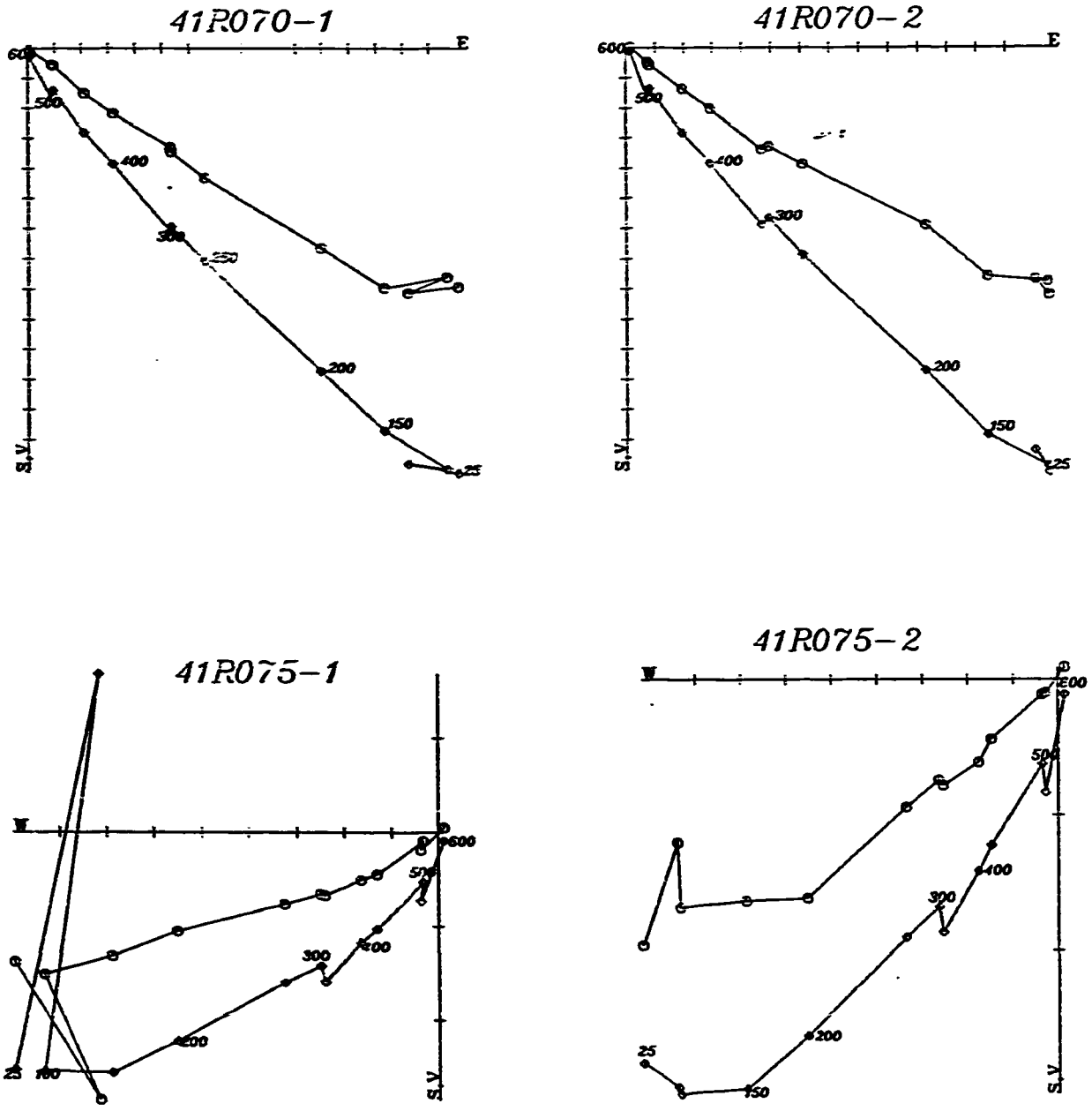

Sets of vector diagrams representing the behavior of remanent magnetization during thermal demagnetization.

Locality 4, Site 2 (Qm1)

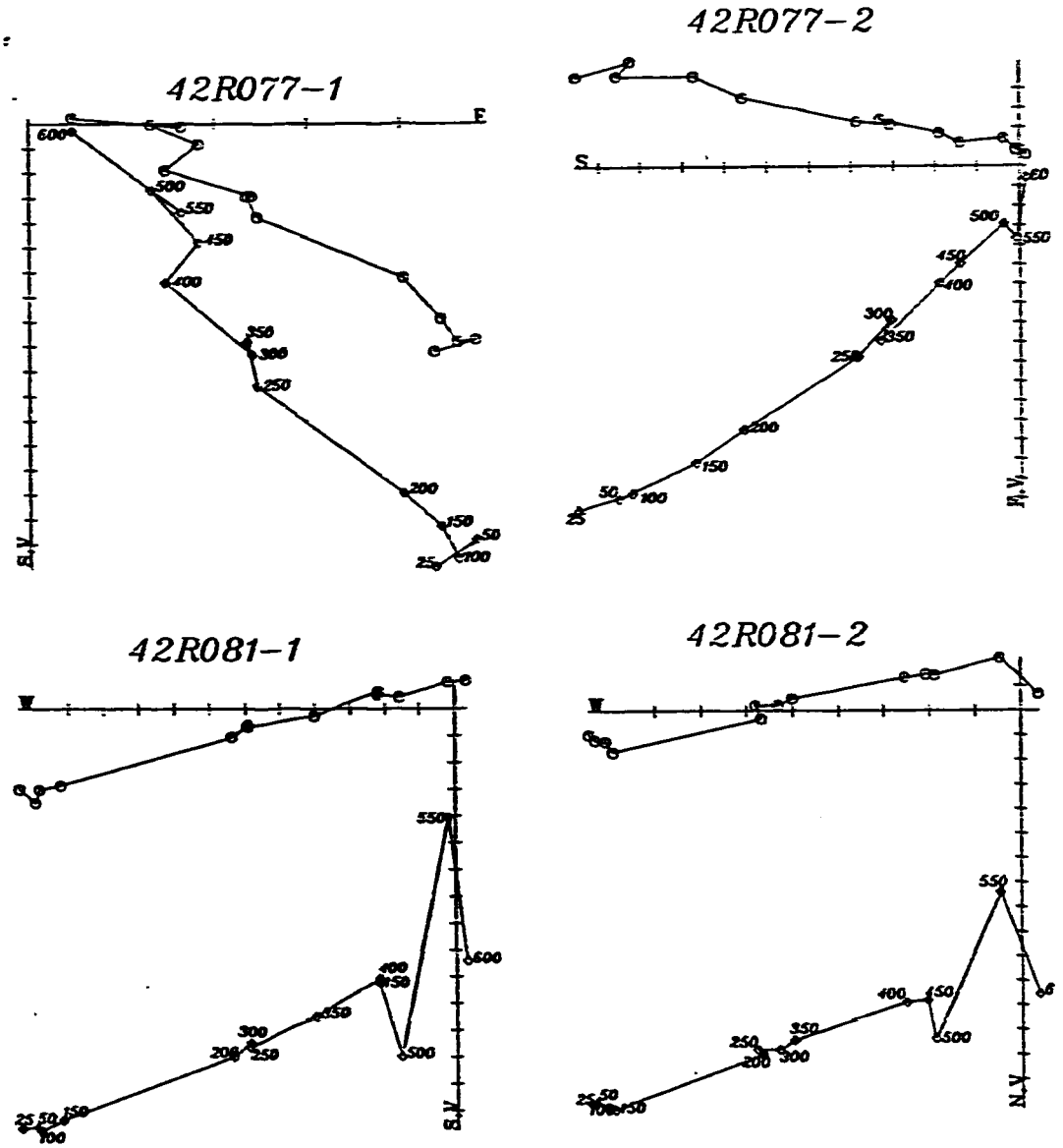

Sets of vector diagrams representing the behavior of remanent magnetization during thermal demagnetization.

Locality 4, Site 3 (Qm1,

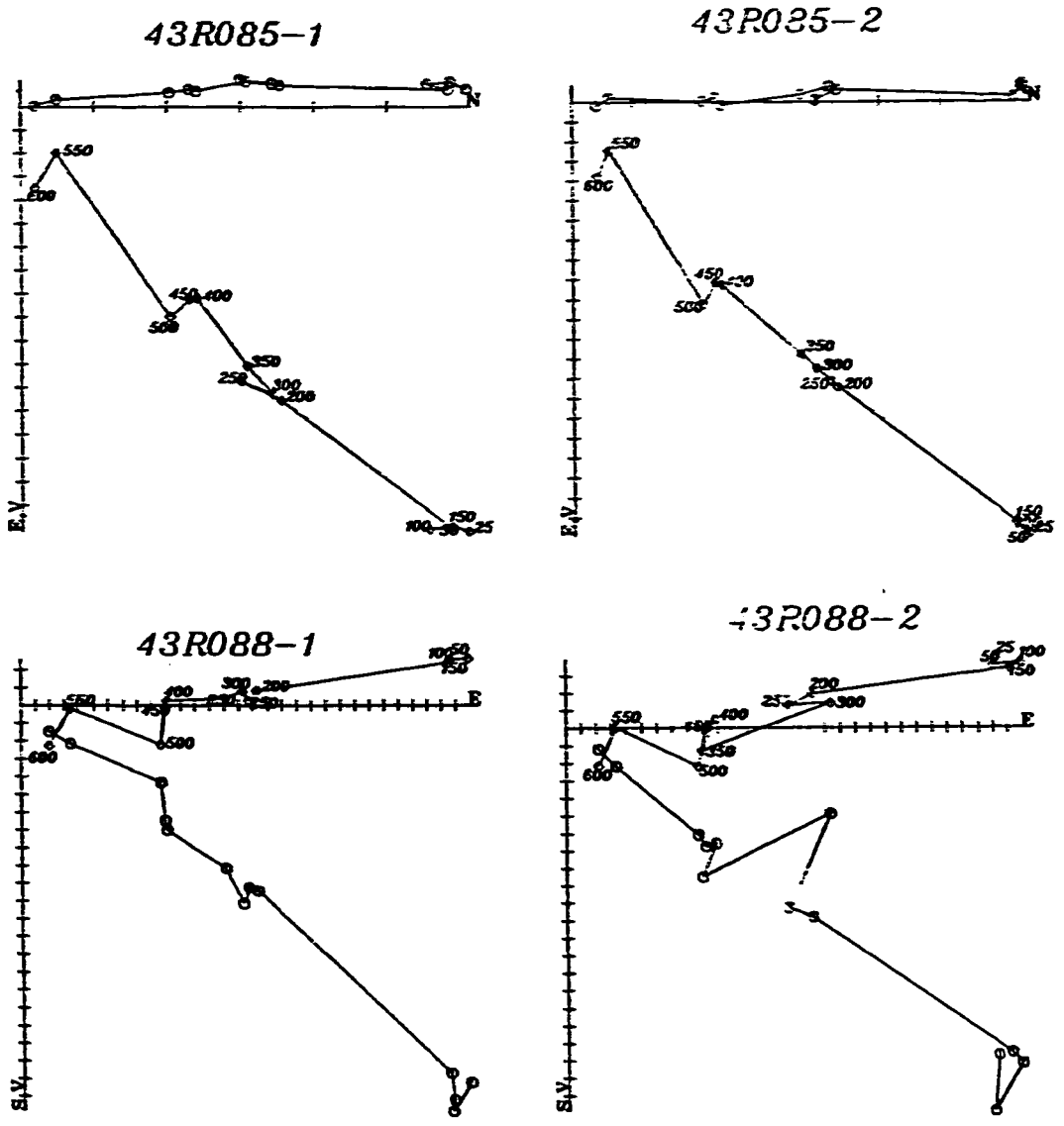

Sets of vector diagrams representing the behavior of remanent magnetization during thermal demagnetization.

Locality 5, Site 1 (Qm2)

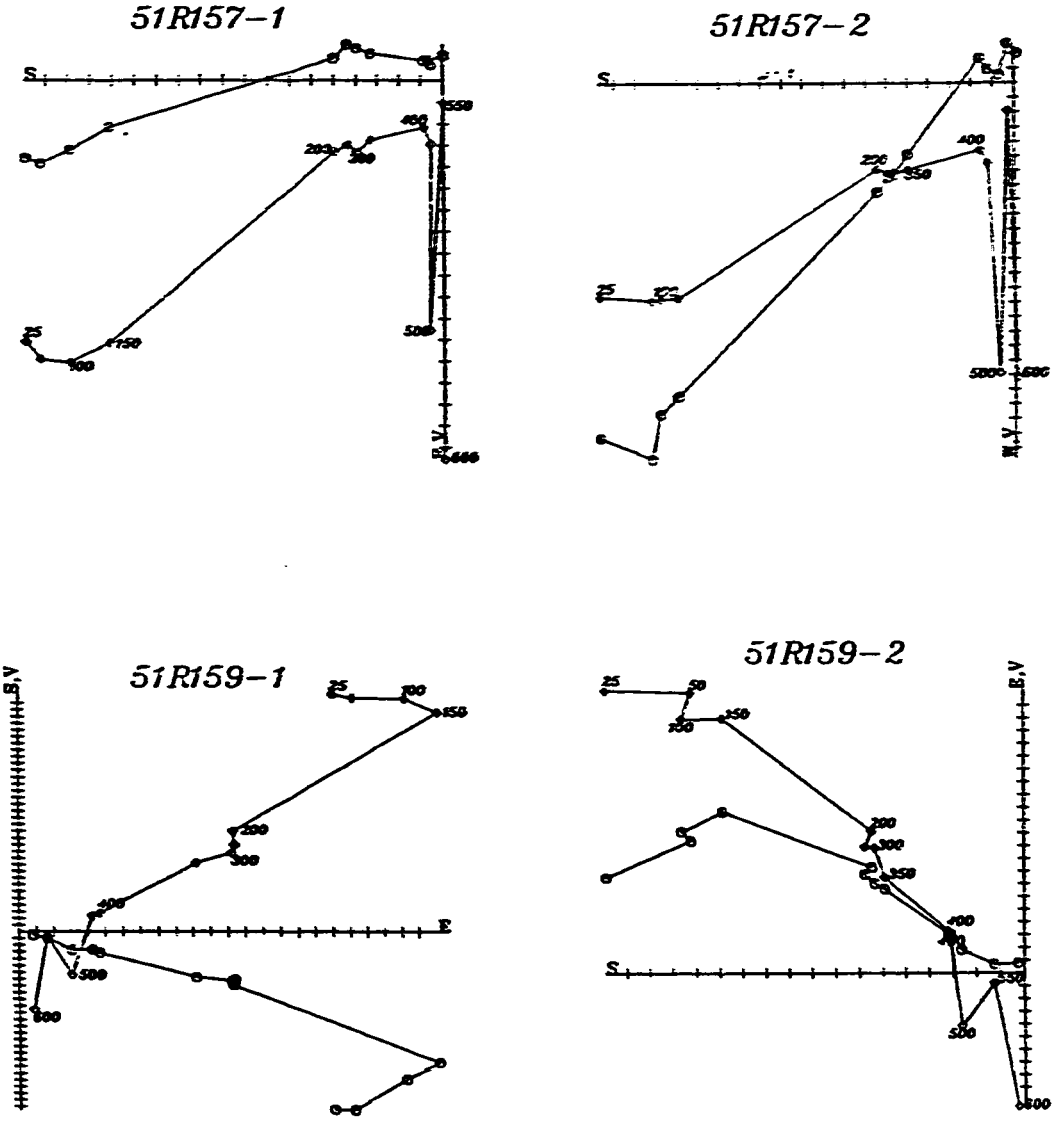

Sets of vector diagrams representing the behavior of remanent magnetization during thermal demagnetization.

Locality 5, Site 2 (Qm2)

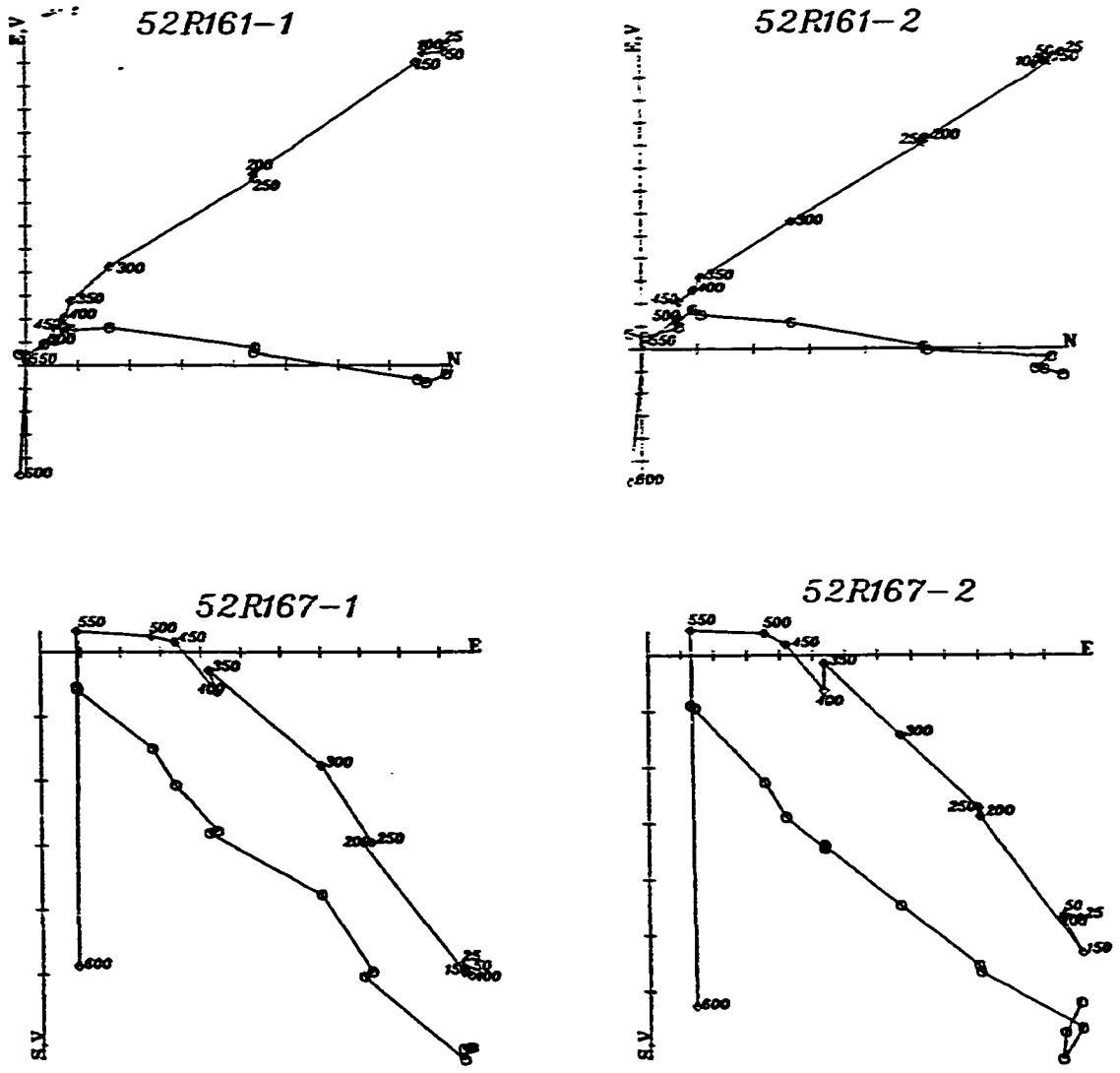

Sets of vector diagrams representing the behavior of remanent magnetization during thermal demagnetization.

Locality 5, Site 3 (Qm3)

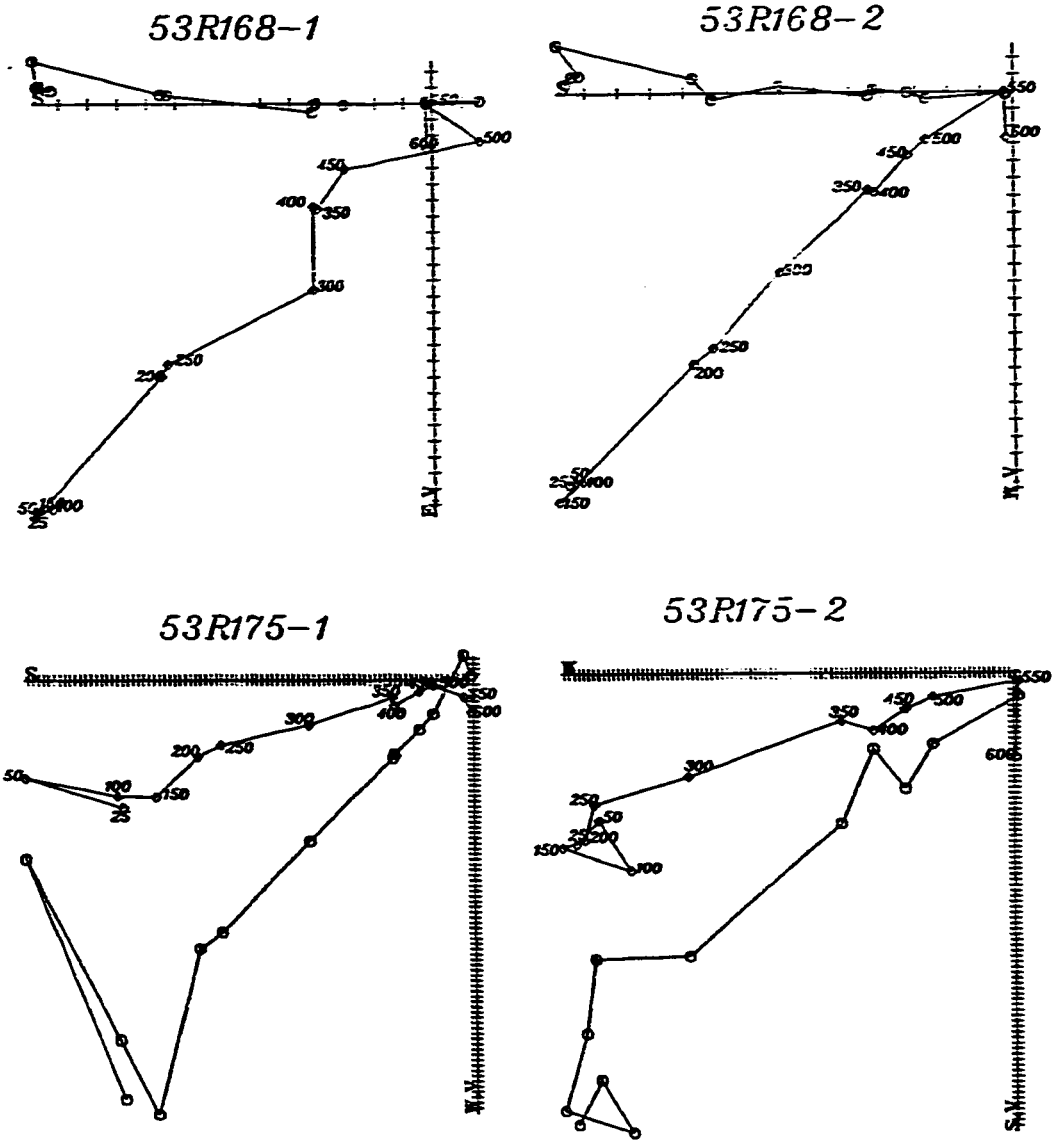

Sets of vector diagrams representing the behavior of remanent magnetization during thermal demagnetization.

Locality 5, Site 4 (Qm5)

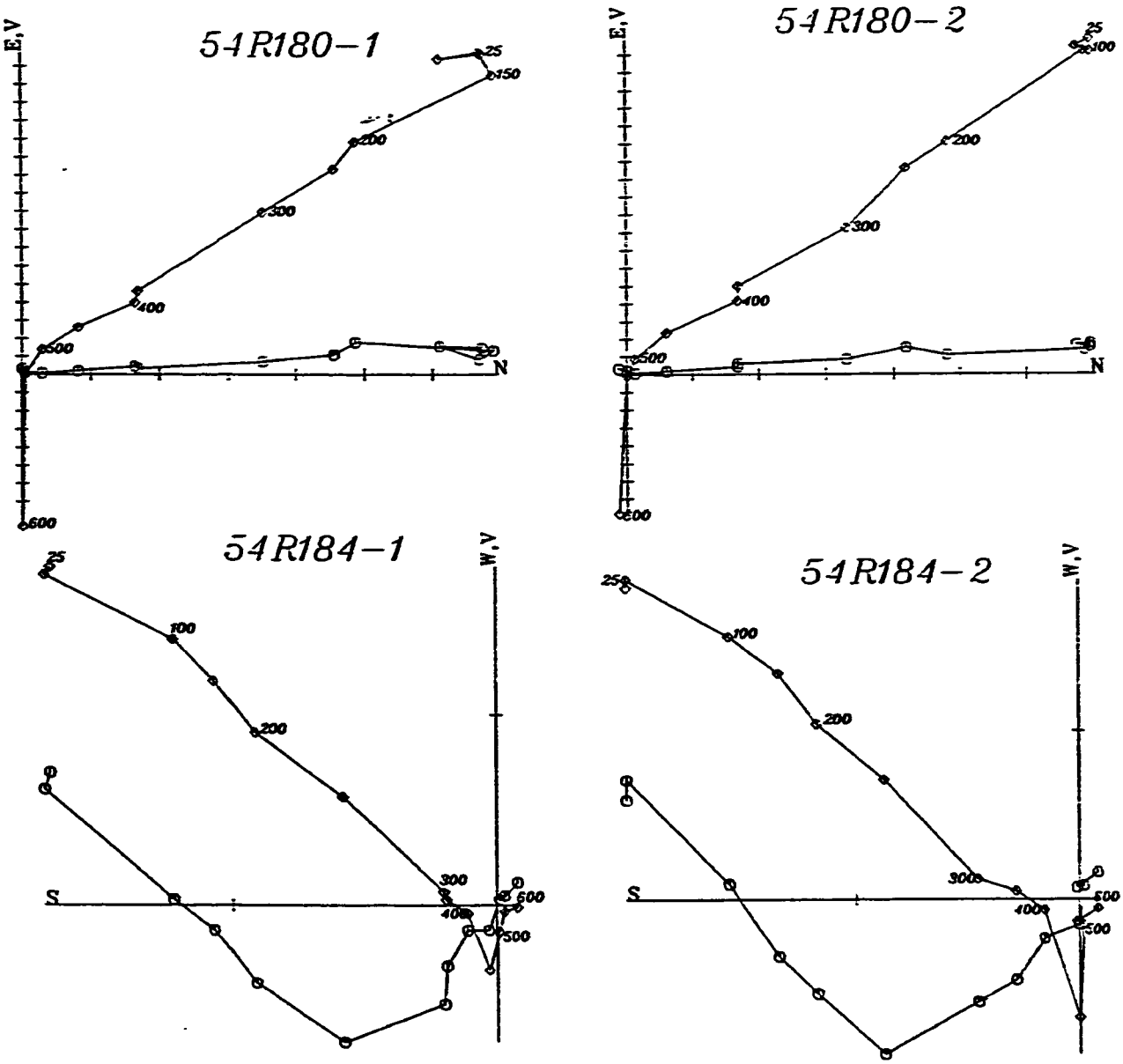

Sets of vector diagrams representing the behavior of remanent magnetization during thermal demagnetization.

Locality 5, Site 5 (Qm3)

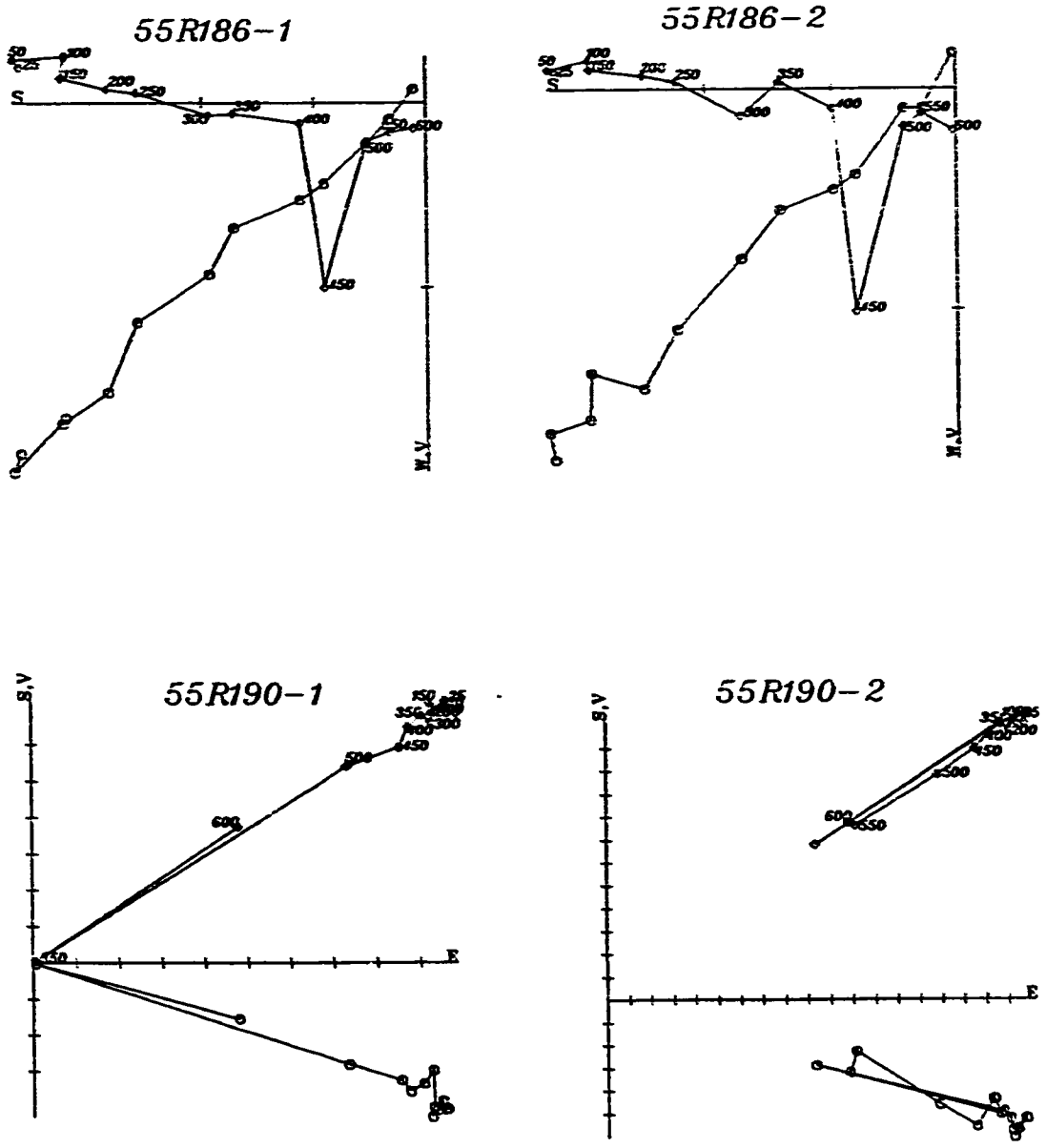

Sets of vector diagrams representing the behavior of remanent magnetization during thermal demagnetization.

Locality 5, Site 6 (Qm3)

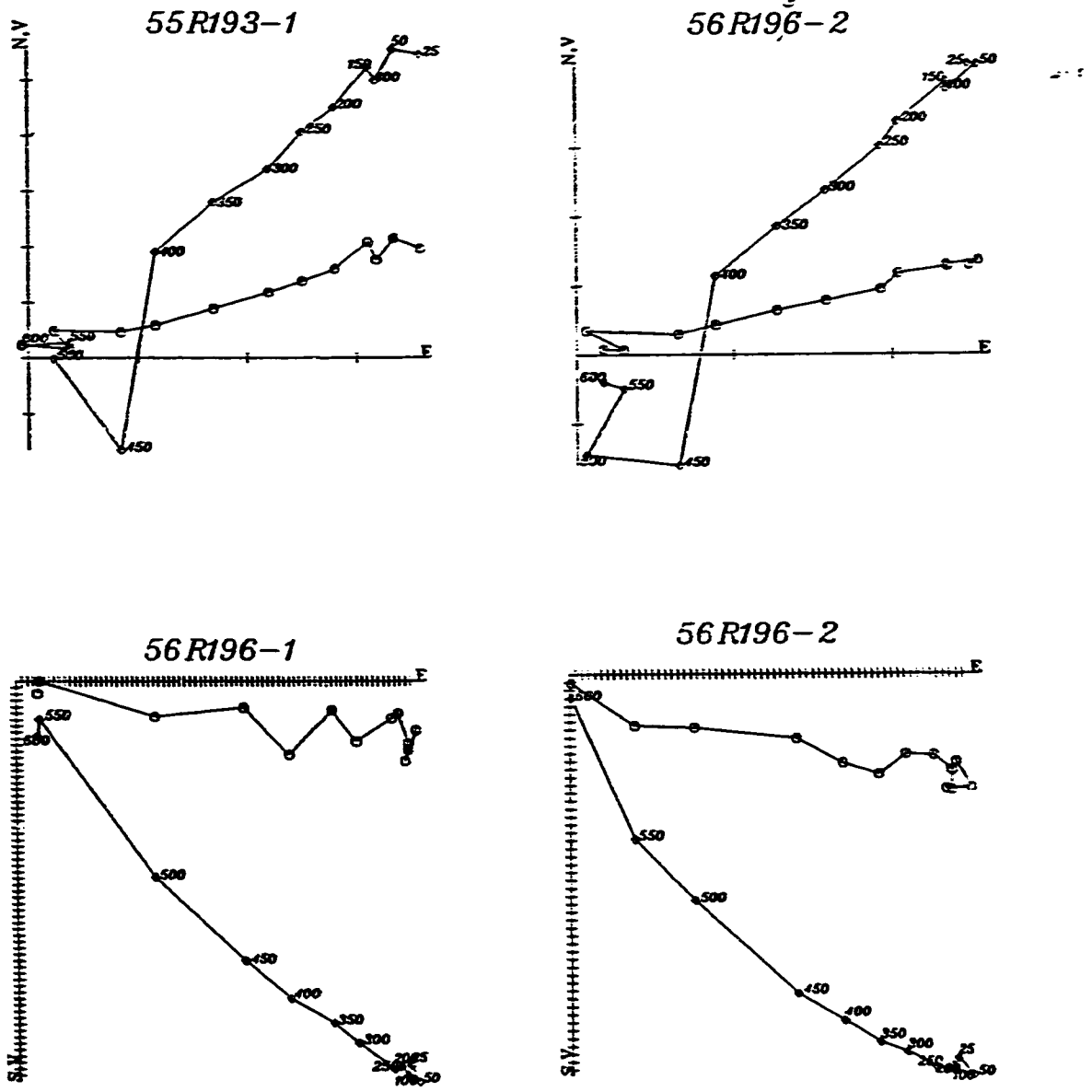

Sets of vector diagrams representing the behavior of remanent magnetization during thermal demagnetization.

Locality 5, Site 7 (Qm2)

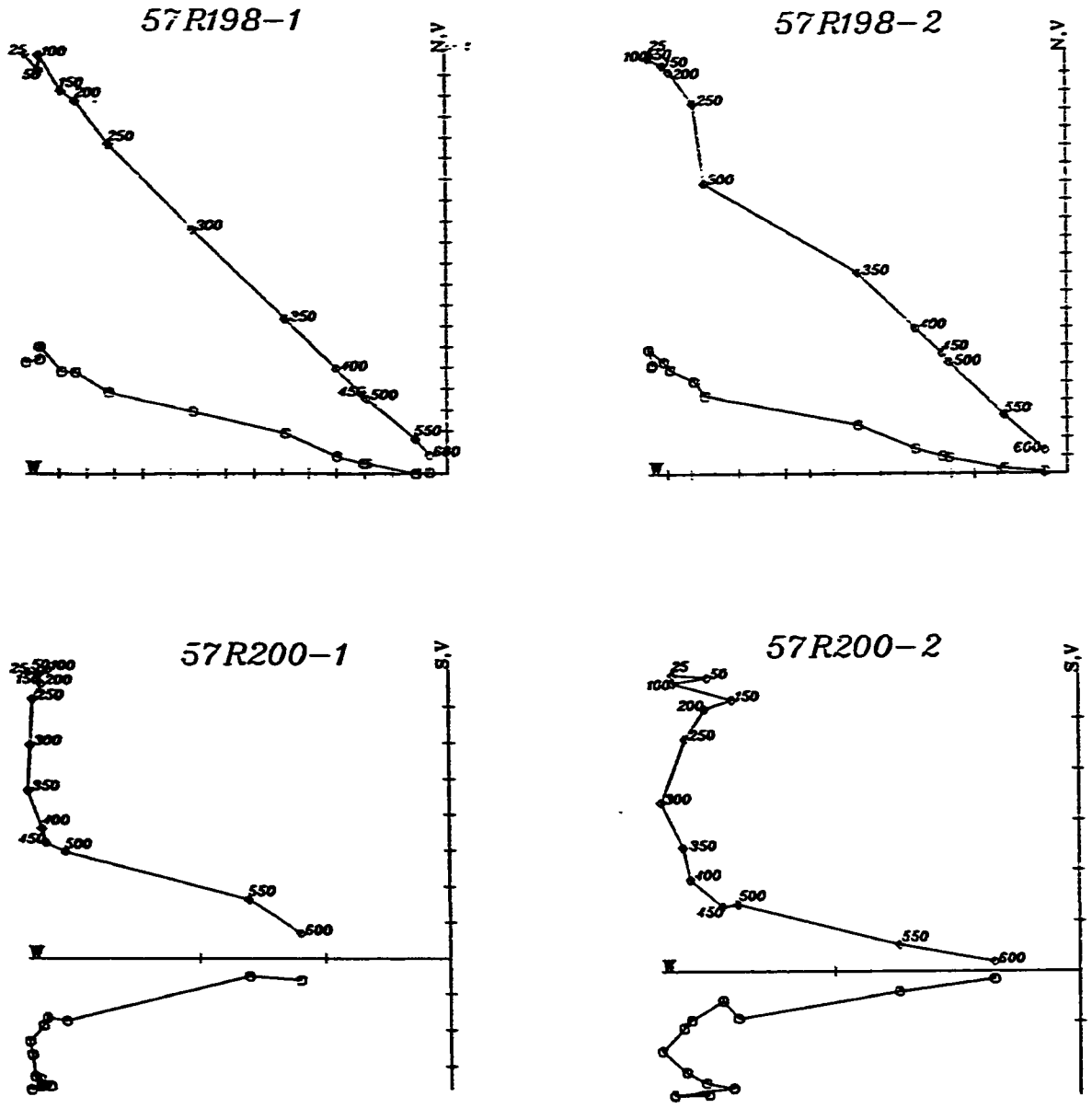

Sets of vector diagrams representing the behavior of remanent magnetization during thermal demagnetization.

Appendix D

This Appendix contains sets of vector diagrams representing the behavior of remanent magnetization during alternating field (a.f) demagnetization.

Horizontal projection

Vertical projcetion

A.F field= mT

Locality 5, Site 4 (Qm5)

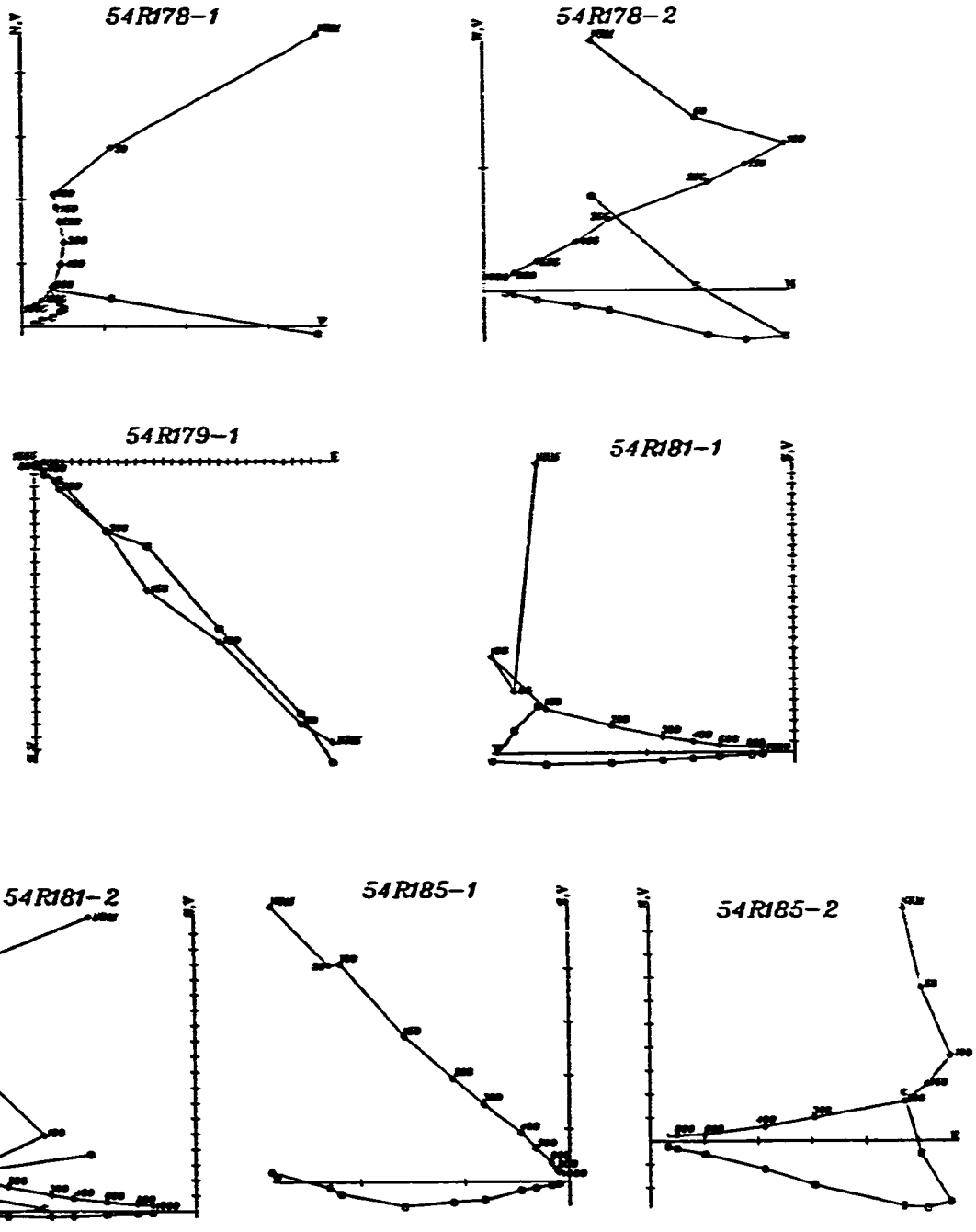

Sets of vector diagrams representing the behavior of remanent magnetization during alternating field (a.f) demagnetization.

Locality 5, Site 6 (Qm3)

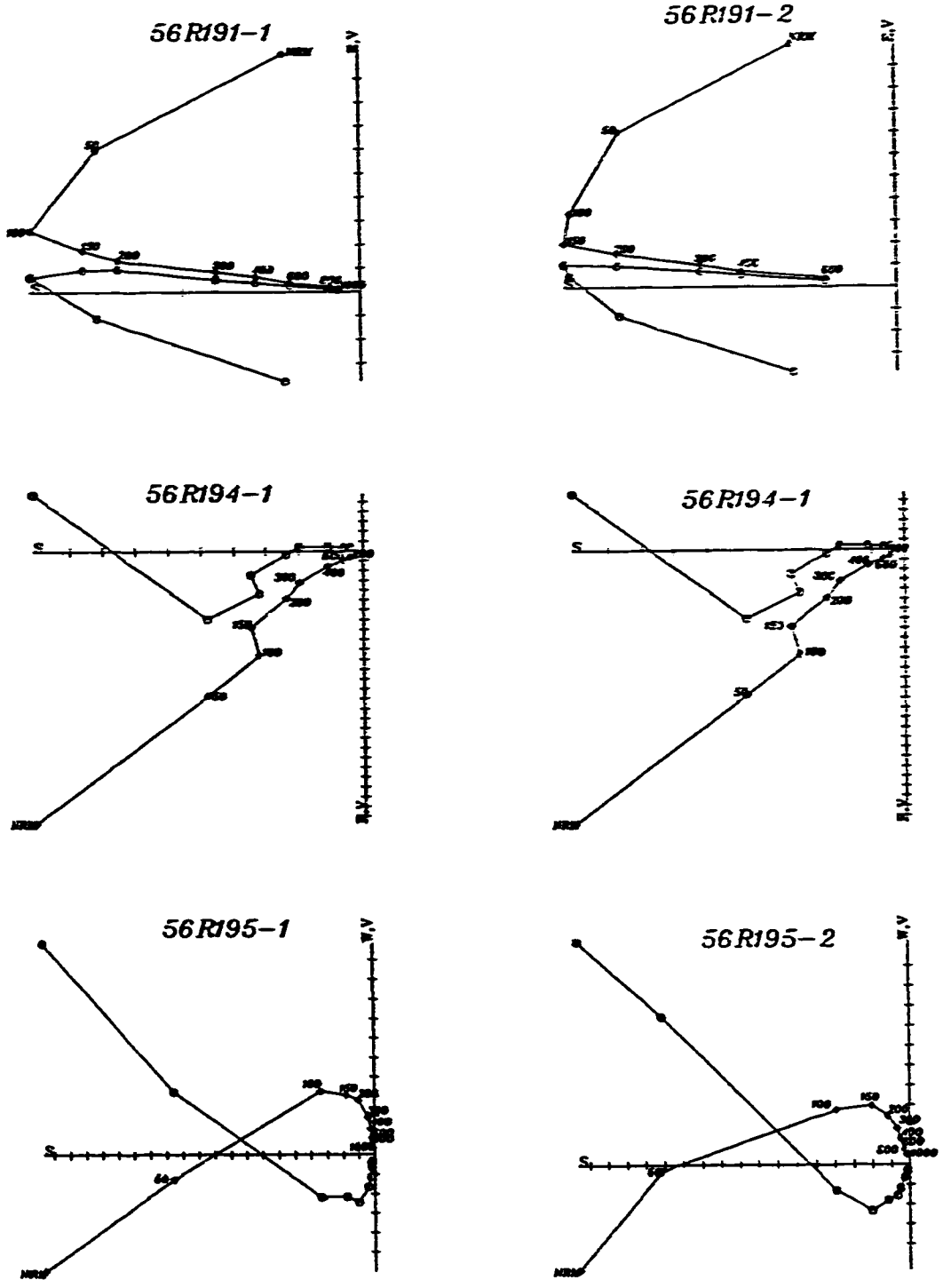

Sets of vector diagrams representing the behavior of remanent magnetization during alternating fields (a.f) demagnetization.

Locality 5, Site5 (Qm3)

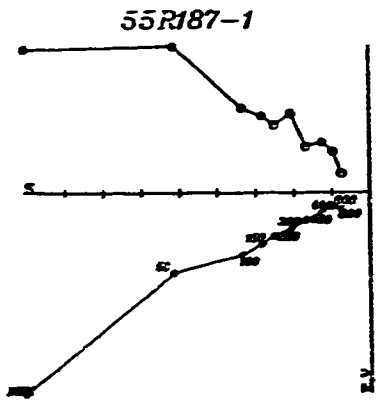

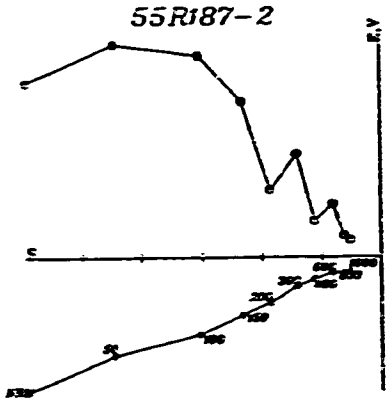

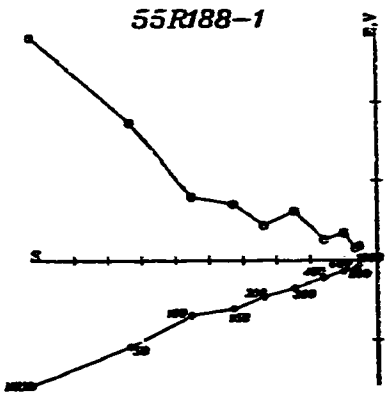

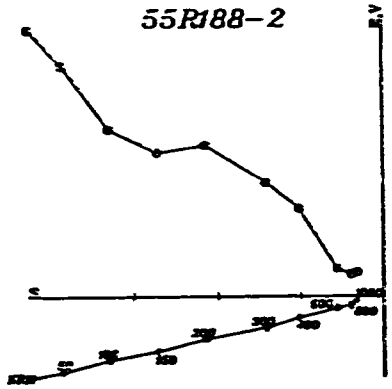

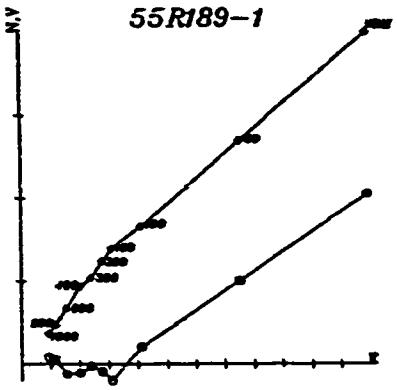

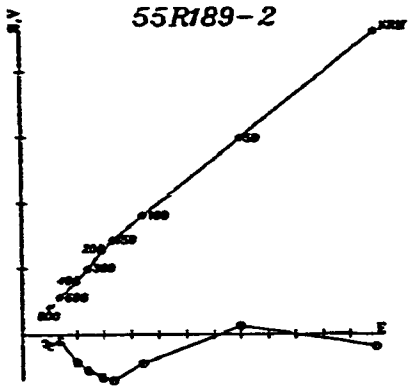

Sets of vector diagrams representing the behavior of remanent magnetization during alternating fields (a.f) demagnetization.

Locality 5, Site 3 (Qm3)

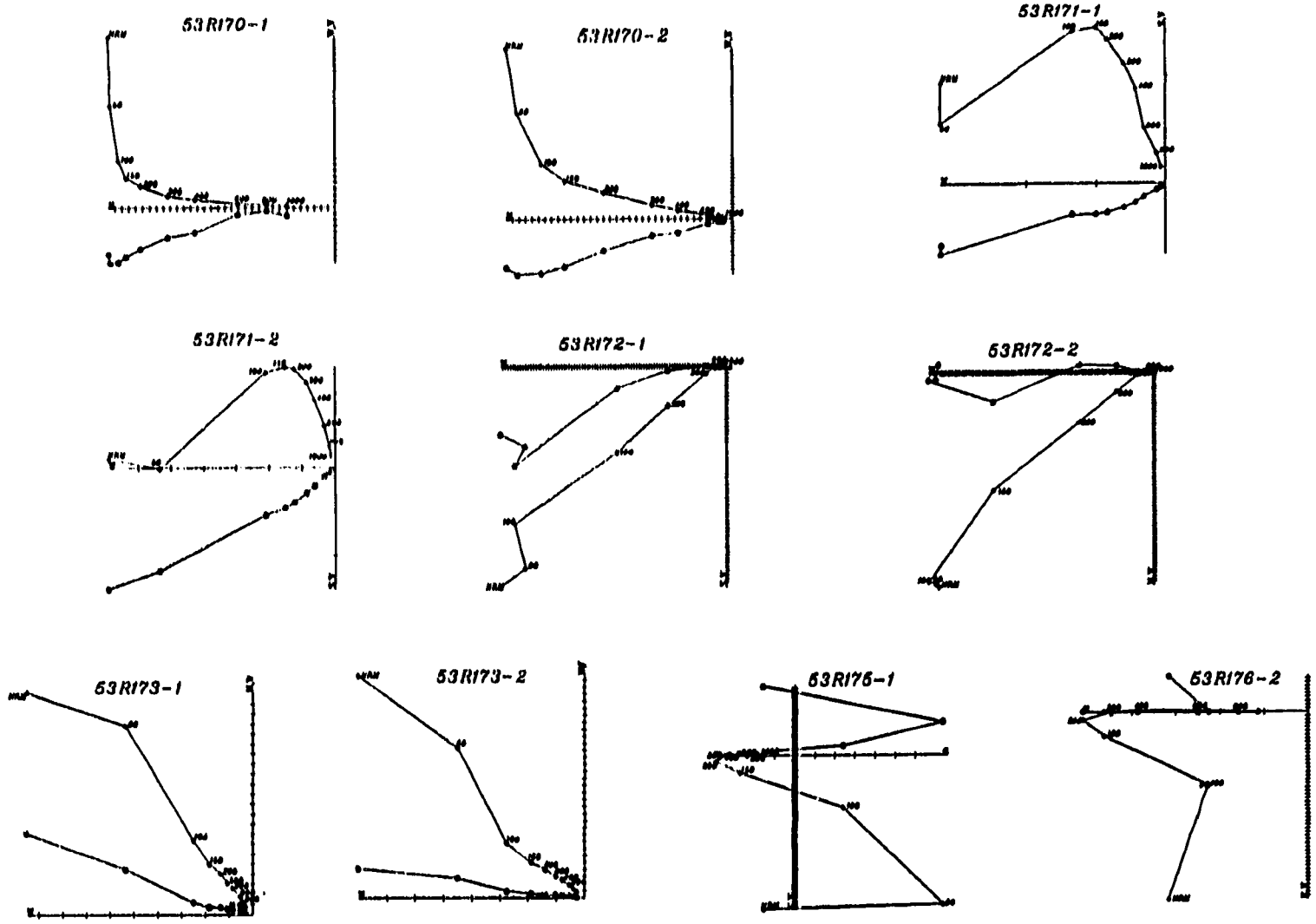

Sets of vector diagrams representing the behavior of remanent magnetization during alternating field (a.f) demagnetization.

Locality 1, Site 2 (Qm2)

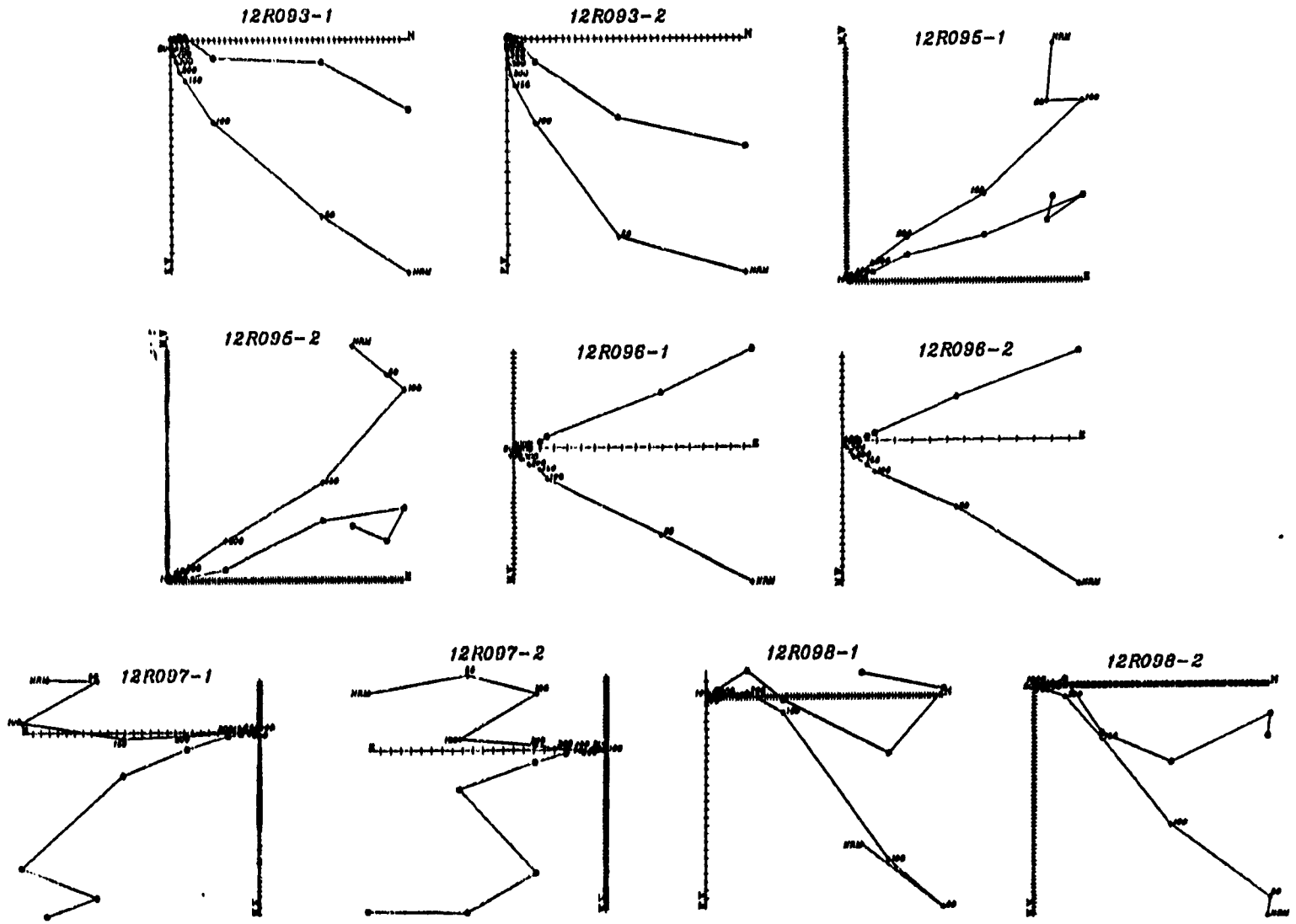

Sets of vector diagrams representing the behavior of remanent magnetization during alternating field (a.f) demagnetization.

Locality 1, Site 7 (Qm2)

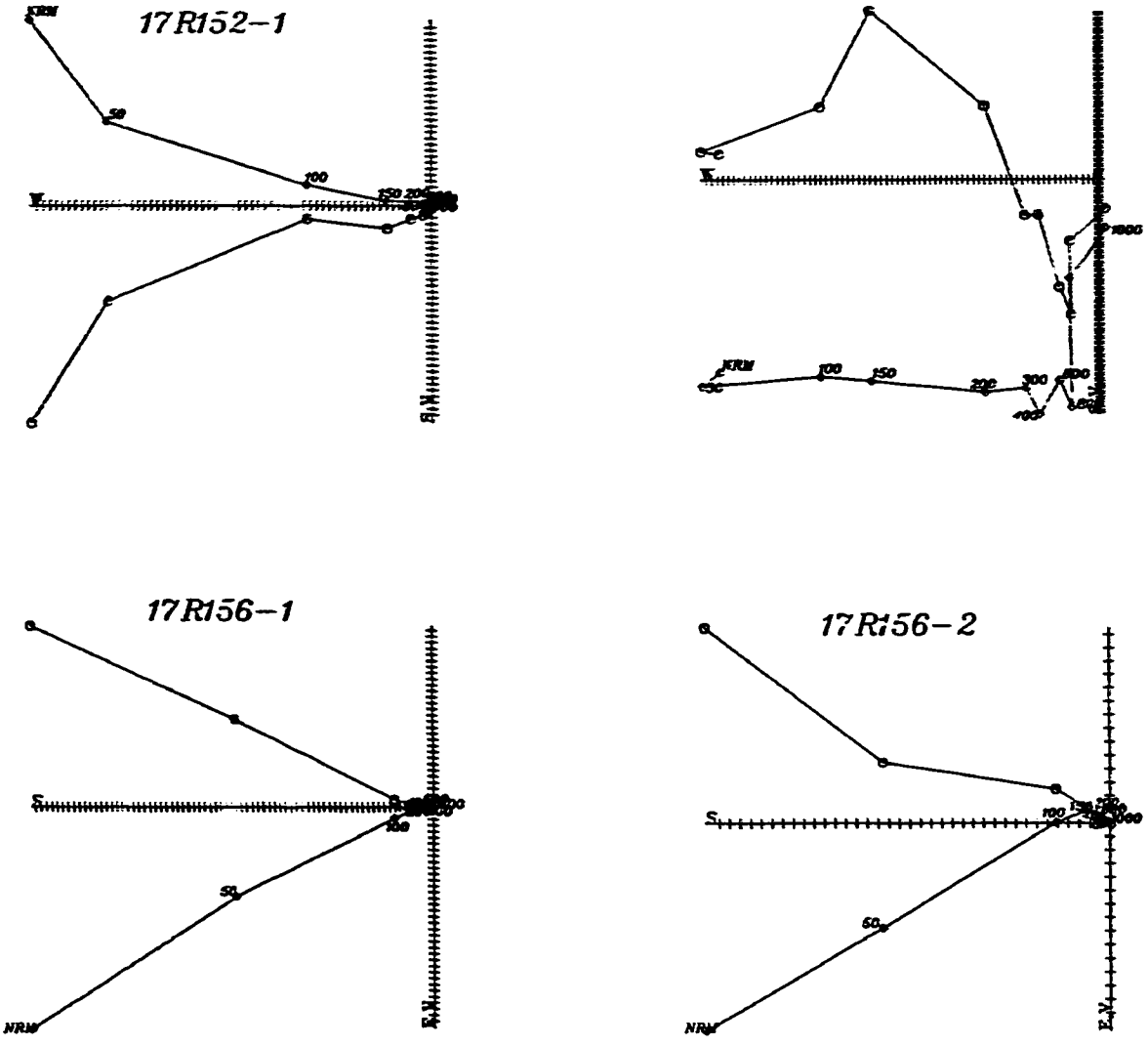

Sets of vector diagrams representing the behavior of remanent magnetization during alternating field (a.f) demagnetization.

Locality 5. Site 1 (Qm2)

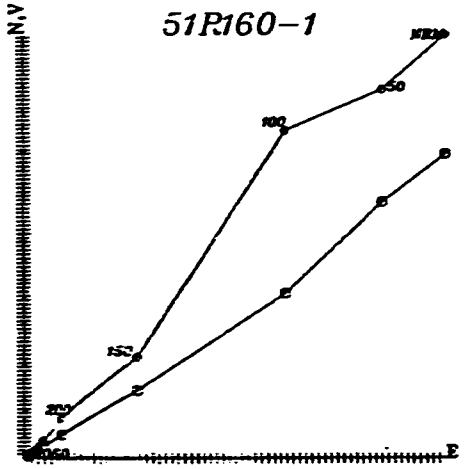

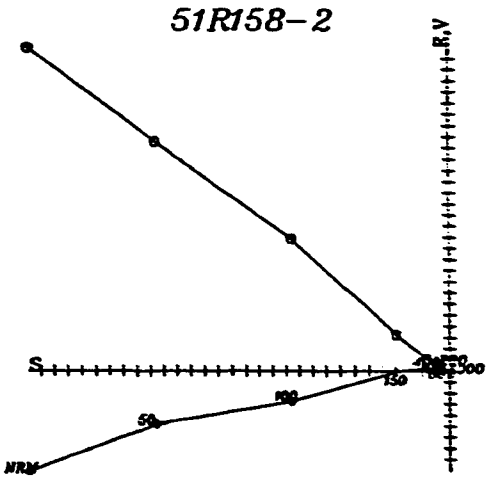

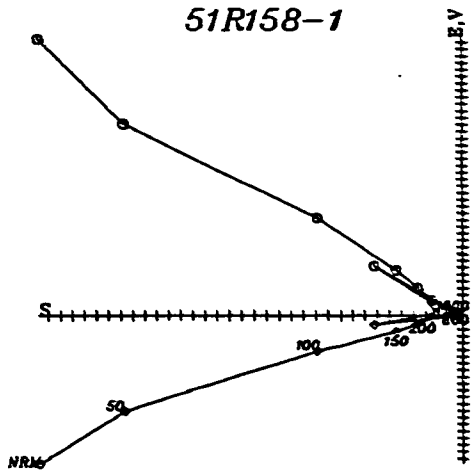

Sets of vector diagrams representing the behavior of remanent magnetization during alternating field (a.f) magnetization.

Locality 5, Site 2 (Qm2)

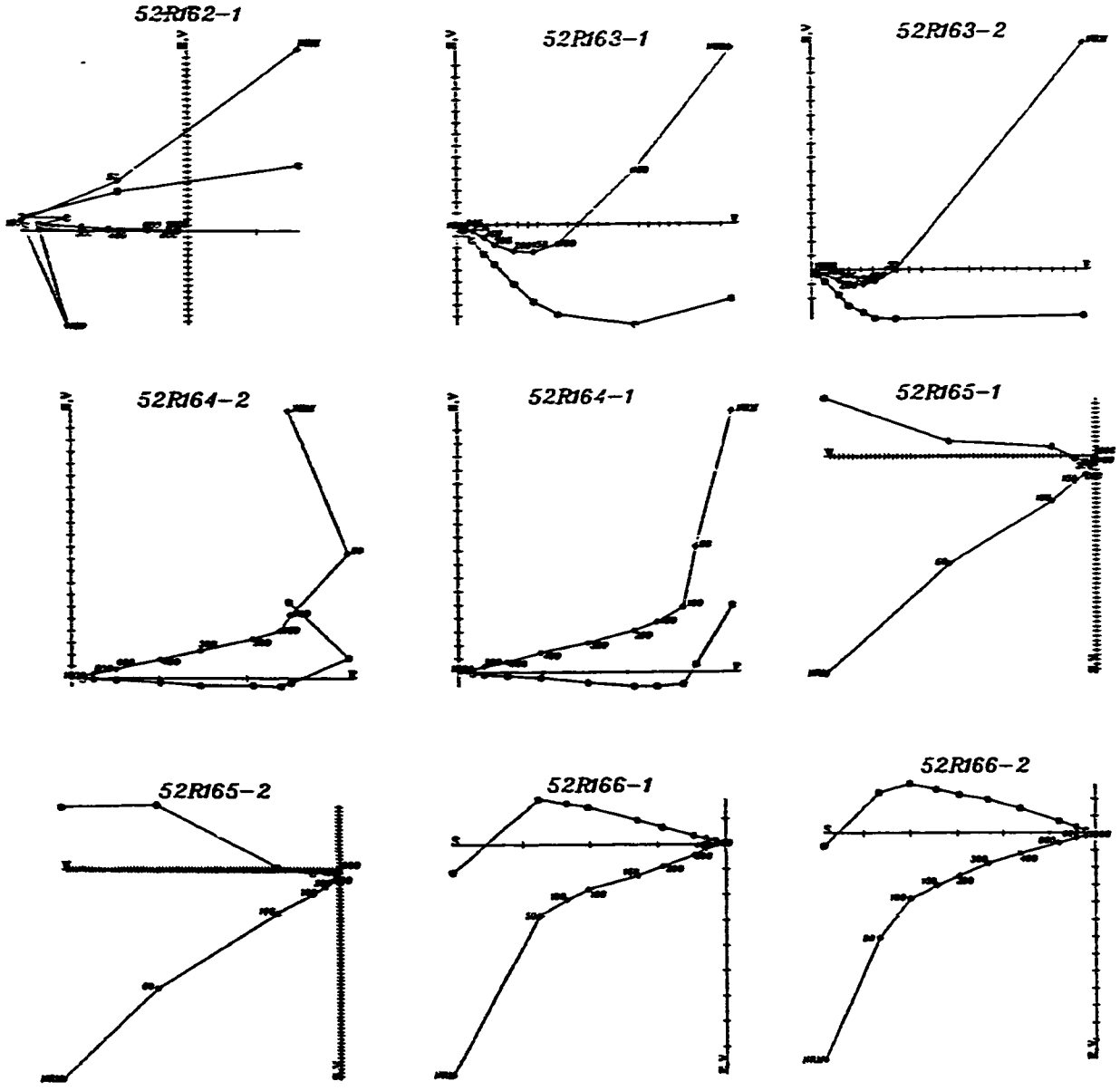

Sets of vector diagrams representing the behavior of remanent magnetization during alternating field (a.f) demagnetization.

Locality 5, Site 7 (Qm2)

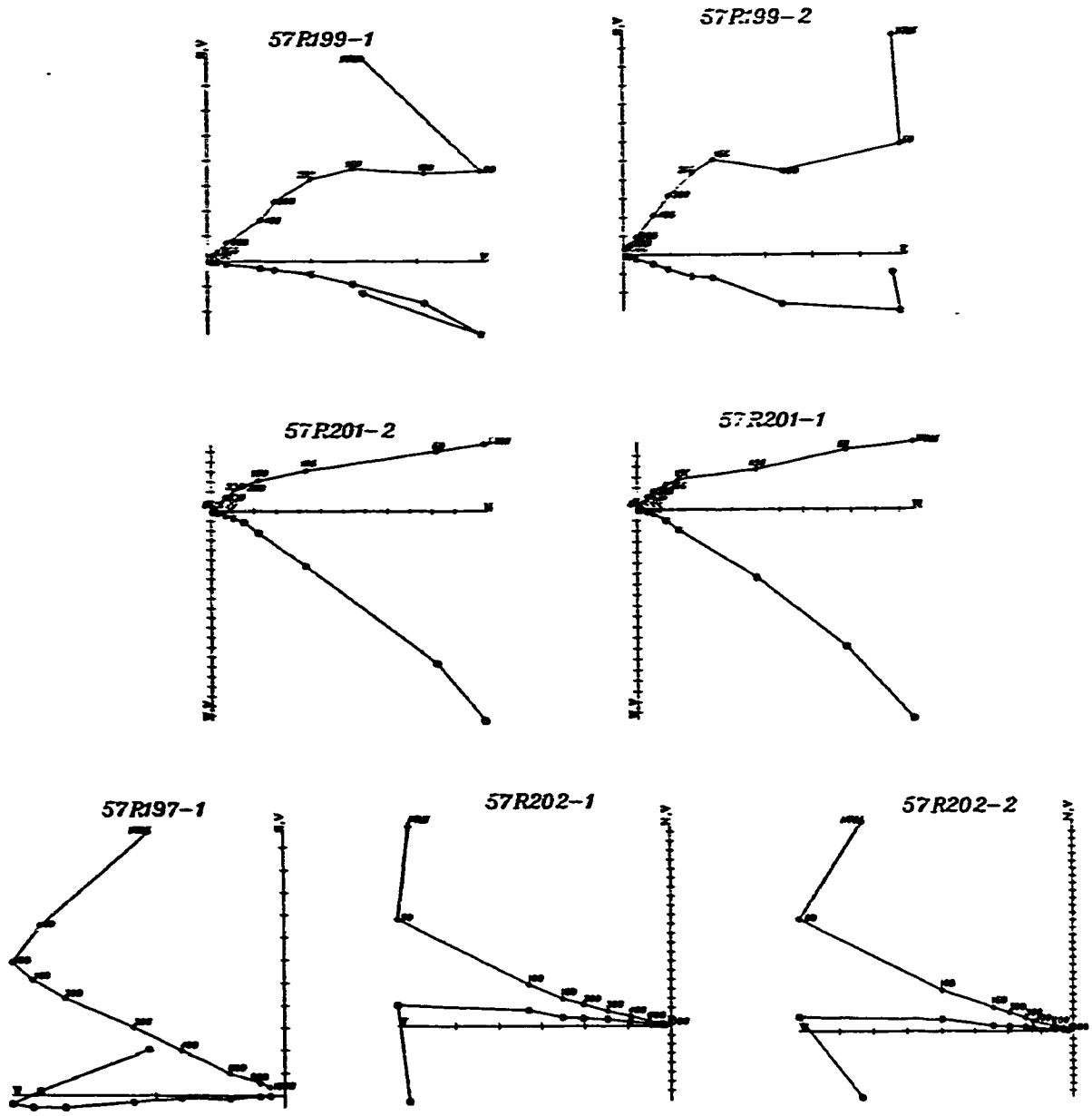

Sets of vector diagrams representing the behavior of remanent magnetization during alternating field (a.f) demagnetization.

Locality 1, Site 3 (Qm1)

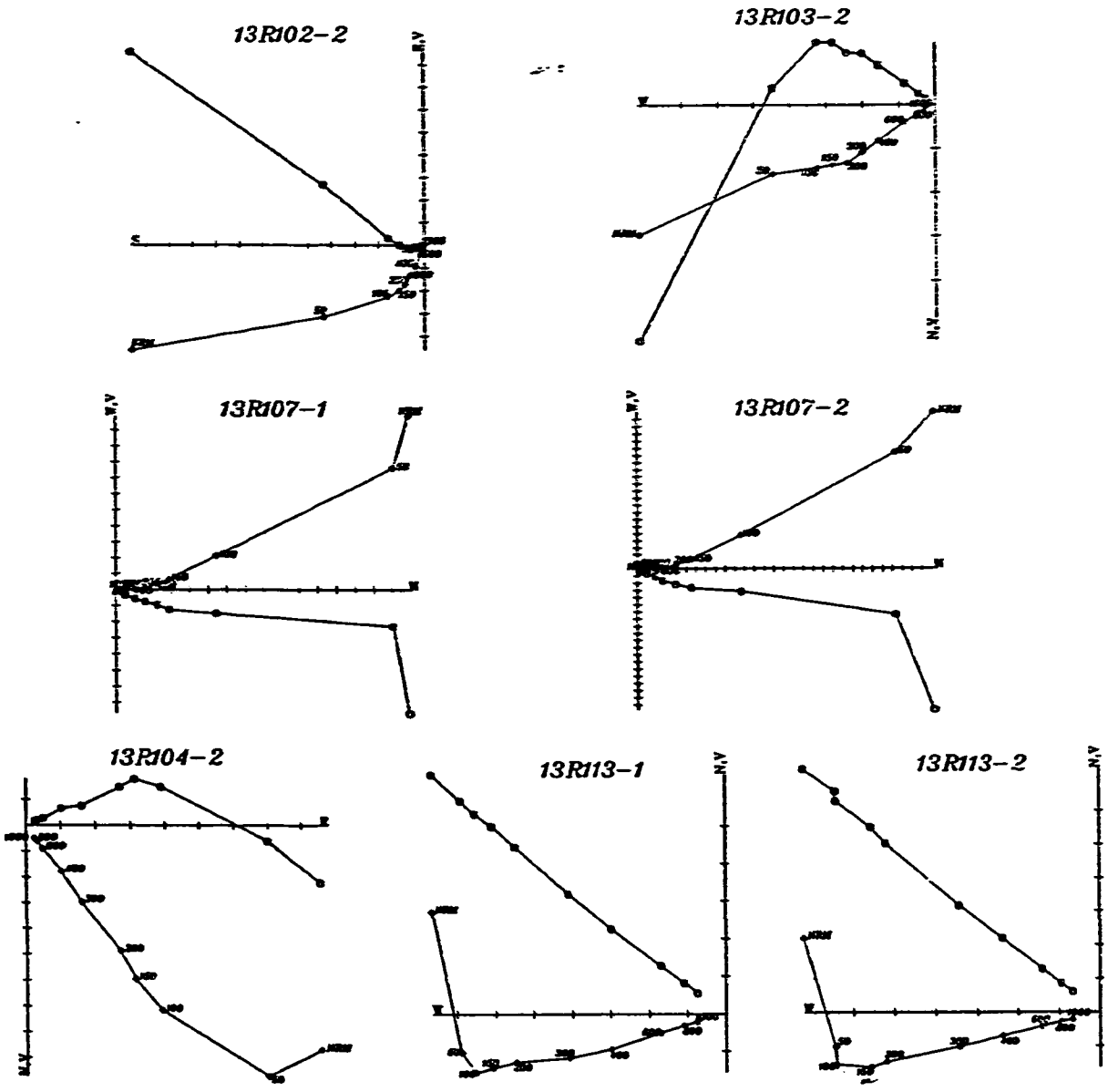

Sets of vctor diagrams representing the behavior ofremanent magnetization during alternating field (a.f) demagnetization.

Locality 1, Site 4 (Qm1)

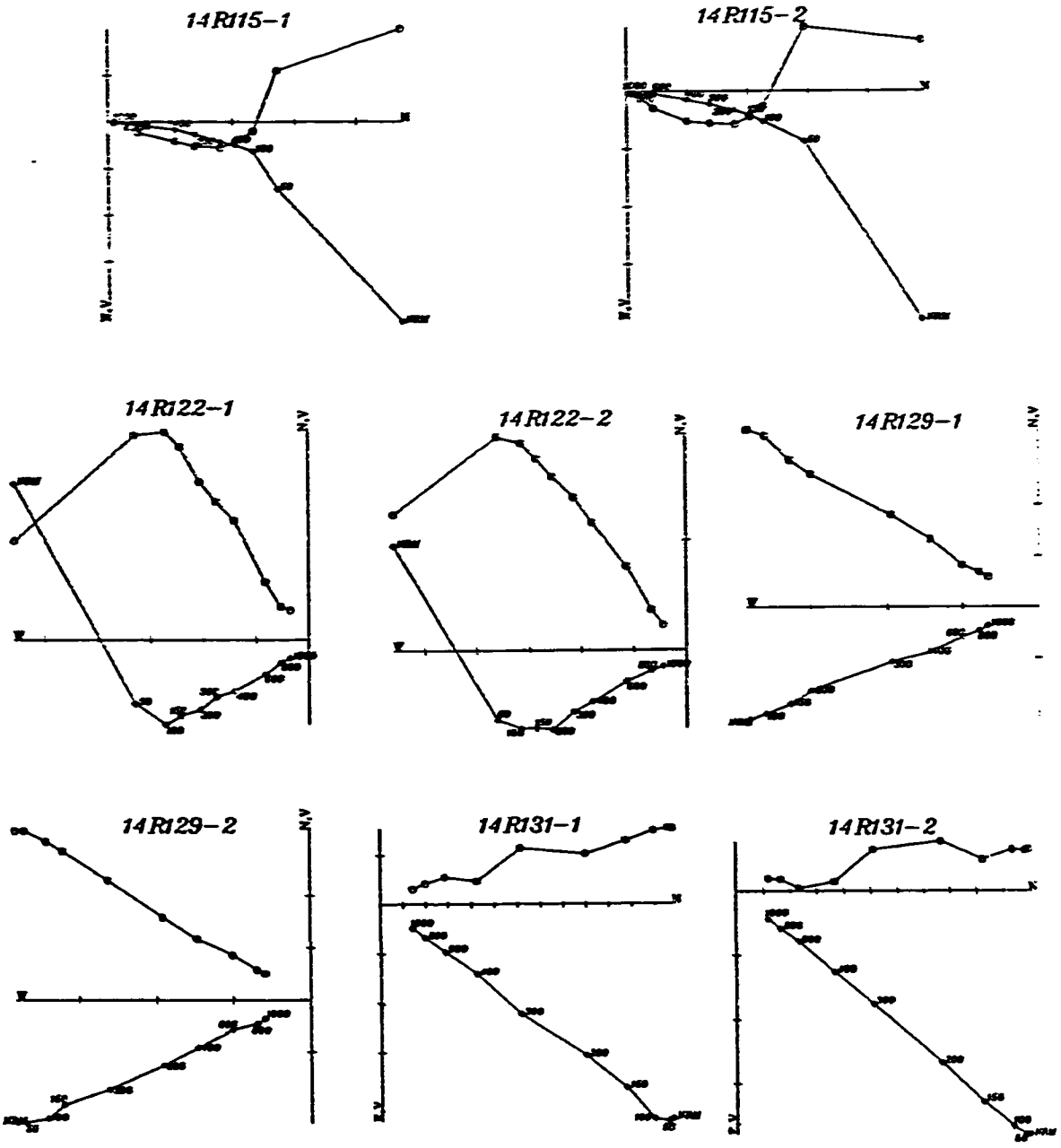

Sets of vector diagrams representing the behavior of remanent magnetization during alternating field (a.f) demagnetization.

Locality 4, Site 2 (Qm1)

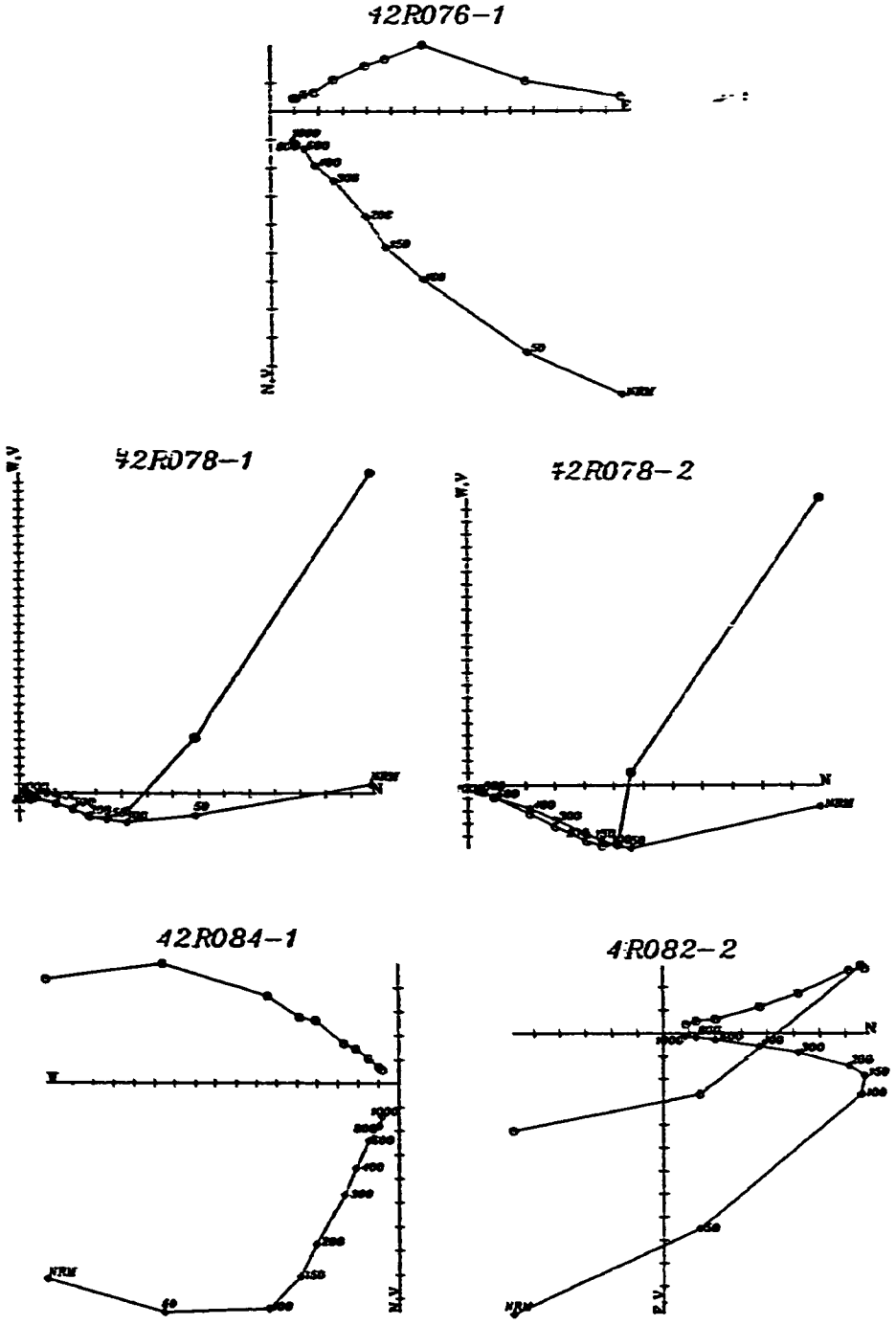

Sets of vector diagrams representing the behavior of remanent magnetization during alternating field (a.f) demagnetization.

Locality 4, Site 2 (Qm1)

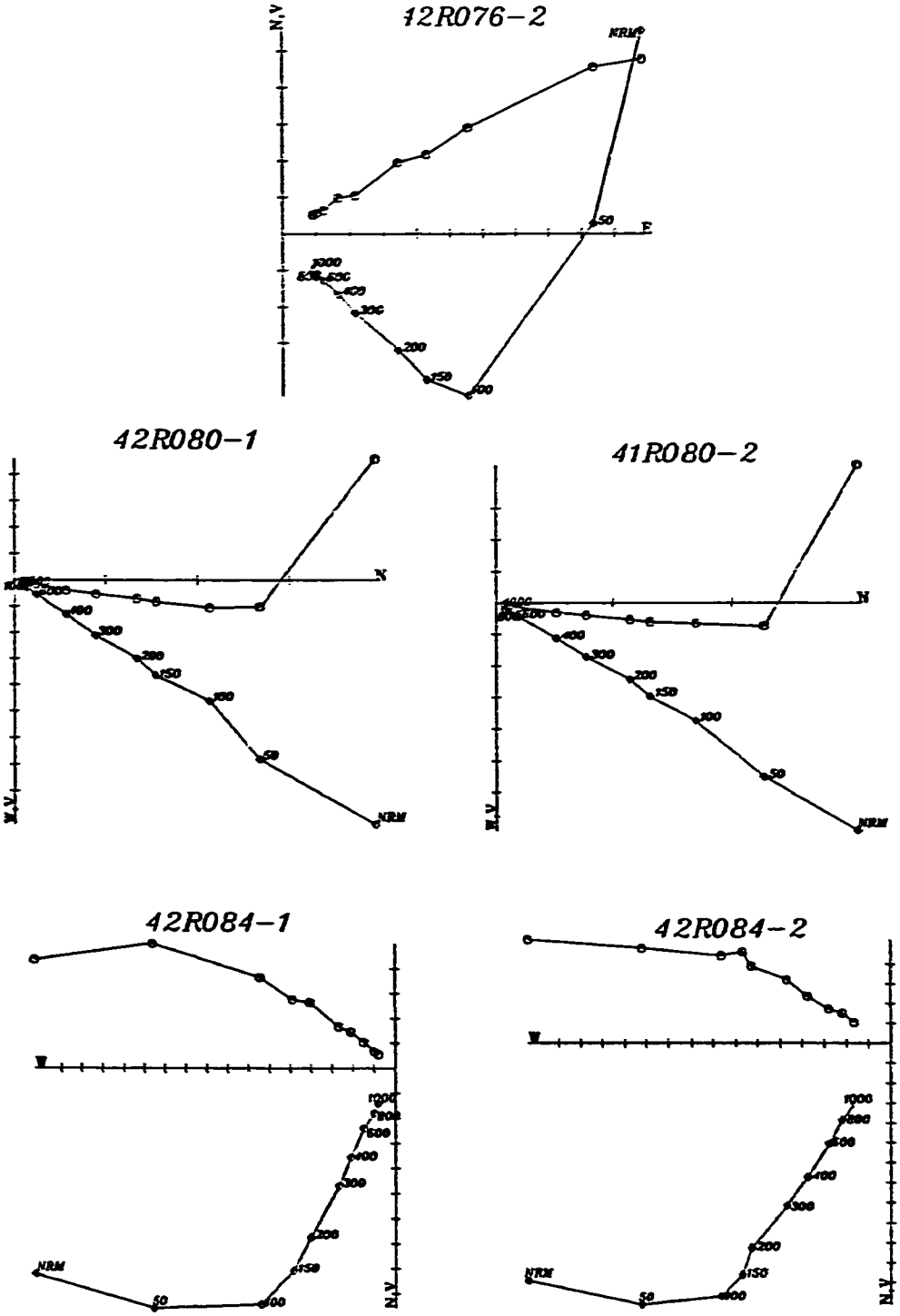

Sets of vector diagrams representing the behavior of remanent magnetization during alternating field (a.f) demagnetization.

Locality 4, Site 3 (Qm1)

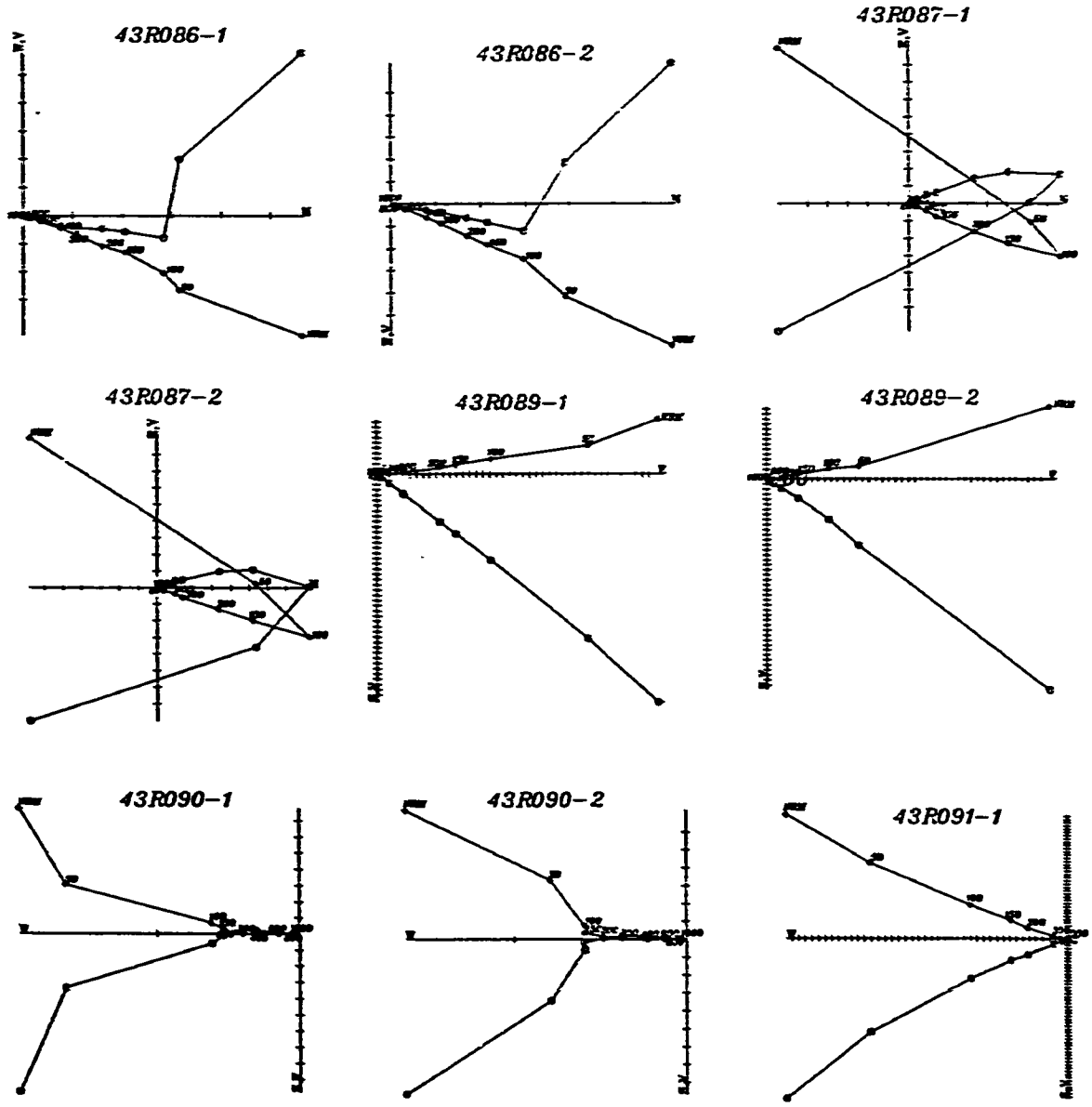

Sets of vector diagrams representing the behavior of remanent magnetization during alternating field (a.f) demagnetization.

Locality 1, Site 5 (Th)

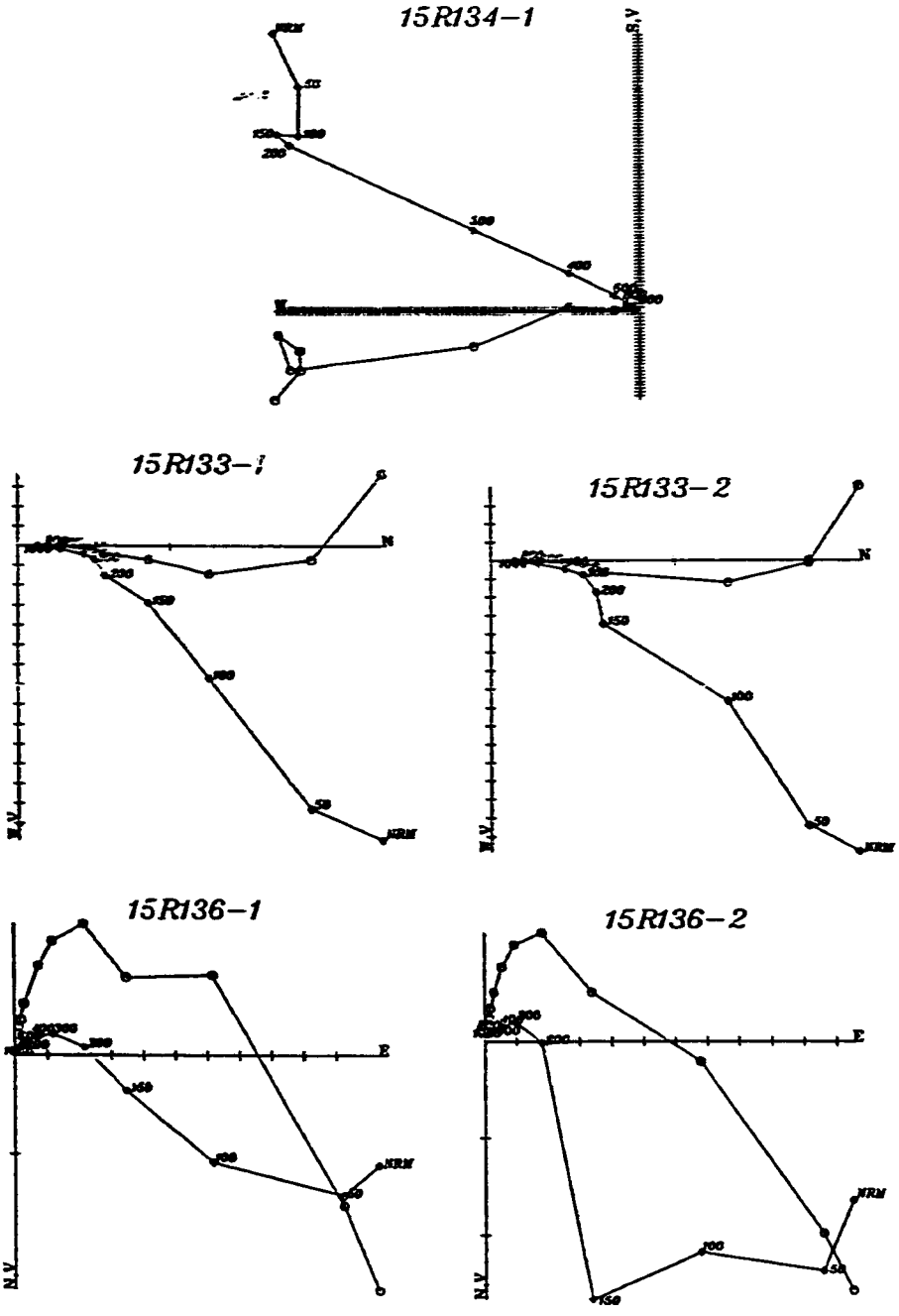

Sets of vector diagrams representing the behavior of remanent magnetization during alternating field (a.f) demagnetization.

Locality 1, Site 6 (Th)

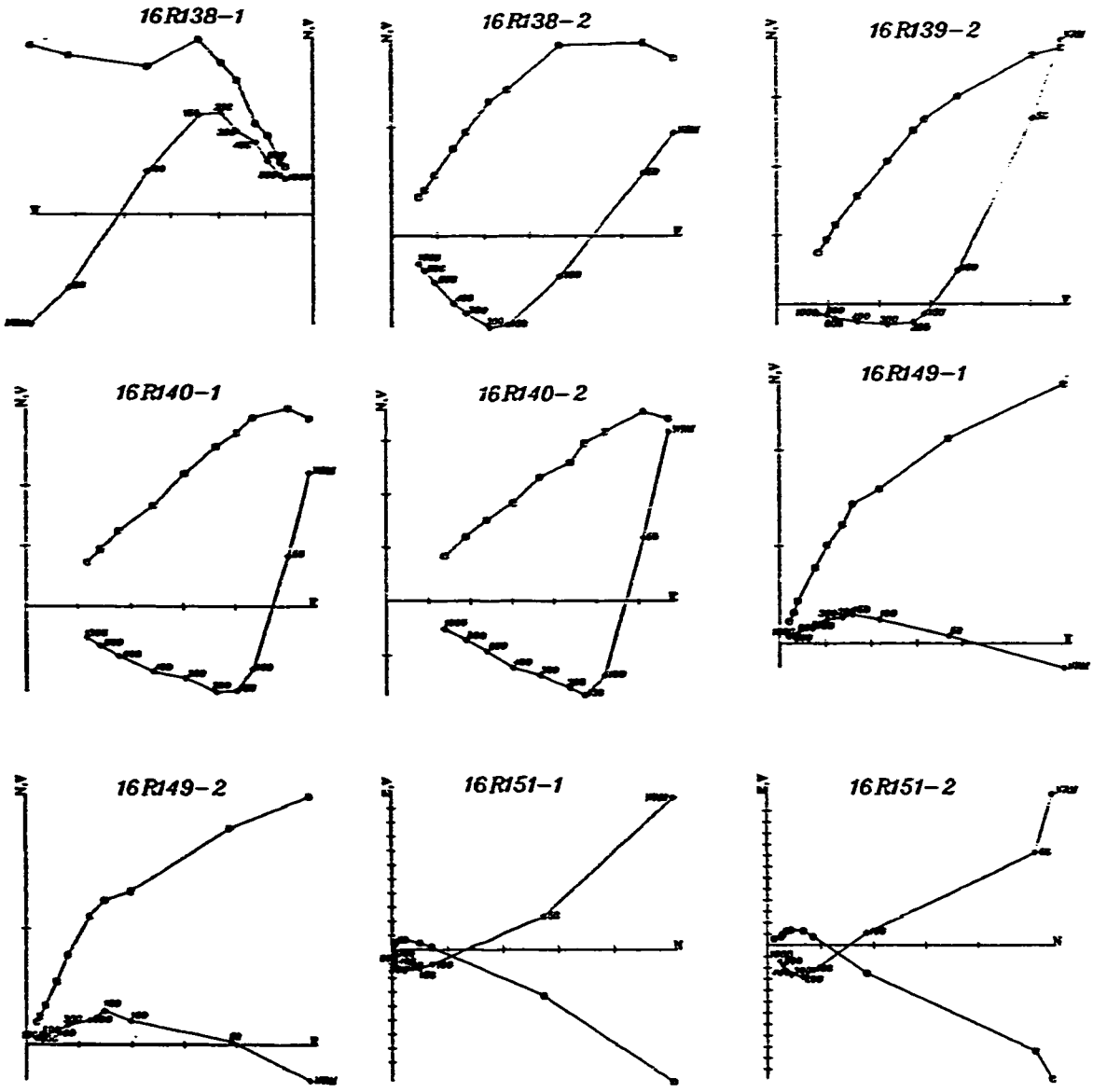

Sets of vector diagrams representing the behavior of remanent magnetization during alternating field (a.f) demagnetization.

Locality 4, Site 1 (Th)

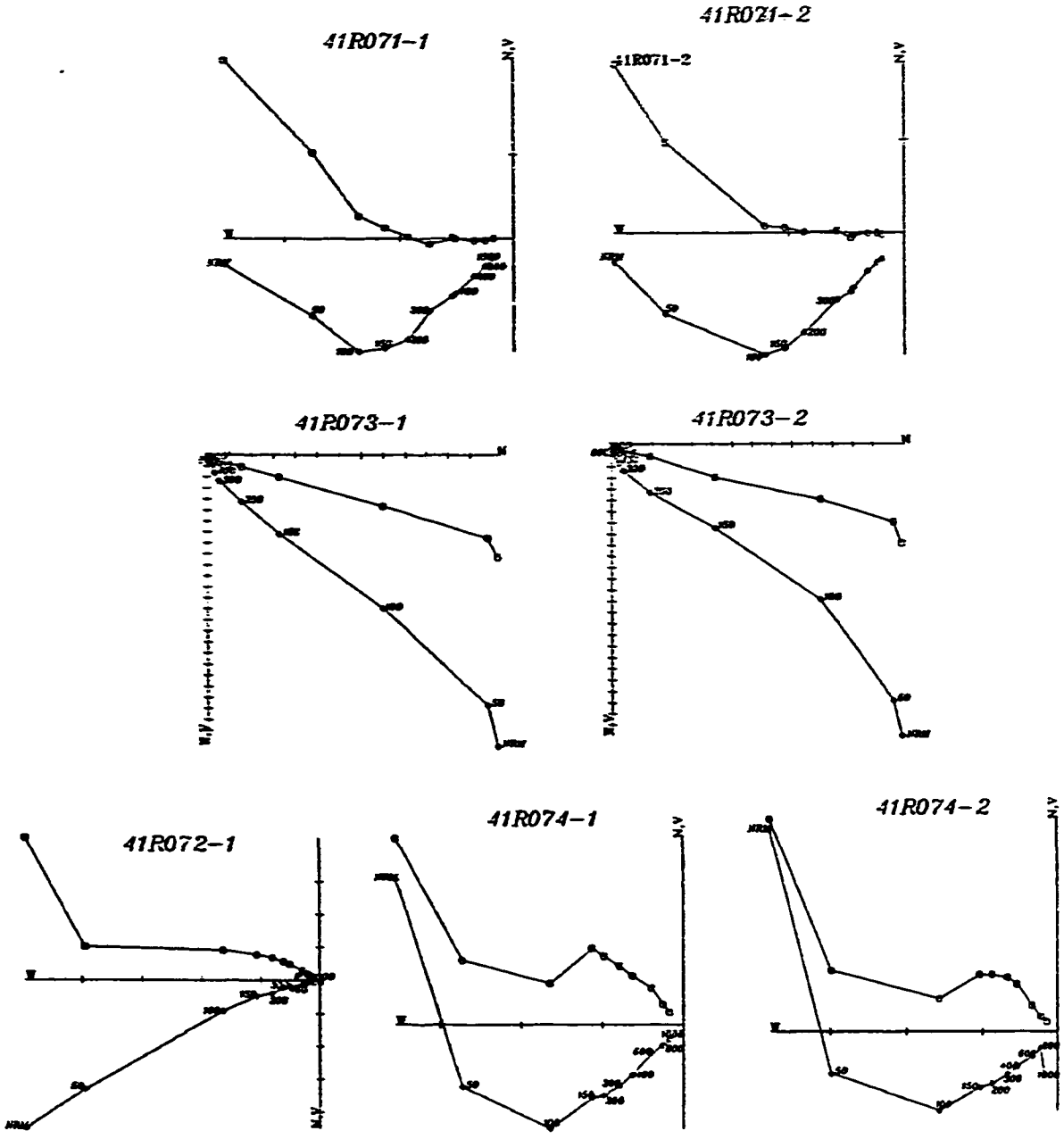

Sets of vector diagrams representing the behavior of remanent magnetization during alternating field (a.f) demagnetization.

Locality 2, Site 1 (Tw1)[244]

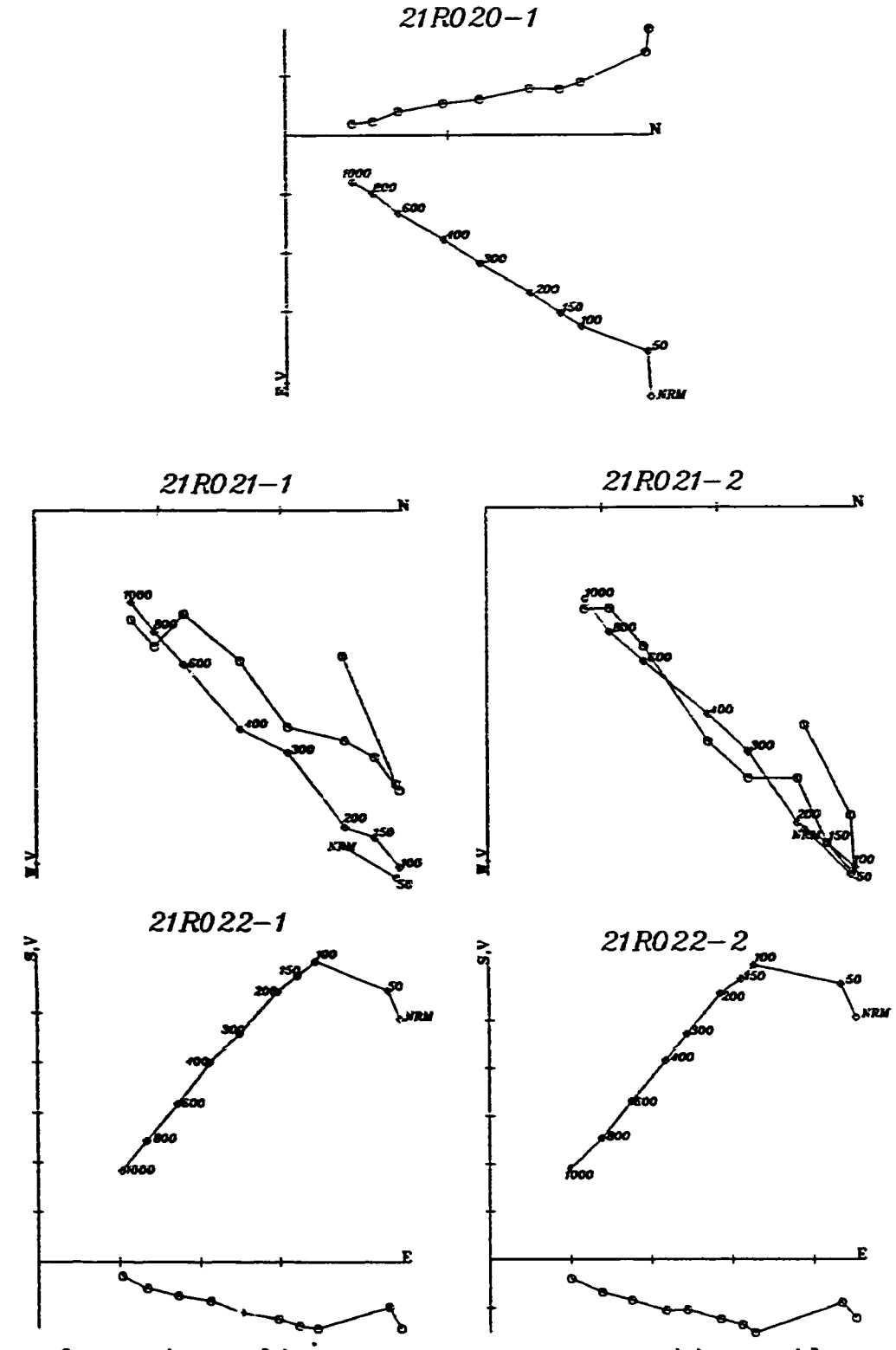

Sets of vector diagrams representing the behavior of remanent magnetization during alternating field (a.f) demagnetization.

Locality 2, Site 2 (Tw1)

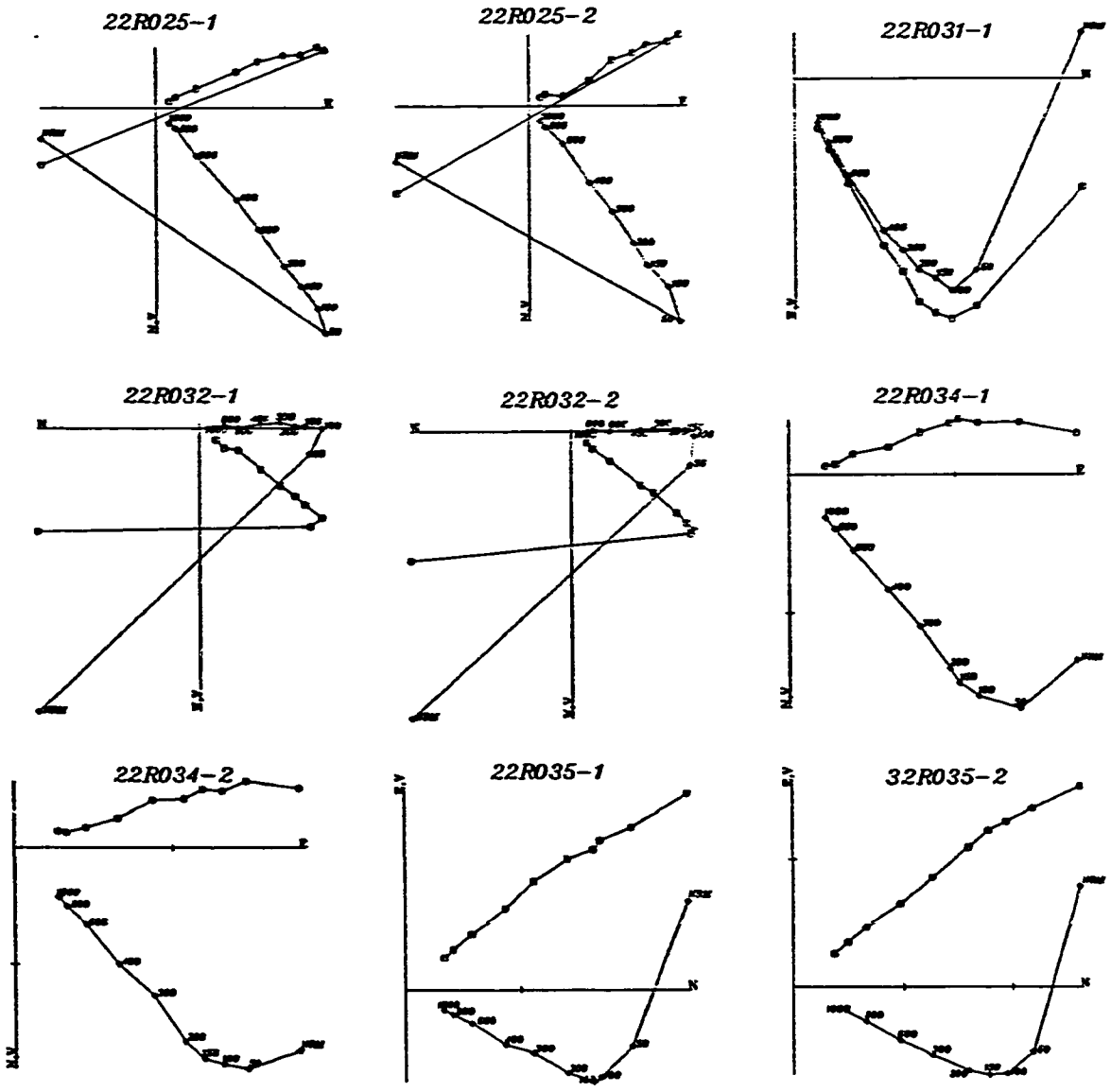

Sets of vector diagrams representing the behavior of remanent magnetization during alternating (a.f) demagnetization.

Locality 2, Site 3 (Tw1)

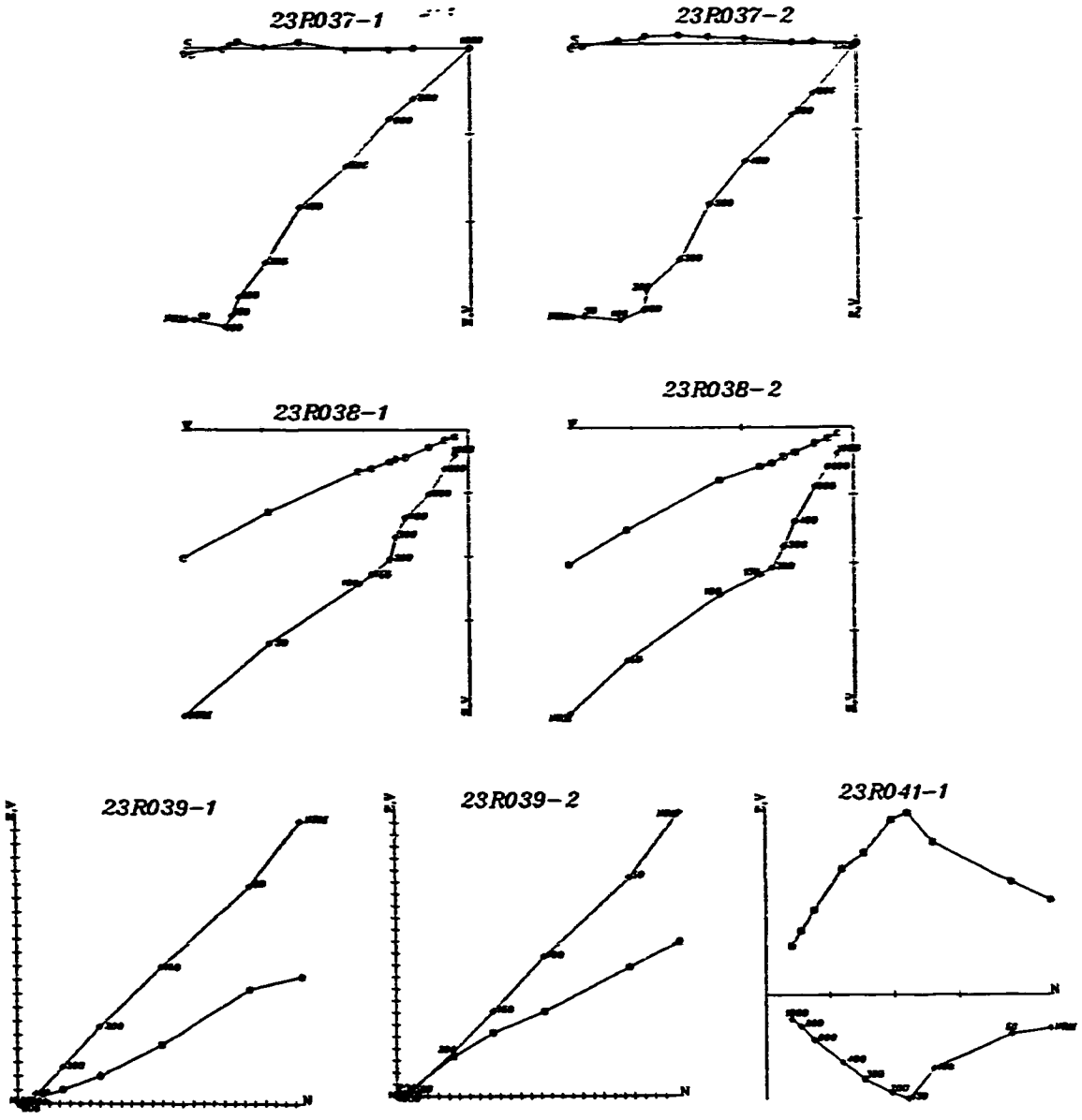

Sets of vector diagrams representing the behavior of remanent magnetization during alternating (a.f) demagnetization.

Locality 3, Site 1 (Tw1)

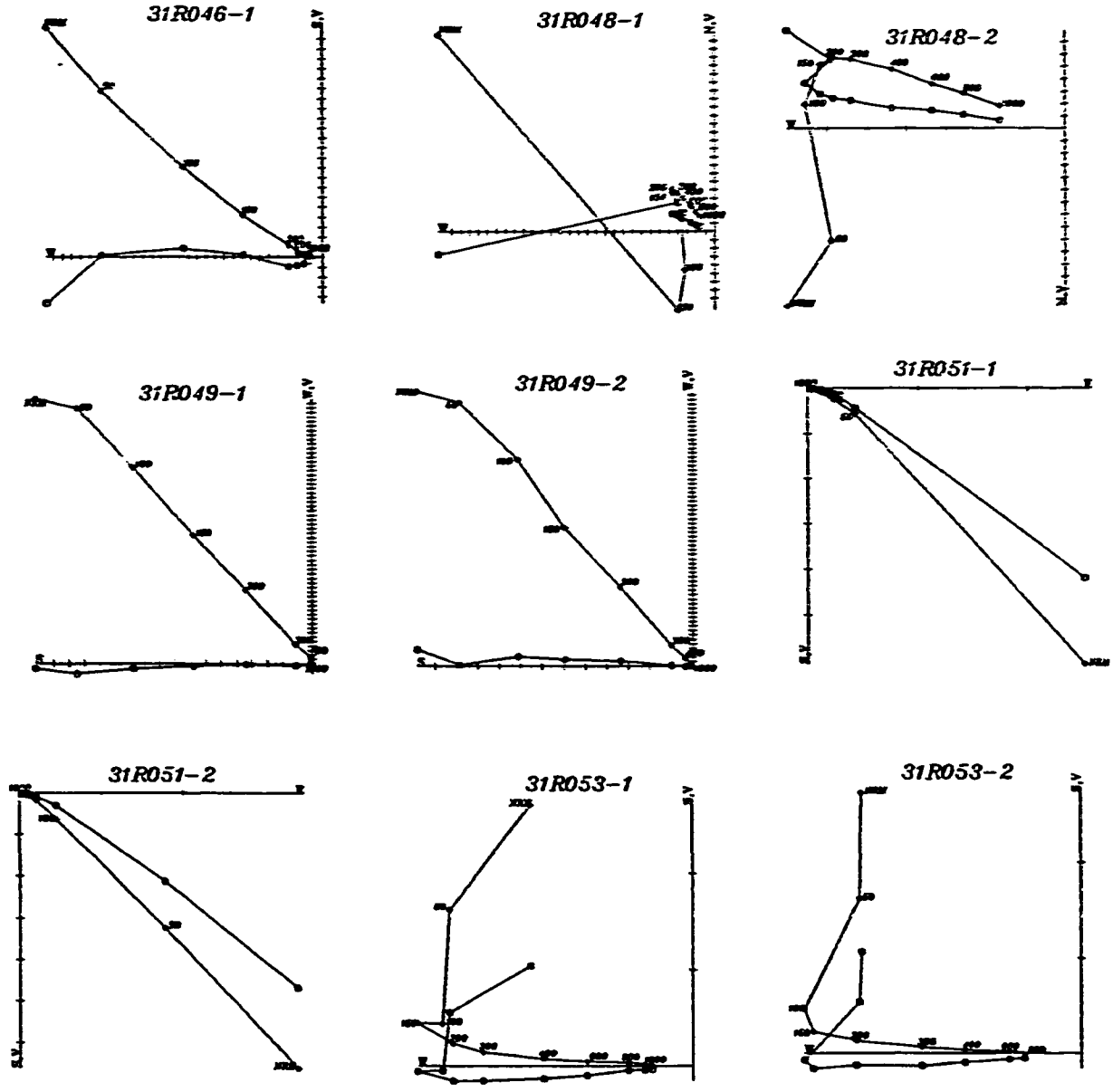

Sets of vector diagrams representing the behavior of remanent magnetization during alternating field (a.f) demagnetization.

Locality 3, Site 2 (Tw1)

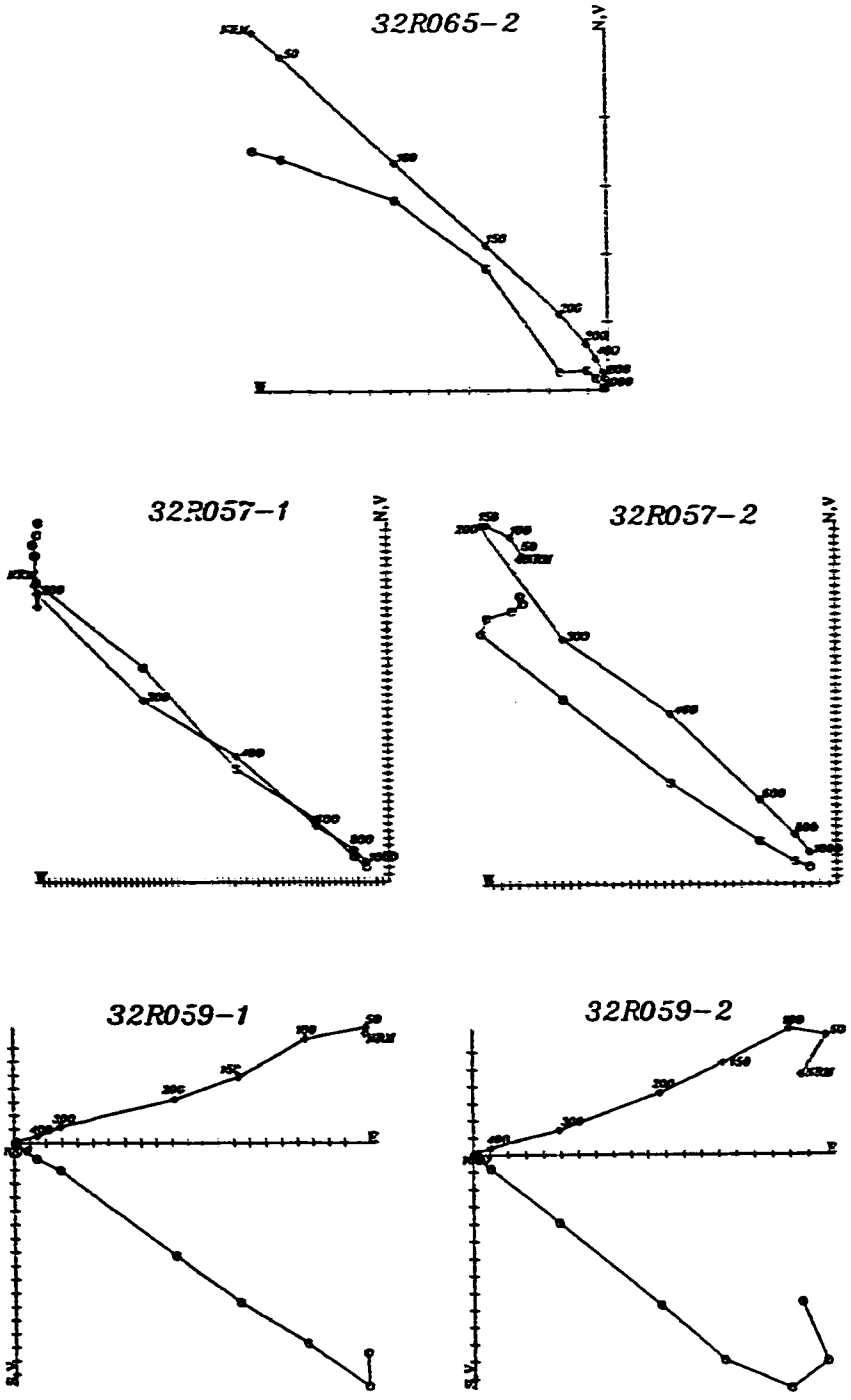

Sets of vector diagrams representing the behavior of remanent magnetization during alternating field (a.f) demagnetization.

Locality 3, Site 3 (Tw1)

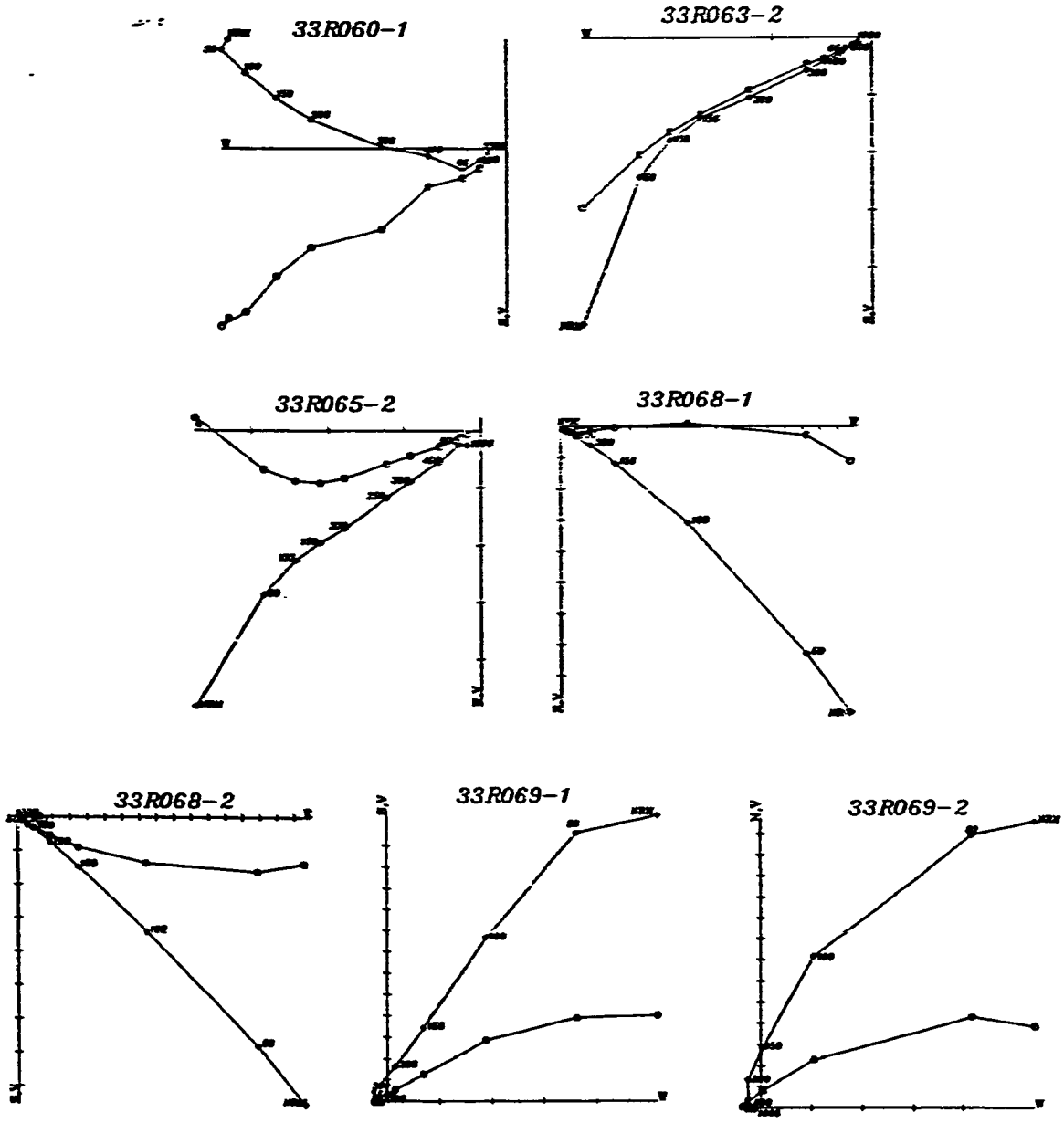

Sets of vector diagrams representing the behavior of remanent magnetization during alternating (a.f) demagnetization.

Locality 1, Site 1 (Tw2)

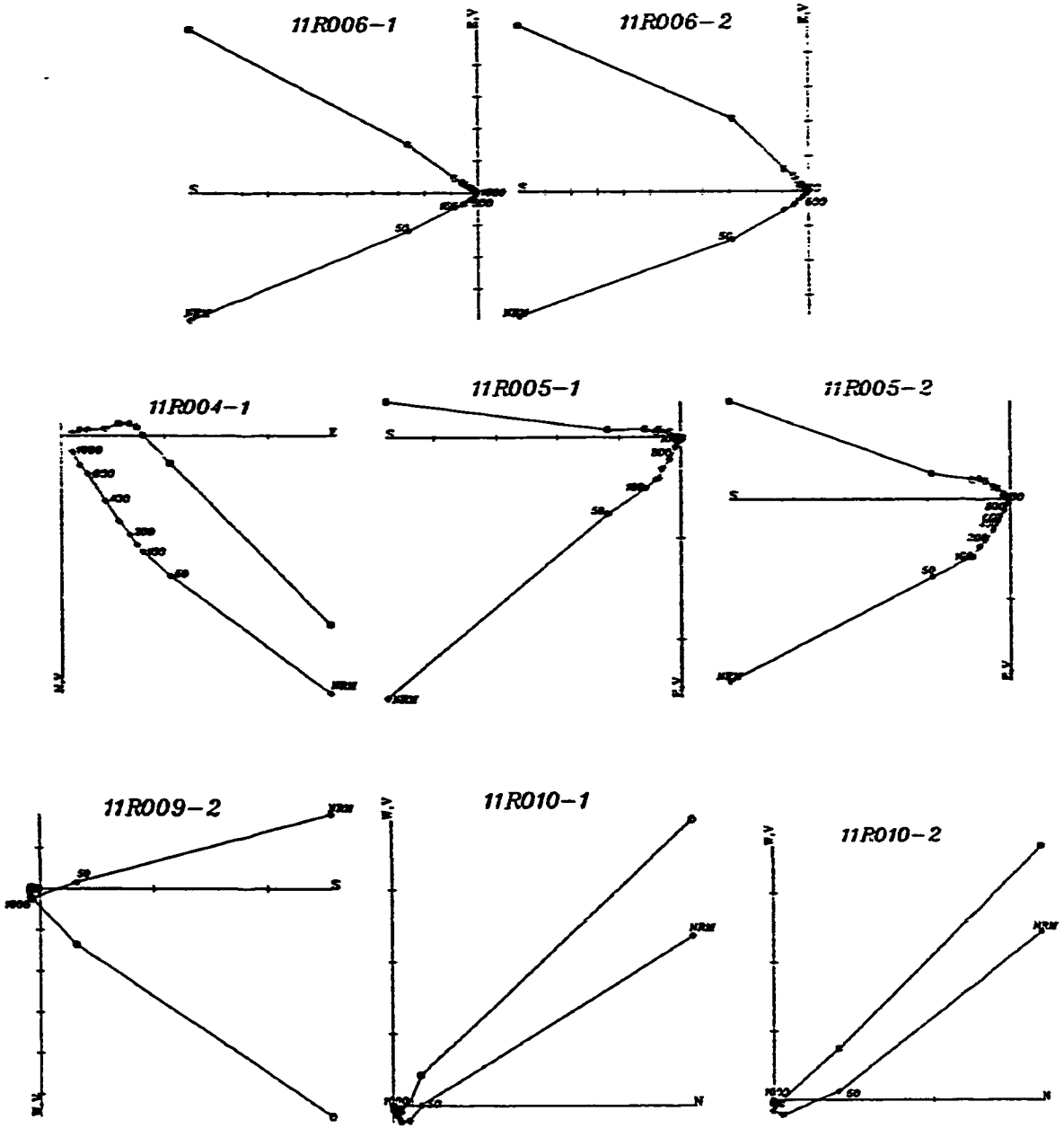

Sets of vector diagrams representing the behavior of remanent magnetization during alternating field (a.f) demagnetization.